AN INVESTIGATION OF THE IMPEDANCE OF A POWERED FLYING CONTROL SYSTEM.

by

J.E.T. Penny. B.Sc.(Eng) G.I. Mech.E.

Submitted in fulfilment of the requirements
for the degree of Doctor of Philosophy.
University of Aston in Birmingham.
September 1966.

Faculty of Engineering.
Dept. of Mech. Eng.

Head of Department,
Prof. A.C. Walshaw.
Supervisor,
Prof. E. Downham.

SYNOPSIS

This thesis describes an investigation to determine the impedance of a powered flying control system.

The first stage of this project investigated the impedance of a hydraulic servomechanism in a rigid environment. The impedance was predicted theoretically and measured experimentally by sinusoidal and random excitation of the output end and also by sinusoidal excitation of the valve input. A qualitative agreement has been shown to exist between the theoretical predictions and the experimental results.

Following the determination of the impedance of the servomechanism in a rigid environment, the analysis and experimental work was extended to include the effect of a flexibility connected to the output end of the servomechanism. It was demonstrated theoretically and verified experimentally that the impedance of this system may be predicted by combining the impedance of the servomechanism with the impedance of the flexibility using the normal laws of impedance addition.

The impedance of the servomechanism has also been determined with its anchorage connected to a flexibility. The theoretical analysis of this system produced a result of some complexity, but it has been shown that as the

frequency of excitation tends to zero and also to infinity, the system impedance can be readily predicted and these predictions have been verified experimentally.

The most recent stage of the project has been to investigate the effect upon the servomechanism of connecting the servo valve input to a flexibility. The analysis of such a system was found to be difficult and the resulting predictions unreliable. The experimental results did not agree with the theoretical predictions for this system, indicating that the effect of valve input flexibility must be obtained experimentally.

CONTENTS

Note: Graphs and diagrams referred to in the text may be found immediately following the chapter to which they refer.

A photograph showing the instrumentation and test rig may be found at the end of this volume.

PART I

INTRODUCTION.

CHAPTER I

Introduction and Formulation of the Problem

The circumstances leading to the adoption of powered flying control systems in aircraft are described and the reasons for determining the impedance of such a system given. The main stages in the proposed research programme are outlined.

1.1 Application of servomechanism to aircraft control systems.

During the middle and late 1940's there occurred a marked increase in aircraft performance caused in part by the development of the gas turbine and in part by the impetus to design brought about by the Second World War. This improved performance presented the aircraft designer with a variety of new problems, one of which being the difficulty of controlling the aircraft during high speed flight. The reason for this was that since the aerodynamic forces acting on the control surfaces increase approximately in proportion to the velocity of flight squared, the increased flight speed led to a situation arising where the aerodynamic forces acting exceeded a level that could reasonably be controlled manually. Designers subsequently were forced to provide some form of power assistance in order that the pilot could control the aircraft, leading ultimately to the present form of the powered flying control system.

1.2 Flutter.

Flutter is the aerodynamic excitation of any part of the aircraft structure causing an oscillatory instability to occur and in which the flexibility of the structure plays an essential part in the instability. The energy required to sustain the instability is taken from the passing air stream.

One form of flutter often encountered is that of the control surface. In a manual flying control system a flutter problem frequently exists but it is accentuated by the adoption of the powered flying control. A manual control system can be regarded as a simple stiff system and classical flutter can be encountered, but with a powered flying control system it is sometimes possible to encounter unstable conditions caused by the coupling of the control surface movement to the servovalve by means of aircraft structural distortion.

To prevent the possibility of flutter in a powered flying control system it is necessary for the system to have either no free movement at the control surface when the pilot's control is fixed, or a stiffness against a moment under these conditions so great that the natural frequency of the system is above any flutter frequency. Unfortunately, to obtain a system which is both stable and stiff presents difficulties, the two properties being interrelated such that an increase in one property leads to a decrease in the other and vice versa.

1.3 Operation of a hydraulic servomechanism.

One type of servomechanism used in a powered flying control system is the hydraulic servomechanism of the jack type, this servomechanism having many advantages, notably light weight and simplicity of design.

Since this type of servomechanism is frequently used in practice, it was chosen for analysis and experimental work. The servomechanism is a power amplifier and is shown diagrammatically in Fig. 1.1. The jack body is connected to the control surface and moves relative to the jack piston which is normally fixed to the aircraft structure. Integral with the jack body is the valve body which contains a four way plate or spool valve. Movement of the spool from the neutral position opens the ports connecting one side of the jack piston to the high pressure hydraulic supply and the opposite side of the jack piston to the drain. This causes the jack body to move in such a manner that the ports close, i.e. the jack body will follow the movement of the spool. The aircraft pilot moves the spool and hence, via the servomechanism, varies the control surface position. If a force, e.g. an aerodynamic force, acts at the output end and causes a displacement of the jack body in one direction, then the valve ports will open resulting in hydraulic forces acting in the opposite direction. This internal hydraulic force, in opposing the applied force, gives rise to the impedance of the servomechanism.

The terms anchorage, output end and valve input are frequently used throughout this work and relate to various positions relative to the servomechanism, as shown in Fig. 1.1.

1.4 Objects and scope of the investigation.

In order to predict the flutter characteristics of a powered flying control system a knowledge of the system impedance is required. Measurement of this impedance by the direct excitation of the aircraft control surface presents many practical difficulties making the method extremely restricted and unreliable. The control system is non-linear and a large excitation force is therefore required to investigate the full performance range of the servomechanism up to conditions of stall. In recent years vibrators, having large force outputs in the frequency range required for flutter investigations, have become commercially available allowing the full performance range of the system to be tested. The application of large forces to the control system, can, however, create further problems in the efforts to measure system impedance. The most serious of these problems is that the excitation of the aircraft structure, frequently in a manner not normally encountered during flight, introduces errors and uncertainties into the measured impedance. Other unknown factors such as anchorage flexibility, free movement in joints and friction effects can also introduce errors of unknown size into the impedance measurements.

In view of these and other difficulties, a new and radically different approach to the problem of determining the impedance of a powered flying control system has been devised. The research project, which resulted from discussions with members of the Structures Dept. R.A.E. Farnborough, has been sponsored and almost entirely financed by the Ministry of Aviation and during the course of the programme contact was maintained with the Structures Dept.

The first stage of the project has been to determine both theoretically and experimentally the impedance of a hydraulic servomechanism in a rigid environment by direct excitation of its output end in a test rig. In this manner it was hoped that a more accurate measurement of impedance than hitherto available would be obtained. The theoretical analysis of this system and the resulting predictions are given in Chapter IV. The experimental programme, which included not only sinusoidal but also random excitation of the servomechanism and the conclusions based on the experimental results, are described in Chapter V.

An attempt has been made to measure the impedance of the servomechanism in a rigid environment by excitation of the servo valve input. The theoretical justifications and limitations of this method are set out in Chapters II and IV and the experimental work described in Chapter VI.

Following the determination of the servomechanism impedance in a rigid environment by two differing methods, the next stage of the programme was to introduce flexibilities into the system under investigation. The effect of these flexibilities has been analysed (Chapter VII) and the experimental work to determine the effect of output, anchorage and valve input flexibilities upon the system impedance is described. (Chapters VIII, IX & X.)

It has already been stated that the principle difficulty encountered when attempting to determine the impedance of a powered flying control system is the large force input to the system required to produce the range of servo valve openings which are necessary for investigation of all performance conditions. Excluding the servomechanism, the remainder of the system does not, however, require large force excitation and thus if the servomechanism was temporarily removed, impedance tests on the remainder of the system could be performed on the aircraft using a relatively low level of force excitation. The problem then resolves into one of finding a suitable temporary replacement for the servomechanism such as a spring, a free rigid link or a link clamped to the aircraft structure, and then devising a method of combining the results obtained from these tests with the impedance of the servomechanism measured in, or predicted from, laboratory tests.

This thesis describes the work that has been done to date in carrying out this programme. In order to take the project to its ultimate conclusion it will be necessary to perform tests upon a control system in an aircraft with the servomechanism removed and to predict the complete system impedance from these tests by combining the results with the impedance of the servomechanism. Finally, notwithstanding the statement at the beginning of this section concerning the difficulty of obtaining the system impedance in an aircraft directly, this will have to be attempted in a very limited and restricted way (both in range and accuracy) so that a comparison can be made between the results obtained by direct excitation of the control system in the aircraft and the results obtained by the method that has been proposed in this thesis.

Because of the extent of the main project, little time has been spent in investigating certain interesting results which arose during the experimental programme. This thesis, therefore, is in the nature of an overall survey of the main problem and must inevitably leave certain topics unexplored and certain phenomena unexplained

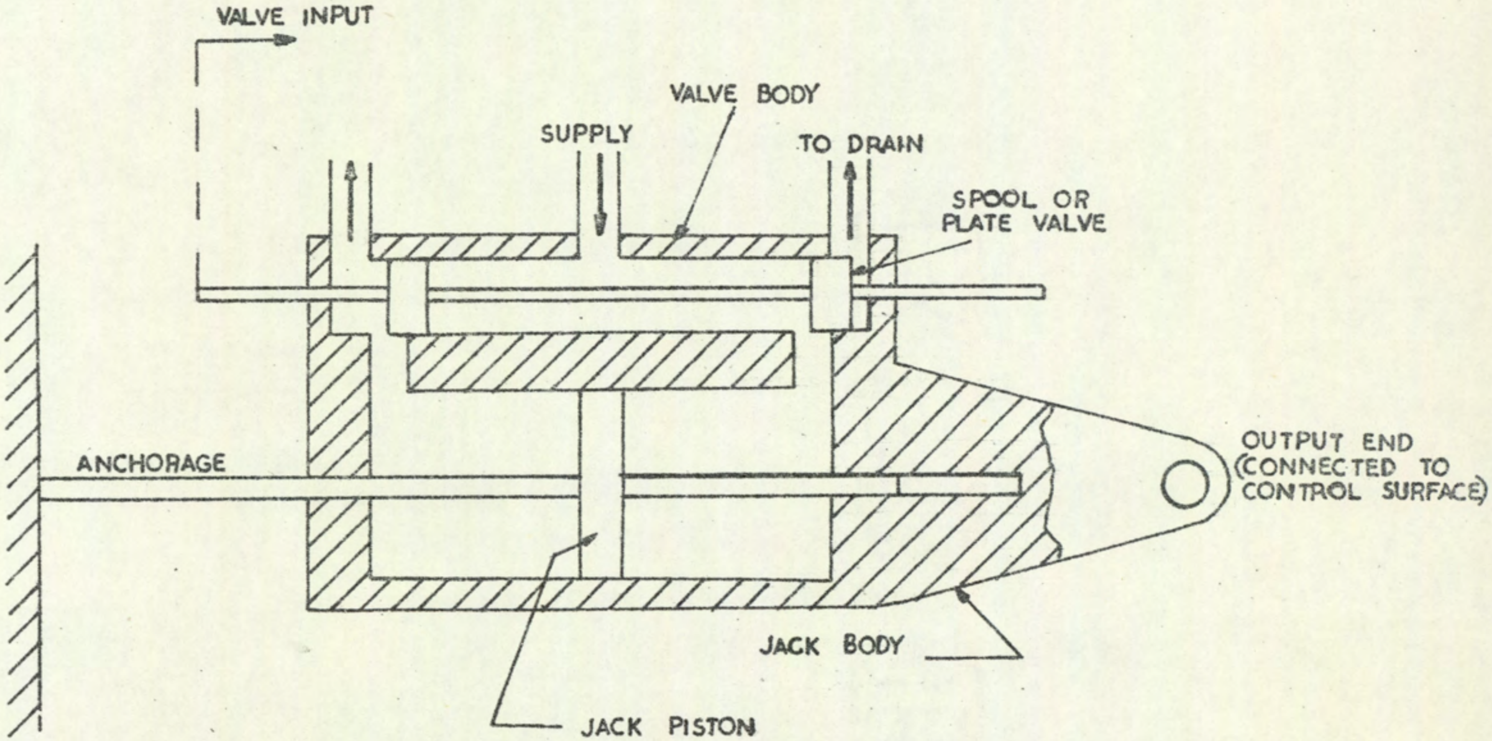

SCHEMATIC DIAGRAM OF A
HYDRAULIC SERVOMECHANISM

FIG 1.1

CHAPTER II

Impedance Techniques in Vibration Analysis.

The basis of the impedance technique in vibration analysis is described together with the related four pole analysis method and using the four pole method the internal impedance of a mechanical generator is developed. The concept of random excitation in vibration analysis is briefly described together with its application to the measurement of system impedance. Non-linear systems are discussed.

2.1 Notation.

The following notation is used throughout this chapter:

c	Damping coefficient
f	Force
j	$\sqrt{(-1)}$
k	Spring stiffness
m	Mass
t	Time
$(T_f)_{ij}$	Force transmissibility between stations i and j
$(T_x)_{ij}$	Displ. " " " "

x Displacement

Z Impedance

δ_{ij}, σ_{ij},

μ_{ij} Four pole parameters

$[\bar{\delta}_{ij}]$ Four pole matrix

ω Excitation frequency

The following superscripts are applied to f, x and Z.

B Blocked condition

F Free condition

The following subscripts are applied to Z.

d Impedance of a damper

g " " generator

m " " mass

s " " spring

ij Impedance between stations i and j

The following notation is used in the random analysis.

B Bandwidth

$G_x(n)$ Power spectral density of x at a frequency of n c/s

$\bar{G}_x(n)$ An approximation to $G_x(n)$

$G_{xf}(n)$ Cross spectral density between x and f

$C_{xf}(n)$ Co-spectral density between x and f

$Q_{xf}(n)$ Quad-spectral density between x and f

n Frequency c/s

$p(x)$ Probability density

T	Averaging time
$\|x\|$	Absolute average value of x
$\overline{x^2}$	Mean square value of x
$\bar{x}$	Mean value of x
x_{rms}	Root mean square value of x
Δn	Incremental bandwidth
σ	Standard deviation

2.2 Historical introduction.

In order to analyse the vibrations caused by the excitation of an elastic system by a sinusoidal force, the classical method is to apply Newton's laws of motion to the system and to solve the resulting differential equations. To investigate the effect of natural or forced vibrations requires a study of the complimentary function or the particular solution of the differential equations respectively, and, in the event of changes being made to the mechanical system under consideration, the equations of motion must be reformulated and solved again.

At the beginning of the present century electrical engineers, when analysing linear circuits carrying alternating currents, began to consider the ratio between the sinusoidal voltage across and the resulting sinusoidal current flow between a pair of terminals. Since the circuits were linear the voltage current ratio was demonstrated to be independent of amplitude and a function of frequency only.

From this beginning an extensive theory was built up in order that all forms of passive circuit elements could be connected together and the voltage current relationship determined for the network. This ratio was termed the network impedance. Subsequently the mathematical similarity between acoustic and electrical circuits was observed and electrical circuits were used as acoustic analogues and analysed by impedance techniques (1).* Later, control engineers adopted the electrical analogue approach to assist in the solution of control problems and finally mechanical engineers used electrical analogues to analyse torsional and lumped parameter systems, (2) & (3). A notable step forward in the early 1940's was the application of impedance methods to mechanical systems without recourse to electrical analogues (4).

2.3 Impedance

Impedance is the sinusoidal force required to produce a unit sinusoidal response in a linear elastic system. The response chosen may be either the displacement, velocity or acceleration response depending upon the type of problem and the frequency of the applied force. At a low frequency the displacement response form of the equation is often chosen since at low frequencies the stress induced into the system is proportional to displacement. At a higher frequency stress tends to become a function of velocity and velocity response is of greater significance; the impedance based on velocity response has a further advantage in that it can be

* A list of references is given on page 173.

represented by a simple electrical analogue. When inertia forces are the predominant cause of excitation, such as in balancing problems, impedance based on acceleration response is frequently favoured particularly because at all but the lowest frequencies of excitation the acceleration response is more easily measured. It can be shown that conversion from one form of impedance to another can be achieved by multiplying or dividing by the factor $j\omega$.

Instead of considering the ratio of force to response, the ratio of response to force can be used and is termed mobility. Depending upon the particular problem, whilst either the impedance or mobility approach can be used to obtain the solution, one will always require less algebraic manipulation and numerical work than the other. At the present time no standard nomenclature exists for the description of the various force to response and response to force ratios, but throughout this thesis the ratio of force to displacement response will be termed impedance. Thus impedance Z is given by

$$Z = f/x \tag{2.1}$$

where f and x are complex quantities making Z complex also. The real part of Z is termed the stiffness or resistance and represents the stored energy, the imaginary part is termed the damping or reactance and represents the dissipated energy. In the analysis which follows it is assumed that the excitation is sinusoidal and the system is linear. In Sections 2.9 and 2.10 the method is extended to include the effect of non-sinusoidal and random excitation and the effect of non-linearities is discussed in Section 2.11.

2.4 Analysis of mechanical elements.

In a mechanical system the primary passive elements are masses, springs and dampers, the active elements being force and displacement generators. Springs and dampers are 'double ended' elements and in a network must always be placed either between two other elements or between one other element and ground. The element displacement must be measured (Fig. 2.1a) with one end blocked or alternatively the displacement must be measured across the element, which is an exact equivalent, since the springs and dampers are assumed to be ideal and without mass.

Spring : Equation of motion $f = kx$

$$\therefore \quad Z_s = k \tag{2.2}$$

Damper : Equation of motion $f = c\dot{x}$

If $f = f \exp j\omega t$ and $x = x \exp j\omega t$

$\dot{x} = j\omega x \exp j\omega t$

$$f \exp j\omega t = j\omega c x \exp j\omega t$$

$$\therefore \quad Z_d = f/x = j\omega c \qquad (2.3)$$

The displacement of a mass must be measured relative to an inertial frame of reference, hence a mass is essentially 'single ended' and must have one end connected to another element and one end free as shown in Fig. 2.1b, e.g. if, in a physical system, a mass is placed between two springs, then for the purpose of analysis the mass must be considered to be placed in parallel with one spring and the spring-mass combination must be connected in series with the other spring.

<u>Mass</u> : Equation of motion $f = m\ddot{x}$

If $f = f \exp j\omega t$ and $x = x \exp j\omega t$

$$\ddot{x} = - \omega^2 x \exp j\omega t$$

$$f \exp j\omega t = - \omega^2 x m \exp j\omega t$$

$$\therefore \quad Z_m = f/x = - m\omega^2 \qquad (2.4)$$

An alternative way of considering the impedance of passive elements is to introduce the concept of blocked and free impedance. The impedance of an element with the output end blocked is written Z^B and with the output end free, Z^F. This notation is particularly useful in the four pole method of analysis (Section 2.6). Applying this notation to the passive elements just evaluated gives:-

For a spring $Z_s^B = k = Z_s$ (2.5)

$$Z_s^F = 0 \tag{2.6}$$

For a damper $Z_d^B = j\omega c = Z_d$ (2.7)

$$Z_d^F = 0 \tag{2.8}$$

For a mass Z_m^B tends to infinity (2.9)

$$Z_m^F = - m\omega^2 = Z_m \tag{2.10}$$

Hence, when springs and dampers are placed in a system between elements or with one end grounded it is the blocked impedance that is effectively used in the analysis; for a mass with one free end, the free impedance is used. Providing these restrictions are observed the superscripts F and B can be dispensed with.

2.5 Network analysis.

In order to analyse a network of mechanical components it is desirable to simplify the system. This can be achieved in the following manner.

Elements connected in series : Mechanical elements are said to be connected in series when the same force acts through all the components at any instant.

Refering to Fig. 2.2a

$$Z = f/x = f/(x_1 + x_2 + x_3)$$

$$\therefore \quad 1/Z = (x_1 + x_2 + x_3)/f$$

$$\therefore \quad \frac{1}{Z} = \frac{1}{Z_1} + \frac{1}{Z_2} + \frac{1}{Z_3}$$

or in general if there are n elements then

$$1/Z = \Sigma(1/Z_r) \text{ where } r = 1 \text{ to } n \tag{2.11}$$

Note : A mass cannot be connected in series with other elements unless it be placed at the free end of a series for the reason previously given.

Elements connected in parallel : Mechanical elements are said to be connected in parallel when all components have the same displacement between their input and output ends.

Refering to Fig. 2.2b

$$Z = f/x = (f_1 + f_2 + f_3)/x$$

$$\therefore \quad Z = Z_1 + Z_2 + Z_3$$

or in general if there are n elements then

$$Z = \Sigma\, Z_r \text{ where } r = 1 \text{ to } n \tag{2.12}$$

Using the parallel and series connection rules, networks can be simplified to determine the impedance of the complete system. In order to further assist in the analysis of mechanical systems, a number of network theorems used in electrical circuit analysis have been adapted for use in the analysis of mechanical systems.

2.6 Four pole parameters.

A method of vibration analysis closely related to the impedance technique is the four pole parameter method. This method is based on the fact that the relationship between the input and output forces and displacements of a linear system having a single input point and a single output point can be given by

$$\left.\begin{aligned} f_1 &= \delta_{11} f_2 + \delta_{12} x_2 \\ x_1 &= \delta_{21} f_2 + \delta_{22} x_2 \end{aligned}\right\} \qquad (2.13)$$

where f_1, x_1 are the input conditions, f_2, x_2 are the output conditions and the positive direction of force and displacement is defined as the direction from the input point to the output point. The so-called four pole parameters δ_{11}, δ_{12}, etc, are defined by this pair of equations

Using matrix notation

$$\begin{bmatrix} f_1 \\ x_1 \end{bmatrix} = \begin{bmatrix} \delta_{11} & \delta_{12} \\ \delta_{21} & \delta_{22} \end{bmatrix} \begin{bmatrix} f_2 \\ x_2 \end{bmatrix} \qquad (2.14)$$

This may be written in the form

$$\begin{bmatrix} f_1 \\ \\ x_1 \end{bmatrix} = \begin{bmatrix} \bar{\delta}_{12} \end{bmatrix} \begin{bmatrix} f_2 \\ \\ x_2 \end{bmatrix}$$

If the output is blocked $x_2 = 0$

$$f_1 = \delta_{11} f_2$$

$$x_1 = \delta_{21} f_2$$

Hence $\delta_{11} = (f_1/f_2)^{2B} = 1/(T_f)_{12}^{2B}$

and $\delta_{21} = (x_1/f_2)^{2B} = 1/Z_{12}^{2B}$

where the superscript 2B indicates that station 2 (the output) is blocked.

If the output is free $f_2 = 0$

$$f_1 = \delta_{12} x_2$$

$$x_1 = \delta_{22} x_2$$

Hence $\delta_{12} = (f_1/x_2)^{2F} = Z_{12}^{2F}$

and $\delta_{22} = (x_1/x_2)^{2F} = 1/(T_x)_{12}^{2F}$

where the superscript 2F indicates that station 2 (the output) is free.

It can be shown that the force and displacement transmissibilities in opposite directions are equal.

Hence $(T_x)^{2F}_{12} = (T_f)^{1B}_{21}$

If it is defined that the station to which the second subscript refers is blocked in the force transmissibility term and free in the displacement transmissibility term then the superscripts F and B need not be used.

Hence $(T_x)_{12} = (T_f)_{21}$

It can also be shown that the transfer impedance between two stations in opposite directions is equal.

Hence $Z^{2B}_{12} = Z^{1B}_{21} = Z^{B}_{12}$ and $Z^{2F}_{12} = Z^{1F}_{21} = Z^{F}_{12}$

Summarising,

$$\delta_{11} = 1/(T_f)_{12} = 1/(T_x)_{21} \tag{2.15}$$

$$\delta_{22} = 1/(T_f)_{21} = 1/(T_x)_{12} \tag{2.16}$$

$$\delta_{12} = Z^{F}_{12} \tag{2.17}$$

$$\delta_{21} = 1/Z^{B}_{12} \tag{2.18}$$

Thus the generalised four pole parameter matrix is

$$\begin{bmatrix} 1/(T_x)_{21} & Z^{F}_{12} \\ 1/Z^{B}_{12} & 1/(T_x)_{12} \end{bmatrix} \tag{2.19}$$

The parameters may be evaluated for mechanical elements either by substituting in the basic equations or by using the generalised definitions for δ_{11}, δ_{12} etc. This gives the following results:-

<u>Mass</u>: $$\begin{bmatrix} 1 & -m\omega^2 \\ 0 & 1 \end{bmatrix} \tag{2.20}$$

<u>Spring</u>: $$\begin{bmatrix} 1 & 0 \\ 1/k & 1 \end{bmatrix} \tag{2.21}$$

<u>Damper</u>: $$\begin{bmatrix} 1 & 0 \\ 1/j\omega c & 1 \end{bmatrix} \tag{2.22}$$

2.7 <u>Network analysis using the four pole method.</u>

It has been shown in Section 2.5 how systems can be simplified by using the method of series and parallel connexions to obtain the system impedance. A similar technique can be used to determine the four pole parameters for the system as follows.

<u>Elements connected in series</u>: The output force and displacement of the first element is equal to the input force and displacement of the second element and so on, as in Fig. 2.3a.

Hence $$\begin{bmatrix} f_1 \\ x_1 \end{bmatrix} = \begin{bmatrix} \delta_{11} & \delta_{12} \\ \delta_{21} & \delta_{22} \end{bmatrix} \begin{bmatrix} \sigma_{22} & \sigma_{23} \\ \sigma_{32} & \sigma_{33} \end{bmatrix} \begin{bmatrix} \mu_{33} & \mu_{34} \\ \mu_{43} & \mu_{44} \end{bmatrix} \begin{bmatrix} f_4 \\ x_4 \end{bmatrix} \tag{2.23}$$

This can be extended for any number of elements. The four pole parameter method places no restriction on the position of the mass element in the system; a mass has an input point and an output point in common with all other elements when this method of analysis is used.

Elements connected in parallel: If elements are connected as shown in Fig. 2.3b, then if

$$A = \Sigma(\delta_{11}/\delta_{21})_r$$

$$B = \Sigma(1/\delta_{21})_r$$

$$C = \Sigma(\delta_{22}/\delta_{21})_r$$

[In this case r = 1 to 3 or generally r = 1 to n where n is the number of elements] then it can be shown that for the combined system

$$\left.\begin{array}{ll} \delta_{11} = A/B & \delta_{21} = 1/B \\ \delta_{12} = (AC - B^2)/B & \delta_{22} = C/B \end{array}\right\} \qquad (2.24)$$

2.8 Mechanical generators.

A mechanical generator consists of two basic components, an ideal generator and an elastic system. The ideal generator exerts a sinusoidal force or displacement at the input of the associated elastic structure, as shown in Fig. 2.4.

Hence $f_s = \delta_{11}f_o + \delta_{12}x_o$ (2.25)

$$x_s = \delta_{21}f_o + \delta_{22}x_o \tag{2.26}$$

where the positive direction of force and displacement is defined as the direction from the input of the elastic structure to the output.

Rearranging the equations gives

$$f_o = (1/\delta_{11})f_s - (\delta_{12}/\delta_{11})x_o \tag{2.27}$$

$$f_o = (1/\delta_{21})x_s - (\delta_{22}/\delta_{21})x_o \tag{2.28}$$

It is not normally possible to separate the mechanical source into its basic components and therefore it is desirable to describe the generator in terms of the quantities that can be measured, the force and displacement at the output point.

Consider an ideal force generator:-

If the output is blocked $x_o = 0$ and $f_o = f_o^B$

From equation (2.25) $f_s = \delta_{11}f_o^B$

Substituting in equation (2.27)

$$f_o = f_o^B - (\delta_{12}/\delta_{11})x_o \tag{2.29}$$

If the output is free $f_o = 0$ and $x_o = x_o^F$

From equation (2.25) $f_s = \delta_{12}x_o^F$

Substituting in equation (2.27)

$$f_o = (\delta_{12}/\delta_{11})x_o^F - (\delta_{12}/\delta_{11})x_o \tag{2.30}$$

Consider an ideal displacement generator:-

If the output is blocked $x_o = 0$ and $f_o = f_o^B$

From equation (2.26) $x_s = \delta_{21} f_o^B$

Substituting in equation (2.28)

$$f_o = f_o^B - (\delta_{22}/\delta_{21})x_o \qquad (2.31)$$

If the output is free $f_o = 0$ and $x_o = x_o^B$

From equation (2.26) $x_s = \delta_{22} x_o^F$

Substituting in equation (2.28)

$$f_o = (\delta_{22}/\delta_{21})x_o^F - (\delta_{22}/\delta_{21})x_o \qquad (2.32)$$

From equations (2.25) & (2.26)

$$\delta_{22}/\delta_{21} = Z_{22}^B \quad \text{and} \quad \delta_{12}/\delta_{11} = Z_{22}^F$$

Hence for a constant force generator

$$\left.\begin{aligned} f_o &= f_o^B - Z_{22}^F x_o \\ f_o &= Z_{22}^F x_o^F - Z_{22}^F x_o \end{aligned}\right\} \qquad (2.33)$$

For a constant displacement generator

$$\left.\begin{aligned} f_o &= f_o^B - Z_{22}^B x_o \\ f_o &= Z_{22}^B - Z_{22}^B x_o \end{aligned}\right\} \qquad (2.34)$$

If the impedance of the generator is measured, either Z_{22}^F or Z_{22}^B is measured depending upon the type of exciter under investigation.

Hence, writing $Z_g = Z_{22}^F$ or Z_{22}^B we have

$$\left.\begin{aligned} f_o &= f_o^B - Z_g x_o \\ f_o &= Z_g x_o^F - Z_g x_o \end{aligned}\right\} \qquad (2.35)$$

Eliminating f_o,

$$Z_g = f_o^B / x_o^F \qquad (2.36)$$

Thus the internal impedance of a generator can be calculated from a knowledge of the block force and free displacement.

2.9 Non-sinusoidal excitation.

It has been previously stated that impedance techniques can be used to analyse the behaviour of a system provided the system is linear and the excitation is sinusoidal. Frequently, in practice, the excitation is not sinusoidal but takes the form of either continuous, periodic but non-sinusoidal excitation or continuous non-periodic random excitation. The former case will be considered here and the latter in Section 2.10.

If a non-sinusoidal function is expanded in the form of a Fourier series, then provided the initial conditions are suitably chosen the resulting series can be shown to be a series of cosine terms,

i.e. $\Phi(f) = f_1 \cos \omega t + f_2 \cos 2\omega t + ----$

Thus the non-sinusoidal excitation may be considered to be an infinite number of sinusoidal exciters operating with various amplitudes (f_1, f_2 etc.) and frequencies (ω, 2ω etc). According to the principle of superposition the response of a system to several simultaneous excitations is the sum of the response of the system to the individual excitations.

Hence, if the impedance of the system at frequencies ω, 2ω etc. is given by Z_1, Z_2, then, $x_1 = f_1/Z_1$, $x_2 = f_2/Z_2$ etc. and the response of the system is a wave, having a Fourier series given by

$\Phi(x) = x_1 \cos \omega t + x_2 \cos 2\omega t + ----$ etc.

If the Fourier analysis of the force and displacement wave forms is known, the impedance of the system can be determined both at the fundamental and also at the harmonic frequencies. At the higher harmonic frequencies, since the amplitude of the excitation and the response is much smaller than at the fundamental frequency, measurement of the impedance becomes progressively more inaccurate and unreliable.

2.10 Random excitation.

A random vibration is one whose instantaneous value is not predictable. The amplitude of a random signal never repeats exactly but the amplitude characteristics of the vibration can be described by its probability density function in the amplitude domain and by infinite averages of its absolute mean, mean square and rms values in the time domain. The spectral characteristics of a random vibration are described by its power spectrum.

Power spectral density: Given a stationary random signal $x(t)$, power spectral density (PSD) is defined thus

$$G_x(n) = \frac{1}{T(\Delta n)} \int_0^T x^2_{\Delta n}(n,t)dt \qquad (2.37)$$

where T tends to infinity and Δn tends to zero. In practice, infinitely narrow frequency intervals and infinitely long averaging times cannot be obtained. An approximate value of PSD can, however, be defined as follows:

$$\bar{G}_x(n) = \frac{1}{BT} \int_0^T x_B^2(n,t)dt \qquad (2.38)$$

where Δn has been replaced by a finite bandwidth B and T is a finite averaging time.

$$\therefore \qquad \bar{G}_x(n) = \overline{x_B^2}/B \qquad (2.39)$$

This assumes a flat spectrum within bandwidth B.

The most commonly occurring amplitude probability curve is the Gaussian or 'normal' density curve as shown in Fig. 2.5. Assuming the mean value of the function to be zero (see equation(2.42)) the function is given by

$$p(x) = \frac{1}{\sigma\sqrt{(2\pi)}} \exp(- x^2/2\sigma^2) \tag{2.40}$$

The absolute average of x in the amplitude domain is given by

$$|x| = 2\int_0^\infty x\, p(x)dx$$

$$|x| = \frac{2}{\sigma\sqrt{(2\pi)}} \int_0^\infty x \exp\,(- x^2/2\sigma^2)dx$$

$$|x| = \frac{2}{\sigma\sqrt{(2\pi)}} [- \sigma^2 \exp\,(- x^2/2\sigma^2]_0^\infty$$

$$\therefore \quad |x| = \sigma \sqrt{(2/\pi)} \tag{2.41}$$

The mean value of x in the amplitude domain is given by

$$\bar{x} = \int_{-\infty}^{\infty} x\, p(x)dx$$

$$\bar{x} = \frac{1}{\sigma\sqrt{(2\pi)}} \int_{-\infty}^{\infty} x \exp\,(- x^2/2\sigma^2)dx$$

$$\bar{x} = \frac{1}{\sigma\sqrt{(2\pi)}} \left[- \sigma^2 \exp\left(- x^2/2\sigma^2\right)\right]_{-\infty}^{\infty}$$

$$\therefore \quad \bar{x} = 0 \tag{2.42}$$

This verifies that the form of the normal density curve chosen assumes the mean value to be zero.

The mean square value of x in the amplitude domain is given by

$$\overline{x^2} = \int_{-\infty}^{\infty} x^2 p(x)dx$$

$$\overline{x^2} = \frac{1}{\sigma\sqrt{(2\pi)}} \int_{-\infty}^{\infty} x.x \exp\left(- x^2/2\sigma^2\right)dx$$

$$\overline{x^2} = \frac{1}{\sigma\sqrt{(2\pi)}}\left[-x\sigma^2\exp(-x^2/2\sigma^2) - \int -\sigma^2\exp(-x^2/2\sigma^2)dx\right]_{-\infty}^{\infty}$$

$$\text{Let} \quad I = \int_{-\infty}^{\infty} \exp(-x^2/2\sigma^2)dx = \int_{-\infty}^{\infty} \exp(-y^2/2\sigma^2)dy$$

$$\therefore \quad I^2 = \int_{-\infty}^{\infty}\int_{-\infty}^{\infty} \exp[-(x^2 + y^2)/2\sigma^2]dxdy$$

Let $x = r\ \mathrm{Sin}\theta$, $y = r\ \mathrm{Cos}\theta$

$$\therefore \quad I^2 = \int_{0}^{\infty}\int_{0}^{2\pi} r \exp(-r^2/2\sigma^2)d\theta dr$$

$$I^2 = [-\sigma^2\exp(-r^2/2\sigma^2)]_{0}^{\infty} [\theta]_{0}^{2\pi}$$

$\therefore \quad I = -\sigma\sqrt{(2\pi)}$

Substituting for I in the equation for $\overline{x^2}$ gives

$$\overline{x^2} = \frac{1}{\sigma\sqrt{(2\pi)}}[0 + \sigma^3\sqrt{(2\pi)}] = \sigma^2$$

$$\therefore x_{rms} = \sigma \qquad (2.43)$$

From equations (2.41) & (2.43), for a normal distribution

$$x_{rms} = \sqrt{(\pi/2)}\,|x| \text{ for a random signal} \qquad (2.44)$$

The relationship between x, x_{rms} and $|x|$ for a sine wave is $x_{rms} = x/\sqrt{2}$ and $|x| = 2x/\pi$

$$\therefore x_{rms} = (\pi/2\sqrt{2})\,|x| \text{ for a sine wave.} \qquad (2.45)$$

Detecting circuits are designed to measure $|x|$ for a sine wave but by introducing the calibration factor $\pi/2\sqrt{2}$ the detector will read the rms value. If such a detector is used to measure a random signal then, as

$$x_{rms}(\text{random}) = (2/\sqrt{\pi})\, x_{rms}(\text{Sine}) \quad \text{and}$$

$$G_x(n) = \overline{x_B^2}/B = \pi|x|_B^2/2B$$

or $G_x(n) = 2\,\overline{x_B^2}/B\sqrt{\pi}$ if $\overline{x_B^2}$ is measured on a sine calibrated detector. (2.46)

<u>Cross power spectral density</u>: Given two stationary random signals x(t) and f(t) the cross power spectral density (CPSD) function is

$$G_{xf}(n) = C_{xf}(n) - jQ_{xf}(n) \tag{2.47}$$

where
$$C_{xf}(n) = \frac{1}{T\Delta n}\int_0^T x_{\Delta n}(n,t)\, f_{\Delta n}(n,t)dt \tag{2.48}$$

and
$$Q_{xf}(n) = \frac{1}{T\Delta n}\int_0^T [\![\overline{x_{\Delta n}(n,t)}]\!] f_{\Delta n}(n,t)dt \tag{2.49}$$

The symbol $[\![---]\!]$ denotes that x(t) is 90° out of phase with f(t). The real part of the CPSD is the co-spectrum and the imaginary part the quad-spectrum. Following the same general analysis as in the case of PSD, it can be shown that

$$C_{xf}(n) = \overline{x_B f_B}/B \tag{2.50}$$

and
$$Q_{xf}(n) = \overline{[\![\overline{x_B}]\!] f_B}/B \tag{2.51}$$

<u>Relationship between input force and system response</u>:
It can be shown (5) that the relationship between the random force acting on a system and the resulting response is related as follows:-

$$G_f(n) = |Z(n)|^2 G_x(n) \tag{2.52}$$

$$G_{xf}(n) = Z(n)G_x(n) \tag{2.53}$$

$$G_f(n) = Z(n)G_{fx}(n) \tag{2.54}$$

Expanding equation (2.53) gives

$$C_{xf}(n) - jQ_{xf}(n) = [Z_R(n) + jZ_I(n)]G_x(n)$$

Real part $\qquad C_{xf}(n) = Z_R(n)G_x(n)$

Imag. part $\qquad -Q_{xf}(n) = Z_I(n)G_x(n)$

To calculate both the real and imaginary components of the impedance a knowledge of the displacement PSD and the force-displacement CPSD is required. The impedance modulus can, however, be determined from the PSD of force and the PSD of displacement since from equation (2.52)

$$|Z(n)| = \sqrt{[G_f(n)/G_x(n)]} \tag{2.55}$$

Rate of analysis and statistical accuracy: When analysing random signals to obtain an estimate of the PSD, a statistical error will exist due to the finite bandwidth and averaging time of the analysis equipment. It can be shown (6) that this error is given by

$$e = \frac{1}{\sqrt{(BT)}} \quad \text{(providing } e \leqslant 0.2\text{)} \tag{2.56}$$

The error between the measured PSD and the true PSD will be $\pm$ e with a confidence factor of 67 per cent. If $e > 0.2$ the deviation becomes a Chi-squared distribution and this must be used instead of equation (2.56). The analysis equipment uses an RC averaging circuit and thus $T = 2RC$ where RC is the detector time constant, T_c.

$$\therefore \quad e = \frac{1}{\sqrt{(2BT_c)}} \quad \text{(providing } e \leqslant 0.2\text{)}$$

If the data for analysis is obtained from a tape loop and T_r is the time length of the record, then

$$e = \frac{1}{\sqrt{(BT_r)}} \quad \text{(providing } e \leqslant 0.2\text{)} \qquad (2.57)$$

It can also be shown (6) that

$$\text{Analysis rate} \leqslant \frac{B}{\frac{4}{B} + T} \qquad \text{and as } \frac{4}{B} \ll T$$

$$\text{Analysis rate} \leqslant \frac{B}{T} \qquad (2.58)$$

2.11 Effect of non-linearities.

In a linear system impedance is defined as the ratio of the applied force to the resulting response, i.e.

$$f = Zx \quad \text{or} \quad Z = f/x$$

where Z is complex and may be written $Z_R + jZ_I$.

In a non-linear system, e.g. $f = Ax^3$, a unit increase in force will not produce the same displacement, but will depend on the initial value of f. Under these circumstances impedance at any point along the force-displacement curve is defined as the local ratio of change in force to change in displacement, i.e. the gradient of the force-displacement curve, df/dx. This definition of impedance is consistent with that used in a linear system, since in a linear system, as $f = Ax$ then $df/dx = A$ and the impedance is constant at a particular frequency.

If a force is applied to a non-linear system, prediction of the response will be complicated by the fact that the system impedance is not constant. It will be shown that for a hydraulic servomechanism the impedance at a particular frequency can converiently be measured or calculated for various values of valve opening. Hence the impedance can be expressed as a function of displacement, in practice a polynomial containing even powers of x only is obtained since the function is even.

$$\therefore \text{ Let } Z = (a_0 + a_2x^2 + a_4x^4 + \text{-----} \; a_nx^n)$$

$$+ j(b_0 + b_2x^2 + b_4x^4 + \text{----} \; b_nx^n) \qquad (2.59)$$

where n, the order of the polynomial, is even.

$$\text{As} \quad Z = df/dx \quad \therefore f = \int Z \, dx$$

$$\therefore \quad f = [\, a_0x + a_2x^3/3 + a_4x^5/5 + \text{----} \; a_nx^{n+1}/(n+1)]$$

$$+j[b_0x + b_2x^3/3 + b_4x^5/5 + \text{----} \; b_nx^{n+1}/(n+1)]$$

$$(2.60)$$

If the system is excited by an ideal displacement generator then $x = x_p \text{Sin } \omega t, x^3 = x_p^3 \text{Sin}^3 \omega t$ etc.

Expanding the powers of Sin ωt

$$x_p^3 \text{Sin}^3 \omega t = x_p^3(-\text{ Sin}3\ \omega t + 3\text{Sin } \omega t)/4$$

$$x_p^5 \text{Sin}^5 \omega t = x_p^5(\text{Sin}5\ \omega t - 5\text{Sin } 3\omega t + 10\text{Sin } \omega t)/16$$

$$x_p^7 \text{Sin}^7 \omega t = x_p^7(-\text{ Sin}7\ \omega t + 7\text{Sin } 5\omega t - 21\text{Sin } 3\omega t + 35\text{Sin } \omega t)/64$$

etc.

Analysis equipment filters the force and displacement signals, rejecting all harmonics and passing the fundamental only.

Hence, $x_p^3 \text{Sin}^3 \omega t$ filters to $x_p^3 (3/4) \text{Sin } \omega t$

$x_p^5 \text{Sin}^5 \omega t$ filters to $x_p^5 (5/8) \text{Sin } \omega t$

$x_p^7 \text{Sin}^7 \omega t$ filters to $x_p^7 (35/64) \text{Sin } \omega t$

and, providing r is odd

$$x_p^r \text{Sin}^r \omega t \text{ filters to } \frac{r!}{[(r+1)/2]![(r-1)/2]!2^{r-1}} \text{Sin } \omega t$$

where the symbol ! denotes factorial.

$$\therefore f = [a_0 x_p + a_2 x_p^3/4 + a_4 x_p^5/8 --- \frac{n! a_n x_p^{n+1}}{[(n+2)/2]![n/2]!2^n}] \text{Sin } \omega t$$

$$+ j[b_0 x_p + b_2 x_p^3/4 + b_4 x_p^5/8 --- \frac{n! b_n x_p^{n+1}}{[(n+2)/2]![n/2]!2^n}] \text{Sin } \omega t$$

(2.61)

As n is even, the order of the polynomial n+1 is odd, thus the function f is odd also. Hence if $f = f_p \operatorname{Sin} \omega t$, f_p can be evaluated for a particular value of x_p.

Using the reversion of series technique (7) the force f, which, in equation (2.60) is expressed as a polynomial in x, can be reversed so that x is given by a power series in f. The coefficients of the power series are functions of a_0, a_2, a_4; b_0, b_2, b_4 etc., and have been calculated up to the 13th term in (7). If the system is excited by an ideal force generator, then x_p can be evaluated for a particular value of f_p from the reversed series using similar reasoning to that used in obtaining equation (2.61).

2.12 Experimental determination of impedance.

In a non-linear system the impedance is a function of both the excitation frequency and the displacement of the system from the equilibrium position, so in order to determine the impedance of a non-linear system, tests must be performed over a frequency range of interest and at various points along the non-linear force displacement curve. The frequency range chosen for this investigation, 5 - 70 c/s, was such as to include the range in which aerodynamic excitation of the control surfaces has been found to occur in practice. Two methods of measuring the servomechanism impedance will be used as follows:-

(a) Excitation of the servomechanism output end: It has been stated that the impedance is the sinusoidal force required to produce a unit sinusoidal displacement in the system. The servomechanism impedance of interest is that measured at the output end of the servomechanism, this being the 'input point' for the purpose of impedance measurement, whilst the servo valve input is the 'output point' and must be blocked. Because the 'input point' is at the servomechanism output end, large force excitation will be required to investigate the full non-linear range of the system.

(b) Excitation of the servomechanism valve input: An alternative method of obtaining the impedance of a servomechanism is to consider the servomechanism as a mechanical generator and determine the impedance by the application of equation (2.36). This method has the advantage that the input to the mechanical generator is the input to the servo valve, and only a small force is required to actuate the valve. The disadvantage of this method is that the analysis developed in Section 2.8 is based upon the assumption that the system is linear. In Chapter IV the limitations and inaccuracies of this assumption are described more fully.

It has been stated that the impedance of a non-linear system is the local ratio of the change in force to the resulting change in displacement at the point on the force displacement curve under consideration, i.e. the gradient of the curve, df/dx. Therefore, to determine the impedance of the system under any particular set of conditions it is necessary to excite the system with infinitely small oscillatory forces or displacements. In practice, however, there is a minimum size of oscillation which can be controlled or measured. The concept of exciting the system using small oscillations has an application to both the experimental and theoretical determination of the impedance of a non-linear system. The method, that of small perturbations, is used to analyse the servo system and is described in Chapter IV.

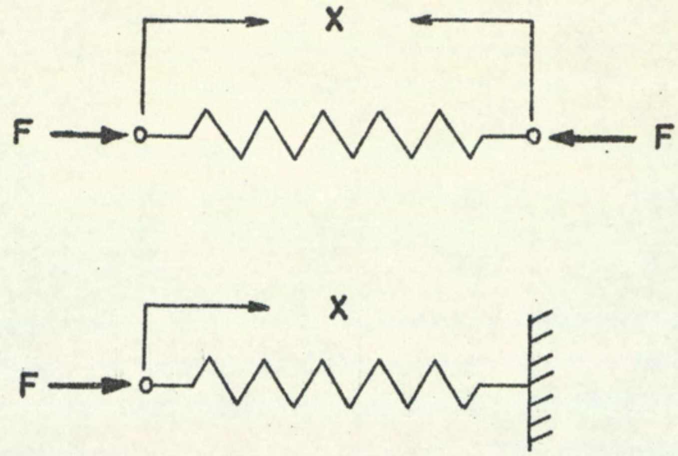

(A) FOR A SPRING (OR DAMPER) X IS MEASURED ACROSS THE ELEMENT OR ALTERNATIVELY WITH ONE END BLOCKED

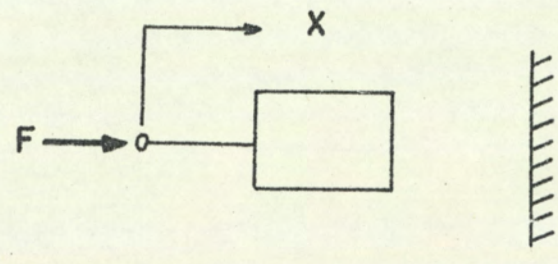

(B) FOR A MASS X IS MEASURED RELATIVE TO AN INERTIAL REFERENCE

PASSIVE MECHANICAL ELEMENTS.
MEASUREMENT OF DISPLACEMENT

FIG 2.1

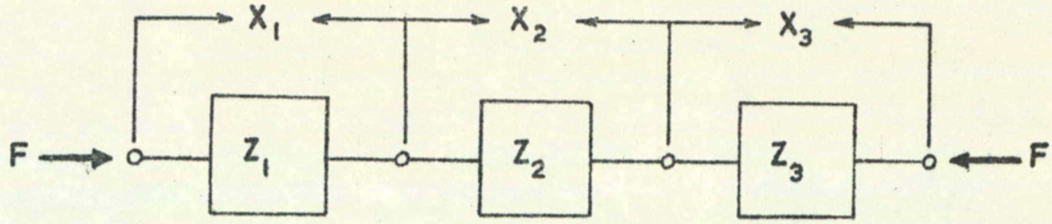

(A) IMPEDANCE ELEMENTS IN SERIES

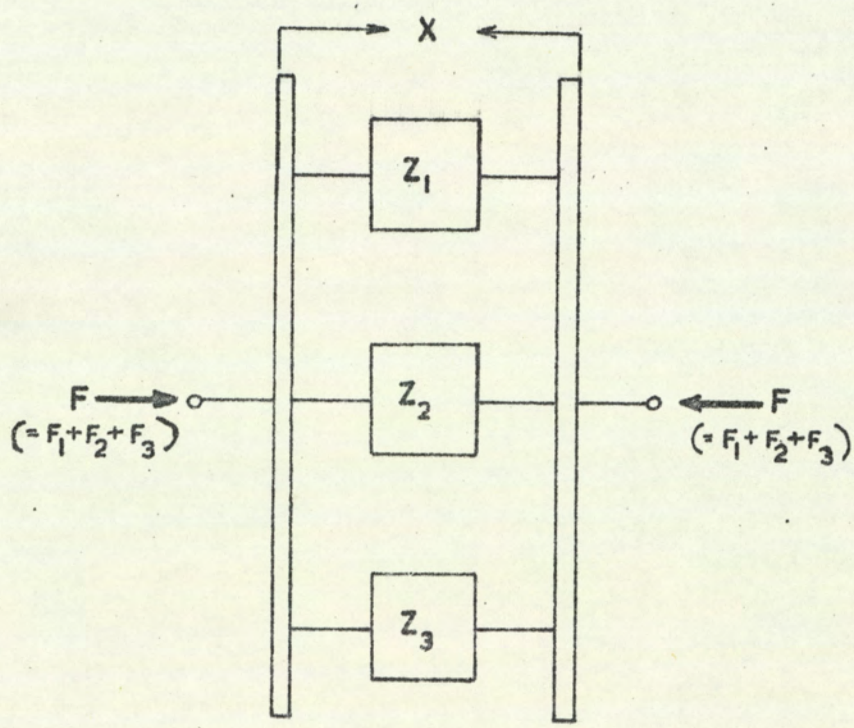

(B) IMPEDANCE ELEMENTS IN PARALLEL

IMPEDANCE ELEMENTS CONNECTED IN SERIES AND IN PARALLEL

FIG 2.2

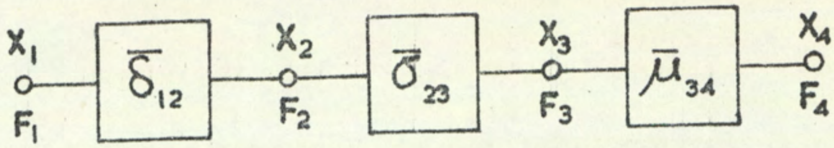

(A) FOUR POLE ELEMENTS IN SERIES

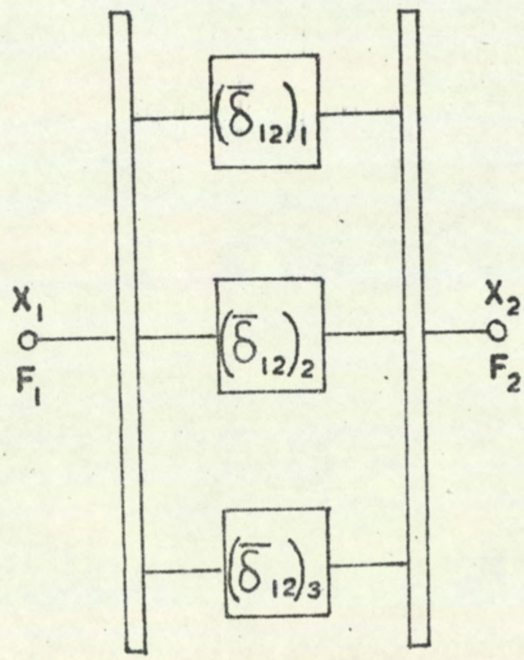

(B) FOUR POLE ELEMENTS IN PARALLEL

FOUR POLE ELEMENTS CONNECTED IN SERIES AND IN PARALLEL

FIG 2.3

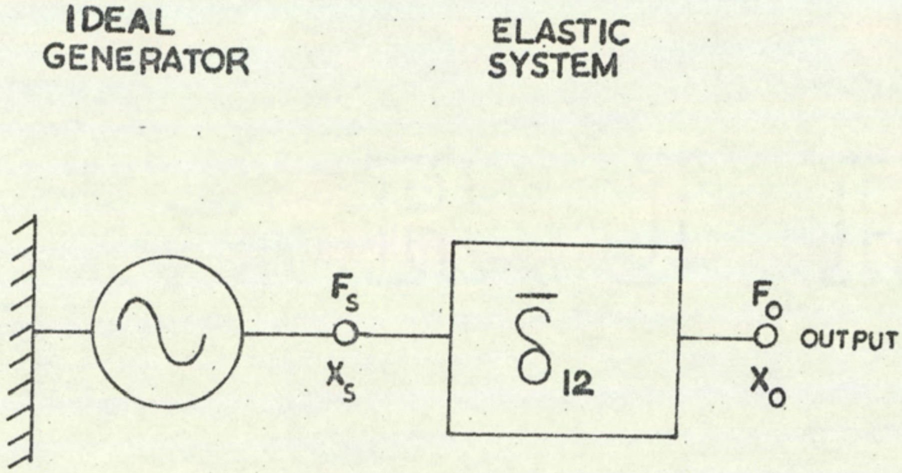

MECHANICAL GENERATOR

FIG 2.4

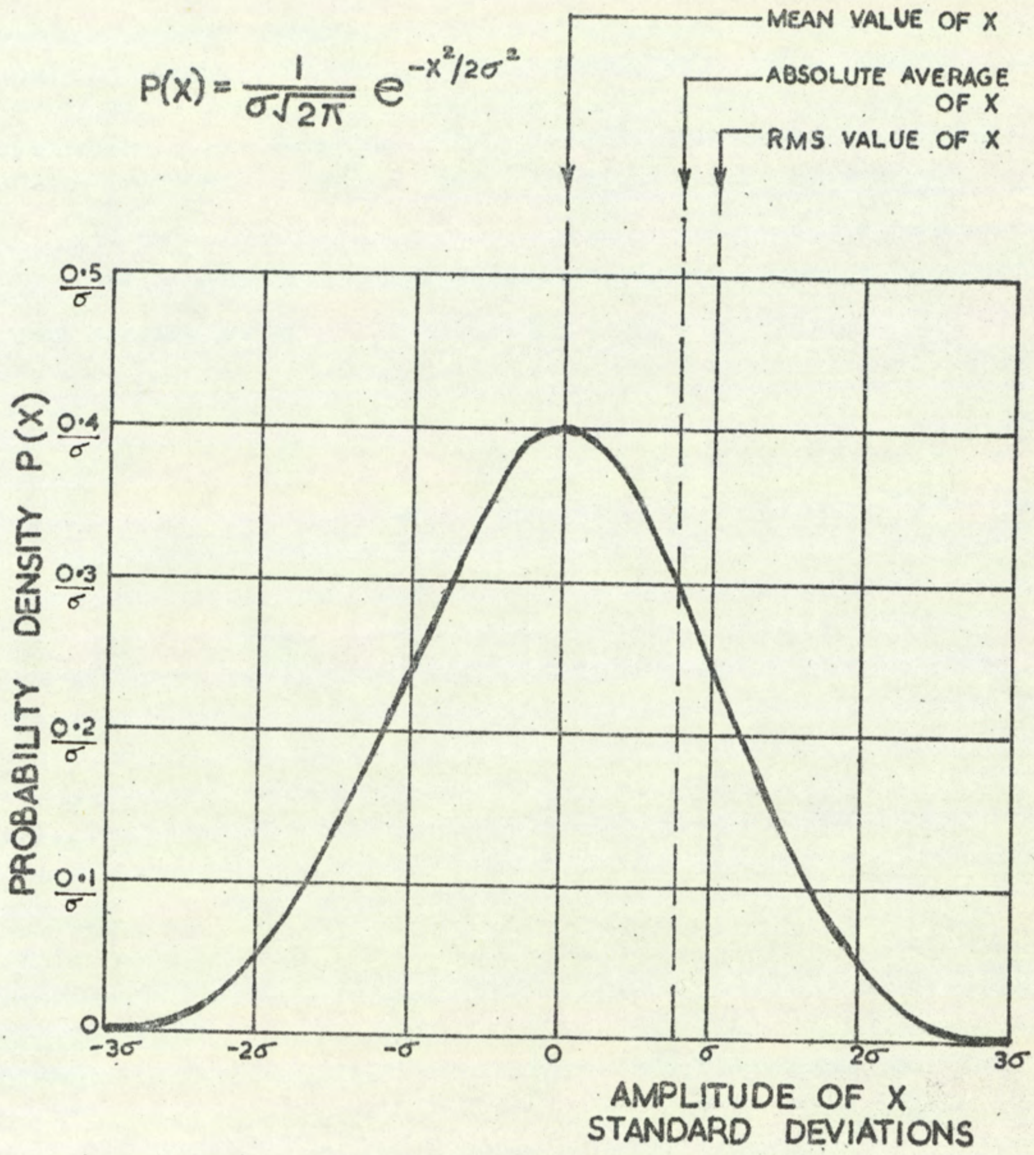

GAUSSIAN OR NORMAL DENSITY CURVE

FIG 2.5

CHAPTER III

The Test Rig, Instrumentation and Analysis Equipment.

The design details of the test rig and the associated instrumentation, based on the requirements outlined in the previous chapter, are described together with the modifications made to complete the various parts of the research programme. A description of the principles of operation of the analysis system is given.

3.1 Test rig for the measurement of the impedance of a servomechanism by excitation of its output end.

A versatile test rig was designed in order that the complete experimental programme could be performed in one basic rig. The rig, as arranged for the measurement of the impedance of the servomechanism in a rigid environment, is described in this section and the modifications to the rig necessary for the completion of other aspects of the experimental programme are described in Sections 3.4 & 3.5.

To eliminate any structural flexibilities giving rise to structural feedback and other undesirable effects, the test rig was made extremely rigid. The general arrangement is shown in Fig. 3.1, the vertical position of the servomechanism being chosen purely in order to conserve floor space, the vibrator and servomechanism functioning equally well in the horizontal or vertical plane. The main frame was constructed of two 2 inch thick mild steel plates, at the top and bottom of which anchorage blocks were fixed by means of fitted bolts passing through the blocks and plates. Additional fitted bolts were passed through the sides of the main frames, the frames being held apart by spacer tubes. The servo-unit under test was fixed to the top anchorage block (the centre section of which could be lifted out to facilitate the easy removal of the servo) by means of a latch which inserted into a recess in the piston rod, the salient points are shown in Fig. 3.2.

The vibrator was connected to the servomechanism by means of a rigid link and to avoid the possibility of the vibrator supplying a sideways component of force to the servomechanism a theodolite was used to check that the vibrator, connecting link and servomechanism were in a straight line and in the vertical plane. The centre of one of the latch support pins was taken as the reference point and the centre line of the servo, connecting link and vibrator were positioned vertically below this point. Since all large forces were reacted within the frame of the test rig, it was not necessary to secure the rig to the floor. The rig stood in an oil drip tray.

The initial arrangement of the servomechanism under test is shown in Fig. 3.3a. The valve was connected to a rigid cantilever but on completion of Test Series I the valve was reversed and connected to a cross bar which was clamped rigidly to the servo piston rod. This arrangement had the advantage that the earthing points of the valve and piston were brought together so that any movement of the latch holding the servomechanism to the top of the anchorage was of no consequence. All further test series' were performed with the valve fixed in this manner as shown in Fig. 3.3b.

A hydraulic vibrator was used to excite the system for the following reasons:-

(a) Force levels of up to 5000 lbf were readily available.

(b) Suitability for work in the frequency range required.

(c) The ease with which a controlled static tensile or compressive force could be applied using force feedback control. Alternatively, a controlled positive or negative movement of the output end of the servomechanism could be obtained using displacement feedback control.

(d) The ease with which the magnitude of the constant force or displacement oscillation could be controlled by force or displacement feedback.

(e) The relatively small physical bulk of the vibrator made it suitable for installation in the test rig.

The vibrator consisted of an equal displacement jack controlled by an electro-hydraulic flow control servo valve. The valve passed a flow which was proportional to the signal input and hence the actuator velocity was proportional to the signal input. The vibrator was powered by a hydraulic pump unit incorporating filters, cooler, accumulator and controls.

3.2 Instrumentation and associated electronics.

Measurement of force: The force which the vibrator applied to the system was measured by means of a link load cell, as shown in Fig. 3.4. The cell, consisting of four unbonded strain gauges forming a Wheatstone Bridge, was energised by a DC supply. Initially DC power packs of various types were used for this purpose but when the vibrator was working under force feedback control, instability was experienced caused by small ripples on the DC level being fed back and amplified. The problem was overcome by using dry batteries to energise the load cell. The signal from the load cell was amplified by a DC pre amplifier and filtered ; the maximum frequency of excitation of the system was 70 c/s and high frequency noise was filtered from the system by a simple RC filter. The force signal could be connected to the feedback circuit and/or the analysis equipment. For analysis purposes a high sensitivity signal was required but since instability could occur if the feedback signal sensitivity was excessively high, the feedback signal was taken from the centre tap of a potential divider, thus reducing its sensitivity.

Measurement of displacement: The displacement of the jack body relative to the jack piston rod was measured by a Linear Variable Differential Transformer, Fig. 3.4 shows the instrumentation block diagram.

This transducer, in which a core moves relative to two sets of transformer windings, thus varying the degree of coupling between the windings, has no physical contact between the moving and fixed parts. The resolution of the transducers was dependent only on the quality of the associated electronics and had no inherent limit as would be the case with a potentiometric transducer. One winding of the transducer was energised by an oscillator and the signal induced into the other winding was demodulated to give an output proportional to displacement.

The signal, which was filtered to remove any high frequency noise by a simple RC network, could be connected to the analysis equipment and/or the feedback circuit via a potential divider.

3.3 Control of the hydraulic vibrator.

The electro-hydraulic Moog valve in the vibrator was driven by a servodrive amplifier controlled by a signal generator together with a feedback signal as shown in Fig. 3.4. The feedback signal was proportional to either force into, or displacement of the system under test. The gain (i.e. the alternating signal output) and the bias (i.e. the steady signal output) of the amplifier were variable, so that a steady load or displacement, together with an alternating load or displacement, could be applied by the vibrator.

3.4 Modification to test rig and instrumentation for measurement of impedance by excitation of the valve input.

To measure the impedance of the servomechanism by exciting the valve input as proposed in Section 2.12b, the test rig was modified as shown in Fig. 3.5. A cross member (9 in. deep X 3 in. thick) was securely fixed between the main frames of the rig using the existing fitted bolts and located by spacers. For the blocked output tests the servomechanism output end was rigidly connected to this cross member via a load cell and for the free output tests the load cell was removed.

An electric motor, which was mounted on top of the main frame, drove a lay shaft by a chain drive. At one end of the lay shaft was fixed an eccentric, the throw of which could be adjusted (see Fig. 3.6), which was connected to the jack valve input by means of a pair of long rods passing through the upper anchorage block. Since the connecting rods were long compared with the eccentricity, the valve was excited sinusoidally.

The speed of the motor was varied by a controller, the controller itself being driven so that the motor spped could be slowly increased over the frequency range of interest. A tachogenerator, which was coupled to the lay shaft, gave a DC output proportional to the lay shaft speed, i.e. excitation frequency. This provided a reference signal for programming the analysis system to keep it in synchronous with the excitation, see Section 3.7. The instrumentation block diagram is shown in Fig. 3.7. Displacement transducers were arranged to measure the valve input displacement and the output end displacement during the free output tests.

3.5 Modifications to test rig and instrumentation for measurement of the impedance of a system consisting of a servomechanism in a flexible environment.

The test rig and instrumentation were modified in the following manner to investigate the effect on the system impedance of the following flexibilities.

Output end flexibility: The modified test rig is shown in Fig. 3.8, the rigid link connecting the load cell and servo of the original arrangement having been replaced by a beam type spring. This particular design of spring was chosen because in moving the end shackles along the beam the stiffness of the spring could be varied. An inductive type of transducer was fitted into the base of the vibrator in order that the displacement of the spring servo system could be measured in addition to the measurement of the displacement of the servomechanism alone, (Fig. 3.9).

Anchorage flexibility: To investigate the effect of anchorage flexibility on the system impedance, the test rig was modified as shown in Fig. 3.10. The servomechanism was connected directly to the load cell and the piston rod was connected to earth via the beam spring. The instrumentation is shown in Fig. 3.11, the displacement transducers being arranged to measure the system and servo deflexion.

Valve input flexibility: For this investigation the valve, instead of being fixed, was connected to the rigid structure by means of a coil spring, as shown in Fig. 3.12. The instrumentation is shown in Fig.3.13.

3.6 Impedance analysis using a transfer function analyser.

This equipment was primarily designed to measure transfer functions. The system consisted of three units; a decade oscillator, a reference resolver and a resolved components indicator, as shown in Fig. 3.14. The function of the resolved components indicator was to compare the alternating component of the signal to be measured with the four phase reference signal generated by the oscillator so that the test signal could be measured in amplitude and phase relative to the oscillator reference signal. The signal to be measured contained harmonic distortion and was filtered by using thermocouple wattmeters. The filtering was achieved by connecting the reference signal to one arm of the thermocouple bridge and the inphase or quadrature component of the test signal to the other arm; it can be shown theoretically that the wattmeter will respond to the fundamental frequency of the input signal only. In practice a high degree of harmonic rejection is achieved, better than 40 db for related and 60 db for unrelated harmonics. The complex result was displayed by the wattmeters in cartesian form but using the reference resolver this complex result could be converted to the polar form, the function of the reference resolver being to'rotate' the four phase reference signal by adding the same angle to each phase.

This form of presentation was used during the experimental programme in order to facilitate the easy division of the complex load by the complex displacement. The oscillator also provided the input signal to the servo drive amplifier in order to excite the system under test. Since the force and displacement signals could not be measured simultaneously and the phase of each signal could only be measured relative to the oscillator reference signal, measurement of impedance by using this type of analysis equipment was a relatively slow process.

3.7 Impedance analysis using automatic mechanical impedance analyser.

Due to the limitations of the transfer function analyser when used for impedance measurements, i.e. slow acquisition of data and the necessity to perform calculations upon this data to obtain impedance, an automatic system for measuring impedance was obtained. The system chosen, a block diagram of which is shown in

Fig. 3.15, was built around the concept of tracking filters, that is, narrow band filters, the centre frequency of which was tuned automatically to the frequency of excitation of the system under test. The filters used had bandwidths of five cycles although plug-in filters as narrow as 1.5 cycles were available. The shape of the filter is shown in Fig. 3.16, the filter having a shape factor of four. The rejection of the first harmonic frequency using one of these filters is shown in Fig. 3.17. At 5 c/s centre frequency a rejection of 22 db was obtained, the rejection improving to better than 60 db at a centre frequency of 10 c/s and above.

The force and displacement signals were connected to a pair of logarithmic voltmeter converters and a pair of tracking filters (dynamic analysers) functioned within the servo loops of the logarithmic converters. This arrangement had the advantages that the dynamic analysers operated on a signal which was relatively constant in amplitude and the logarithmic converters operated on a clean sinusoidal signal thus giving DC signals proportional to the filtered input signals. The dynamic analysers developed constant frequency (100 kc/s), constant amplitude phase coherent signals which were connected to the phase meter. The phase meter operated very accurately at this one particular frequency and gave a DC output proportional to the phase difference between the input signals.

The outputs of the logarithmic converters, being DC proportional to the logarithm of their inputs, were connected to the master control unit. The function of the master control unit was to perform any differentation or integration required, depending upon the form of the input signals and to give a DC output proportional to the difference between the two logarithmic input signals. This ratio was the system impedance, transmissibility or mobility depending upon the input signals. A sweep oscillator produced an excitation signal to drive the servo drive amplifier, the oscillator being connected to the servo drive amplifier via an amplitude servo monitor. The amplitude servo monitor continually varied the amplitude of the input to the servo drive amplifier in order to maintain the force or displacement signal level constant by comparing a feedback with the output from the sweep oscillator; the feedback signal contained the fundamental frequency only, having been first filtered by a dynamic analyser. The oscillator also provided a sinusoidal reference signal for the three dynamic analysers and a DC signal proportional to the logarithm of the excitation frequency for the master control unit and the Y axis of the XY plotter. The DC outputs from the master control unit and the phase meter were connected to the X axis of the XY plotter via a sampling unit. The unit sampled each signal and connected it in turn to the plotter for a period of about 3 seconds. The oscillator could be programmed externally by a DC signal proportional to frequency.

3.8 Analysis of random signals.

The analysis system is shown in Fig. 3.18 in the form of a block diagram. A random signal generator, having the facility to generate either a wide band of white noise or white noise of specified bandwidth and centre frequency, was used to drive the servo drive amplifier and excite the system. Although the input to the servo drive amplifier was a pure white noise up to a frequency of 20 kc/s, due to the attenuation of frequencies much above 100 c/s the system was not excited by a pure white noise. The force and displacement signals from the transducers were recorded on an FM tape recorder and to analyse the recorded signals the signals were replayed on to an endless tape loop. The recorder and loop deck were not compatable and thus it was necessary to demodulate the FM recordings and then re-record onto the loop deck at a different carrier frequency. The signals were then played continuously from the loop deck and after demodulation connected to a narrow band analyser. The bandwidth, sweep rate and averaging time constant of the analyser could be adjusted independently in order that optimum analysis conditions could be achieved. To analyse random signals narrow band analysis with slow sweep rates and long averaging time was required, as shown in Section 2.10. The output from the analyser was connected to one axis of an XY plotter. The analyser also gave a DC signal output proportional to the instantaneous frequency of the analyser. This signal was connected to the other axis of the XY plotter in order that a plot of a signal against frequency could be obtained.

3.9 Harmonic analysis.

A similar system to that described in the previous section was used for the harmonic analysis of the signals. The system under test was excited by an oscillator and the output signals recorded and transfered to the loop recorder. The signals were analysed by the narrow band analyser and the harmonic analysis was plotted on an XY plotter. Because the signals to be analysed were periodic the analysis sweep rate was far more rapid than was the case when analysing random signals.

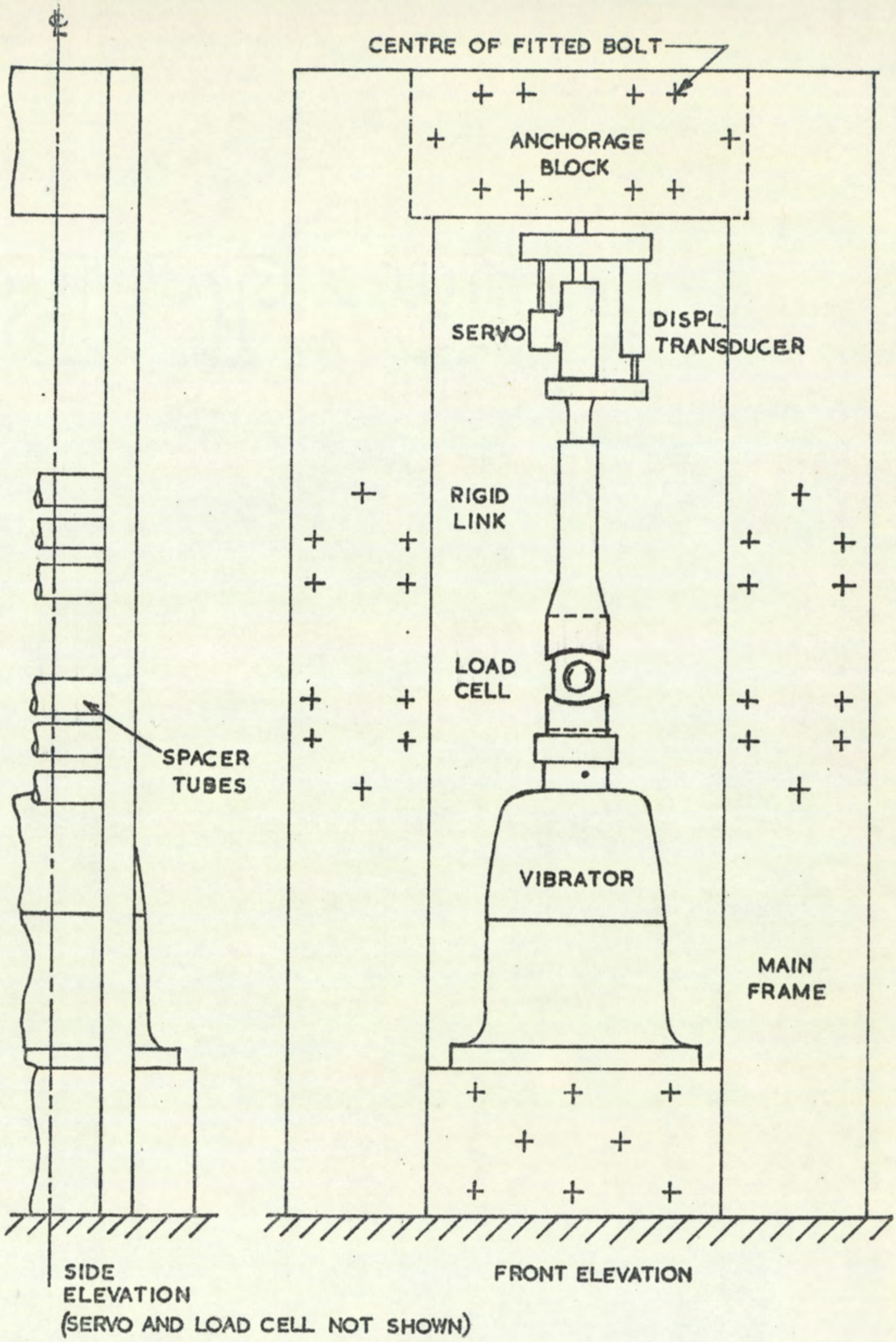

GENERAL ARRANGEMENT OF TEST RIG.
SERVOMECHANISM IN A RIGID ENVIRONMENT

FIG 3.1

METHOD OF CONNECTING JACK PISTON TO TEST RIG

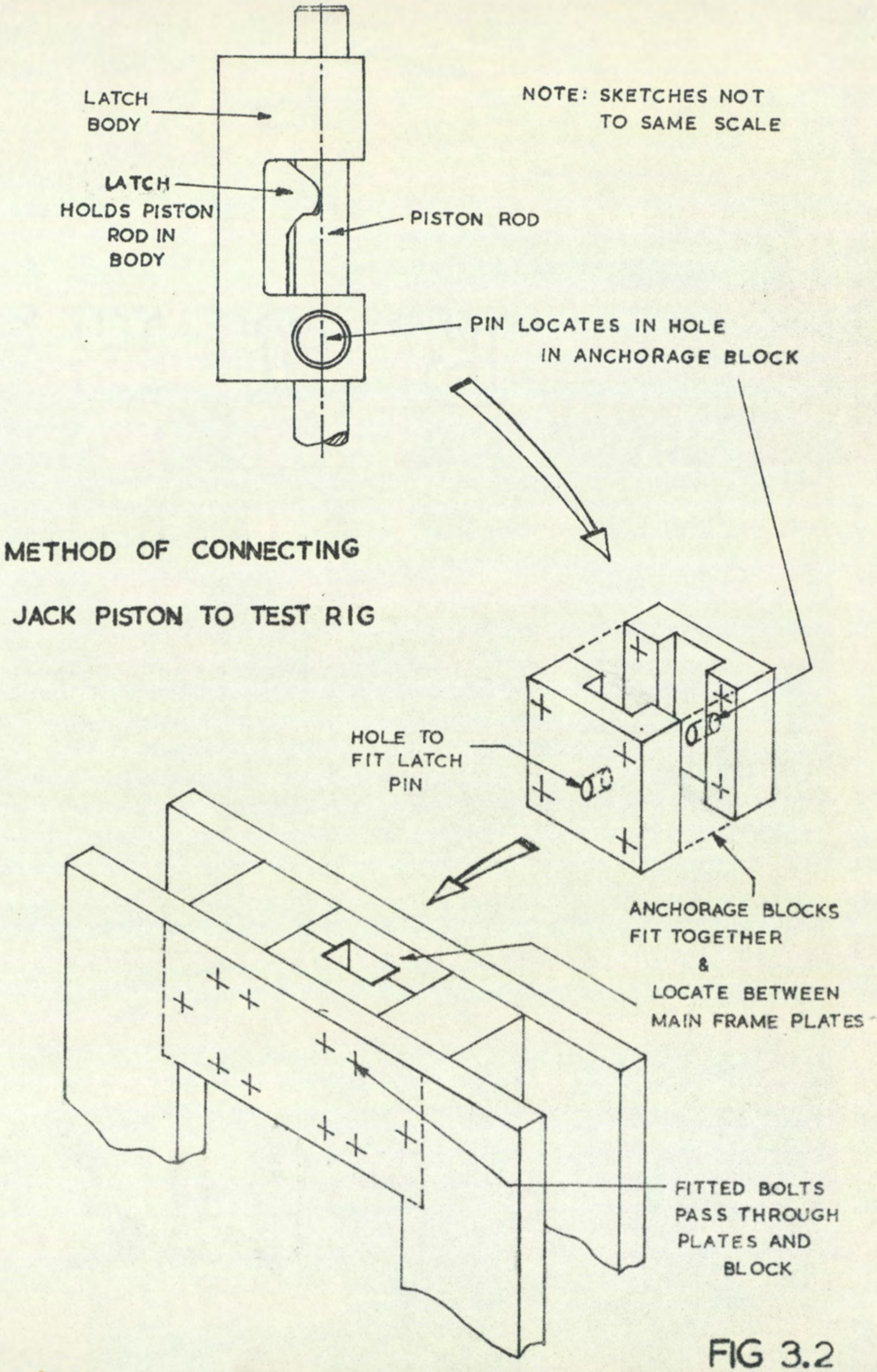

FIG 3.2

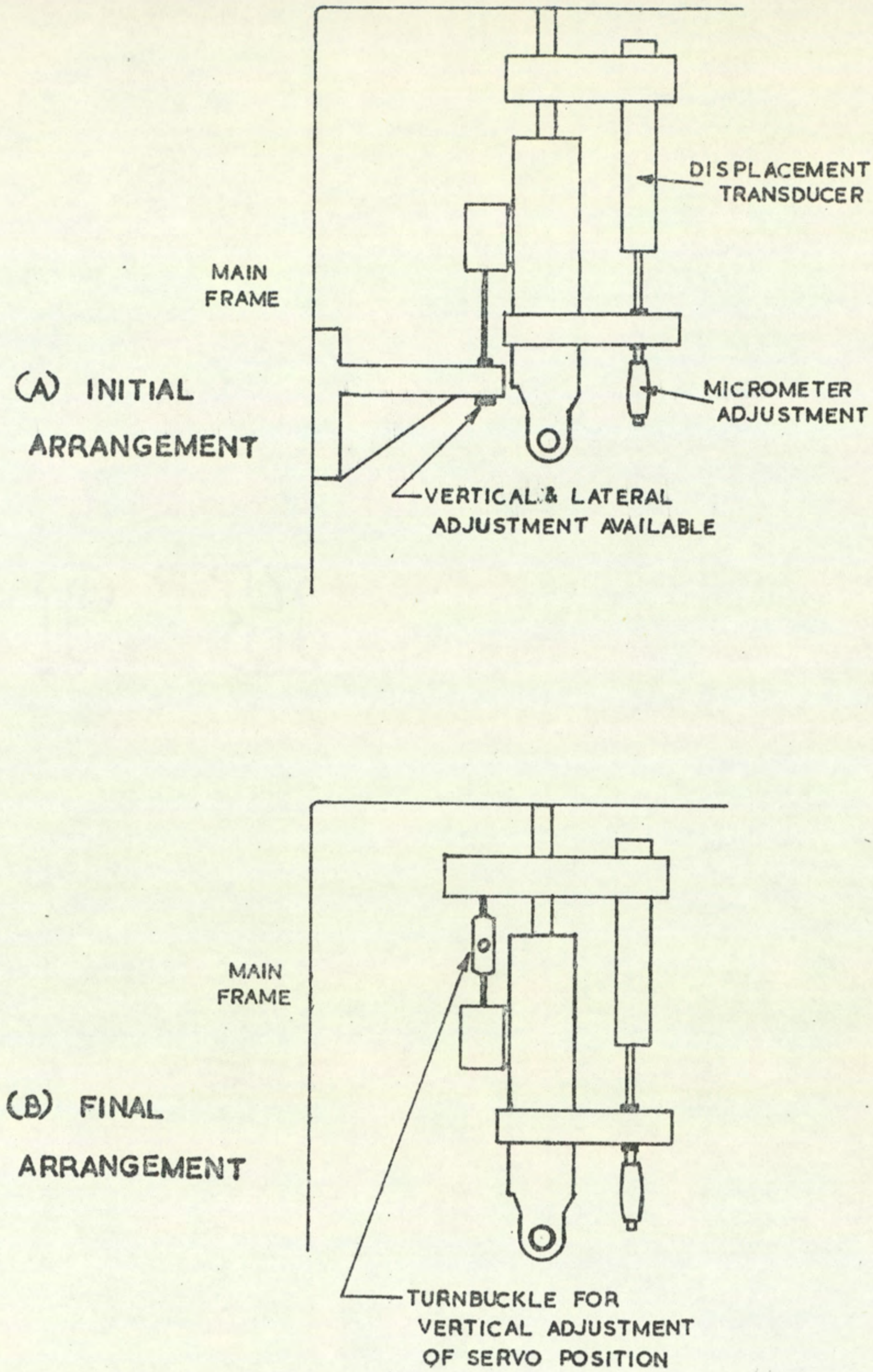

METHOD OF LOCKING VALVE INPUT TO TEST RIG

FIG 3.3

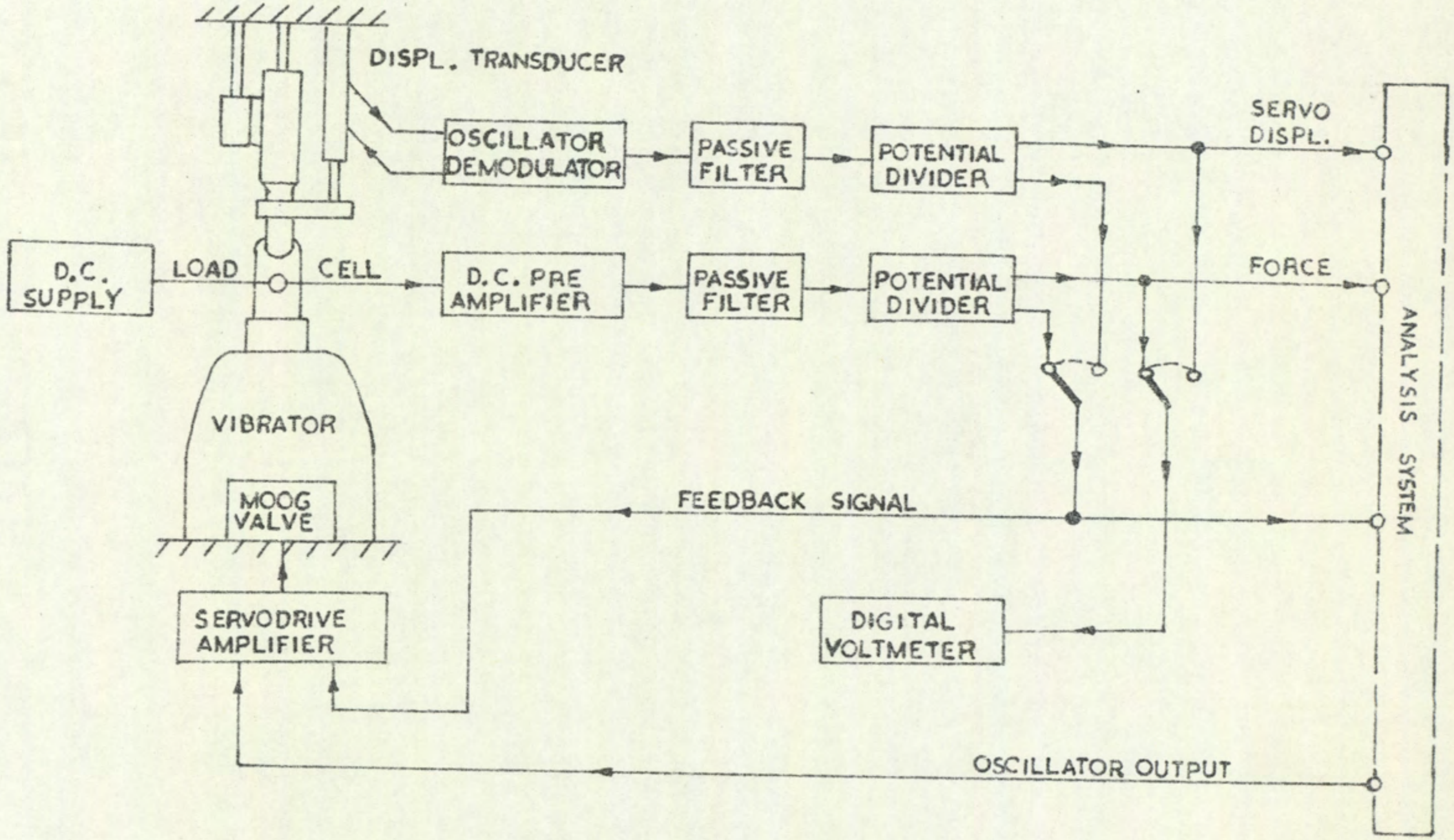

INSTRUMENTATION.
SERVOMECHANISM IN A RIGID ENVIRONMENT

FIG 3.4

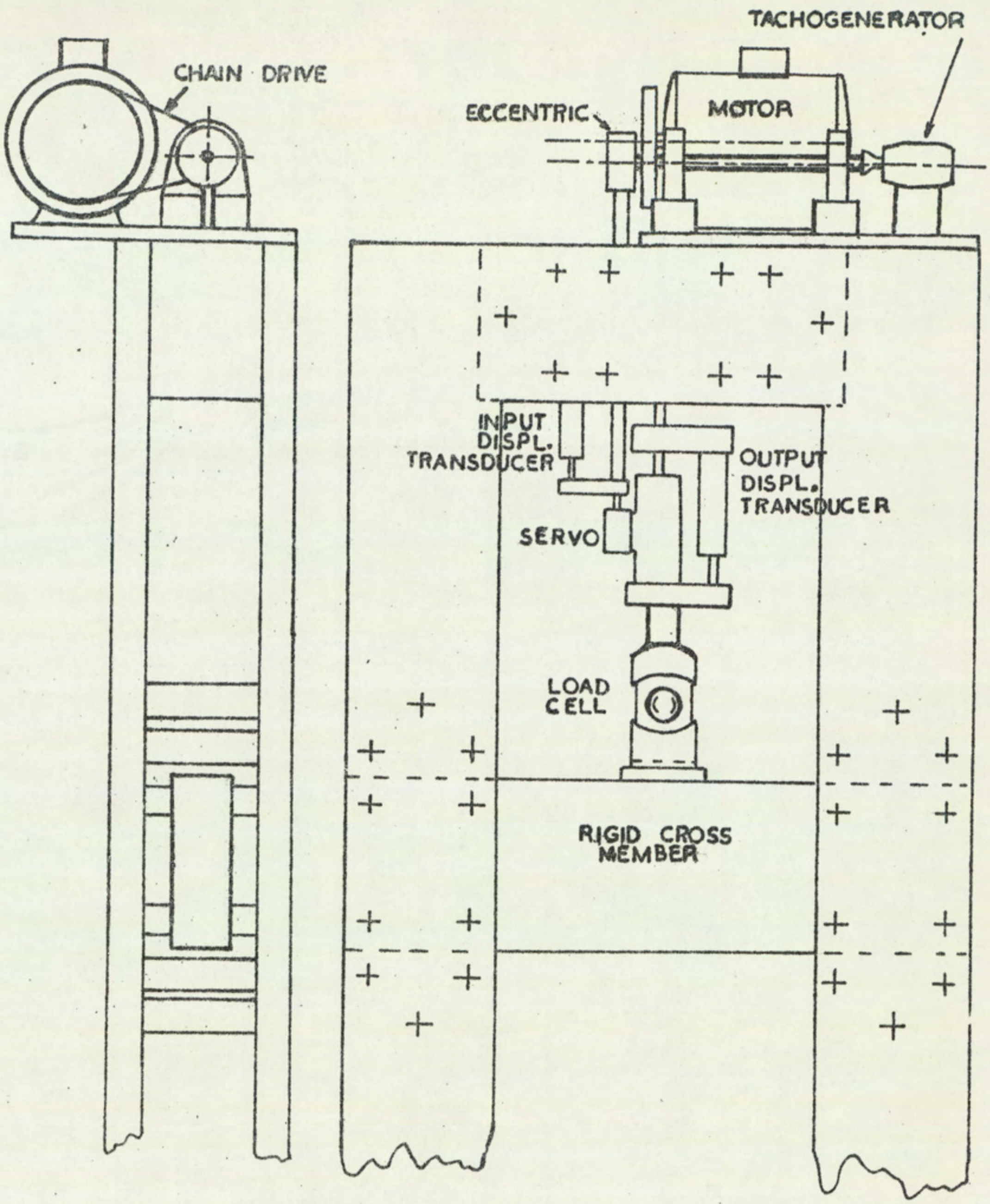

GENERAL ARRANGEMENT OF TEST RIG.
EXCITATION OF THE SERVOMECHANISM
VALVE INPUT

FIG 3.5

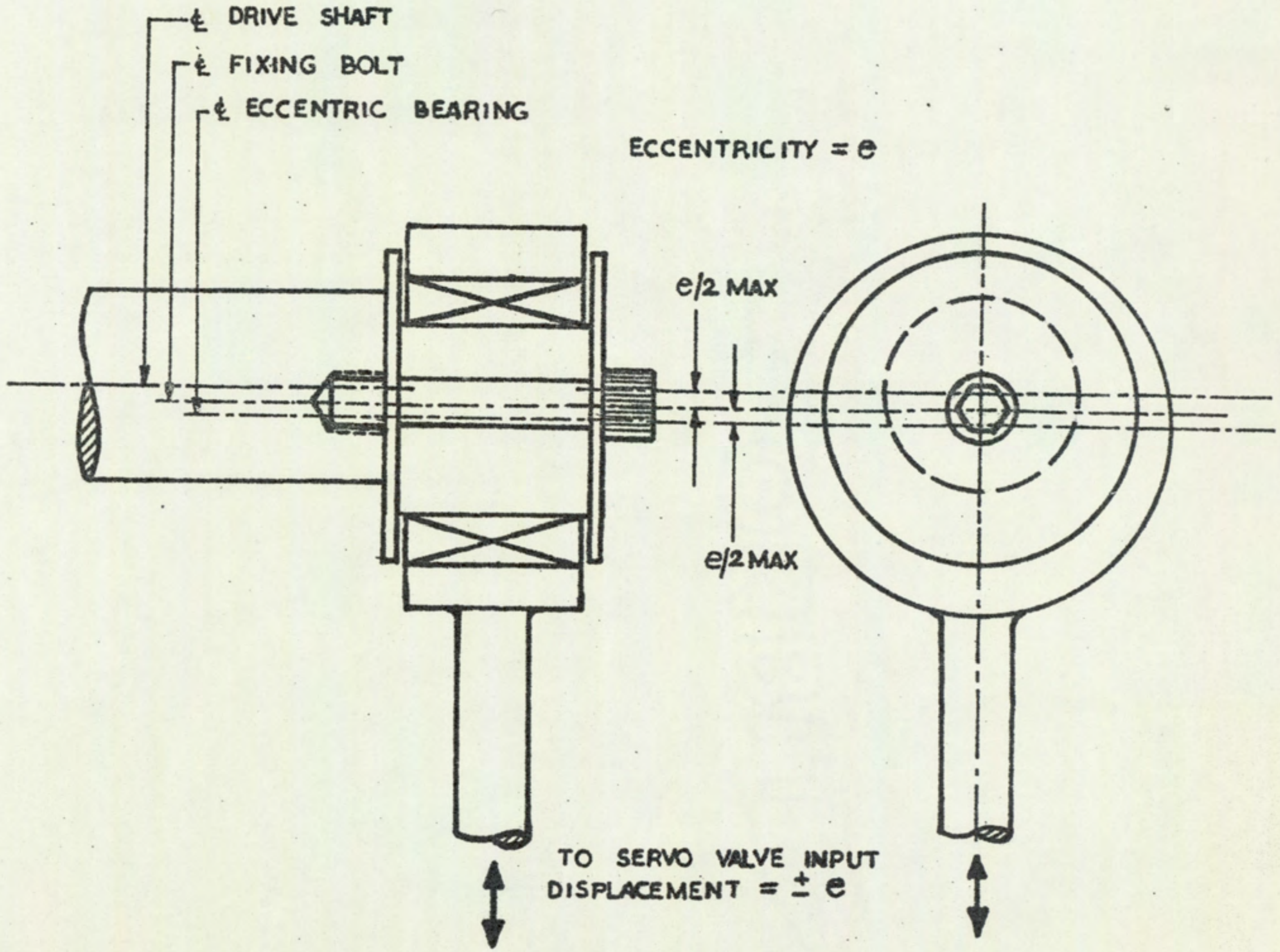

GENERAL ARRANGEMENT OF ADJUSTABLE ECCENTRIC

FIG 3.6

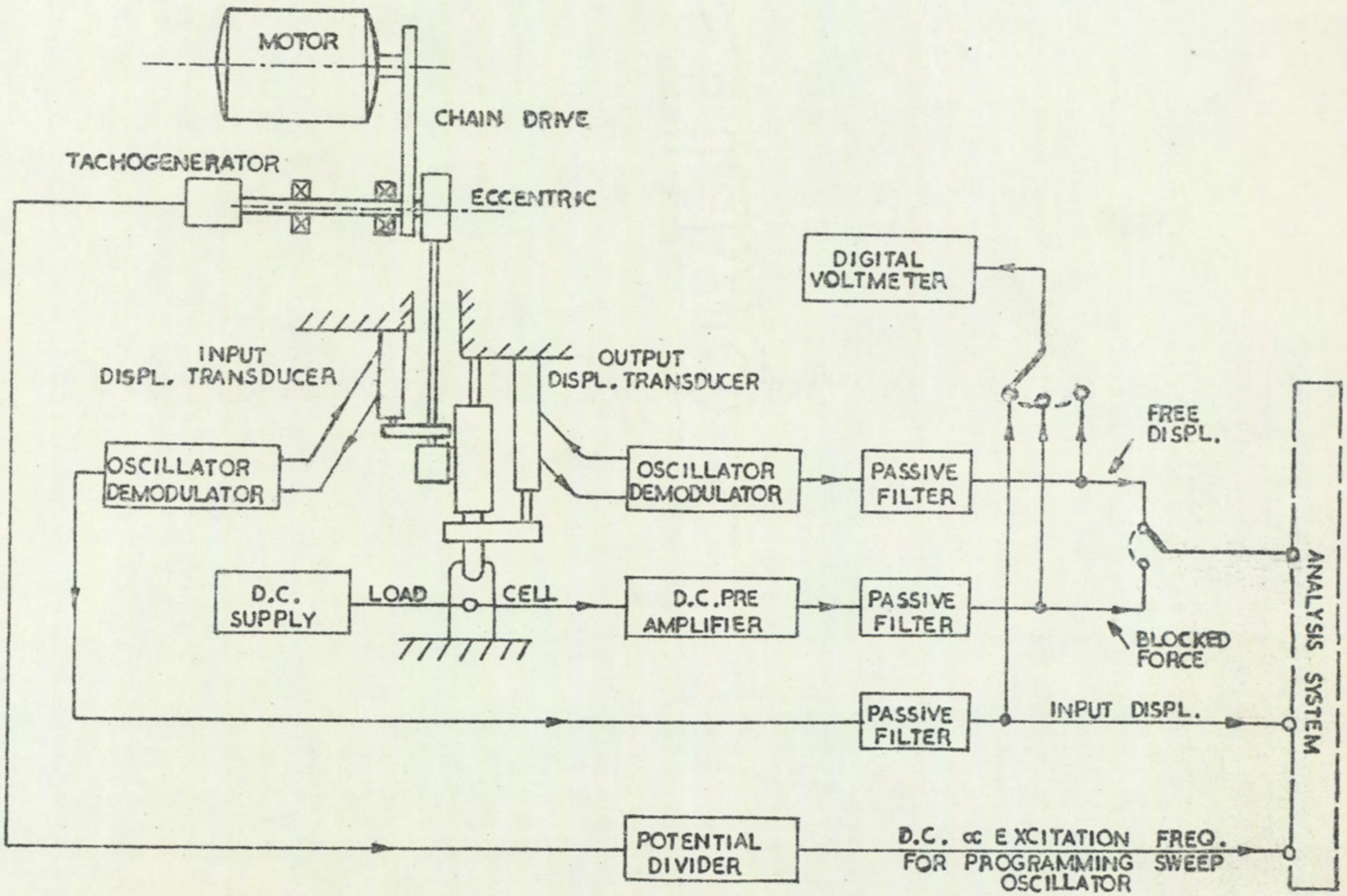

INSTRUMENTATION.

EXCITATION OF THE SERVOMECHANISM VALVE INPUT

FIG 3.7

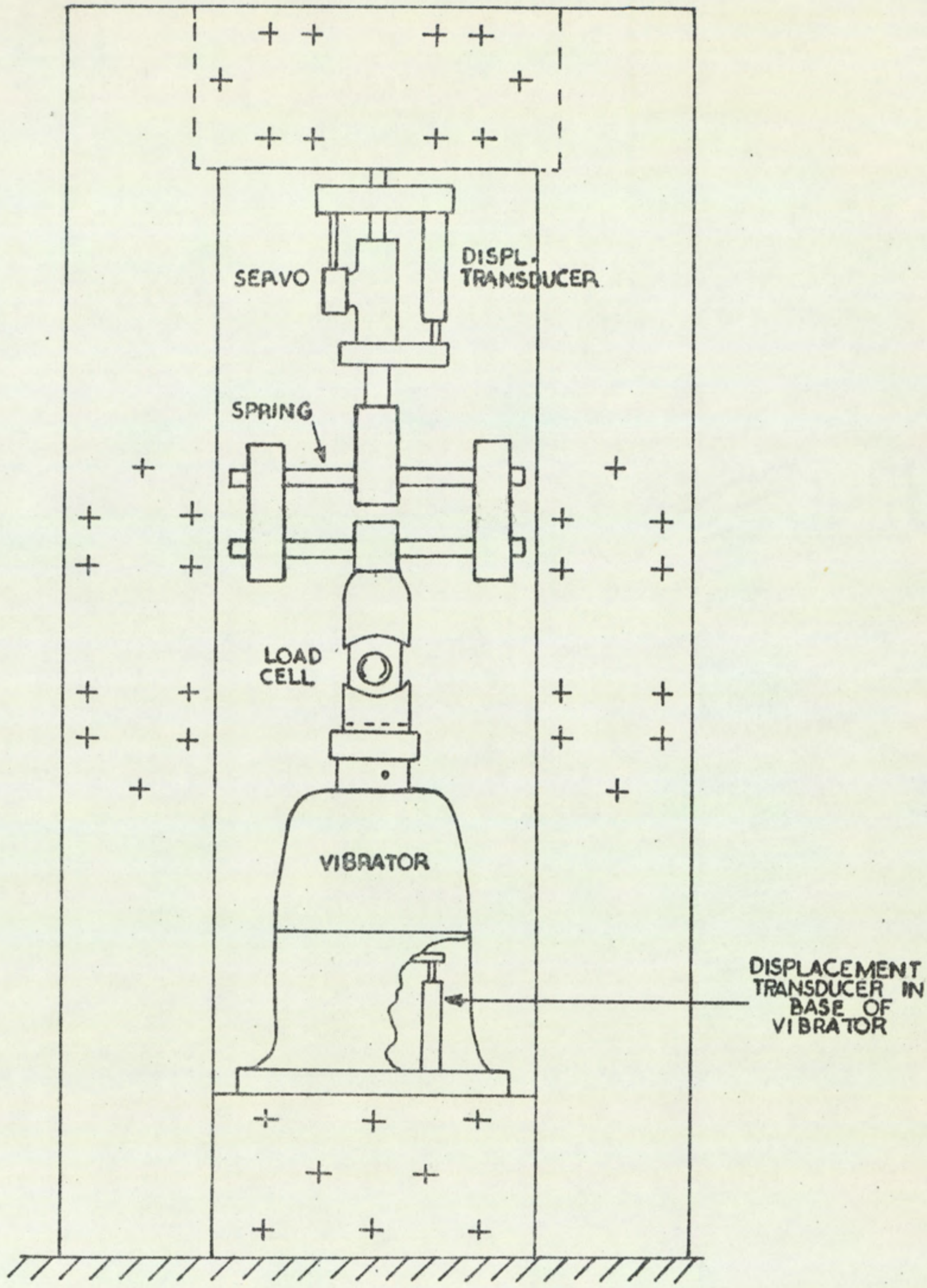

GENERAL ARRANGEMENT OF TEST RIG.
SERVOMECHANISM WITH A FLEXIBILITY
CONNECTED IN SERIES AT ITS OUTPUT END

FIG 3.8

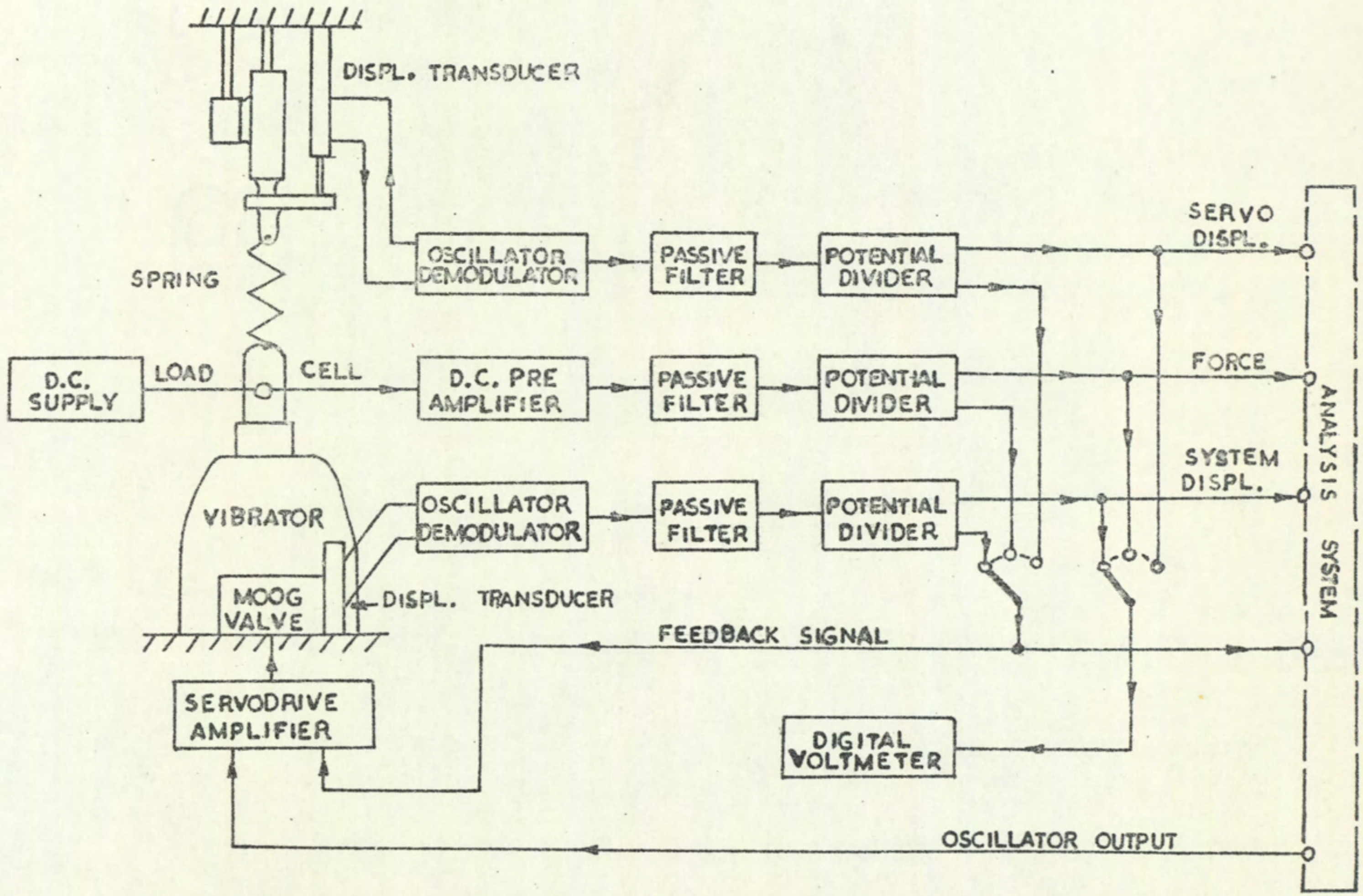

INSTRUMENTATION.
SERVOMECHANISM WITH A FLEXIBILITY
CONNECTED IN SERIES AT ITS OUTPUT END

FIG 3.9

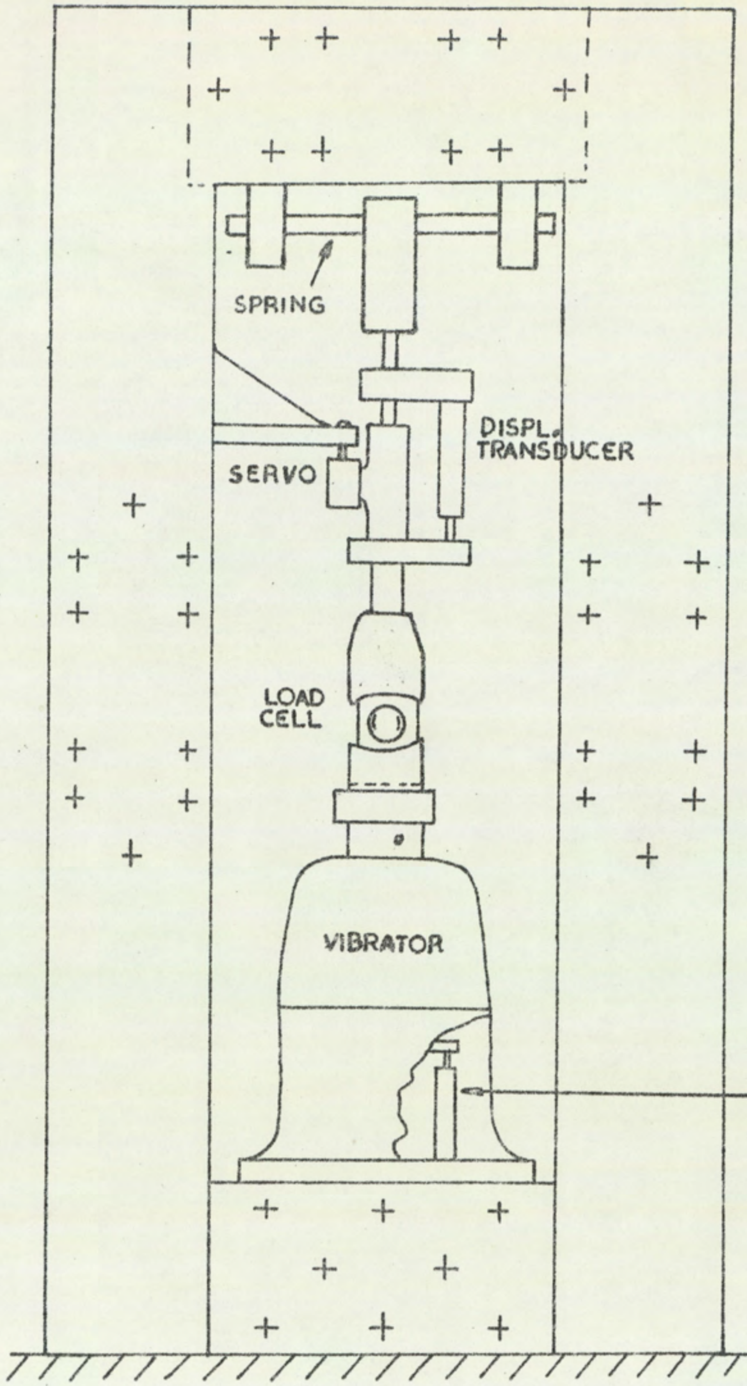

GENERAL ARRANGEMENT OF TEST RIG.
SERVOMECHANISM WITH ITS ANCHORAGE
CONNECTED TO A FLEXIBILITY

FIG 3.10

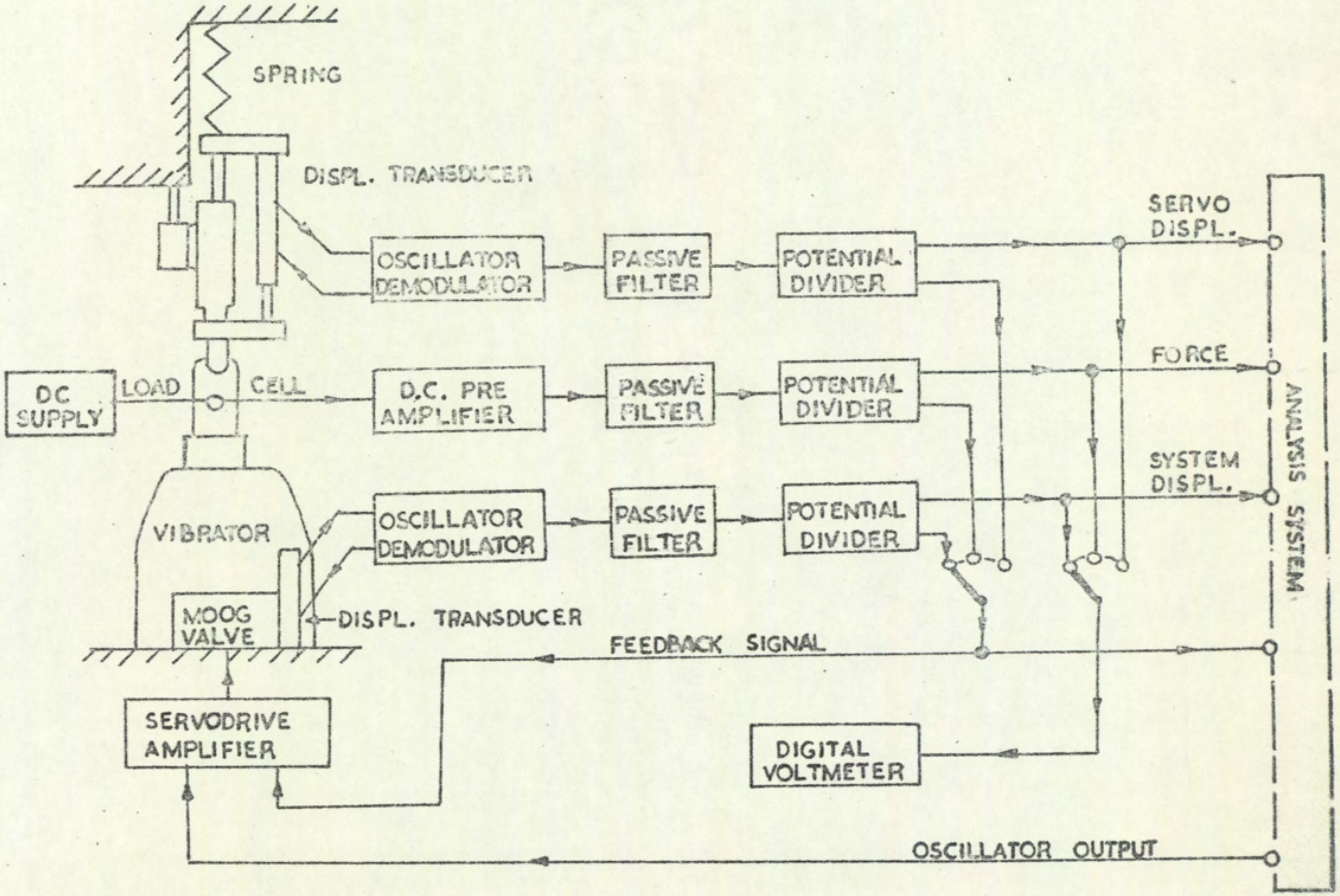

INSTRUMENTATION.
SERVOMECHANISM WITH ITS ANCHORAGE
CONNECTED TO A FLEXIBILITY

FIG 3.11

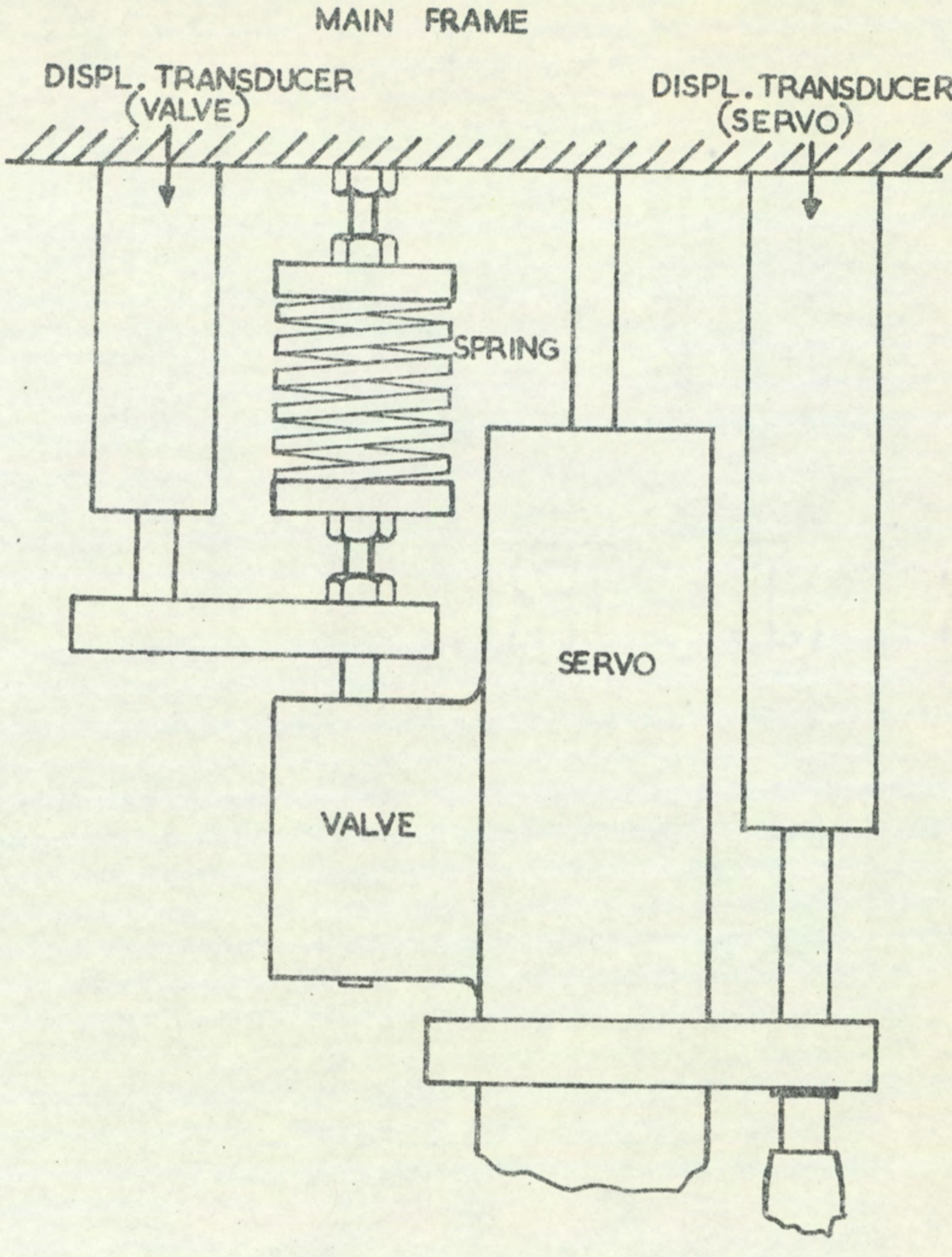

DETAIL OF TEST RIG.
SERVOMECHANISM WITH ITS VALVE INPUT
CONNECTED TO A FLEXIBILITY

FIG 3.12

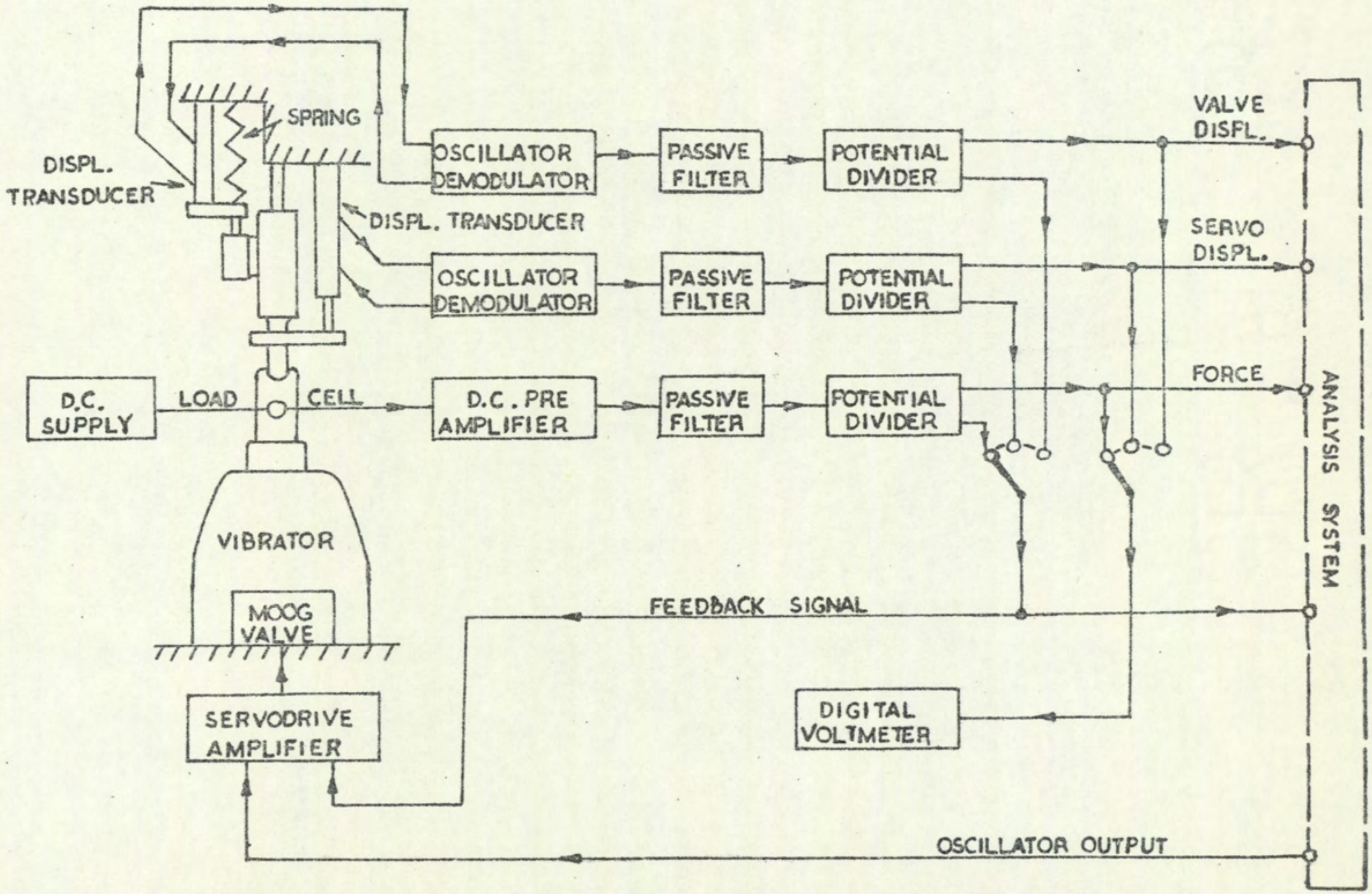

INSTRUMENTATION.
SERVOMECHANISM WITH ITS VALVE INPUT
CONNECTED TO A FLEXIBILITY

FIG 3.13

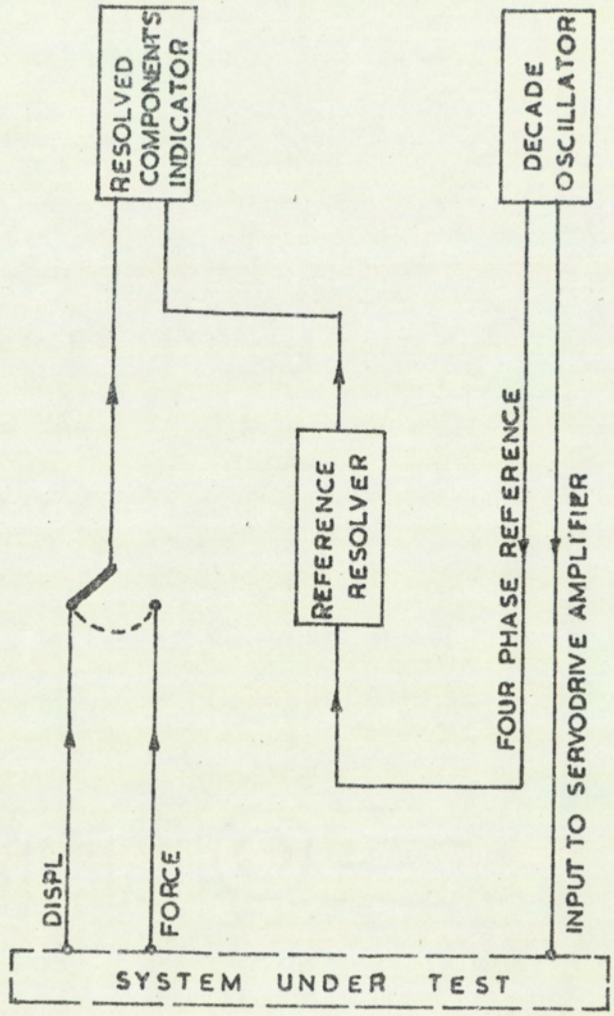

TRANSFER FUNCTION ANALYSIS SYSTEM

FIG 3.14

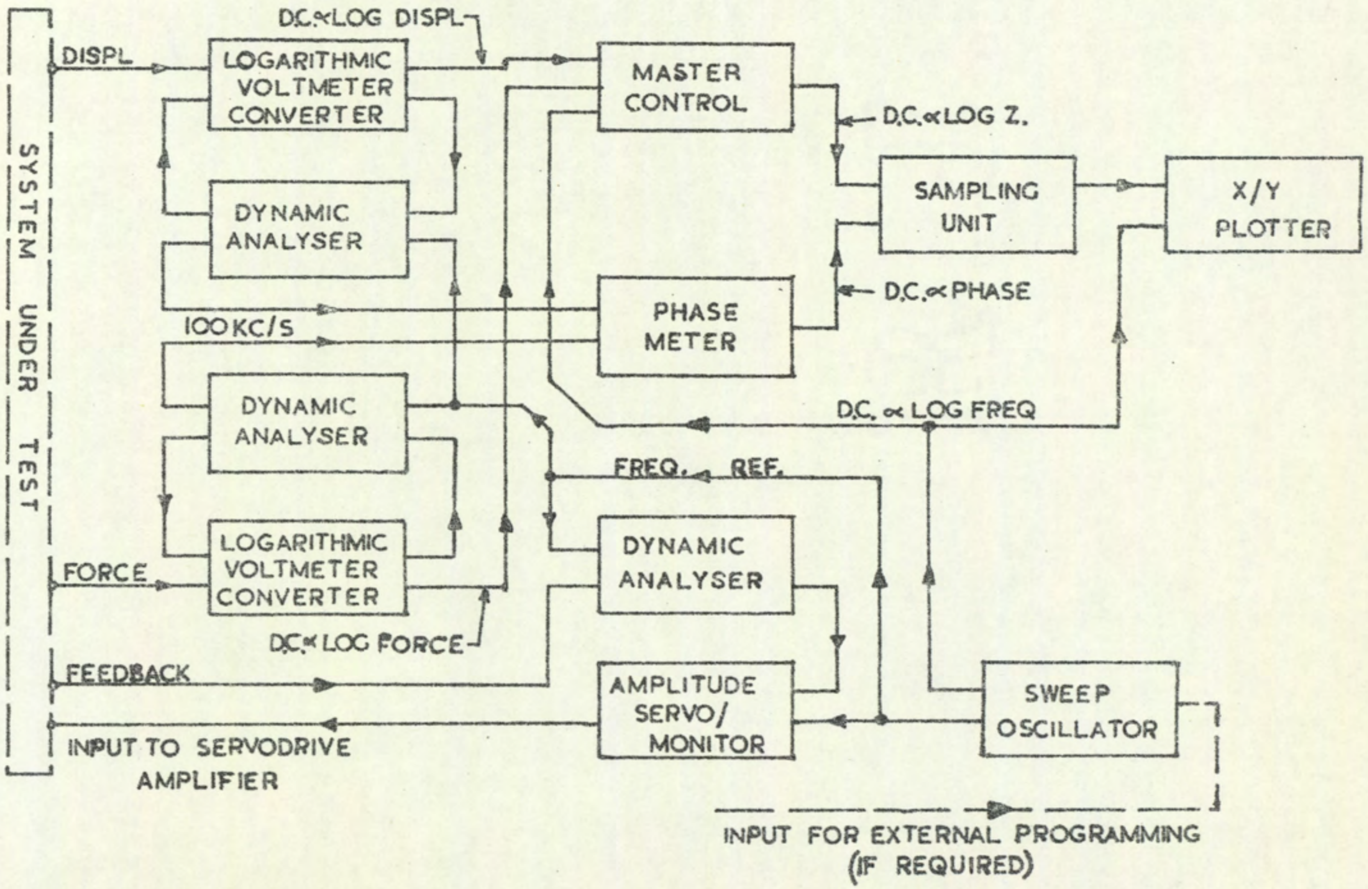

AUTOMATIC MECHANICAL IMPEDANCE ANALYSIS SYSTEM

FIG 3.15

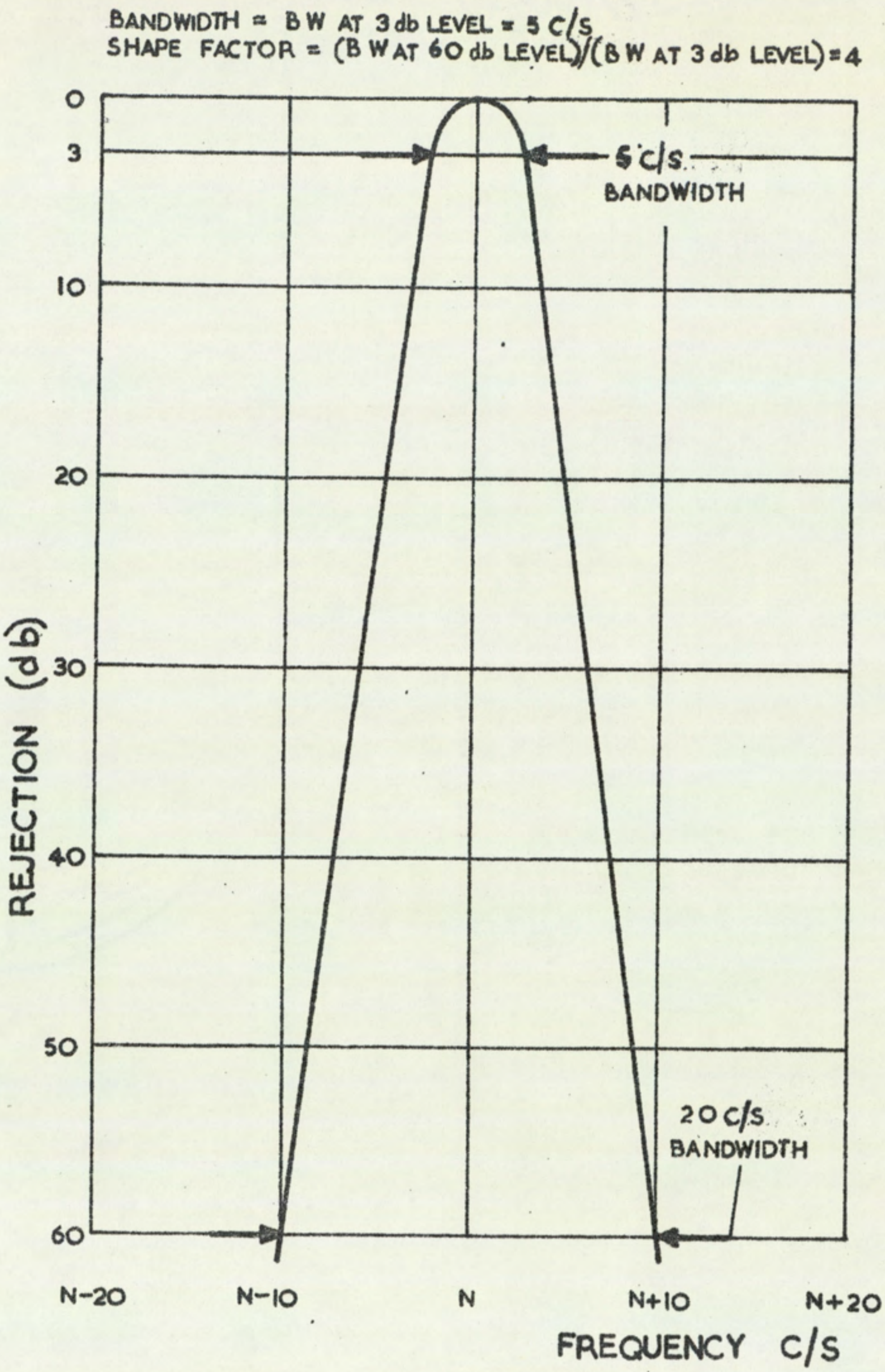

RESPONSE OF CONSTANT BANDWIDTH FILTER

FIG 3.16

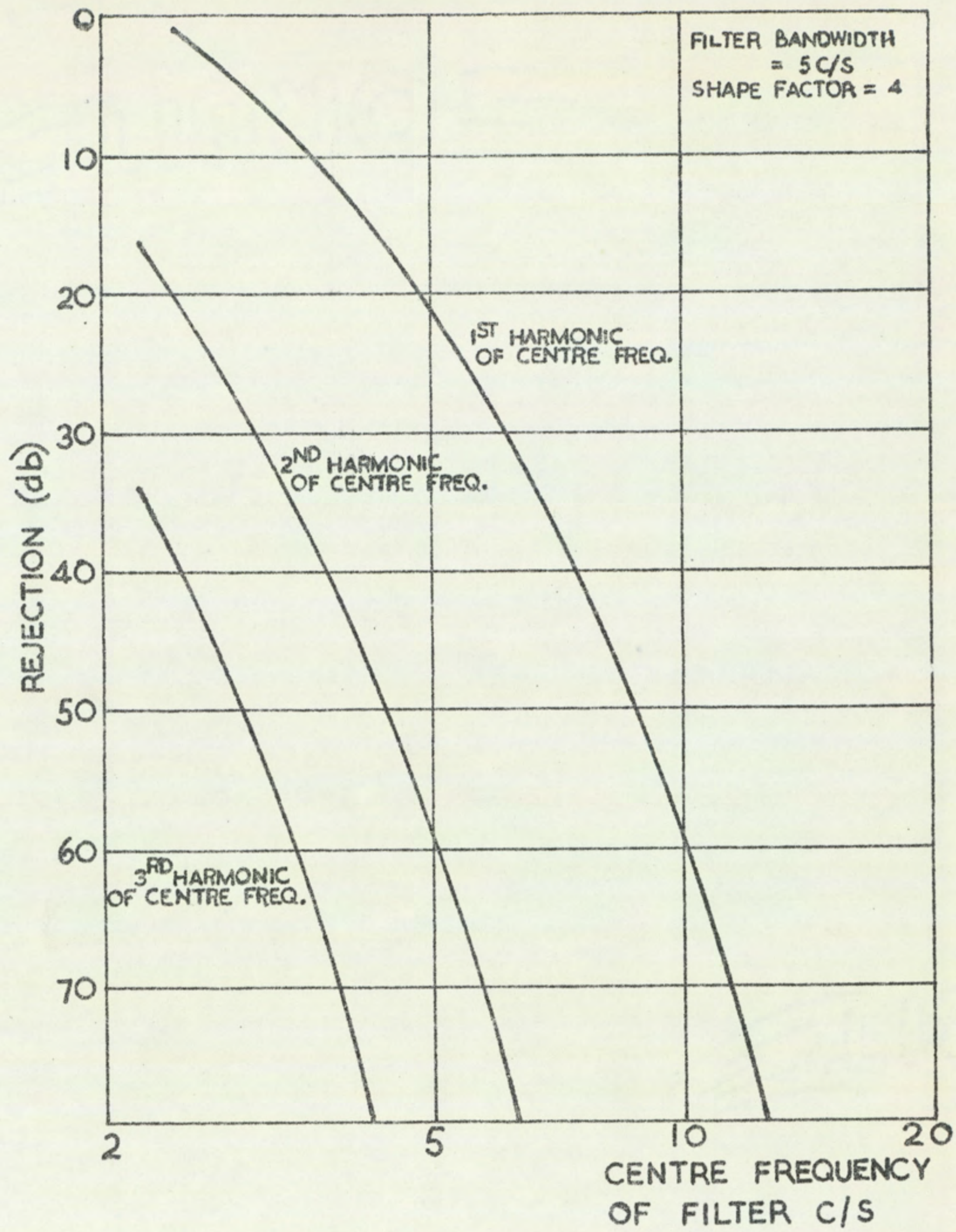

HARMONIC FREQUENCY REJECTION OF A CONSTANT BANDWIDTH FILTER

FIG 3.17

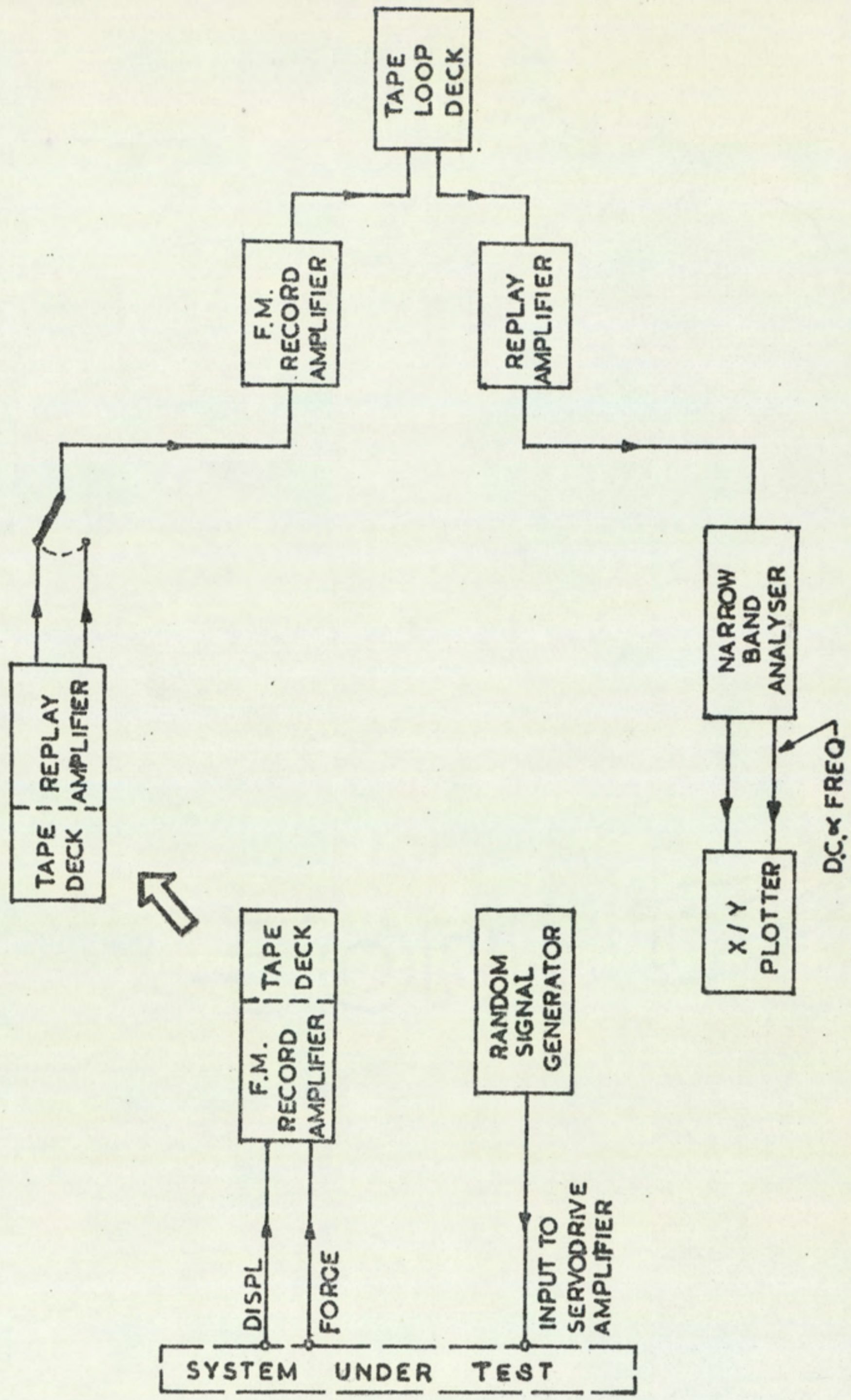

RANDOM EXCITATION. ANALYSIS SYSTEM

FIG 3.18

PART II

THE IMPEDANCE OF A SERVOMECHANISM IN A RIGID ENVIRONMENT.

CHAPTER IV

Theoretical Analysis of a Hydraulic Servomechanism.

The impedance equation for both output end and valve input excitation of the servomechanism is derived from considerations of the internal hydraulic pressures and flows. Approximate values of flow coefficients are obtained and the effect of Coulomb and viscous friction analysed. Using the appropriate values for the system parameters, the theoretical impedance of the servomechanism is evaluated and the results discussed.

4.1 Notation.

The following notation is used in this Chapter:

A	Cross sectional area of jack piston.
C_e	Valve flow coefficient $\partial Q/\partial E$.
C_p	Valve flow coefficient $2\partial Q/\partial P_v$.
C_{jp}	Leakage coefficient (around jack piston) dQ_j/dP_j.
C_{op}	Leakage coefficient (out of jack) dQ_o/dP_1, dQ_o/dP_2.
C_p'	$= C_p + 2C_{jp} + C_{op}$.
c	Viscous damping coefficient.
E_b	Initial or boundary value of E.
F_c	Coulomb friction force.

j	$\sqrt{(-1)}$.
K_e	$= A\omega$.
K_p	$= V\omega/2N$.
K_j	Leakage constant (around jack piston).
K_o	Leakage constant (out of jack).
K_v	Valve flow constant.
m	Mass of moving parts of jack.
N	Bulk modulus of fluid.
Q_{j1}	Leakage around piston out of No. 1 chamber.
Q_{j2}	Leakage around piston into No. 2 chamber.
Q_{o1}	Leakage from No. 1 chamber.
Q_{o2}	Leakage from No. 2 chamber.
P_s	Supply pressure.
t	Time.
V	Swept volume of jack.
W	Energy dissipated/cycle.
X_{ob}	Initial or boundary value of X_o.
Z	Impedance.
Z_s	Impedance of a particular system.
Z_p	Impedance of a servomechanism with an impedance element in parallel with it.
Z_u	Impedance of servomechanism unit.
ω	Excitation frequency.

In the following notation the upper case letters (left hand column) refer to the steady state condition, and the lower case letters (right hand column) refer to the small perturbation about the steady state condition.

E	e	Valve error or opening.
F_o	f_o	Applied force in the direction of X_o.
Q_1	q_1	Flow into one side of jack. (No.1 chamber)
Q_2	q_2	Flow out of other side of jack. (No. 2 chamber)
P_1	p_1	Pressure in No. 1 chamber.
P_2	p_2	Pressure in No. 2 chamber.
P_j	p_j	Pressure drop across jack piston, $(P_1 - P_2)$.
P_v	p_v	Total pressure drop across valves, $(P_s - P_j)$.
X_i	x_i	Input displacement.
X_o	x_o	Output displacement.

4.2 Introduction and historical survey.

The equations of motion for a hydraulic servomechanism of the four way valve and jack type have been formulated and solved in several published papers. A method frequently used to solve the non-linear equations is to linearise them by considering small perturbations about a steady state condition. The method was employed by Conway and Collinson (8) and Harpur (9). Harpur included the effect of oil compressibility and developed the equations of motion into the impedance form as well as the more usual response equation. Sung and Watanabe (10) followed Harpur's approach but expanded the equations by the inclusion of various leakage effects and internal friction. Williams (11) obtained and solved the equations of motion using the same method as Harpur but included the effect of oil momentum forces on the valve. Glaze (12) formulated the equations of motion and included the effect of Coulomb friction and leakage, but solved the equation using an analogue computer. In two recent papers Lambert and Davies (13) & (14) investigated the response of a servomechanism connected both rigidly and flexibly to an inertial load. The theoretical analysis of the system which follows is based on the work of Harpur with refinements suggested by Sung and Watanabe.

4.3 Analysis of a hydraulic servomechanism.

In the analysis it is assumed that the servomechanism is of symmetrical design and there is leakage around the piston and out of the jack. The valve has a small amount of overlap, i.e. there will be no leakage due to underlap.

Leakage effects around the valves have been neglected since the analysis of these leakages is very much dependent upon the geometry of the particular valve used. It is assumed that the supply pressure is constant and the return pressure is zero.

Consider the effect of compressing a fluid of bulk modulus N in a closed chamber.

By definition,

$$N = - V\, dP/dV$$

Differentiating w.r.t time,

$$\frac{dV}{dt} = - \frac{V}{N}\frac{dP}{dt}$$

With reference to the notation defined in Section 4.1 and the diagram of the servomechanism, Fig. 4.1,

Flow into jack through valve $Q_1 = \phi_1\ (E,\ P_1)$ (4.1)

Flow out of jack through other valve $Q_2 = \phi_2\ (E,\ P_2)$ (4.2)

Flow into jack

= (flow to compress fluid confined to one side of jack)

+ (flow corresponding to jack velocity)

+ (leakage flow across jack Q_{j1})

+ (leakage flow out of jack Q_{o1}).

$$\therefore \quad Q_1 = \frac{V_1}{N}\frac{dP_1}{dt} + A\frac{dX_o}{dt} + Q_{j1} + Q_{o1} \qquad (4.3)$$

where $Q_{j1} = \phi_{j1}(P_1 - P_2) = \phi_{j1}(P_j)$

and $Q_{o1} = \phi_{o1}(P_1)$

Similarly flow out of jack may be written as

$$Q_2 = \frac{V_2}{N}\frac{dP_2}{dt} + A\frac{dX_o}{dt} + Q_{j2} - Q_{o2} \tag{4.4}$$

where $Q_{j2} = \phi_{j2}(P_1 - P_2) = \phi_{j2}(P_j)$

and $\quad Q_{o2} = \phi_{o2}(P_2)$

The small perturbation technique is based on an approximation obtained from a Taylor series expansion of a function. For example, if δY is a small change in Y, then

$$f(Y + \delta Y) = f(Y) + \delta Y f'(Y) + \frac{(\delta Y)^2}{2!} f''(Y) + \text{-----}$$

Neglecting higher terms

$$f(Y + \delta Y) \simeq f(Y) + \delta Y f'(Y)$$

It is assumed that although Y is not really a constant it varies so slowly that it may be regarded as a constant. The steady state term is $f(Y)$ and the small perturbation term is $\delta Y f'(Y)$. In this term $f'(Y)$ is assumed constant and thus the perturbation term is a linear function in δY. Applying this technique to equations (4.1), (4.2), (4.3) and (4.4) and using lower case letters to denote incremental quantities (i.e. $y = \delta Y$) we have ,

From (4.1)

$$Q_1 + q_1 = \phi_1(E, P_1) + \frac{\partial Q_1}{\partial P_1} p_1 + \frac{\partial Q_1}{\partial E} e \tag{4.5}$$

and from (4.3)

$$Q_1 + q_1 = \frac{V_1}{N}\frac{dP_1}{dt} + A\frac{dX_o}{dt} + Q_{j1} + Q_{o1} + \frac{V_1}{N}\frac{dp_1}{dt}$$

$$+ A\frac{dx_o}{dt} + \frac{dQ_{j1}}{dP_j}p_j + \frac{dQ_{o1}}{dP_1}p_1 \qquad (4.6)$$

Eliminating the steady state terms from equations (4.5) and (4.6) we have

$$q_1 = \frac{\partial Q_1}{\partial P_1}p_1 + \frac{\partial Q_1}{\partial E}e \qquad (4.7)$$

and

$$q_1 = \frac{V_1}{N}\dot{p}_1 + A\dot{x}_o + \frac{dQ_{j1}}{dP_j}p_j + \frac{dQ_{o1}}{dP_1}p_1 \qquad (4.8)$$

Similarly the small perturbation flow out of the other side of the jack becomes, from equation (4.2)

$$q_2 = \frac{\partial Q_2}{\partial P_2}p_2 + \frac{\partial Q_2}{\partial E}e \qquad (4.9)$$

and from equation (4.4)

$$q_2 = -\frac{V_2}{N}\dot{p}_2 + A\dot{x}_o + \frac{dQ_{j2}}{dP_j}p_j - \frac{dQ_{o2}}{dP_2}p_2 \qquad (4.10)$$

Since the servomechanism is symmetrical

Let

$$\frac{\partial Q_1}{\partial E} = \frac{\partial Q_2}{\partial E} = C_e \qquad (4.11)$$

$$-\frac{\partial Q_1}{\partial P_1} = \frac{\partial Q_2}{\partial P_2} = C_p \qquad (4.12)$$

$$\frac{dQ_{j1}}{dP_j} = \frac{dQ_{j2}}{dP_j} = C_{jp} \tag{4.13}$$

$$\frac{dQ_{o2}}{dP_1} = \frac{dQ_{o2}}{dP_2} = C_{op} \tag{4.14}$$

Furthermore, if the piston is in the mid stroke position

$$V_1 = V_2 = V/2$$

Equating equations (4.7) & (4.8) and (4.9) & (4.10) and substituting for $\partial Q_1/\partial E$ etc,

$$q_1 = - C_p p_1 + C_e e = \frac{V}{2N}\dot{p}_1 + A\dot{x}_o + C_{jp}p_j + C_{op}p_1 \tag{4.15}$$

and

$$q_2 = C_p p_2 + C_e e = - \frac{V}{2N}\dot{p}_2 + A\dot{x}_o + C_{jp}p_j - C_{op}p_2 \tag{4.16}$$

Adding these two equations

$$- C_p(p_1 - p_2) + 2C_e e = \frac{V}{2N}(\dot{p}_1 - \dot{p}_2) + 2A\dot{x}_o + 2C_{jp}p_j$$

$$+ C_{op}(p_1 - p_2)$$

$$\therefore\ 2C_e e - p_j(C_p + 2C_{jp} + C_{op}) = \frac{V}{2N}\dot{p}_j + 2A\dot{x}_o$$

$$\text{or}\quad 2C_e e - p_j C_p' = \frac{V}{2N}\dot{p}_j + 2A\dot{x}_o \tag{4.17}$$

where $\quad C_p' = C_p + 2C_{jp} + C_{op}$

This is the performance equation for the servomechanism and from it can be developed the frequency response or impedance equation.

4.4 Impedance equation for a servomechanism excited at its output end.

Since for impedance testing the valve input is locked, $x_i = 0$ and thus $e = - x_o$. Considering small perturbations

$$f_o = - p_j A$$

where f_o is the force required to move the jack in the direction of x_o.

Substituting for e and p_j in equation (4.17) we have

$$- 2C_e x_o + \frac{f_o}{A} C_p' = - \frac{V}{2NA} \dot{f}_o + 2A\dot{x}_o$$

If the exciting force at the output end is sinusoidal then the response is also sinusoidal (since the system is assumed linear over the perturbated range).

$$\therefore \quad f_o = f_o \exp j\omega t \qquad \text{and} \qquad x_o = x_o \exp j\omega t$$

$$\dot{f}_o = j\omega f_o \exp j\omega t \qquad\qquad \dot{x}_o = j\omega x_o \exp j\omega t$$

Hence $$\left(j\frac{V\omega}{2N} + C_p'\right) \frac{f_o}{A} = 2(jA\omega + C_e)x_o \tag{4.18}$$

Writing $V\omega/2N = K_p$ and $A\omega = K_e$ and since $Z_u = f_o/x_o$ we have

$$Z_u = \frac{2A}{C_p'^2 + K_p^2}\left[(C_e C_p' + K_e K_p) + j(C_p' K_e - C_e K_p)\right] \qquad (4.19)$$

where C_p' includes the effect of leakage.
The real part of the equation represents stiffness and the imaginary part represents damping.

4.5 Static stiffness.

As ω tends to zero $K_e = K_p = 0$ and thus

$$Z_u(\text{static}) = 2AC_e/C_p' = 2AC_e/(C_p + 2C_{pj} + C_{op}) \qquad (4.20)$$

The damping is zero and the effect of leakage is to decrease the static stiffness.

4.6 Infinite frequency stiffness.

As ω tends to infinity C_e and C_p' become insignificant compared to K_e and K_p. Thus

$$Z_u(\text{inf. freq.}) = 2AK_e/K_p = 4A^2N/V \qquad (4.21)$$

Under these conditions the valve motion is no longer significant and the piston is bouncing on the oil in the jack. The damping is zero.

4.7 Criterion for stability.

For the servo to be stable the damping must be positive.

i.e. $C_p'K_e > C_eK_p$ or $C_p'/C_e > V/2NA$ (4.22)

The effect of leakage is to increase C_p to C_p' and hence improve stability. From equations (4.17) & (4.18)

$$C_p'/C_e = 2A/Z_u(\text{static})$$

and $V/2NA = 2A/Z_u(\text{inf. freq.})$

Substituting in equation (4.19) gives

$Z_u(\text{inf. freq.}) > Z_u(\text{static})$ (4.23)

This is an alternative form of the stability criterion.

4.8 Locus of the Argand diagram.

It has been shown that the stiffness of a servomechanism varies from $2AC_e/C_p'$ when $\omega = 0$ to $2AK_e/K_p$ when ω tends to infinity, whilst the damping increases from zero when $\omega = 0$ to a maximum value and back to zero when ω tends to infinity. The maximum value of damping can be determined by differentiation of the imaginary part of equation (4.19) w.r.t ω.

From equation (4.19)

$$Z_{uI} = \frac{2A}{C_p'^2 + K_p^2}[C_p'K_e - C_eK_p] = \frac{2A\omega}{C_p'^2 + (\frac{V\omega}{2N})^2}[C_p'A - C_e \frac{V}{2N}]$$

$$\therefore \frac{dZ_{uI}}{d\omega} = \frac{2A[AC_p' - \frac{VC_e}{2N}][C_p'^2 + (\frac{V\omega}{2N})^2 - \omega(\frac{V}{2N})^2 \, 2\omega]}{[C_p'^2 + (\frac{V\omega}{2N})^2]^2}$$

$\therefore$ For maximum condition

$$C_p'^2 - (\frac{V\omega}{2N})^2 = 0$$

$$\omega = 2NC_p'/V$$

Substituting for ω in the equation for Z_{uI} gives

$$\text{Max. } Z_{uI} = \frac{A}{C_p'^2}[\frac{2NA}{V}C_p'^2 - C_eC_p']$$

$$\therefore \text{ Max } Z_{uI} = A\left[\frac{K_e}{K_p} - \frac{C_e}{C_p'}\right]$$

If it is assumed that the Argand diagram is part of a circle then the coordinates of the centre of the circle, C, are given by

$$A\left[\frac{C_e}{C_p'} + \frac{K_e}{K_p}\right], 0$$

or

$$A\left[\frac{C_e}{C_p'} + \frac{2NA}{V}\right], 0.$$

Refering to Fig. 4.2,

$$\mu = \frac{2A}{C_p'^2 + K_p^2}(K_c C_p' - K_p C_c) \tag{4.24}$$

and $$\rho = \frac{2A}{C_p'^2 + K_p^2}(C_e C_p' + K_e K_p) - A\left[\frac{C_e}{C_p'} + \frac{K_e}{K_p}\right]$$

$$\therefore \quad \rho = \frac{A}{C_p'^2 + K_p^2}\left[\left\{\frac{C_e}{C_p'} - \frac{K_e}{K_p}\right\}(C_p'^2 - K_p^2)\right] \tag{4.25}$$

Squaring and adding equations (4.24) & (4.25) gives

$$\mu^2 + \rho^2 = A^2\left[\frac{C_e}{C_p'} - \frac{K_e}{K_p}\right]^2$$

$$\therefore \quad \overline{R} = \pm A\left[\frac{C_e}{C_p'} - \frac{K_e}{K_p}\right] \text{ and as } K_e/K_p = 2NA/V$$

$$\therefore \quad \overline{R} = \pm A\left[\frac{C_e}{C_p'} - \frac{2NA}{V}\right] \tag{4.26}$$

It can be seen that $\overline{R}$ and the coordinates of C are independant of ω and are constant provided that C_e, C_p', N, V and A are constants. Thus the initial supposition that the Argand diagram forms part of a circle is shown to be valid.

In Section 4.7 the stability criterion for the system was discussed and it was shown that for stability the damping must be positive, a corollary of this being that the static stiffness must be less than the infinite frequency stiffness. This criterion can be shown on the Argand diagram, Fig. 4.3. Here it is shown that as the static stiffness is increased to a value greater than the infinite frequency stiffness, the radius of the circle becomes negative causing negative damping.

4.9 Impedance of a system consisting of a servomechanism with an impedance connected to it in parallel.

This analysis is an extension of that given in Section 4.4. In the system which is shown in Fig. 4.4a, the servo valve is rigidly connected to earth and thus $x_i = 0$ and $e = -x_o$. Considering small force perturbations,

$$f_o = -p_j A + Z_p x_o$$

where Z_p is the impedance in parallel with the servo. Substituting for p_j and e in equation (4.18) and assuming the excitation and response to be sinusoidal, etc,

$$\left(j\frac{V\omega}{2N} + C_p'\right)\left(\frac{f_o}{A} - \frac{Z_p x_o}{A}\right) = 2(jA\omega + C_e)x_o$$

Writing $V\omega/2N = K_p$ and $A\omega = K_e$ we have

$$(C_p' + jK_p)\,\frac{f_o}{A} = 2x_o\left[\left(C_e + \frac{Z_p}{2A}C_p'\right) + j\left(K_e + \frac{Z_p}{2A}\right)\right]$$

Since $Z_s = f_o/x_o$

$$Z_s = \frac{2A}{C_p'^2 + K_p^2}[(C_e C_p' + K_e K_p) + j(C_p' K_e - C_e K_p)] + Z_p \tag{4.27}$$

or $\quad Z_s = Z_u + Z_p$

where Z_u is the impedance of the servo unit.

Therefore, it is shown that when a servomechanism is connected in parallel to another impedance the normal rules of connecting impedance in parallel, as discussed in Section 2.5 , apply.

4.10 Impedance of a system consisting of a servomechanism with an output mass.

The system is shown in Fig. 4.4b. From equation (4.27), as $Z_p = - m\omega^2$,

$$Z_s = Z_u - m\omega^2 \tag{4.28}$$

4.11 Impedance of a servomechanism including the effect of viscous damping.

One example of the presence of viscous damping is the valve damper which is arranged as shown diagrammatically in Fig. 4.4c. Since the valve is rigidly connected to earth the damper will effectively be in parallel with the servomechanism. Hence $Z_p = j\omega c$ and from equation (4.27),

$$Z_s = Z_u + j\omega c \tag{4.29}$$

Even if the servomechanism is not fitted with a valve damper, there will be some viscous damping in the system due to seal friction, etc. The effect of this damping is to increase the stability of the servomechanism.

4.12 The impedance of a servomechanism including the effect of Coulomb friction.

To include the effect of Coulomb friction into the analysis of the system the effect of Coulomb friction must be linearised and an equivalent viscous damping coefficient determined. Two methods of producing this equivalence are as follows:

(a) Equating energy dissipated: The analysis is based on that given in (13). The equivalent viscous damping coefficient can be obtained by equating the energies dissipated by each form of damping.

If damping is small the motion will be approximately sinusoidal, thus $x_o = x_o \sin \omega t$

Viscous damping force = $c\dot{x}_o$

$\therefore$ Energy dissipated/cycle,

$$W = \oint c\dot{x}_o dx_o$$

$$= \int_0^{2\pi/\omega} (c\dot{x}_o)\dot{x}_o dt$$

$$= x_o^2 c \int_0^{2\pi} \omega(\cos^2\omega t)d(\omega t)$$

$$\therefore \qquad W = \pi c\omega x_o^2$$

Coulomb damping force $= F_c(\text{sgn } \dot{x}_o)$

$\therefore$ Energy dissipated/cycle,

$$W = \int_0^{2\pi} F_c(\text{sgn } \dot{x}_o)\ \dot{x}_o dt$$

$$= \dot{x}_o \int_0^{2\pi} F_c(\text{sgn } \dot{x}_o)(\cos \omega t)d(\omega t)$$

$$\therefore \qquad W = 4F_c x_o$$

Equating the energy dissipated,

$$4F_c x_o = \pi c\omega x_o^2$$

$$\therefore \qquad c = 4F_c/\pi\omega x_o$$

Hence c is the equivalent viscous damping.

(b) Fourier Analysis : If a Coulomb damper is excited by a sinusoidal force, F_c will always oppose the motion. Thus the force will be a square wave and the Fourier expansion for such a wave having an amplitude of F_c is given by:-

$$f(F_c) = \frac{4}{\pi} F_c(\sin \omega t + \frac{1}{3} \sin 3 \omega t + \frac{1}{5} \sin 5 \omega t ----)$$

Neglecting all terms but the fundamental

$$f(F_c) = \frac{4}{\pi} F_c \sin \omega t$$

Approximate Coulomb damping force

$$= \frac{4}{\pi} F_c \sin \omega t$$

Viscous damping force

$$= c\dot{x}_o$$

$$= c\omega x_o \sin \omega t$$

Equating damping forces

$$\frac{4}{\pi} F_c \sin \omega t = c\omega x_o \sin \omega t$$

$$\therefore c = 4F_c/\omega x_o$$

It can be seen that neglecting all terms but the fundamental term in a Fourier expansion is tantamount to equating energy dissipation and leads to the same result,

$$c = 4F_c/\omega x_o \qquad (4.30)$$

This value for c may now be substituted into equation (4.29) giving

$$Z_s = Z_u + j\,\frac{4F_c}{\pi x_o} \tag{4.31}$$

Therefore Coulomb friction increases the stability of the servomechanism.

4.13 Evaluation of leakage coefficients.

Approximate values of the leakage coefficients may be obtained as follows:

Assuming lamina flow conditions,

$$Q_j \doteq K_j p_j$$

$$\therefore \quad C_{jp} = \frac{dQ_j}{dP_j} \doteq K_j \tag{4.32}$$

$$Q_{o1} \doteq K_o P_1 \quad \text{hence} \quad \frac{dQ_{o1}}{dP_1} \doteq K_o$$

and $$Q_{o2} \doteq K_o P_2 \quad \text{hence} \quad \frac{dQ_{o2}}{dP_2} \doteq K_o$$

$$\therefore \quad C_{op} = \frac{dQ_{o1}}{dP_1} = \frac{dQ_{o2}}{dP_2} \doteq K_o \tag{4.33}$$

4.14 Approximate evaluation of the servo valve coefficients.

Approximate values for the valve coefficients C_e and C_p may be obtained thus:

As $Q_1 \doteqdot K_v E\sqrt{(P_s - P_1)}$ where K_v is a constant of the valve.

$$\frac{\partial Q_1}{\partial E} \doteqdot K_v\sqrt{(P_s - P_1)} \text{ and since } P_s - P_1 = P_v/2$$

$$\frac{\partial Q_1}{\partial E} \doteqdot K_v\sqrt{(P_v/2)} \qquad (4.34a)$$

Similarly

$$Q_2 \doteqdot K_v E\sqrt{P_2}$$

$$\frac{\partial Q_2}{\partial E} \doteqdot K_v\sqrt{P_2} \qquad \text{and since } P_2 = P_v/2$$

$$\frac{\partial Q_2}{\partial E} \doteqdot K_v\sqrt{(P_v/2)} \qquad (4.34b)$$

From equations (4.34a) & (4.34b)

$$\therefore \quad C_e = \frac{\partial Q_1}{\partial E} = \frac{\partial Q_2}{\partial E} \doteqdot K_v\sqrt{(P_v/2)} \qquad (4.35)$$

$$-\frac{\partial Q_1}{\partial P_1} \doteqdot K_v E\ \tfrac{1}{2}(P_s - P_1)^{-\frac{1}{2}}$$

$$-\frac{\partial Q_1}{\partial P_1} \doteqdot \frac{K_v E}{2\sqrt{(P_v/2)}} \qquad (4.36a)$$

$$\frac{\partial Q_2}{\partial P_2} \simeq \frac{K_v E}{2\sqrt{P_2}}$$

$$\frac{\partial Q_2}{\partial P_2} \simeq \frac{K_v E}{2\sqrt{(P_v/2)}} \qquad (4.36b)$$

From equations (4.36a) & (4.36b)

$$\therefore \quad C_p = -\frac{\partial Q_1}{\partial P_1} = \frac{\partial Q_2}{\partial P_2} \simeq \frac{K_v E}{2\sqrt{(P_v/2)}} \qquad (4.37)$$

Note: As $P_s - P_1 = P_v/2$ and $P_2 = P_v/2$

$$C_p = -\frac{\partial Q_2}{\partial P_1} = -\frac{\partial Q}{\partial P_s} + \frac{\partial Q}{\partial (P_v/2)} = 2\,\frac{\partial Q}{\partial P_v} \qquad (4.38a)$$

Similarly

$$C_p = \frac{\partial Q_2}{\partial P_2} = \frac{\partial Q}{\partial (P_v/2)} = 2\,\frac{\partial Q}{\partial P_v} \qquad (4.38b)$$

Combining equations (4.37) & (4.38)

$$C_p = -\frac{\partial Q_1}{\partial P_1} = \frac{\partial Q_2}{\partial P_2} = 2\,\frac{\partial Q}{\partial P_v} \simeq \frac{K_v E}{2\sqrt{(P_v/2)}} \qquad (4.39)$$

4.15 <u>Experimental evaluation of the servo valve coefficients.</u>

In equations (4.11), (4.12) & (4.38) C_e and C_p are defined as follows,

$$C_e = \partial Q/\partial E \text{ and } C_p = \partial Q_2/\partial P_2 = 2\partial Q/\partial P_v$$

As $E = - x_o$, then $C_e = - \partial Q/\partial X_o$. Under these conditions, however, Q is a negative quantity so that C_e will remain positive whether X_o or E are positive or negative. Hence we may write $C_e = \partial Q/\partial X_o$.

To obtain values for these coefficients the relationship between the valve opening and the resulting flow, and also between the valve pressure drop and the resulting flow is required. The valve flow characteristic against valve opening for lines of constant valve pressure drop is shown in Fig. 4.5, which is based on experimental data supplied by the valve manufacturers. Hence, the gradient of these lines at any point represents $\partial Q/\partial X_o$, i.e. C_e. Similarly, Fig. 4.6, which is a cross plot of Fig. 4.5 using the same data, shows the flow characteristic against valve pressure drop for lines of constant valve opening. Thus the gradient of these lines at any point represents $\partial Q/\partial P_v$, i.e. $C_p/2$. These coefficients C_e and C_p have been plotted against valve opening and pressure drop, Figs. 4.7 and 4.8. From values taken from these graphs a plot of C_p against C_e is obtained showing lines of constant valve pressure drop and valve opening, Fig. 4.9. Also shown are lines of constant C_e/C_p ratio. In equation (4.20) it was shown that

$$Z_u(\text{static}) = 2AC_e/C_p$$

i.e. $Z_u(\text{static}) \propto C_e/C_p$

Hence, regions of high and low static stiffness can be indicated in Fig. 4.9. Regions of high and low stability can also be indicated in Fig. 4.9, since from equation (4.22), the criterion for stability is given by

$$C_p/C_e > V/2NA$$

4.16 Relationship between valve opening and valve pressure drop.

It has been shown in the previous two sections that C_e and C_p are both functions of valve opening and valve pressure drop. Valve opening and valve pressure drop are not, however, independent variables and thus the relationship between them must be established by considering the basic equation of motion for the servomechanism.

From equation (4.17),

$$2C_e e - p_j C_p' = \frac{V}{2N}\dot{p}_j + 2A\dot{x}_o$$

With the valve input locked for impedance testing $e = -x_o$ and

$$2C_e(-x_o) - p_j C_p' = \frac{V}{2N}\dot{p}_j + 2A\dot{x}_o$$

If the jack output end is excited sinusoidally

$x_o = x_o \exp j\omega t$ and $p_j = p_j \exp j\omega t$.

Hence, $- 2(C_e + j\omega A)x_o = (C_p' + j \frac{V\omega}{2N}) p_j$

Writing $K_e = A\omega$ and $K_p = V\omega/2N$

then $$\frac{p_j}{x_o} = - \frac{2}{C_p'^2 + K_p^2}[(C_e C_p' + K_e K_p) + j(K_e C_p' - C_e K_p)]$$

From which

$$\left|\frac{p_j}{x_o}\right| = - 2\sqrt{[(C_e^2 + K_e^2)/(C_p'^2 + K_p^2)]}$$

$$\therefore \quad \left|\frac{dP_j}{dX_o}\right| = - 2\sqrt{[(C_e^2 + K_e^2)/(C_p'^2 + K_p^2)]}$$

As $P_j = P_s - P_v$ and $E = - X_o$

$$\therefore \quad \left|\frac{dP_j}{dX_o}\right| = \left|\frac{dP_v}{dE}\right| = - 2\sqrt{[(C_e^2 + K_e^2)/(C_p'^2 + K_p^2)]}$$

and $$\left|\frac{dP_j}{dE}\right| = \left|\frac{dP_v}{dX_o}\right| = 2\sqrt{[(C_e^2 + K_e^2)/(C_p'^2 + K_p^2)]} \qquad (4.40)$$

The effect of leakage is included in C_p'.

These equations relate valve opening and valve pressure drop in a differential form. The equation can be solved, however, by means of a step by step integration process in conjunction with the information contained in

Fig. 4.9. Before the integration process can be commenced initial or boundary conditions must be specified. The most obvious initial condition is that when the valve opening is zero the full supply pressure acts across the valve. Under these conditions, in the absence of leakage, C_e and C_p theoretically tend to zero, as can be seen from Fig. 4.9. Indeed, under static conditions the equation relating valve opening and valve pressure drop becomes indeterminate. A further difficulty arises from the fact that the values of C_e and C_p are not known for valve openings of less than 0.002 in., see Fig. 4.9.

Because of these difficulties a compromise solution had to be chosen. It is assumed that when the valve opening is 0.002 in., the pressure drop across the valve is equal to the supply pressure. Values of C_e and C_p corresponding to the initial condition were obtained from Fig. 4.9 and, using the appropriate values of K_e and K_p, dP_v/dX_o was evaluated. Thus the change in valve pressure drop for a given incremental change in valve opening was known. Hence, a pair of corresponding values of P_v and X_o were obtained and the integration process could be recommenced and continued indefinately. A curve relating X_o and P_v for a particular set of conditions can then be plotted on the C_e/C_p diagram. A family of these curves for various frequencies is shown in Fig. 4.10. In order to clarify the diagram lines of constant C_e, C_p and C_e/C_p have been omitted.

Using the X_o - P_v relationship for a particular set of conditions the impedance of the servo can now be calculated by using the appropriate pair of C_e and C_p values applicable to the specific conditions of valve opening and valve pressure drop.

Using the technique described above the impedance of the servomechanism has been calculated and the effect of varying selected parameters is described in the sections which follow. The values of the various system parameters used are given below.

$$A = 0.623 \text{ in}^2.$$

$$K_j + K_o/2 = 8 \times 10^{-5} \text{in}^5/\text{lbfsec}.$$

$$N = 120{,}000 \text{ lbf/in}^2.$$

$$P_s = 3{,}000 \text{ lbf/in}^2.$$

$$V = 1.63 \text{ in}^2.$$

4.17 <u>Effect of bulk modulus.</u>

Although the bulk modulus of the hydraulic fluid used, DTD585, was nominally 190,000 lbf/in^2., due to the effects of aeration and dilation of the jack body, it was possible that the effective bulk modulus was in fact lower than this. Lambert and Davies (13) used a bulk modulus of 50,000 $lbf/in.^2$ after making allowances for aeration and dilation. Values of N = 190,000 $lbf/in.^2$; 120,000 $lbf/in.^2$ and 80, 000 $lbf/in.^2$ were used to determine what effect the bulk modulus had on impedance.

The effect of bulk modulus on stiffness and damping is shown in Figs. 4.11 and 4.12 respectively. It has been shown in equation (4.21) that at an infinite frequency the stiffness tends to $2AK_c/K_p$ ($= 4A^2N/V$), i.e. the piston is bouncing on the oil in the jack. A sufficiently high frequency for all other effects to be neglected provided that the valve opening is small is 70 c/s. Thus, in Fig. 4.11, the flat portion of the 70 c/s curve is equal to the infinite frequency stiffness for the particular value of bulk modulus used. In Section 5.9 it will be shown that the stiffness obtained experimentally at a frequency of 70 c/s was approximately 115,000 lbf/in. providing that the valve opening was small. This corresponds to an effective bulk modulus of 120,000 $lbf/in.^2$ which was the value chosen for all further theoretical calculations. Also shown in Fig. 4.11 is the static stiffness curve which is unaffected by variations in bulk modulus. The effect of bulk modulus on damping is shown in Fig. 4.12. The slight negative damping when the valve opening is small shows the presence of instability which disappears when the valve opening increases and the damping becomes positive. The curves in Figs. 4.11 and 4.12 use a boundary value of X_o = 0.002 in. and it is assumed that there is no leakage or Coulomb friction.

4.18 Effect of boundary conditions.

It has been previously stated that P_v = 3000 lbf/in.^{2} and X_o = 0.002 in. were chosen as reasonable boundary conditions for the step by step integration. To investigate what effect these assumptions have on the resulting impedance, boundary conditions of P_v = 3000 lbf/in.^{2} ; X_o = 0.005 in. and P_v = 3000 lbf/in.^{2} ; X_o = 0.0005 in. were also tried. In order to locate the approximate starting point of the integration on the C_p/C_e diagram for the latter assumption, the line corresponding to X_o = 0.0005 in. was found by extrapolating along the line corresponding to P_v = 3000 lbf/in.^{2} from X_o = 0.002 in.

The influence of boundary conditions on stiffness is shown in Fig. 4.13. The static stiffness curves produced by various assumed boundary conditions, are of the same shape, but as each curve starts at a different initial valve opening the curves are displaced relative to each other along the X_o axis. At high frequency, 70 c/s, the effect of boundary conditions is much reduced. The curves are coincident when the valve opening is small, and only when the valve opening increases do small differences in the curves become apparent. Similarly, boundary conditions have very little effect on the damping curves at 70 c/s, see Fig. 4.14.

4.19 Effect of using approximations for C_e and C_p.

In equations (4.35) & (4.39), it was shown that approximate values for C_e and C_p may be obtained and are given by $C_e \triangleq K_v\sqrt{(P_v/2)}$

and $$C_p \triangleq \frac{K_v E}{2\sqrt{(P_v/2)}}$$

These approximations do not make the theoretical analysis easier since the value of K_v is not known. Under static conditions, however,

$$\text{Static stiffness} = 2AC_e/C_p$$

and substituting the approximate values for C_e and C_p gives

$$\text{Static stiffness} = 2AP_v/E$$

Under static conditions the equation relating P_v and E simplifies to

$$dP_v/dE = -\ 2C_e/C_p$$

and substituting for C_e and C_p gives

$$dP_v/dE = -\ 2P_v/E$$

If the boundary conditions $P_v = P_s$ and $E = E_b$ are assumed then

$$\int_{P_s}^{P_v} dP_v/P_v = -\ 2\int_{E_b}^{E} dE/E$$

Thus $$P_v = P_s(E_b/E)^2$$

This value of P_v may be substituted in the impedance equation giving

$$\text{Static stiffness} = \frac{2AP_sE_b^2}{E^3}$$

or

$$\text{Static stiffness} = \frac{2AP_sX_{ob}^2}{X_o^3}$$

The static stiffness was evaluated using this equation for various valve openings, an initial or boundary value for X_o being first assumed.

The static stiffness obtained using the approximation $C_e/C_p = P_v/X_o$ and the relationship $P_v = P_s(X_{ob}/X_o)^2$ is shown in Fig. 4.15. It can be seen that a good agreement exists between the impedance calculated using the approximation approach and the impedance obtained using the step by step integration method for the same initial or boundary value of X_o.

Whilst this approximation leads to a result which is easily computed and quite accurate, the effects of leakage and frequency cannot easily be introduced, restricting the value of this method.

4.20 Effect of leakage.

It has been shown that the effect of leakage is to modify the valve flow coefficient C_p by the addition of the term $(2C_{jp} + C_{op})$.

From equations (4.32) & (4.33):

$$C_{jp} \triangleq K_j$$

and $$C_{op} \triangleq K_o$$

Hence $$2C_{jp} + C_{op} \triangleq 2K_j + K_o$$

Thus C_p is modified by the addition of two constant coefficients. If we write

$$2K_j + K_o = 2(K_j + \frac{K_o}{2}) \text{ then } K_j + \frac{K_o}{2} \text{ may be}$$

referred to as the leakage coefficient.

Lambert and Davies (13) used a value of $K_j = 3.9 \times 10^{-5} in^5/lbfsec$. During impedance testing the jack was excited over a small displacement in virtually one position over a long period of time and 5×10^6 is a conservative estimate of the number of reversals the jack has experienced during the present testing programme. Taking this fact into consideration and also the cumulative effect the influence of $K_o/2$ will have a leakage coefficient of $8 \times 10^{-5} in^5/lbfsec.$ was chosen as being representative.

The stiffness curves for various frequencies without and with leakage respectively are shown in Figs. 4.16 and 4.17. It is seen that the effect of leakage is to reduce the stiffness when the valve opening is small. The effect of leakage, which is significant at low frequencies, becomes progressively smaller as the excitation frequency is increased, until at about 40 c/s and above the leakage has no significant effect at all. Similarly, the effect of leakage on damping can be obtained by a comparison of Figs. 4.18 and 4.19, which show damping curves for various frequencies without and with leakage respectively. The leakage, which has a stabilising effect, greatly reduces the amount of negative damping present when the valve opening is small. As the frequency decreases the negative damping increases under conditions of small valve opening. This trend does not continue indefinately, however, as Fig. 4.20 shows, a graph of damping against excitation. The damping reaches a peak negative value at a very low frequency and then increases to zero. It is shown in Fig. 4.20 that the effect of leakage is to reduce the amount of negative damping and also to change the frequency at which the maximum negative damping occurs.

4.21 Effect of neglecting K_e and K_p in the step by step integration.

If K_e and K_p were neglected in the equation (4.40) the amount of labour involved in the step by step integration would be greatly reduced. In order to determine the effect of this assumption the impedance was calculated for certain conditions using values of C_e and C_p obtained from the static P_v - X_o relationship.

The results obtained are shown graphically in Figs. 4.21 and 4.22. The effect of neglecting K_e and K_p when obtaining the P_v - X_o relationship appears to be relatively small when the final impedance is calculated.

Comparison of Figs. 4.17 and 4.21 shows that the basic shape of the stiffness curve is unaffected. Similarly, Figs. 4.19 and 4.22 show that the basic shape of the damping curve is unaltered.

4.22 Impedance equation for a servomechanism with valve input excitation.

This analysis is based on the method of obtaining the servomechanism impedance proposed in Section 2.12b.

Output end blocked condition: Refering to Fig. 4.23b, since the output is blocked $X_o = 0$ and thus $e = x_i$.

Now $\quad p_j = f_o^B/A$

where f_o^B is the blocked output force.

Substituting for e and p_j in equation (4.17) and assuming sinusoidal excitation and response

$$[C_p'^B + j\,\frac{V\omega}{2N}]\,\frac{f_o^B}{A} = 2C_e^B x_i$$

Writing $V\omega/2N = K_p$

$$x_i = \frac{[C_p'^B + j\,K_p]}{2C_e^B\,A}\,f_o^B \tag{4.42}$$

or

$$\frac{f_o^B}{x_i} = \frac{2A}{(C_p'^B)^2 + K_p^2}\,[C_e^B\,C_p'^B - j\,C_e^B\,K_p] \tag{4.43}$$

It has been shown in Sections 4.14 and 4.15 that C_e and C_p' are functions of valve opening and valve pressure drop. Thus this relationship between valve opening and valve pressure drop under blocked output conditions must be established. The technique for doing this is similar to that previously used for determining the required relationship under output end excitation conditions. From equation (4.42) and substituting $f_o = p_j A$ gives

$$x_i = \frac{(C_p'^B + jK_p)}{2C_e^B} p_j$$

$$\therefore \quad p_j = \frac{2C_e^B}{C_p'^B + jK_p} x_i$$

$$\therefore \quad \frac{p_j}{x_i} = \frac{dP_j}{dX_i} = \frac{2C_e^B}{\sqrt{[(C_p'^B)^2 + K_p^2]}}$$

$$\text{or} \quad \frac{dP_v}{dX_i} = -\frac{2C_e^B}{\sqrt{[(C_p'^B)^2 + K_p^2]}} \tag{4.44}$$

This equation relates valve input (i.e. valve opening) with pressure drop in a differential form and can be solved using a step by step integration process in conjunction with the information contained in Fig. 4.9. The process is entirely similar to that given in Section 4.16.

Output end free condition: Refering to Fig. 4.23a, since the output is free $P_j = p_j = 0$ and $e = x_i - x_o^F$. Substituting for e and p_j in equation (4.17) and assuming sinusoidal excitation and response

$$2C_e^F(x_i - x_o^F) = j2A\omega x_o^F$$

writing $A\omega = K_e$

$$x_i = \frac{C_e^F + jK_e}{C_e^F} x_o^F \tag{4.45}$$

or
$$\frac{x_o^F}{x_i} = \frac{[(C_e^F)^2 - jC_e^F K_e]}{(C_e^F)^2 + K_e^2} \tag{4.46}$$

The function x_o^F/x_i can be evaluated for various valve openings by using the appropriate values of C_e. These can be obtained from Fig. 4.7 since the valve pressure drop is known and is equal to the supply pressure. Eliminating x_i from equations (4.43) & (4.46) gives

$$\frac{f_o^B}{x_o^F} = \frac{2AC_e^B}{[(C_p'^B)^2 + K_p^2]C_e^F}[(C_e^F C_p'^B + K_e K_p) + j(K_e C_p'^B - K_p C_e^F)] \tag{4.47}$$

From equation (2.36), $Z = f_o^B/x_o^F$ and hence equation (4.47) gives the impedance of the servomechanism.

If the valve and leakage coefficients were constants then

$$C_p'^B = C_p'$$

and
$$C_e^B = C_e^F = C_e$$

then equation equation (4.47) reduces to the normal form of the impedance expression, as given in equation (4.19). This method of determining the servomechanism impedance produces a result which, whilst of the same form as equation (4.16), is not its equivalent since

$$C_p'^B \neq C_p'$$

and $$C_e^B \neq C_e^F \neq C_e$$

In Chapter VI the problems involved in attempting to measure the experimental ratios f_o^B/x_i and x_o^F/x_i are discussed and the experimental work described.

The real and imaginary parts of the x_o^B/x_i ratio have been calculated using equation (4.44), the information contained in Fig. 4.9 and the appropriate system parameters. The results of this are shown in Figs. 4.24 and 4.25, where a leakage coefficient of $8 \times 10^{-5} in^5/lbfsec.$ has been assumed. Similarly, the real and imaginary parts of the x_o^F/x_i ratio have been evaluated using the information contained in Fig. 4.7 and the results are shown in Figs. 4.26 and 4.27. If, for a particular valve opening and excitation frequency, f_o^B/x_i is divided by x_o^F/x_i the servomechanism stiffness and damping may be determined, as shown in Figs. 4.28 and 4.29.

A comparison between Fig. 4.17 and Fig. 4.28 shows that a good agreement exists between the two sets of stiffness curves produced by each method of analysis, i.e. excitation of the servomechanism output end and excitation of the servo valve input. Only at a high frequency does the valve input excitation method lead to a result which is significantly different from that produced by the direct approach.

A reasonable agreement exists between the system damping as predicted by the two methods of analysis, this is shown in a comparison between Fig, 4.19 and Fig. 4.29. When the valve opening is large, however, the damping predicted by the valve excitation method was slightly positive and did not reach the positive value predicted by the normal method.

4.23 Effect of exciting the output end and the valve input simultaneously on the servomechanism impedance.

In Section 4.4 the impedance of the servomechanism was developed assuming the valve input was locked and the excitation applied at the output end. In this section the analysis is extended to investigate the effect of exciting the valve input and output end simultaneously.

From equation (4.17)

$$\frac{V}{2N}\dot{p}_j + C_p'p_j + 2A\dot{x}_o + 2C_e x_o = 2C_e x_i$$

Let $x_o = x_o \exp j\omega t$, $p_j = p_j \exp j\omega t$ and $x_i = x_i \exp j(\omega t + \theta)$ where θ is the phase angle between x_i and x_o.

Substituting for x_o, x_i and p_j and writing $V\omega/2N = K_p$ and $A\omega = K_e$ gives

$$(jK_p + C_p')p_j + 2(C_e + jK_e)x_o = 2C_e x_i \exp j\theta$$

$$(C_p' + jK_p)p_j + 2(C_e + jK_e)x_o = 2C_e x_i(\text{Cos}\theta + j\ \text{Sin}\theta)$$

As $p_jA = -f_o$ and writing $x_i/x_o = r$, then

$$Z_u = \frac{2A}{C_p'^2 + K_p^2}\left[\{(C_e - C_e r\ \text{Cos}\theta)C_p' + (K_e - C_e r\ \text{Sin}\theta)K_p\}\right.$$
$$\left. + j\{(K_e - C_e r\ \text{Sin}\theta)C_p' - (C_e - C_e r\ \text{Cos}\theta)K_p\}\right]$$

$$Z_u = \frac{2A}{C_p'^2 + K_p^2}\left[\{C_eC_p' + K_eK_p - rC_e(C_p'\ \text{Cos}\theta + K_p\ \text{Sin}\theta)\}\right.$$
$$\left. + j\{K_eC_p' - C_eK_p - rC_e(C_p'\ \text{Sin}\theta - K_p\ \text{Cos}\theta)\}\right]$$

<u>Effect of varying θ</u> :

$$\frac{dZ_u}{d\theta} = \frac{2A}{C_p'^2 + K_p^2}\left[-rC_e(-C_p'\ \text{Sin}\theta + K_p\ \text{Cos}\theta)\right.$$
$$\left. + j\{-rC_e(C_p'\ \text{Cos}\theta + K_p\ \text{Sin}\theta)\}\right]$$

For maximum and minimum values of Z_u $dZ_u/d\theta = 0$

For the real part of the equation

$$-rC_e(-C'_p \sin\theta + K_p \cos\theta) = 0$$

$$\therefore \tan\theta = K_p/C'_p$$

For the imaginary part of the equation

$$-rC_e(C'_p \cos\theta + K_p \sin\theta) = 0$$

$$\therefore \tan\theta = -C'_p/K_p$$

Substituting these two values of $\tan\theta$ into the impedance equation gives:

$$Z_u = \frac{2A}{C'^2_p + K^2_p}\left[\left\{C_e C'_p + K_e K_p \pm rC_e\sqrt{(C'^2_p + K^2_p)}\right\} + j(K_e C'_p - C_e K_p)\right]$$

and

$$Z_u = \frac{2A}{C'^2_p + K^2_p}\left[(C_e C'_p + K_e K_p) + j\left\{K_e C'_p - C_e K_p \pm rC_e\sqrt{(C'^2_p + K^2_p)}\right\}\right]$$

It can be seen that when the stiffness is a maximum or a minimum value the damping has its normal value and when the damping is a maximum or a minimum value the stiffness has its normal value.

A brief reference was made to the effect of exciting the valve during impedance testing in a paper by Watson (15).

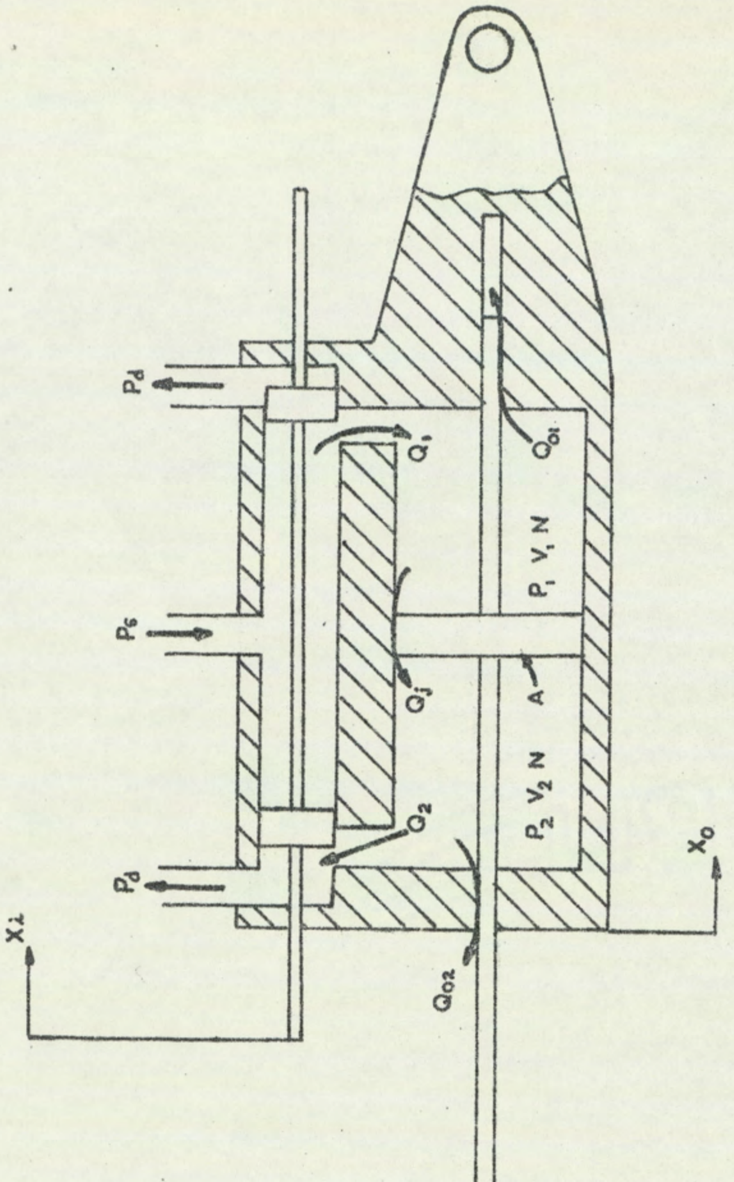

SCHEMATIC DIAGRAM OF A
HYDRAULIC SERVOMECHANISM

FIG 4.1

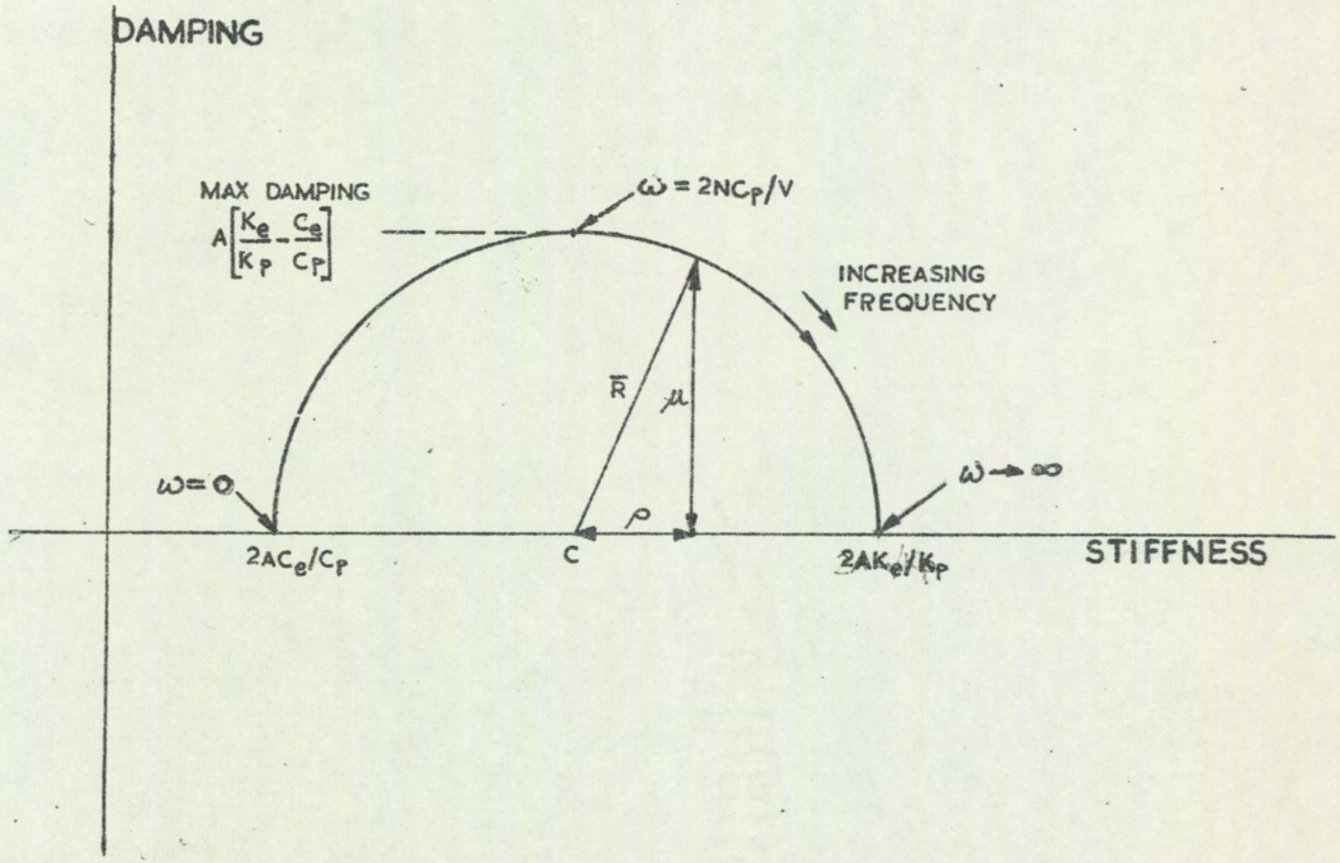

CONSTRUCTION OF ARGAND DIAGRAM

FIG 4.2

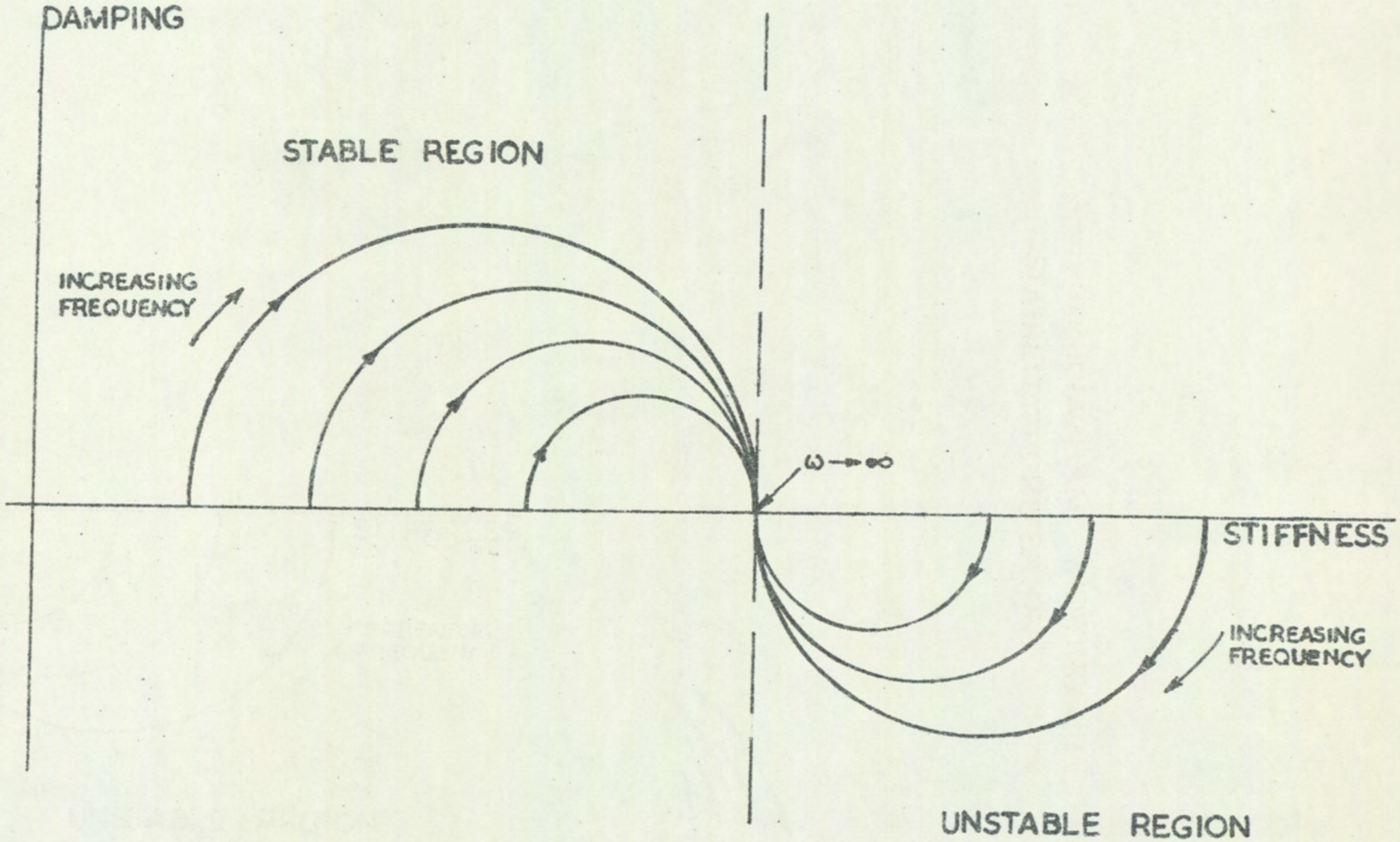

ARGAND DIAGRAM SHOWING
STABILITY CRITERION

FIG 4.3

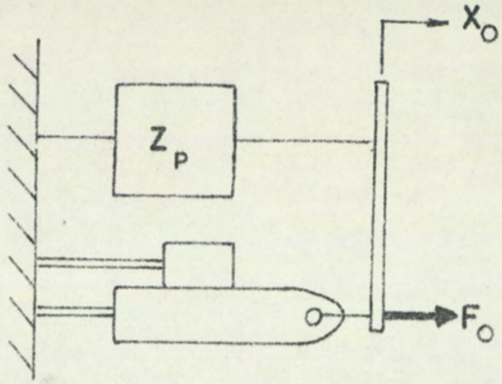

(A) SERVOMECHANISM WITH AN IMPEDANCE CONNECTED IN PARALLEL

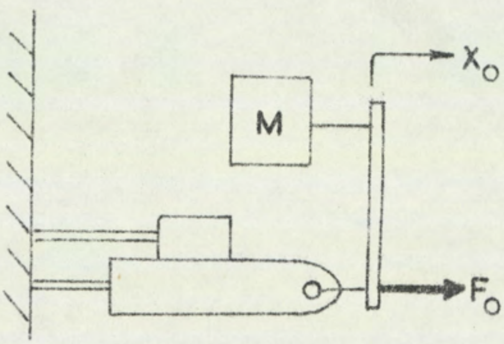

(B) SERVOMECHANISM WITH A MASS AT THE OUTPUT END

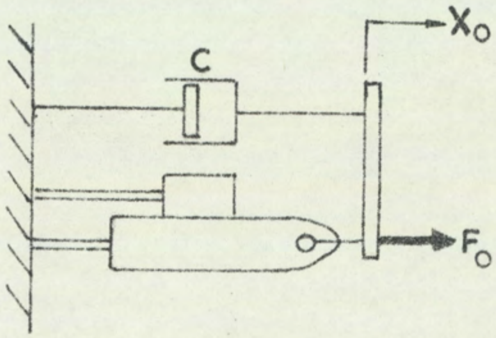

(C) SERVOMECHANISM WITH A DAMPER CONNECTED IN PARALLEL

SYSTEMS CONSISTING OF A SERVOMECHANISM AND AN IMPEDANCE CONNECTED IN PARALLEL

FIG 4.4

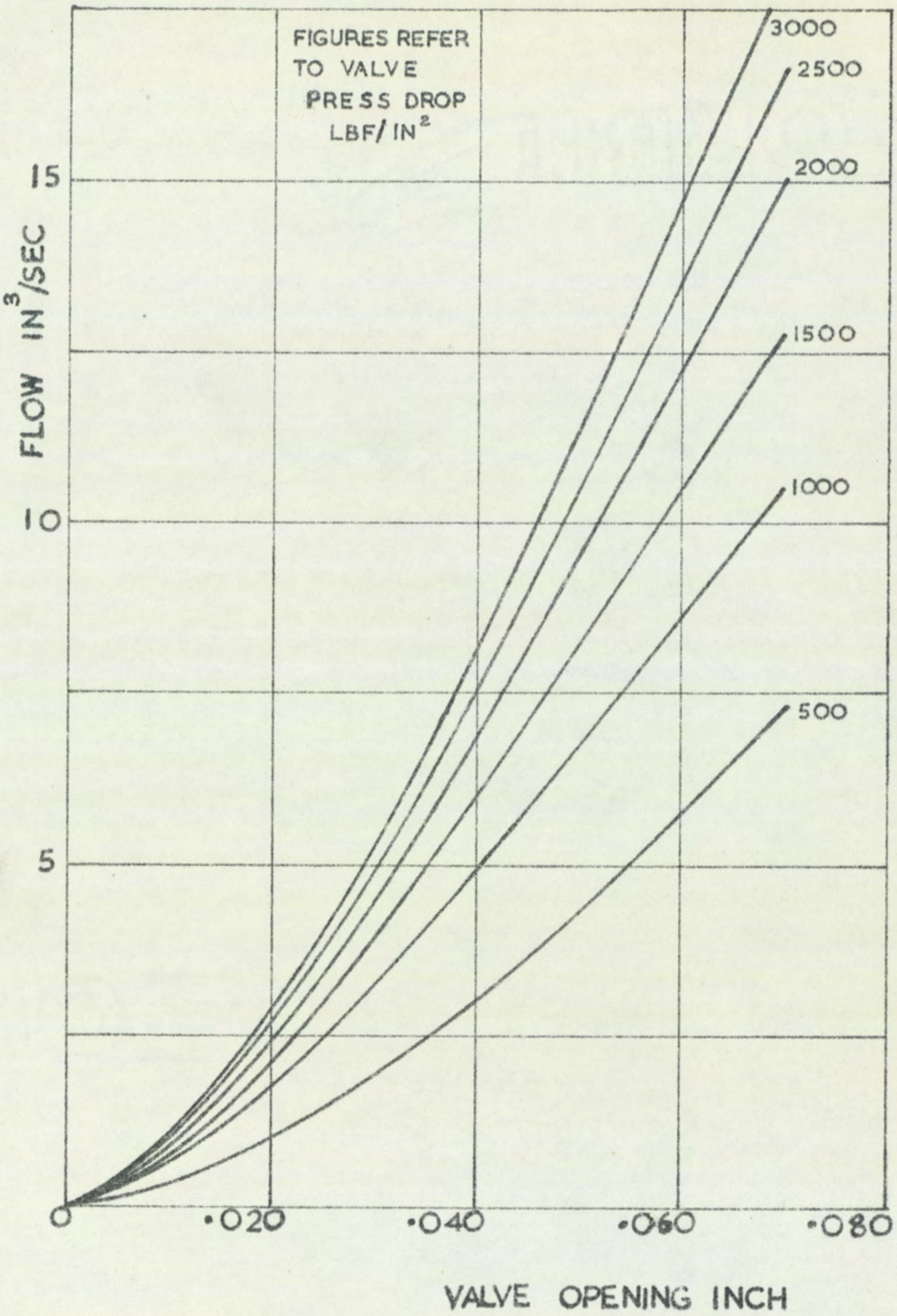

VALVE FLOW/OPENING CHARACTERISTIC

FIG 4.5

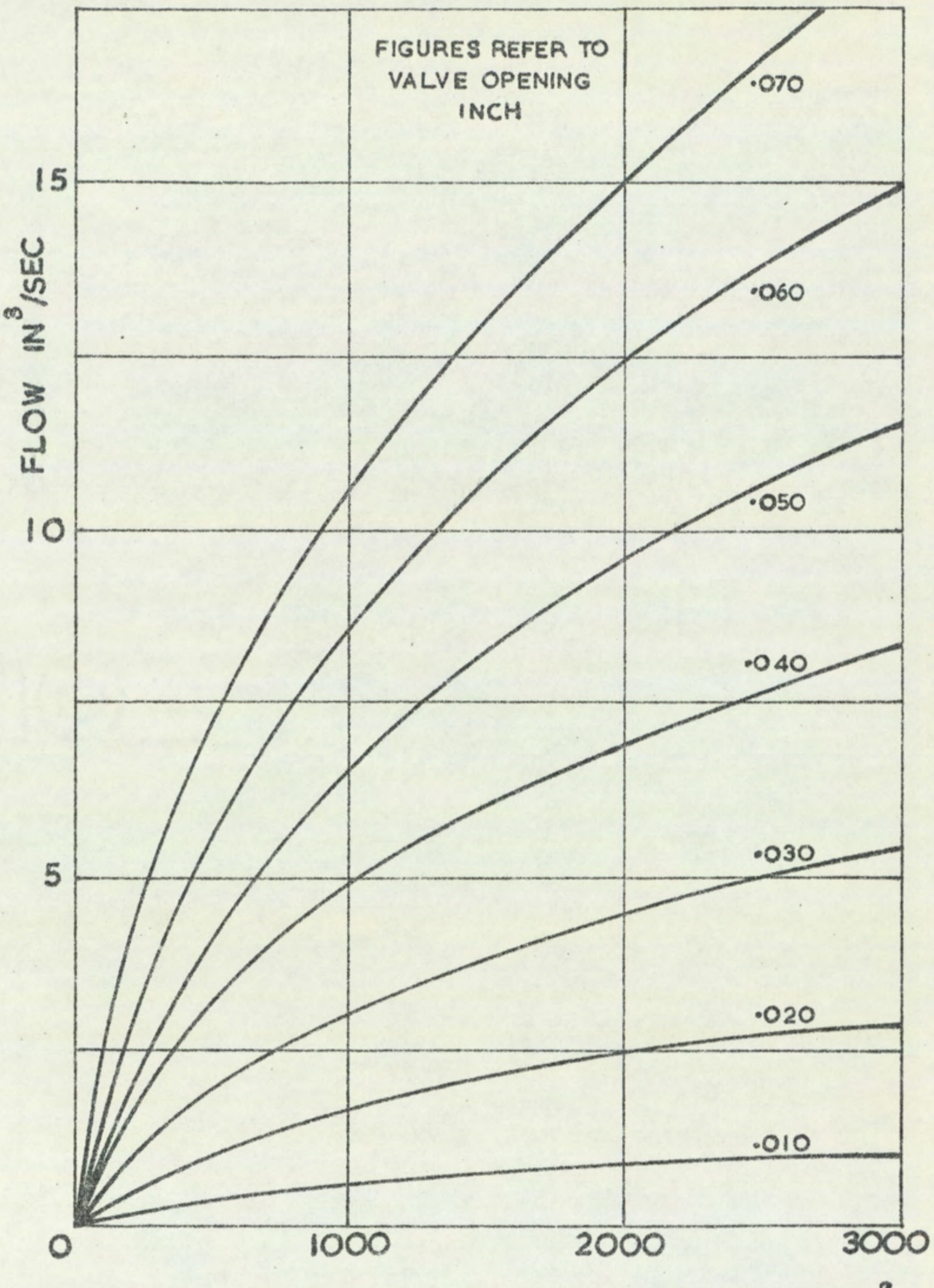

VALVE FLOW / PRESS. DROP CHARACTERISTIC

FIG 4.6

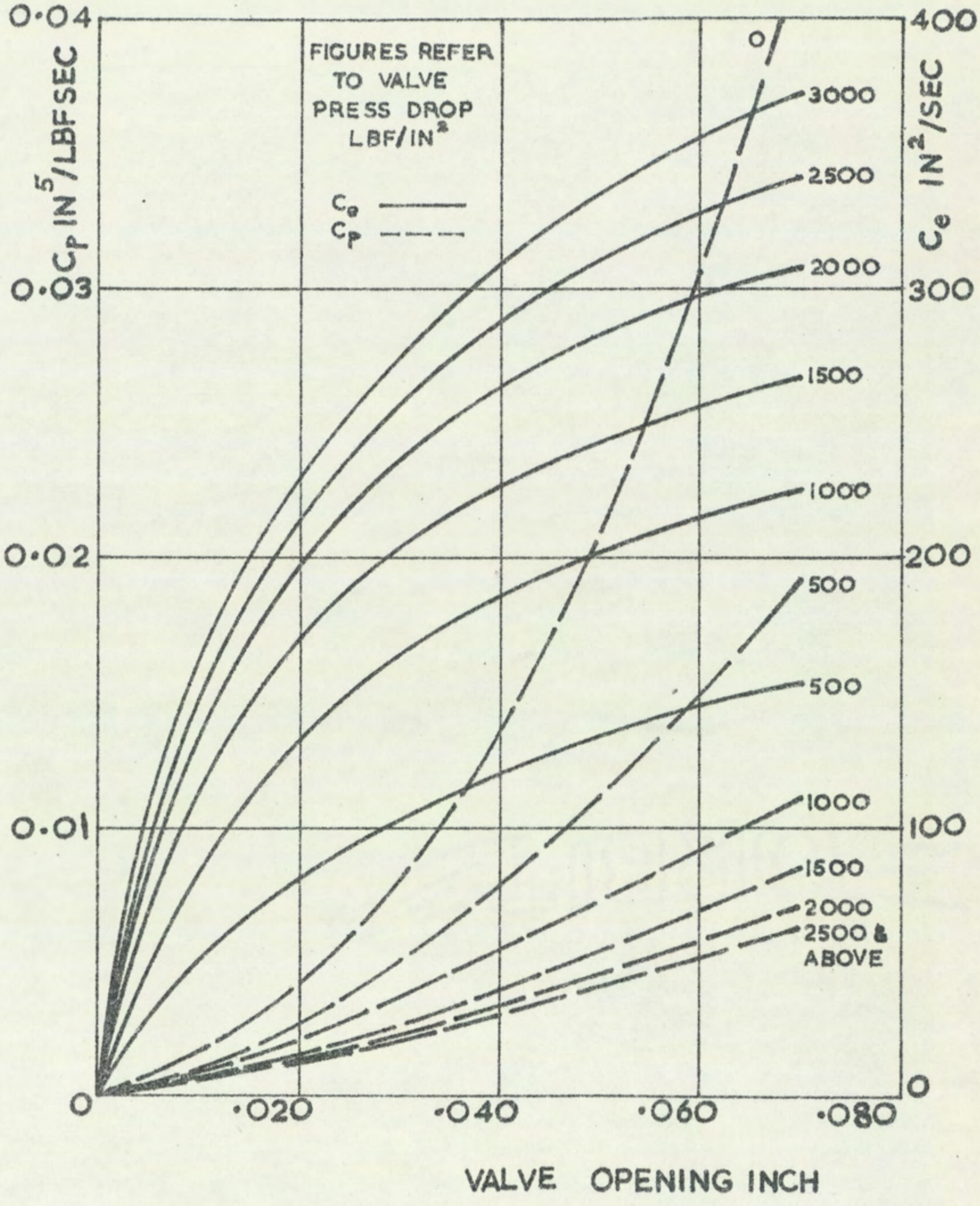

VALVE FLOW COEFFICIENTS / OPENING

FIG 4.7

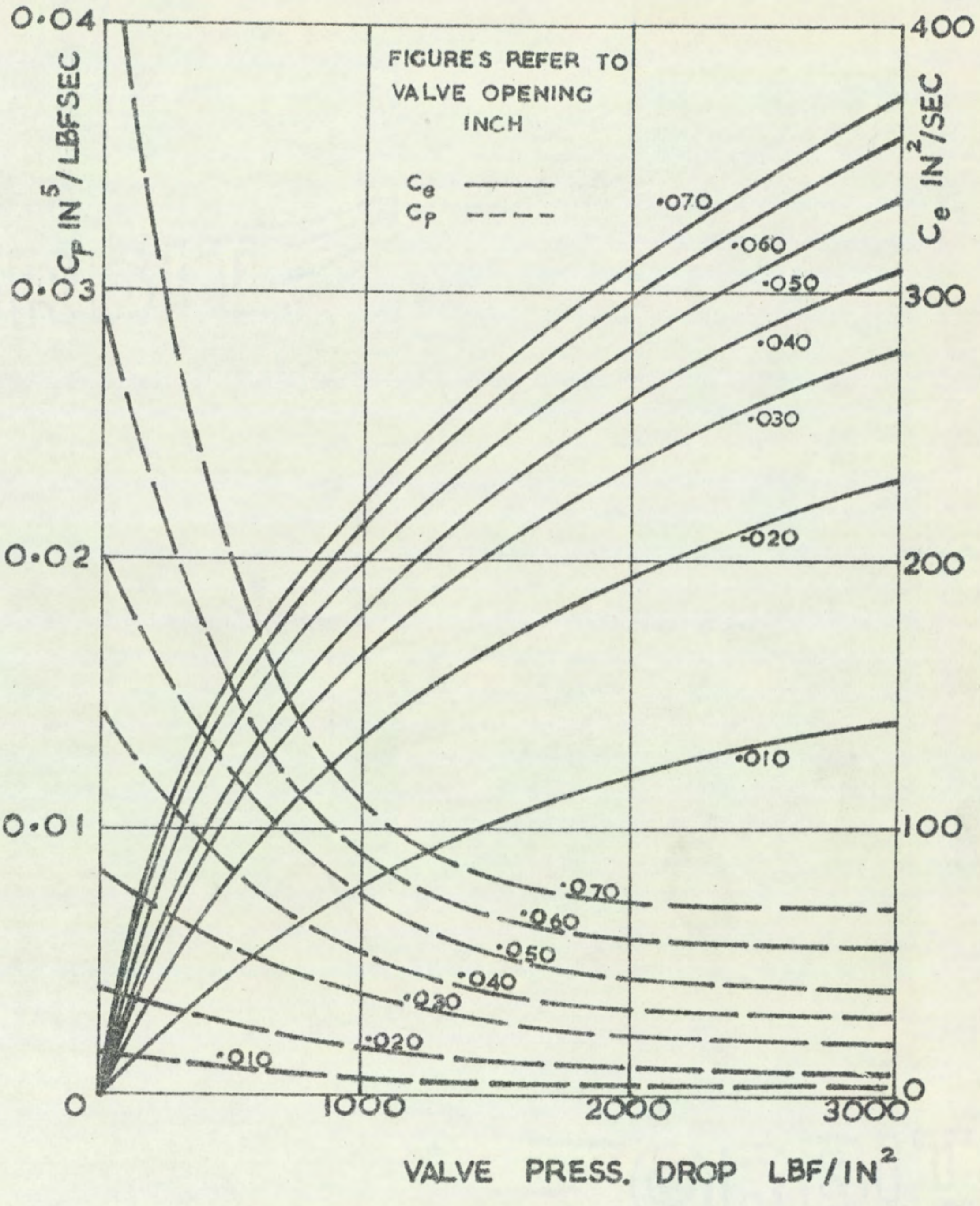

VALVE FLOW COEFFICIENTS / PRESS. DROP

FIG 4.8

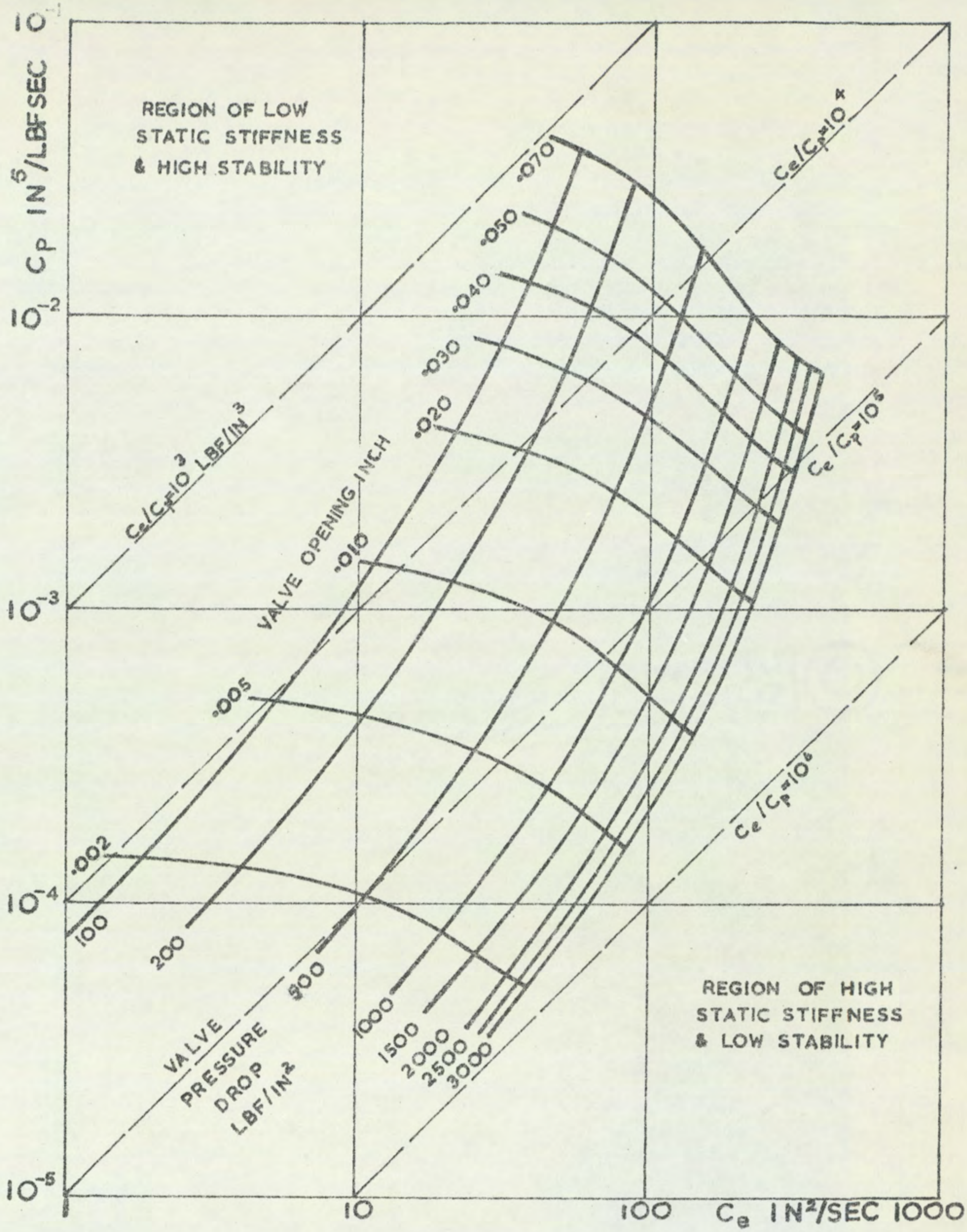

Cp/Ce DIAGRAM SHOWING LINES OF CONSTANT VALVE OPENING & VALVE PRESSURE DROP.

FIG 4.9

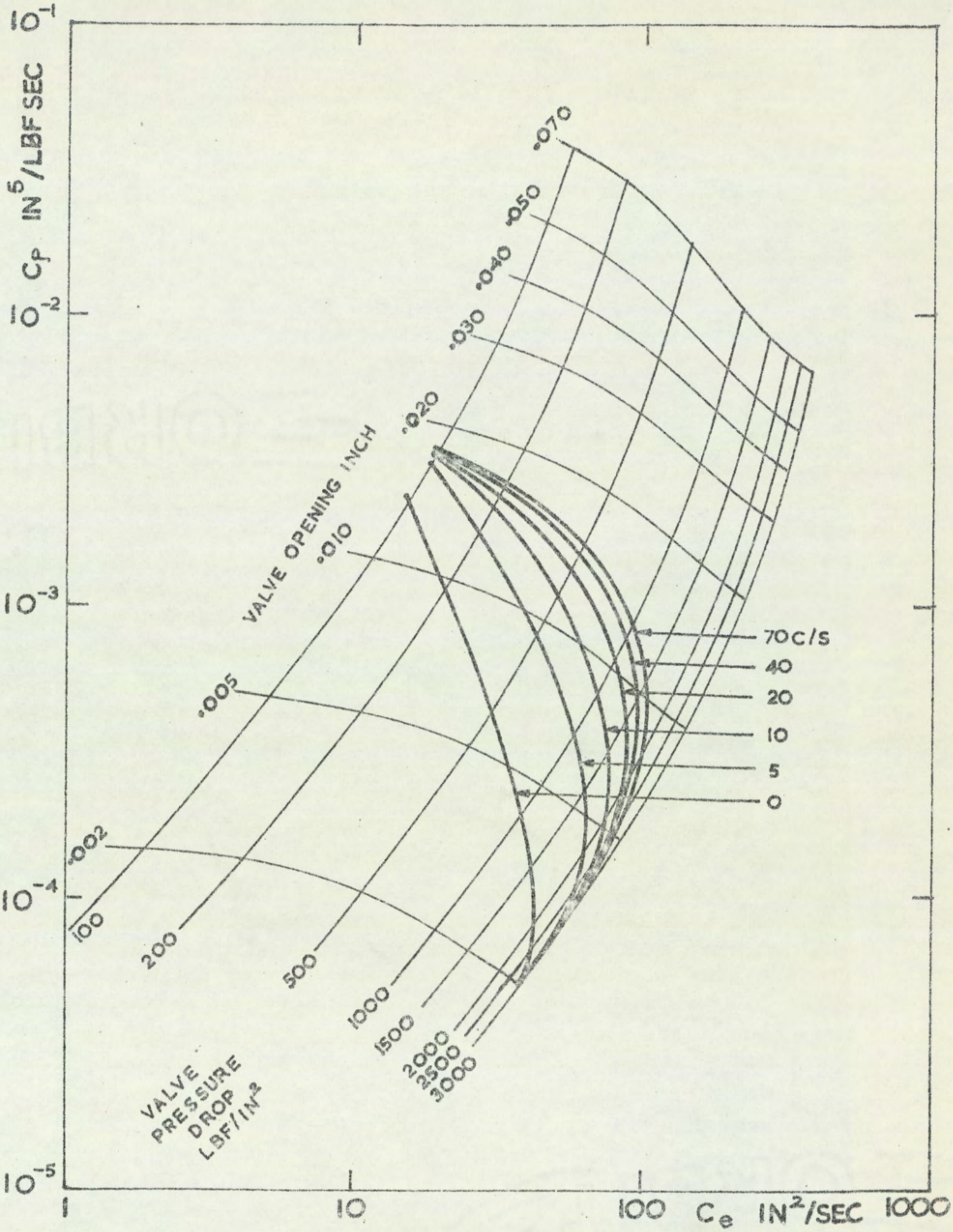

C_p/C_e DIAGRAM SHOWING TYPICAL RELATIONSHIP BETWEEN P_v & X_o AT VARIOUS FREQUENCIES. NO LEAKAGE.

FIG 4.10

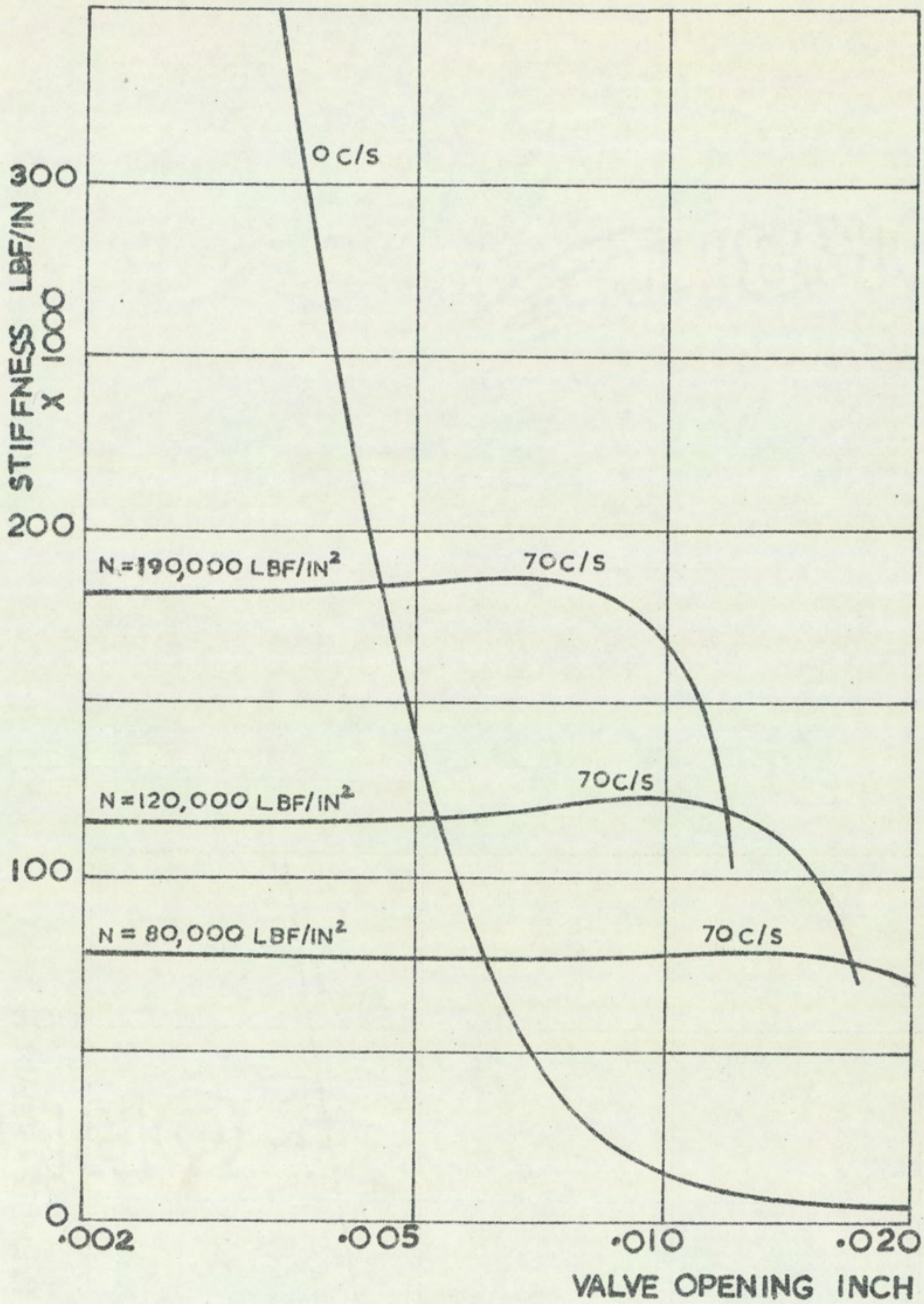

THEORETICAL STIFFNESS CURVES
EFFECT OF VARIATION OF BULK MODULUS.

FIG 4.11

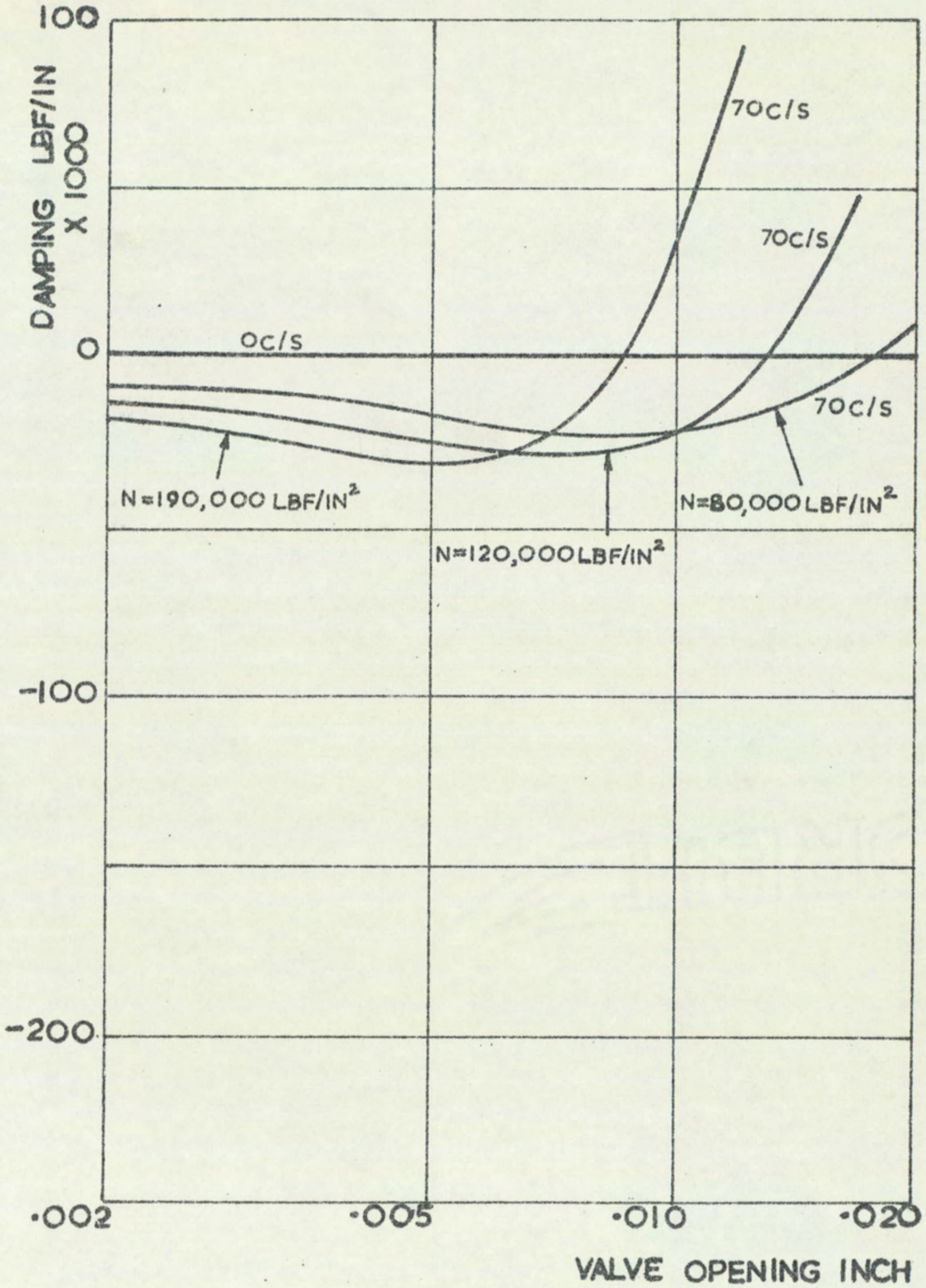

THEORETICAL DAMPING CURVES

EFFECT OF VARIATION OF BULK MODULUS

FIG 4.12

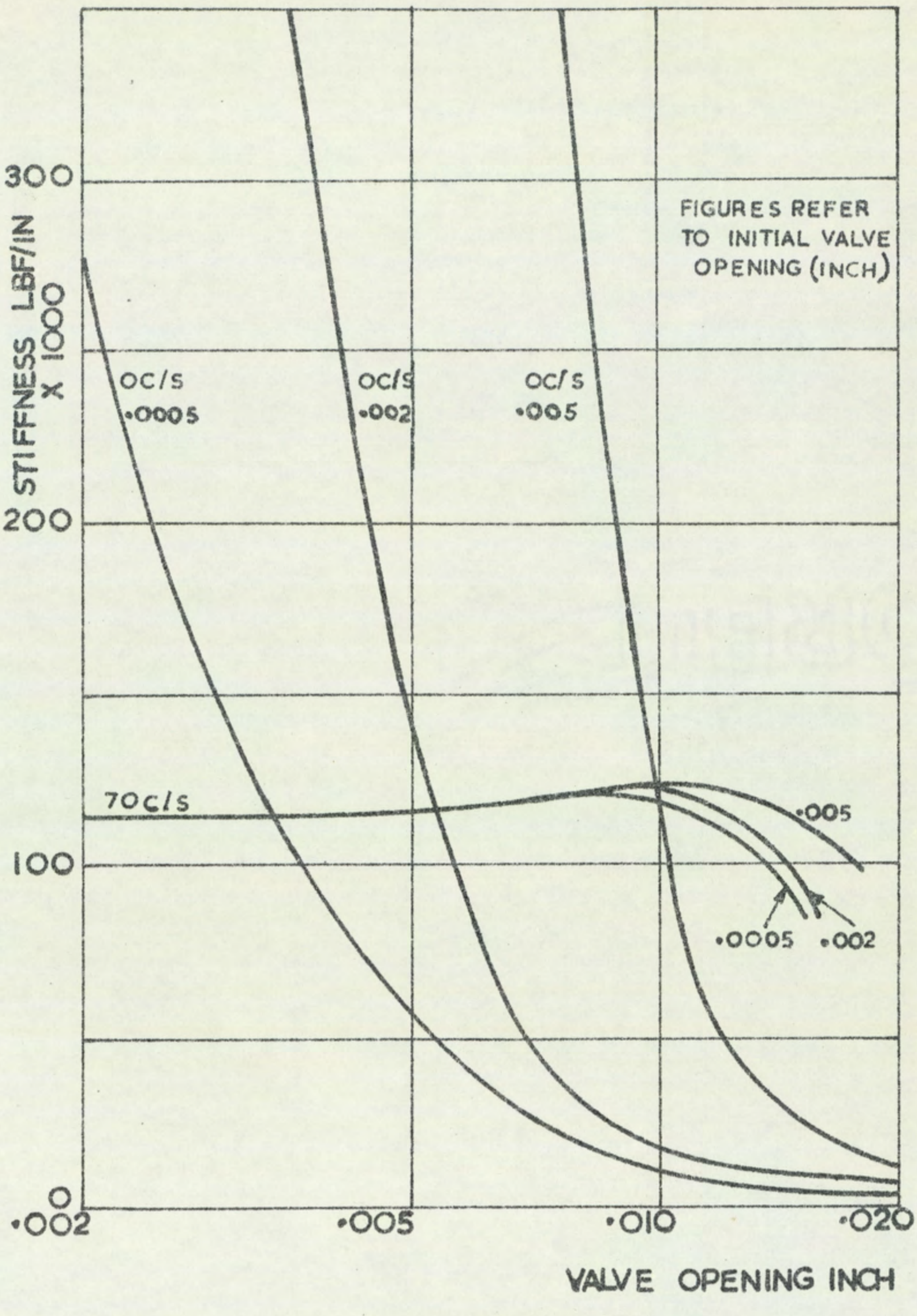

THEORETICAL STIFFNESS CURVES
EFFECT OF VARIATION OF BOUNDARY CONDITIONS

FIG. 4.13

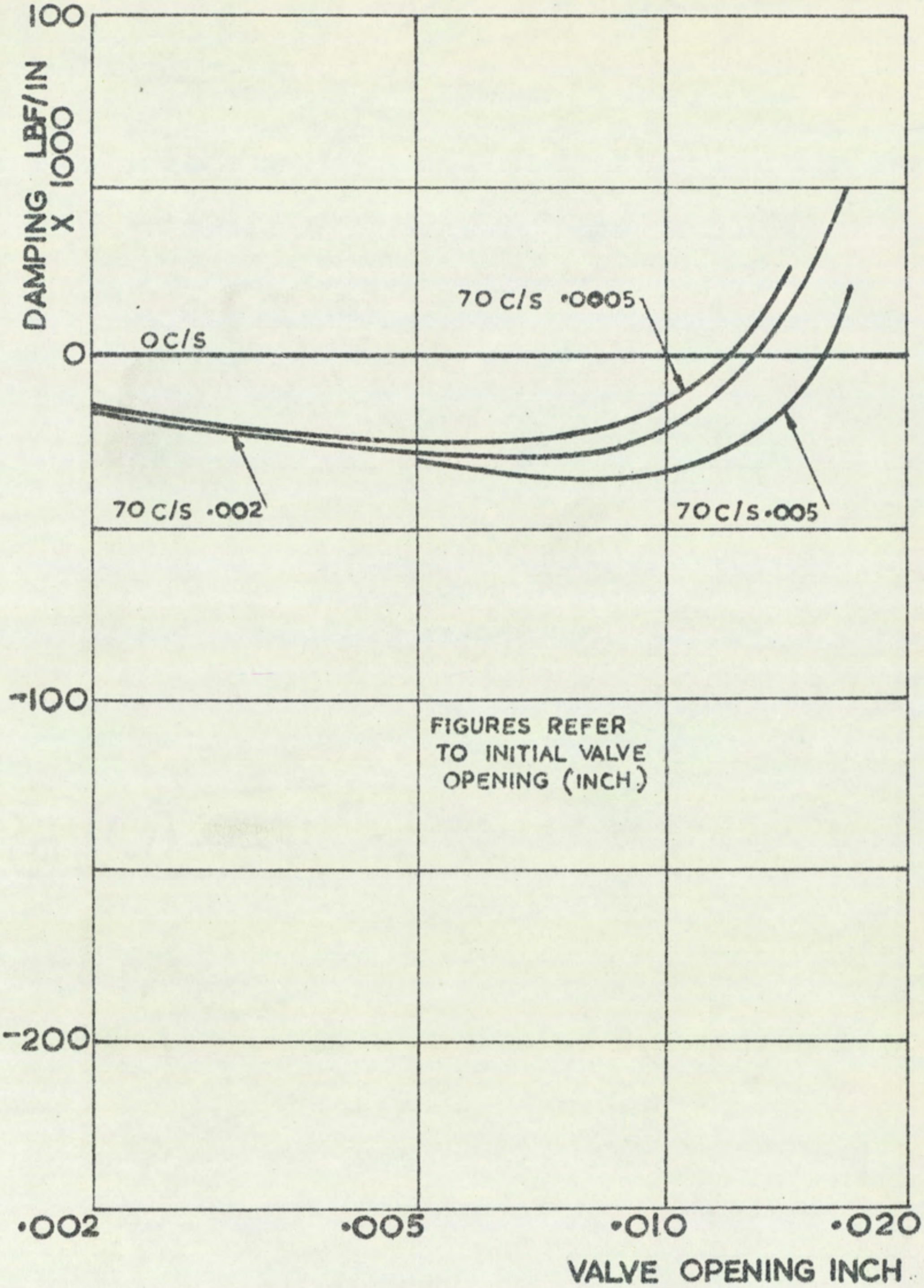

THEORETICAL DAMPING CURVES

EFFECT OF VARIATION OF BOUNDARY CONDITIONS

FIG 4.14

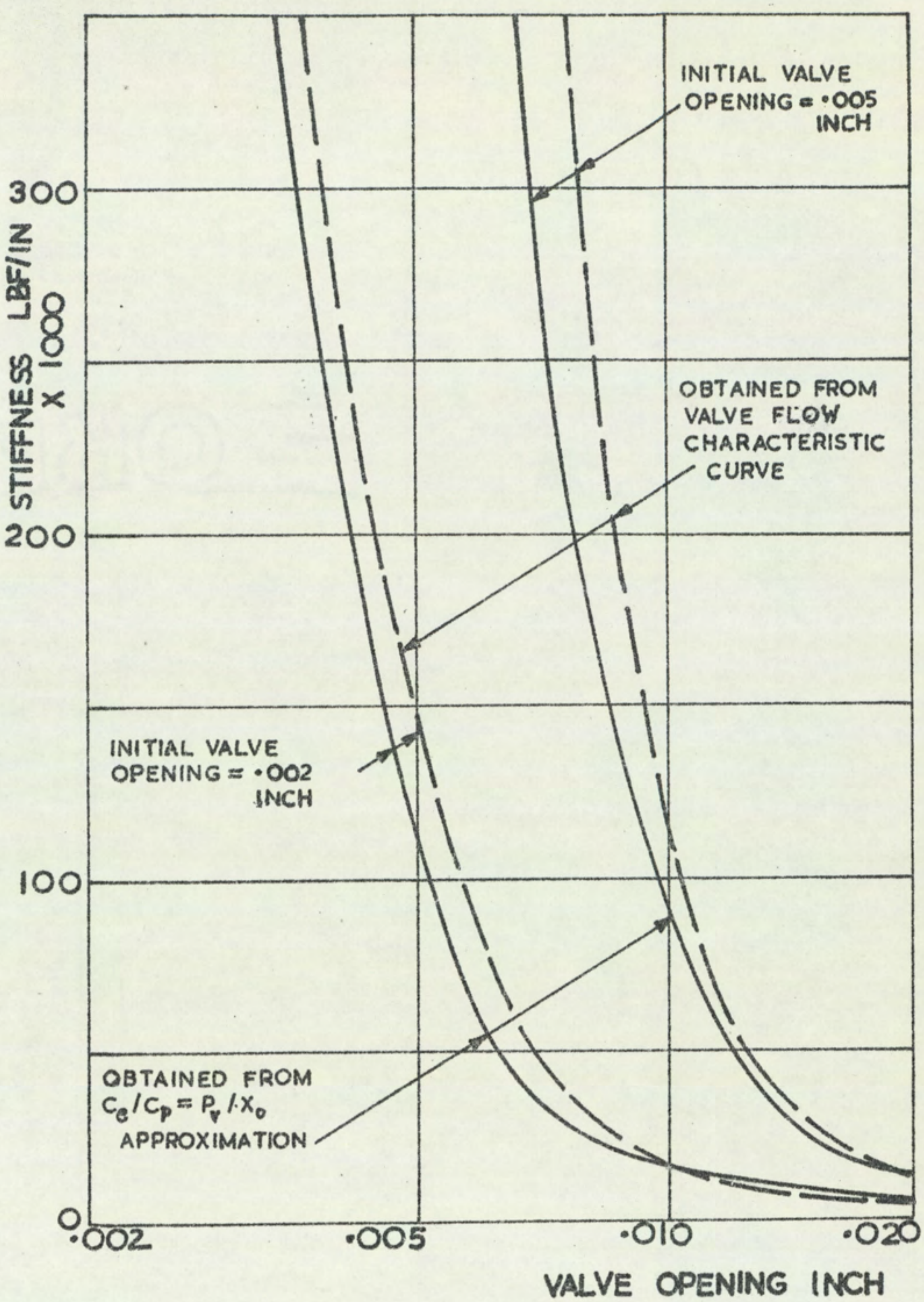

THEORETICAL STATIC STIFFNESS CURVES

NO LEAKAGE

FIG 4.15

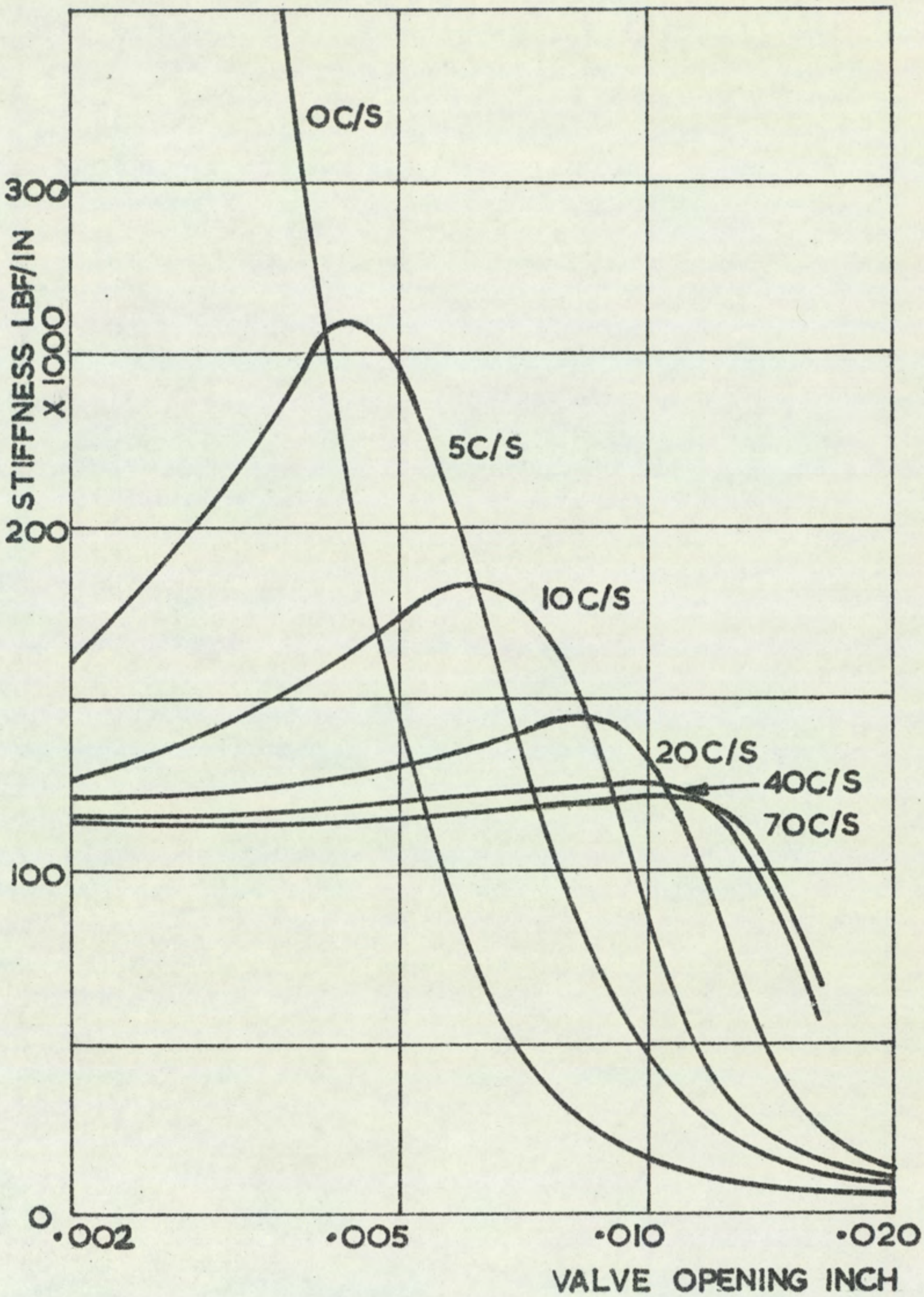

THEORETICAL STIFFNESS CURVES
NO LEAKAGE

FIG 4.16

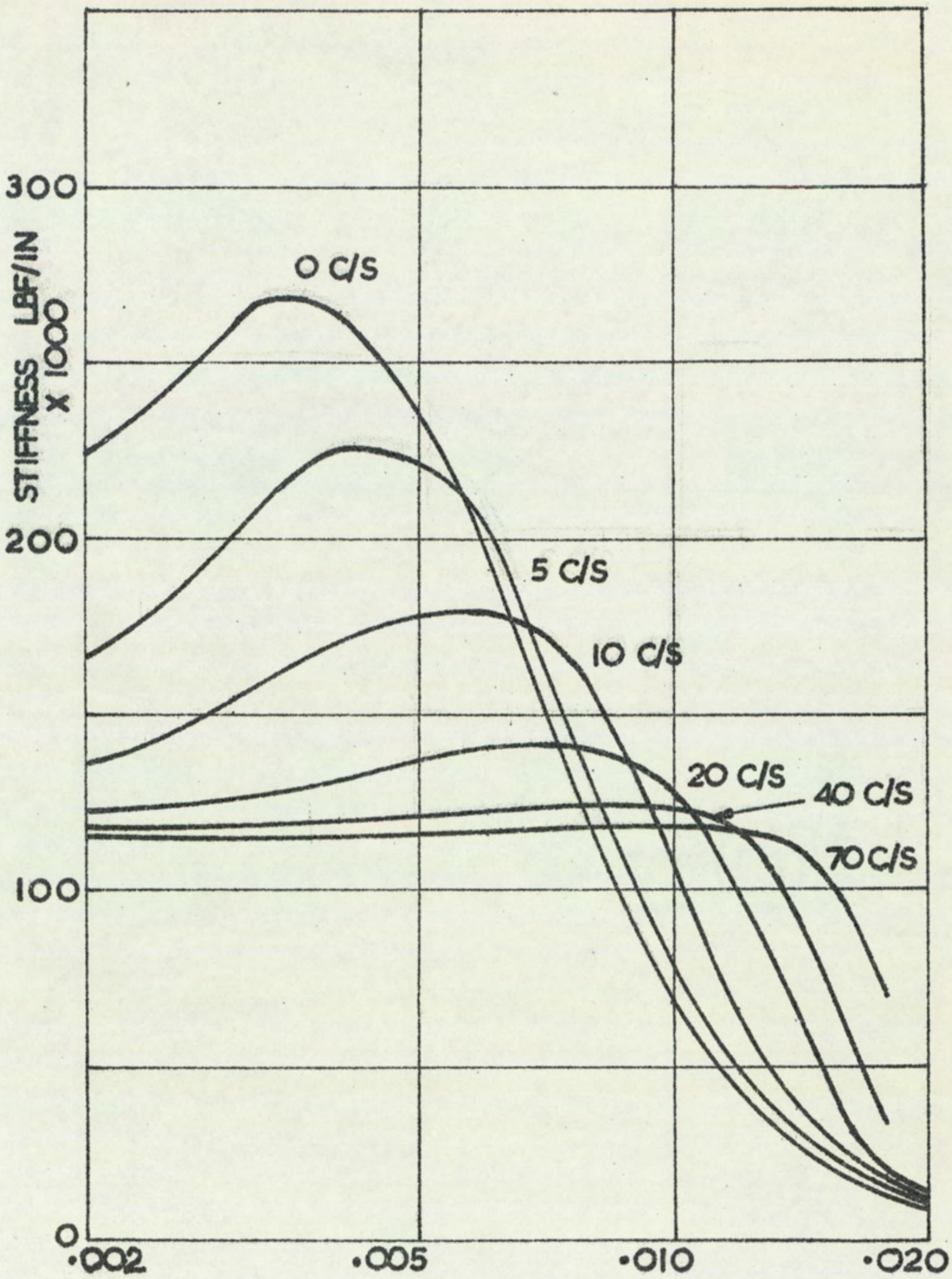

THEORETICAL STIFFNESS CURVES
LEAKAGE COEFF = 8×10^{-5} IN^5/LBF SEC

FIG 4.17

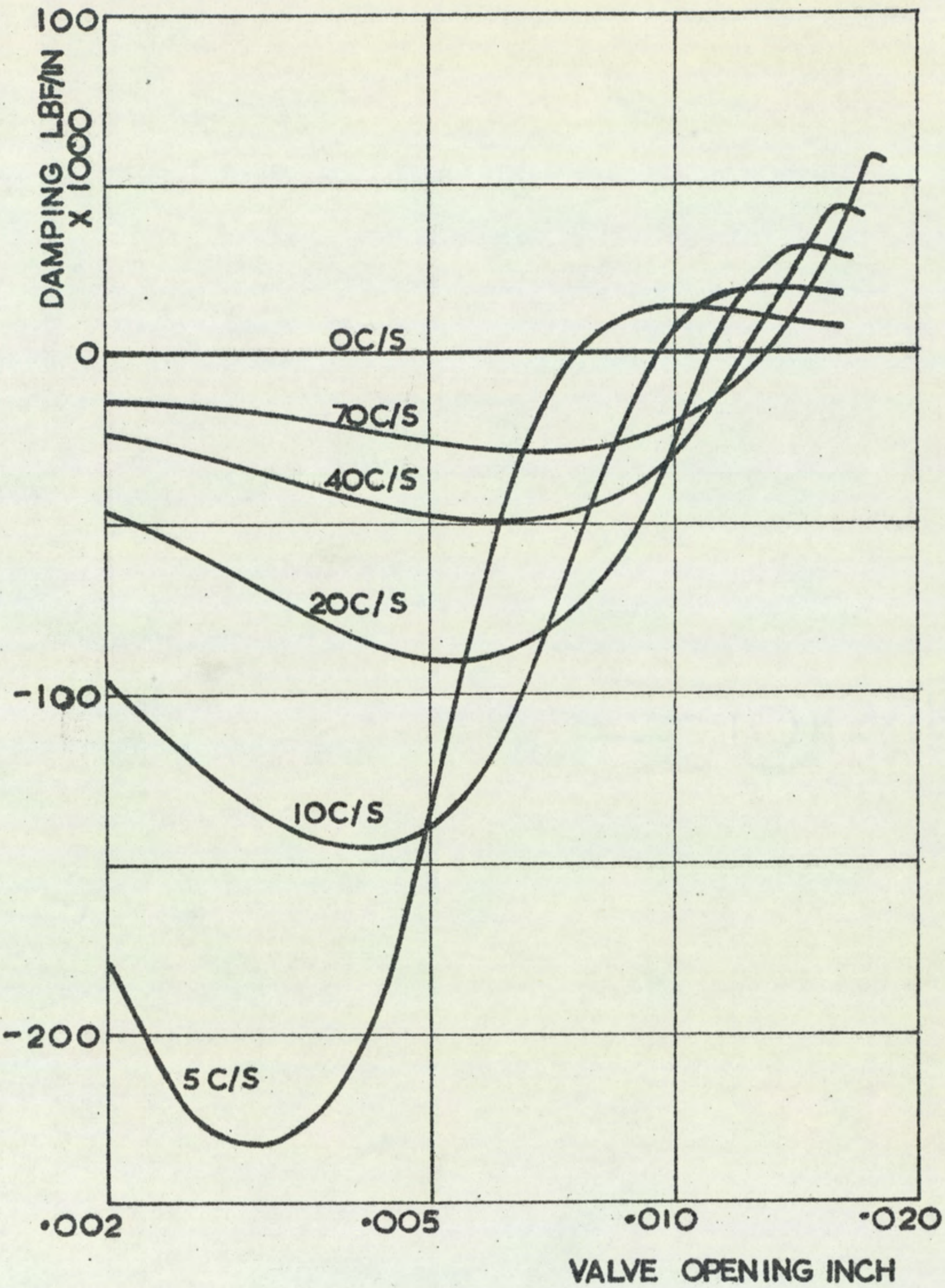

THEORETICAL DAMPING CURVES
NO LEAKAGE

FIG 4.18

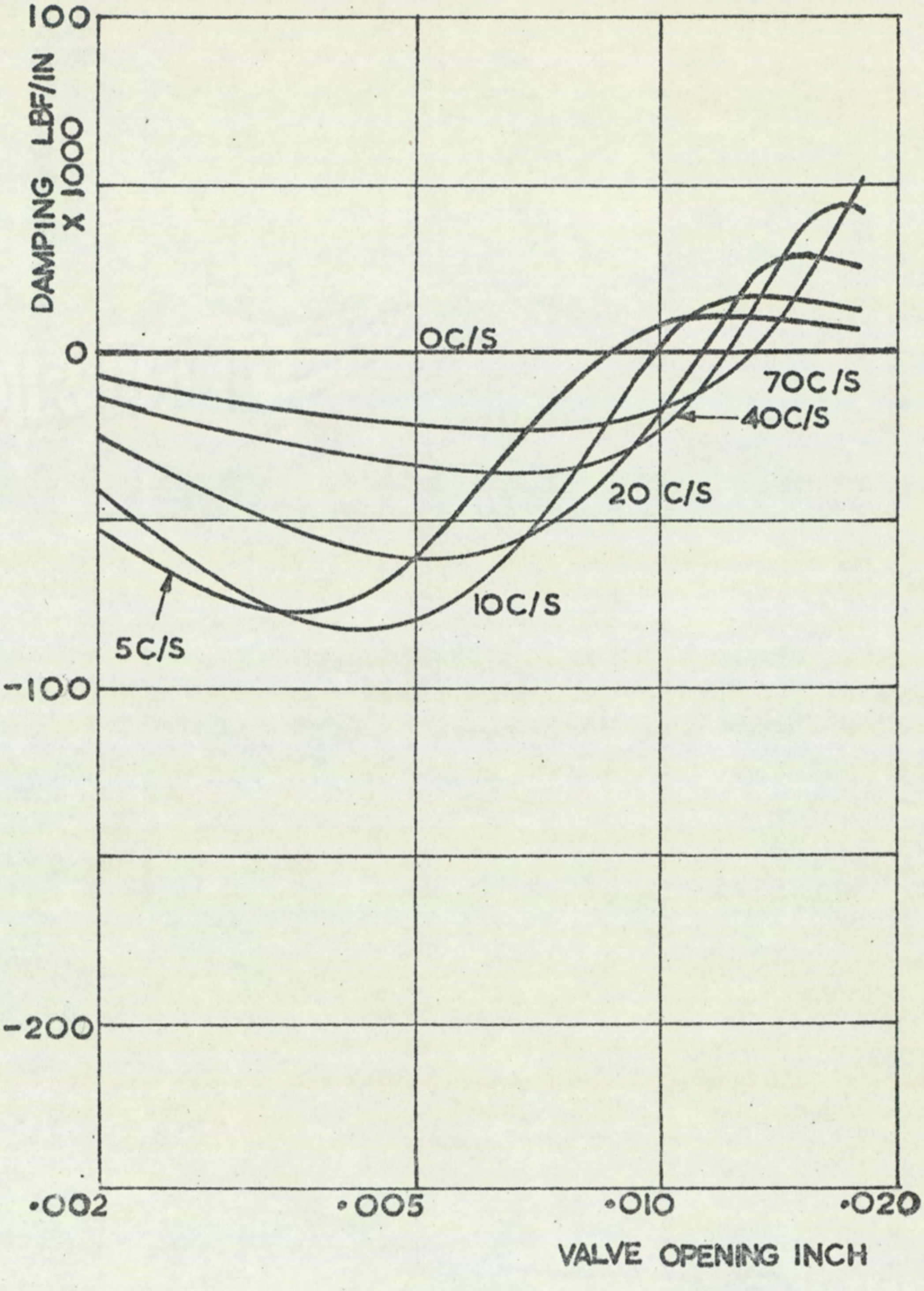

THEORETICAL DAMPING CURVES
LEAKAGE COEFF = 8×10^{-5} IN^5/LBF SEC

FIG 4.19

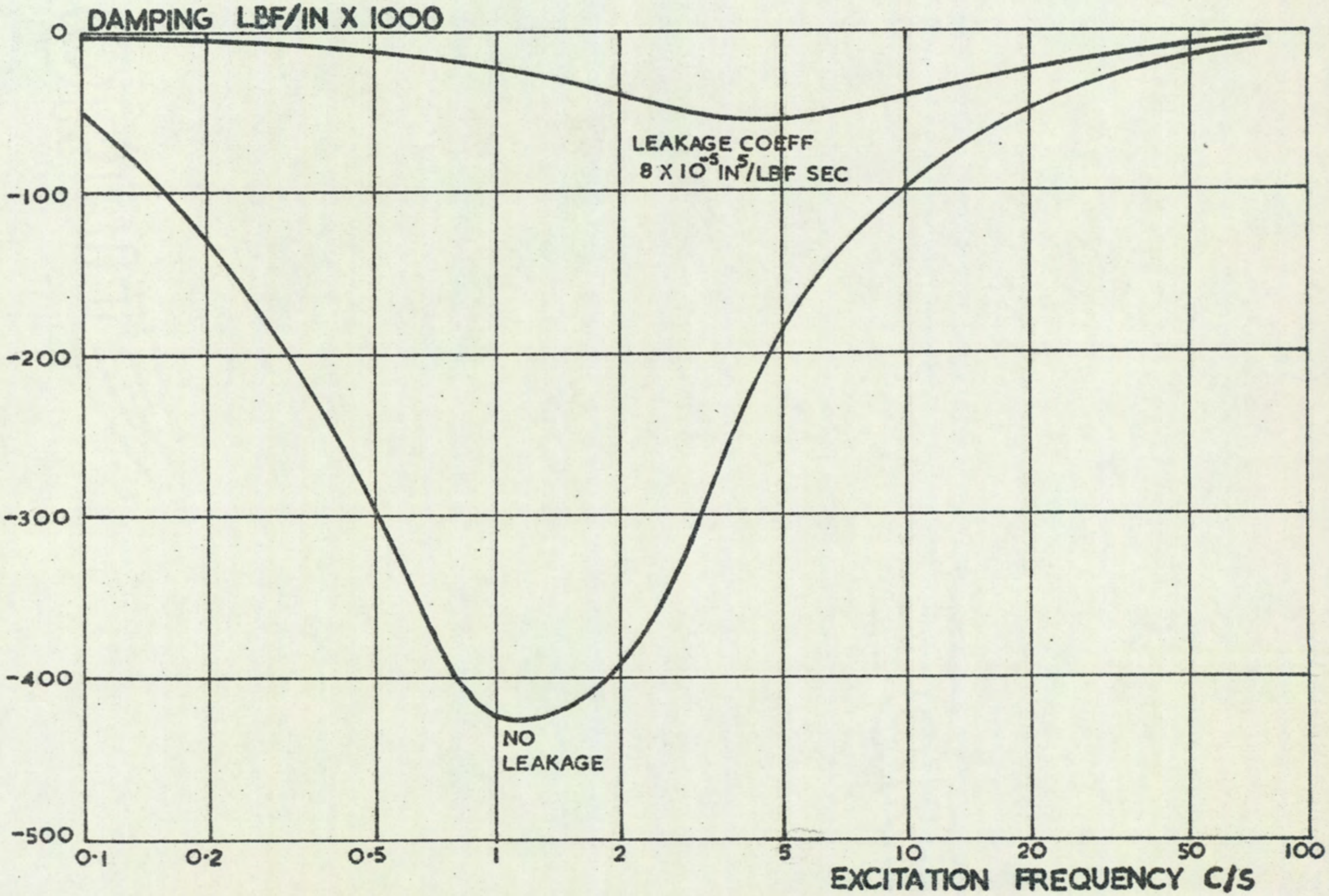

VARIATION OF DAMPING WITH EXCITATION FREQUENCY.

VALVE OPENING = ·002 INCH

FIG 4.20

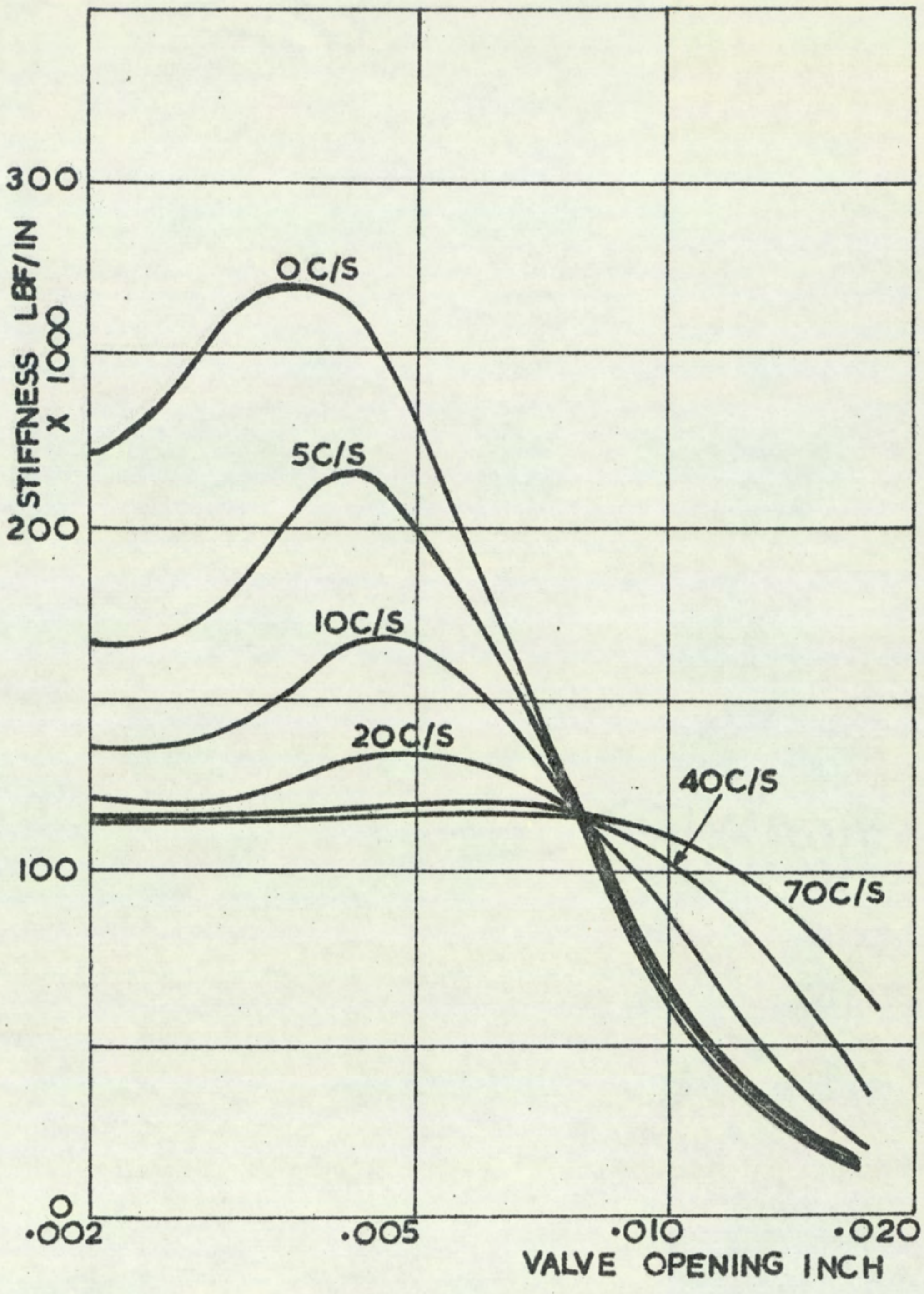

THEORETICAL STIFFNESS CURVES CALCULATED FROM STATIC $P_v - X_o$ RELATIONSHIP.
LEAKAGE COEFF. = 8×10^{-5} IN^5/LBFSEC.

FIG 4.21

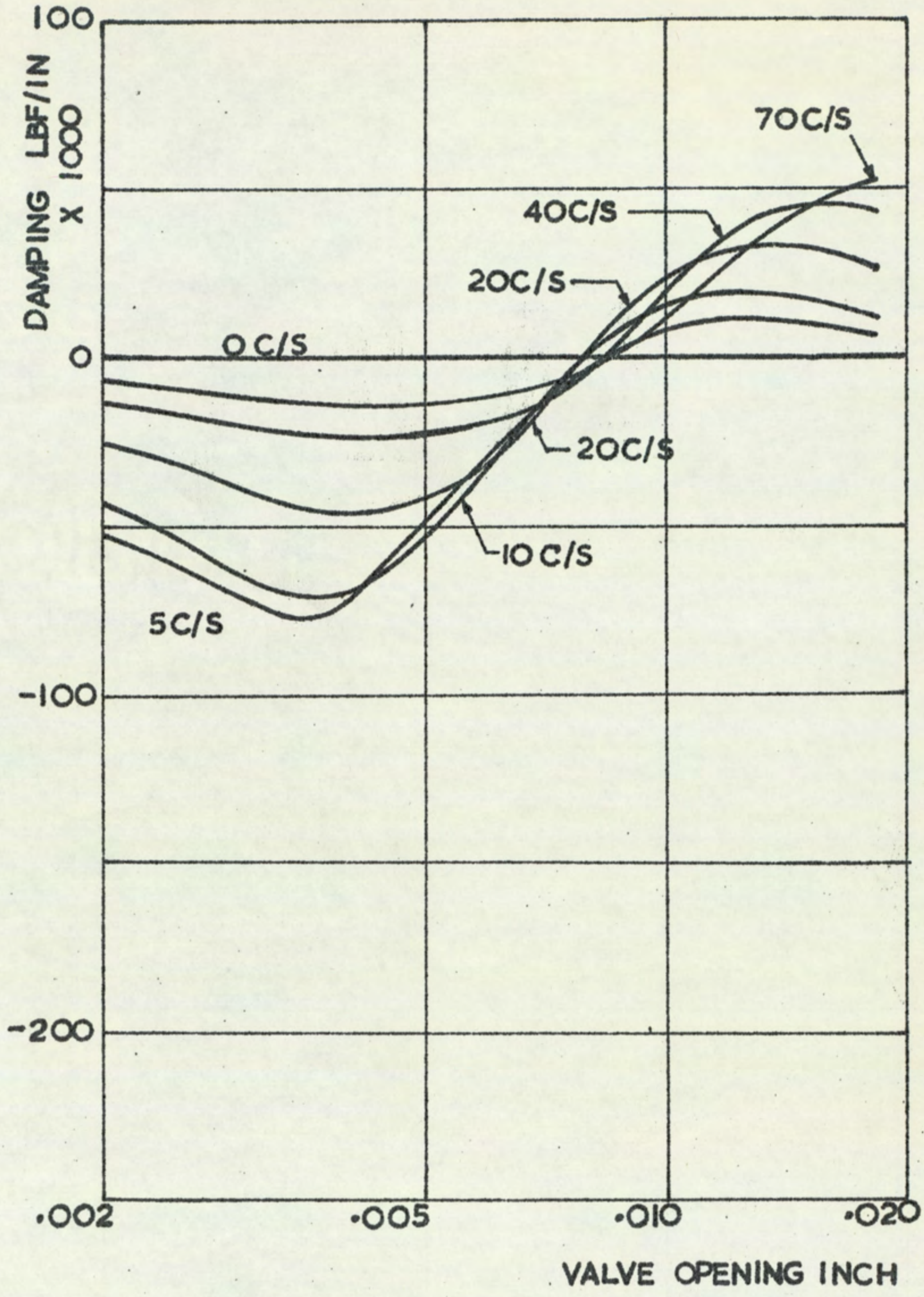

THEORETICAL DAMPING CURVES CALCULATED FROM STATIC $P_v - X_o$ RELATIONSHIP.
LEAKAGE COEFF. = 8×10^{-5} IN^5/LBFSEC.

FIG 4.22

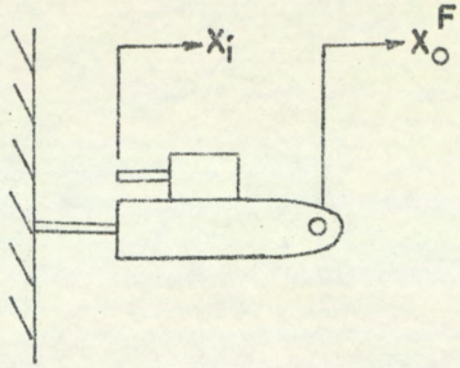

(A) SERVOMECHANISM EXCITED AT ITS VALVE INPUT WITH OUTPUT END FREE

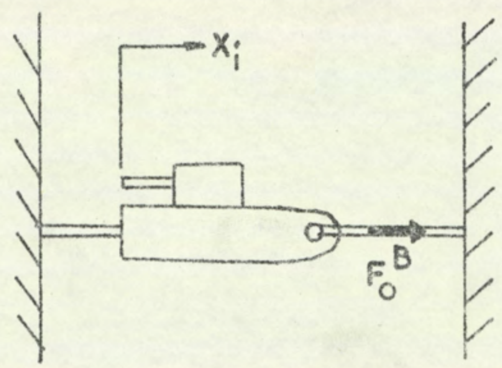

(B) SERVOMECHANISM EXCITED AT ITS VALVE INPUT WITH OUTPUT END BLOCKED

EXCITATION OF SERVOMECHANISM
VALVE INPUT

FIG 4.23

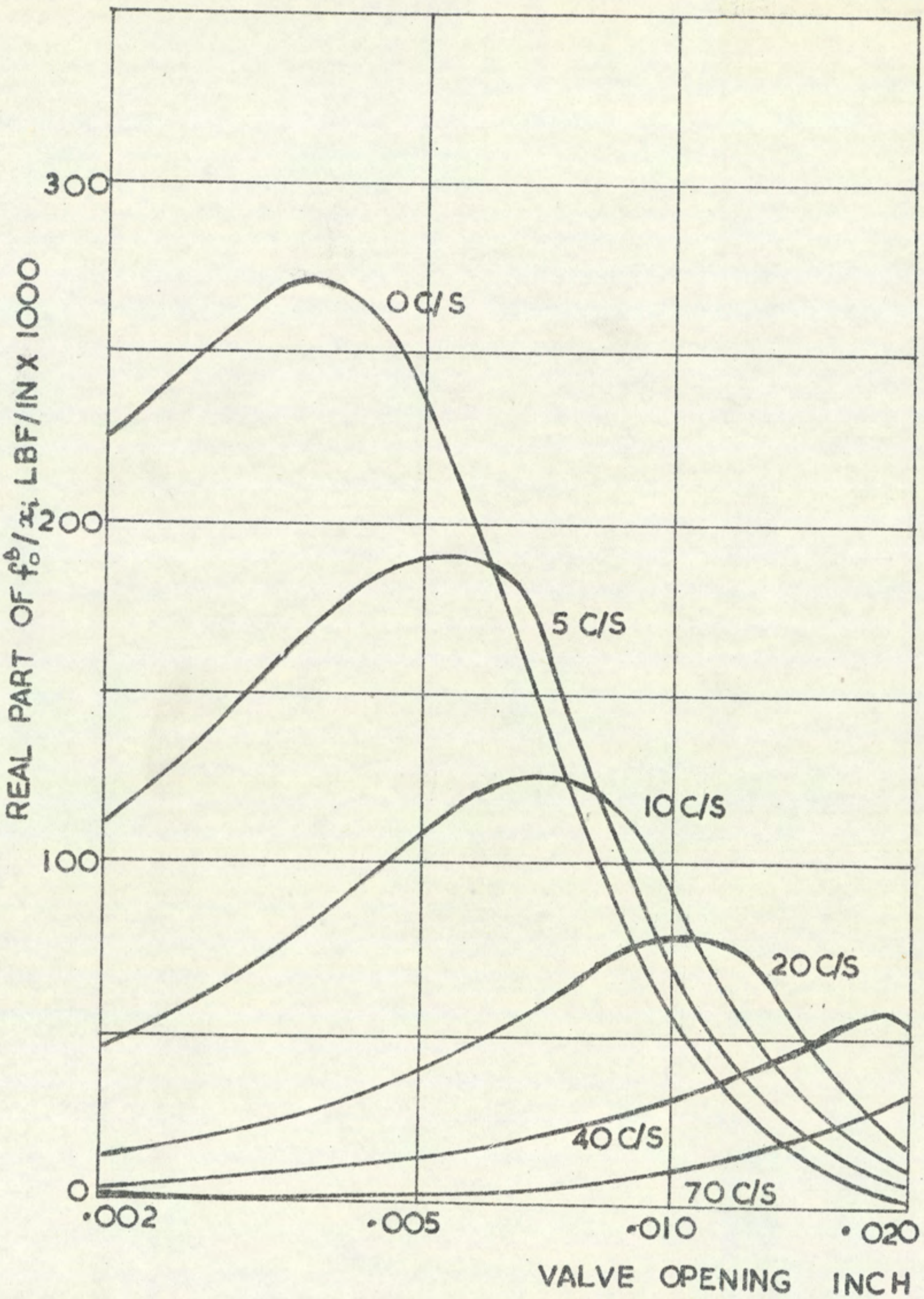

THEORETICAL CURVES FOR REAL PART OF f_o^B/x_i
LEAKAGE COEFF.= 8×10^{-5} IN^5/LBF SEC

FIG 4.24

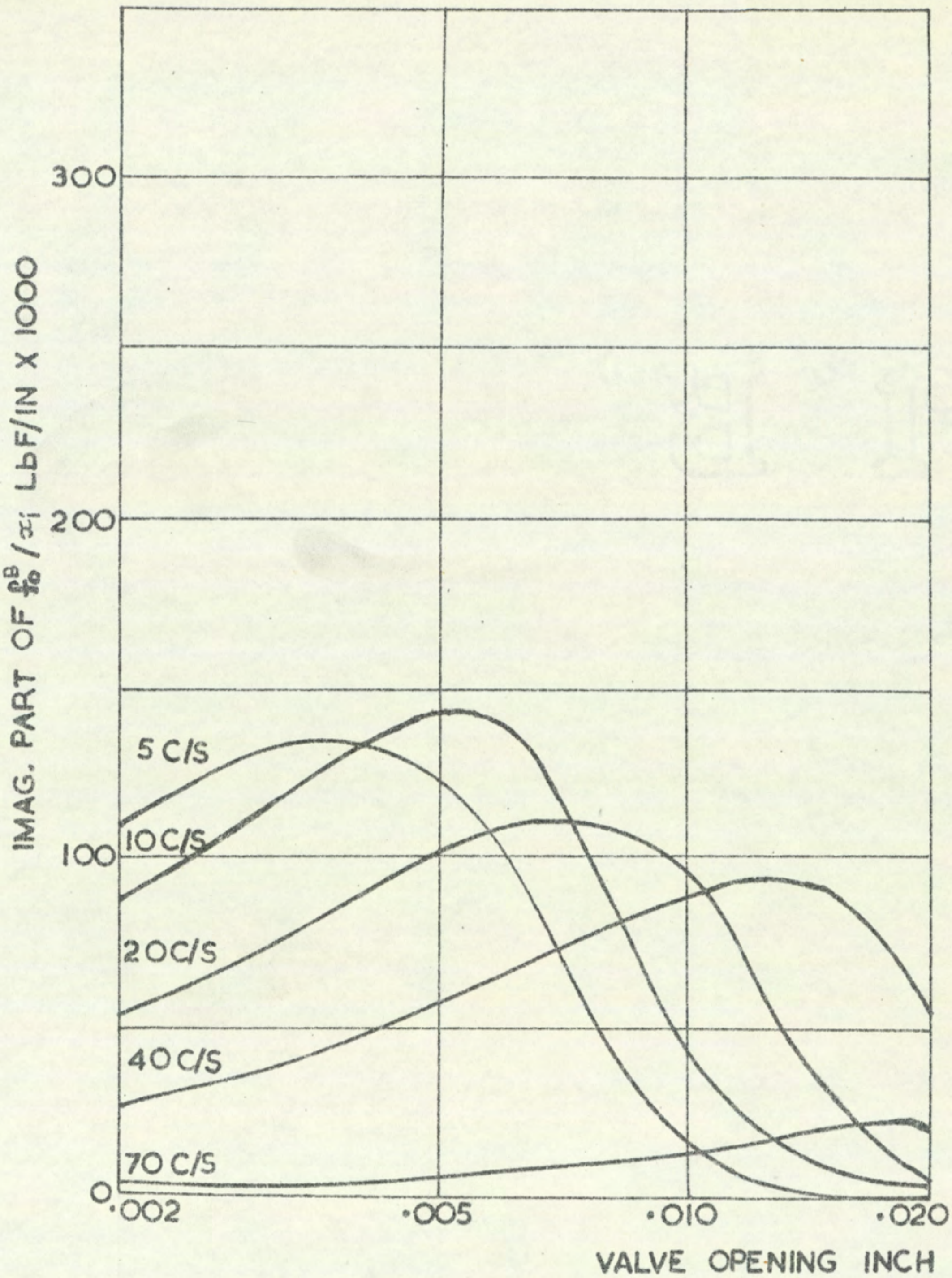

THEORETICAL CURVES FOR IMAG. PART OF f_o^B/x_i
LEAKAGE COEFF. = 8×10^{-5} IN^5/LBF SEC

FIG 4.25

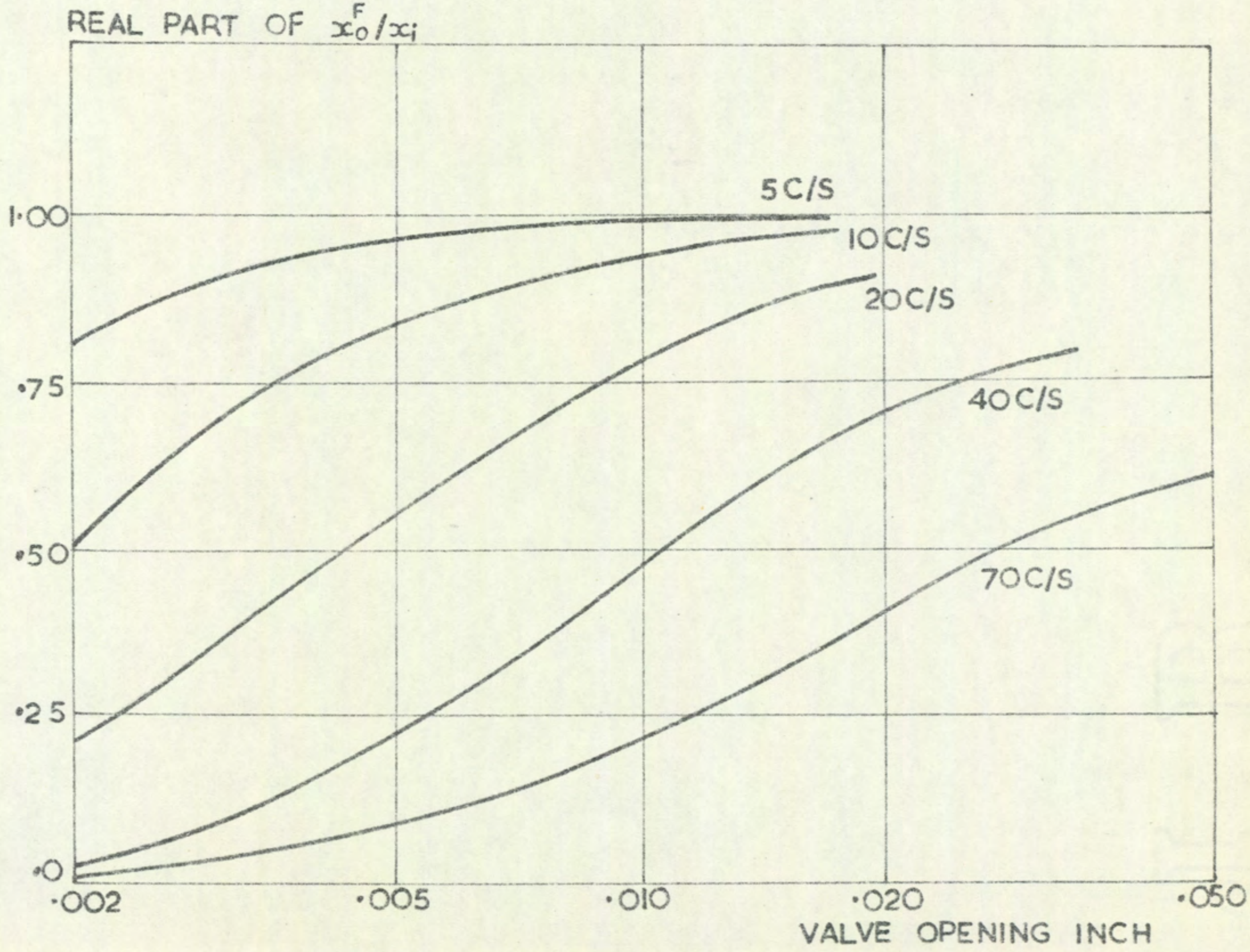

THEORETICAL CURVES FOR REAL PART OF x_o^F/x_i

FIG 4.26

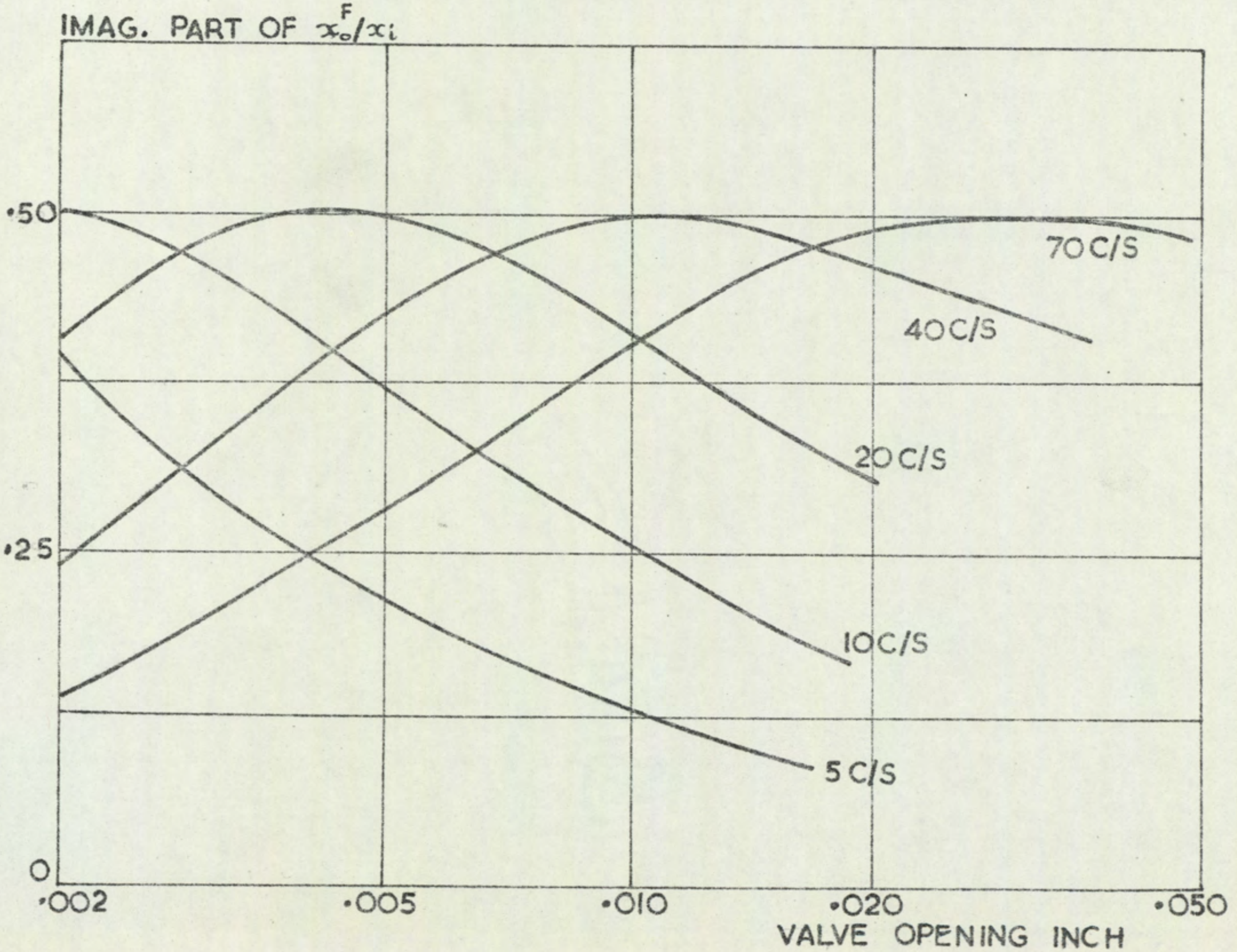

THEORETICAL CURVES FOR IMAG. PART OF x_o^F/x_i

FIG 4.27

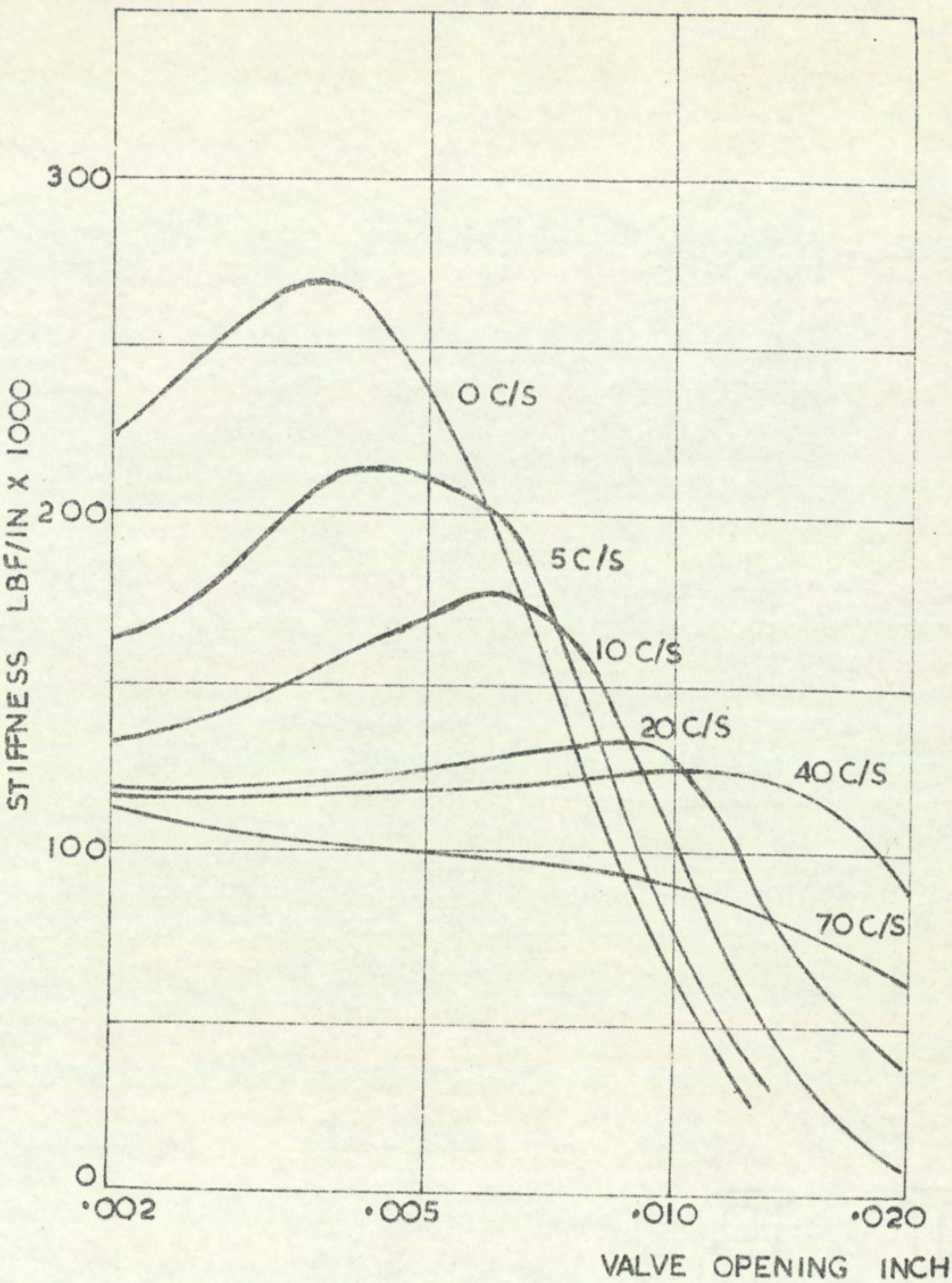

THEORETICAL STIFFNESS CURVES

VALVE INPUT EXCITATION

LEAKAGE COEFF. = 8 X 10^{-5} IN^{5}/LBF SEC

FIG 4.28

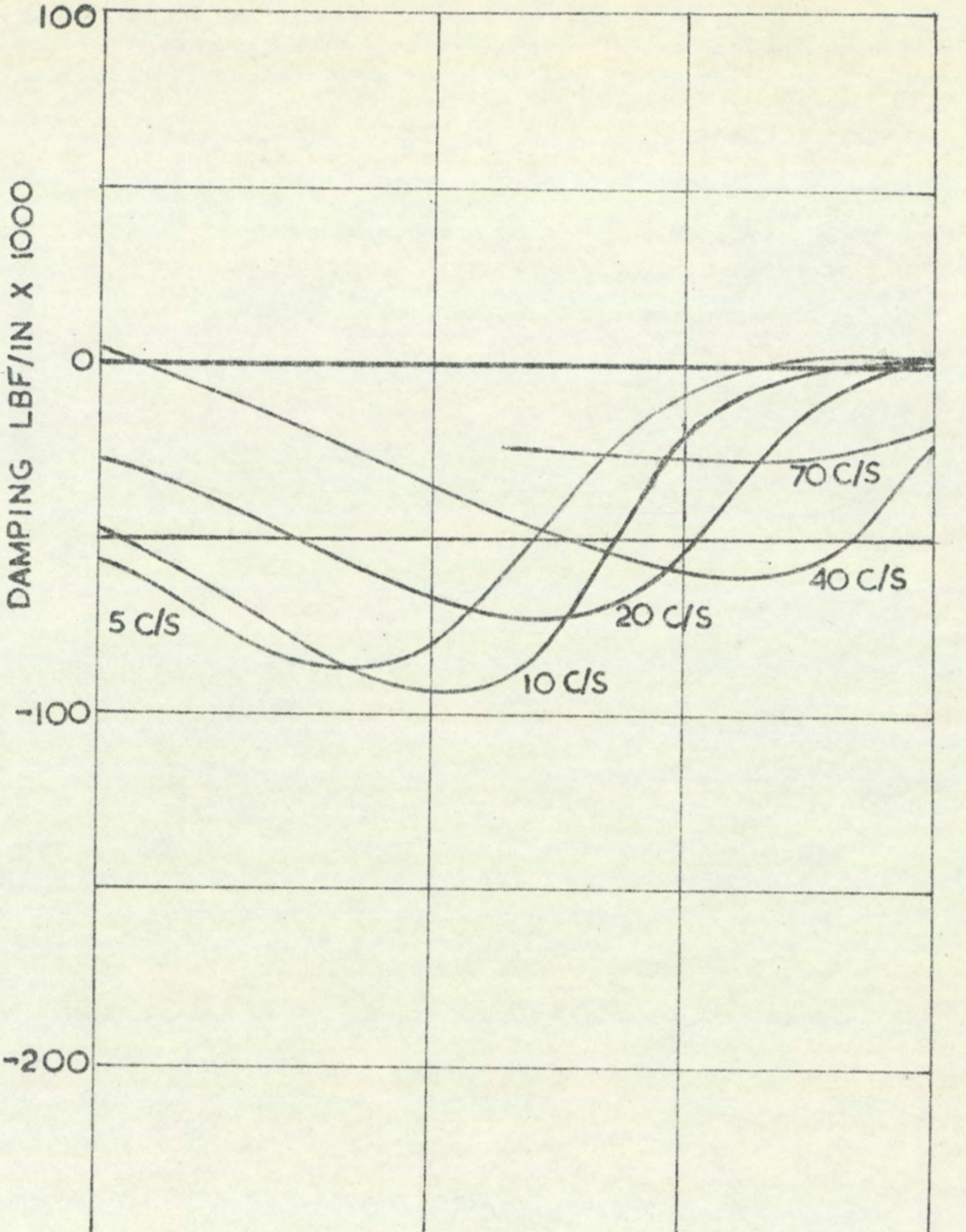

THEORETICAL DAMPING CURVES
VALVE INPUT EXCITATION
LEAKAGE COEFF. = 8×10^{-5} IN^5/LBF SEC

FIG 4.29

CHAPTER V

Experimental determination of the impedance of a servomechanism in a rigid environment by excitation of its output end.

The experimental work done to determine the impedance of the servomechanism by the excitation of its output end is described and the results discussed. A comparison is drawn between these results and the theoretical predictions made in the previous chapter.

5.1 Calibration of transducers and instrumentation.

Load cell: The load cell was calibrated in a Denison 2000 lbf tensile test machine. The calibration, which included the gain of the DC pre amplifier, was found to be 0.352 mV/lbf.

Displacement transducer: The transducer was calibrated by means of a micrometer head mounted integral with it. The calibration was set at 5 V/in.

Amplitude and phase response of the instrumentation: A signal from an oscillator was fed into the force circuit DC pre amplifier and the output from the circuit was compared with the oscillator signal to ascertain that the amplitude response was constant and the phase lag was zero in the frequency range DC to 100 c/s. This was found to be the case. The test was then repeated to check the response of the displacement measuring circuit. It was not possible to check the response of the oscillator/demodulator and consequently the test signal was fed into the filter. The test showed that the amplitude response was constant and the phase lag zero.

5.2 Large amplitude low frequency excitation tests.

In order to investigate the behaviour of the servomechanism when excited at the output end with the valve input locked, very low frequency tests were performed. Initially an attempt was made to measure the static stiffness of the servomechanism but this was found to be virtually impossible in practice because of creep which was due to leakage. Lambert and Davies (16) have shown that the combined effects of valve overlap, Coulomb friction, leakage and silting up of the valve clearances can cause a low frequency instability or relaxation oscillation.

To overcome this difficulty the servomechanism was excited at a very low frequency with a large displacement amplitude, the force/displacement relationship being displayed using the X-Y plates of the oscilloscope. A series of still photographs were taken, a selection of which are shown; Figs, 5.1, 5.2 & 5.3.

5.3 Measurement of Coulomb friction.

(a) Static tests: Coulomb friction within the jack was measured in the following manner. The jack was fixed to a base plate and the valve locked in the fully open position. In order to make seal friction realistic, the seals were pressurised by the hydraulic supply which was connected to both the inlet and exhaust ports of the valve at half the normal supply pressure. A weight hanger was connected to the piston rod by a cable passing over a low friction pulley. A displacement transducer was fixed between the moving piston and earth. Since both sides of the equal area piston were pressurised equally, the externally applied force had only to overcome the friction force to cause motion to take place. Using an ultra violet recorder a trace of displacement against time was obtained for various applied loads. A graph of load against velocity was drawn, the intercept on the force axis representing Coulomb friction force. The test was repeated for various supply pressures. The force/velocity graph is shown in Fig. 5.4.

(b) Dynamic tests: Using the experimental rig as described in Section 3.1, low frequency tests were performed on the servomechanism. The servomechanism, which had the valve locked fully open and the fluid supply at a pressure of 1500 lbf/in^2, i.e. half pressure, connected to both the inlet and exhaust, was excited at 0.2 c/s over a small displacement; the output signals from the load and displacement transducers being displayed against time on the oscilloscope. The displacement signal was sinusoidal, but the force signal was trapezoidal in form, i.e. a distorted square wave. Variation of the input displacement in the range 0.006 in. to 0.028 in. peak to peak, had virtually no effect on the force which remained constant with an amplitude of 150 lbf. peak to peak, i.e. a Coulomb friction force of 75 lbf.

(c) Large amplitude low frequency excitation tests: This experiment has been previously described in Section 5.2. A horizontal overlap, caused by the effect of friction forces is shown in Figs. 5.1, 5.2 and 5.3, the load increment representing twice this force.. The value of this force scaled off the diagram was found to be approximately 160 lbf., i.e. a frictional force of 80 lbf.

5.4 Measurement of impedance by means of small perturbations.

Experiments were performed with the servomechanism piston in the mid stroke position. Before testing commenced it was necessary to select either force or displacement feedback. In the force feedback mode the force applied to the servomechanism could be controlled between zero and the maximum force output of the servomechanism, 1860 lbf., but in practice a force of more than about 80 per cent maximum was not applied to the servomechanism since with larger forces there was a danger that the valve would suddenly become fully open. When this occurred damage to the valve could be caused since with force feedback there was no position control. This restriction presented no difficulties because the prohibited region could be investigated in the displacement feedback mode. In this mode the displacement across the servomechanism was controlled.

When Test Series' I to V were originally performed the Transfer Function Analyser described in Section 3.6 was used to measure impedance. When the Automatic Mechanical Impedance Analyser described in Section 3.7 became available, Test Series' I to V were repeated to verify that both analysis systems gave the same result. Test Series VI was analysed using the system described in Section 3.8.

Tests were performed in the frequency range 5 - 70 c/s, the oscillatory force applied to, and the oscillatory displacement across the servomechanism being measured under various conditions as follows:-

Test Series I : The valve was locked to earth using the cantilever extension fixed to the main test rig as shown in Fig. 3.3a. Controlling the vibrator with displacement feedback, tests were performed with static valve openings in the range 0.002 in. to 0.050 in., perturbation amplitudes of ± 0.002 in., ± 0.005 in. and ± 0.010 in. being used. Tests were also performed with the valve opened 0.030 in. and 0.040 in. using a perturbation amplitude of ± 0.020 in.

Test Series II : These tests were identical to those performed in Test Series I except that the valve was locked to earth via the cross bar on the piston rod for this and all subsequent tests. During these tests selected force and displacement signals were recorded on tape for harmonic analysis using the analysis system described in Section 3.9.

Test Series III : The vibrator was controlled by force feedback and tests were performed with a static force varying from 0 to 1550 lbf. applied to the servomechanism and a perturbation amplitude of 200 lbf. and 500 lbf.

Test Series IV : Test Series II was repeated with a non-return valve fitted 2 ft. from the servo valve inlet port.

Test Series V : In order to examine the effect of operating the servomechanism with the jack piston not in the mid stroke position, the piston was offset by a $\frac{1}{2}$ inch making the ratio of the chamber volumes equal to 9 : 4. Under these conditions Test Series II was repeated.

Test Series VI : The system was excited by a random signal, the vibrator being controlled by displacement feedback. Tests were performed with a valve opening of 0.040 in., in order that a comparison could be made between the impedance measurements obtained from the power spectral analysis of the random signals and the impedance measurements obtained from sinusoidal excitation of the system under otherwise identical conditions.

Test Series VII : The system was excited by a random signal, the vibrator being controlled by displacement feedback. Tests were performed with the static valve openings in the range 0.002 in. to 0.050 in. The force and displacement signals were not analysed to obtain the signal power spectral densities, instead average levels were measured using a valve voltmeter. Average perturbation amplitudes of $\pm$ 0.002 in., $\pm$ 0.004 in. and $\pm$ 0.008 in. were employed.

5.5 Discussion of results obtained from static tests.

The force-displacement curves for the servomechanism obtained at three differing excitation frequencies, Figs. 5.1, 5.2 and 5.3, all exhibit certain hysteretic effects. In Section 5.3c the cause of the vertical separation when the valve opening was large has been attributed to the effect of Coulomb friction force present between the jack piston and body, but the cause of the horizontal separation is difficult to explain in a satisfactory manner. It may be caused by a valve overlap effect but the phenomena will have to be the subject of further investigation before a definite conclusion can be reached.

The force-displacement curves show that the $F_o - X_o$ relationship varies with excitation frequency, the $F_o - X_o$ curve becoming more rounded as the frequency increases. From this it may be deduced that the $P_v - X_o$ relationship will be varied also, since $F_o/A = (P_s - P_v)$. This verifies the prediction made in Section 4.16 where it was shown that the $P_v - X_o$ relationship varied with frequency.

A comparison of the diagrams obtained working under force or displacement feedback control show no significant differences. Under displacement feedback control the horizontal parts of the curves were controlled, the servomechanism tending to 'jump' between the two controlled conditions. In the force feedback mode the vertical sections of the curves were controlled, the servomechanism becoming unstable outside of this range. This problem has already been referred to in Section 5.4.

5.6 Discussion of results obtained from the measurement of Coulomb friction .

The Coulomb friction present between the jack piston and body has been measured by a variety of methods as previously described. The results are summarised thus:

(i) From static test rig [Sect. 5.3a] = 18-30 lbf

Dependent on pressure.

(ii) From dynamic test rig [Sect. 5.3b] = 75 lbf

(iii) From static stiffness test [Sect. 5.3c] = 80 lbf

Note: (ii) & (iii) - Tests performed on same jack.

(i)- Test performed on jack of same design and type as tests (ii) & (iii).

The following values of Coulomb friction have been used by other workers:

Glaze (12) Breakaway 150 - 200 lbf

Running 125 - 175 lbf

Dependent on pressure.

Lambert and Davies (13)		150 lbf
Lambert and Davies (16)	Breakaway	200 lbf
	Running	100 lbf

Although these figures refer to differing designs and sizes of jack, they are, with the exception of (i), of the same approximate magnitude. The lower values obtained by experiment compared with the figures used by other workers may be due to the combined effects of a smaller jack and the use of low friction seals.

The experimental investigations show that a Coulomb friction force of 50 lbf approximately was present between the servo piston and body. This is, however, clearly an over simplification of the situation since the force acting between the piston and body would be composed of a variety of components. These would include Coulomb friction, seal deformation and viscous effects, etc. The investigations do serve, however, to give an approximation to the size of the friction force which might be expected.

5.7 Effect of the method of valve earthing.

A comparison of results obtained under similar conditions during Test Series' I and II shows that a good agreement was obtained. This indicated that the two methods of locking valve to earth (described in

Section 3.1) were equally suitable. Furthermore, since one method connected the valve directly directly to earth, i.e. the rig, whereas the other one connected the valve to earth via the piston rod and latch, it may be concluded that the effect of any flexibilities in the latch or anchorage was negligible.

5.8 Harmonic analysis of the force and displacement signals.

The harmonic analysis curves for typical force and displacement signals obtained from Test Series II are shown in Figs. 5.5 & 5.6. It is seen that the components of frequency of the second and higher harmonics were very small compared to the fundamental. This demonstrates the unsuitability of an attempt to measure the impedance of the system at frequencies other than the fundamental frequency of excitation. Attempts have been made to do this but even the use of the third harmonic frequency results in errors of up to 50 per cent compared to the value obtained from exciting the system at the frequency of the third harmonic and taking values of force and displacement from the fundamental components. The harmonic analysis curves show that only relatively small amounts of distortion were present in the signals analysed.

5.9 Discussion of the results obtained from the measurement of impedance.

It has already been stated that tests were carried out with the vibrator controlled by a feedback signal proportional to the force applied to, or the displacement across the servomechanism, depending upon the region of the $F_o - X_o$ curve under investigation. It should be noted that when the system was being controlled by force feedback the static force applied to the system was accurately controlled and known. This force, however, caused a valve opening in the region of zero to 0.005 in. Thus, the results obtained under force feedback control can be considered as an extension of those obtained under displacement feedback.

The stiffness curves under four different conditions are shown in Figs. 5.7 to 5.10 inclusive. The measured stiffness was adjusted by adding an appropriate $m\omega^2$ term to compensate for the inertial forces in the linkage connecting the vibrator and load cell to the servomechanism. If Figs. 5.7 and 5.8 or Figs. 5.9 and 5.10 are compared with Fig. 4.17 it is seen that the basic shape of the experimental and theoretical curves are in agreement. At low frequency the stiffness, whether measured under force or displacement feedback control, never reached the large value predicted by the theoretical analysis. In fact, when the vibrator was controlled by a force feedback signal, i.e. the valve opening was very small, the difference between the stiffness obtained at 5 c/s and 70 c/s was so small that due to experimental errors the measured values of stiffness at various frequencies showed no trends, the results being completely intermingled. For this reason the graphs show the band in which the results lie.

The experimental damping curves are shown in Figs. 5.11 to 5.14 inclusive. Comparison between Figs. 5.12 or 5.14 and Fig. 4.19 shows that the experimental curves are of the same shape as the theoretical curves although the experimental peak damping for a given frequency tends to occur at a smaller valve opening than that predicted in the theory. The large negative damping which is predicted in the theoretical analysis when the valve opening was small, did occur in practice, but was much reduced in amplitude. Measurement of the amount of negative damping present in the system when the valve opening was small and excitation frequency was low, was found to be difficult and the negative damping apparently varied considerably from test to test for various reasons. It is possible that this variation in damping was caused by fluctuation in some parameter in the system which was not controlled or measured, e.g. hydraulic fluid temperature. Alternatively, the amount of damping may not vary and the apparent variation might be caused by inaccuracies in the measurement of such quantities as phase and valve opening. A small error in phase measurement could have a considerable effect upon the measured damping and the accurate measurement of the valve opening when this is small also presents problems as explained below.

A comparison between Fig. 5.13 and Fig. 4.19 shows that the predicted negative damping was present in the system when the vibrator was controlled by a force feedback signal, thus making the valve opening very small. When the perturbation was decreased, Fig. 5.11, the negative damping disappeared, this phenomena may have been caused by a valve overlap effect.

A general comparison between the theoretical and experimental results shows that only a qualitative agreement exists between them. One of the reasons for this must be due to a difficulty already mentioned, that of determining the steady state valve opening when the valve opening was small. In practice it was difficult to measure this because the valve neutral or zero position moved due to the low frequency relaxation oscillations within the overlap range as indicated by Lambert and Davies (16).

In Section 4.18 it is explained that the theoretical curves are calculated assuming an initial or boundary value of the valve opening X_{ob}. It was shown that the effect of this assumption was not to change the shape of the resulting impedance curves but merely to move their position along the X_o axis, and hence to introduce an error into the theoretically predicted impedance at any given valve opening. Another possible source of inaccuracy in the theoretical analysis involves the values of the coefficients C_e and C_p. These were evaluated from the valve flow characteristic curves, which themselves were determined experimentally and thus subjected to errors, for steady state conditions only. These conditions do not exist in practice.

The variation in stiffness and damping with frequency is shown in Figs. 5.15 to 5.18 inclusive, using the same data as used to construct Figs. 5.7 to 5.14 inclusive. A plot of valve opening against excitation frequency, Fig. 5.19, shows the region of stable and unstable operation of the servomechanism. The boundary condition, which was experimentally determined, is shown in this diagram.

5.10 Effect of perturbation amplitude.

Experimental results show that when the valve opening was large the measured values of damping and stiffness decreased with increase in perturbation amplitude as shown in Figs. 5.20 and 5.21. When the valve opening was small, however, this effect was not clearly defined, i.e. under some conditions the stiffness and damping increased with increase in perturbation amplitude and sometimes decreased with increase in perturbation amplitude.

One possible explanation for these observations may be deduced from the theoretical analysis of the effect of Coulomb friction on the impedance of the servomechanism. It is shown in equation (4.31) that the effect of the Coulomb friction force is to increase the damping component alone by $4F_c/\pi x_o$. As x_o, the perturbation amplitude, decreases, $4F_c/\pi x_o$ increases and so the measured value of damping increases. Since, when the valve opening is large the damping due to a small change in valve opening is small, the effect of a change in perturbation amplitude will virtually only change the value of $4F_c/\pi x_o$. When the valve opening is small the change in damping due to a small change in valve opening can be large, hence a change in the perturbation amplitude under these conditions can cause a positive or negative change in true damping irrespective of the change in $4F_c/\pi x_o$. Thus, although ideally the smaller the perturbation amplitude the more accurately can the damping be measured (since ideally damping and stiffness is the limit of $\delta F_o/\delta X_o$ as δX_o tends to zero) in practice this will cause the term $4F_c/\pi x_o$ to become large which results in misleading values for the system damping. It should be noted that $4F_c/\pi x_o$ can be very large, e.g. if $F_c = 50$ lbf., $X_o = 0.002$ in. then $4F_c/\pi x_o = 32{,}000$ lbf/in.

The experimental results depart from the theoretical predictions, however, in that the stiffness as well as damping is affected by perturbation size as previously stated. The vector diagrams for some conditions of valve opening and frequency have been drawn, Figs. 5.22 & 5.23. The measured value of impedance is the vector sum of the true impedance vector plus the friction force vector $4F_c/\pi x_o$. Thus the extremity or tip of the measured impedance vector should lie on the friction force vector. The measured impedance vector tip values lie quite close to the friction force vector as shown in Figs. 5.22 and 5.23 (broken line in diagrams). Hence as the perturbation amplitude decreases, the vector $4F_c/\pi x_o$ increases and the measured vector is rotated away from the true impedance vector. It is seen that the Coulomb force vector, which should be 90° out of phase relative to the stiffness vector, is in practice only about 45° out of phase. This indicates that the friction force is composed of components other than Coulomb friction. This fact has already been referred to, Section 5.6. The possibility that other non-linearities cause the variation in stiffness and damping with perturbation size cannot be excluded.

5.11 Discussion of the variations in stiffness and damping occuring at a frequency of approximately 30 c/s.

The variation of stiffness and damping with frequency is shown in Figs. 5.15 to 5.18 inclusive. It is seen that as the valve opening is increased the system damping peaks up above the general level at a frequency of 30 c/s. Similarly, the stiffness decreases at 25 c/s and increases at 35 c/s to a peak value before decreasing to the general level.

It has already been stated, Section 5.7, that the method of valve earthing had no effect upon the measured impedance. Thus, this unpredicted variation in stiffness and damping does not appear to have been caused by any factor in the mechanical environment.

When the tests were repeated with a non-return valve (NRV) in the hydraulic supply line, it was found that the variations in stiffness and damping occuring in the frequency range 25 - 35 c/s disappeared, see Figs. 5.24 and 5.25, suggesting that the cause of the variations was the hydraulic rather than the mechanical environment.

5.12 Discussion of the effect of the non-return valve.

As Test Series' II and IV were identical except for the non-return valve (NRV) in the fluid supply line, a direct comparison can be made between these tests to determine what effect if any the presence of the NRV had upon the impedance of the servomechanism. Apart from the effect discussed in Section 5.11 the NRV was found to have very little effect upon the system impedance. When controlled by displacement feedback neither the stiffness nor the damping was significantly affected although the system stiffness was marginally increased as shown in Figs. 5.24 and 5.26. The damping curves are shown in Figs. 5.25 and 5.27.

5.13 Effect of offsetting the servomechanism piston from the midstroke position.

Test Series' II and V were identical except that in Test Series V the servomechanism piston was offset from the midstroke position by a $\frac{1}{2}$ inch. A comparison between the measured values of the servomechanism stiffness and damping obtained from the two sets of experimental conditions shows that offsetting the servomechanism piston had no effect on the system impedance.

5.14 Comparison of random and sinusoidal excitation of the servomechanism.

A typical pair of power spectral density curves for force and displacement obtained from the random analysis system are shown in Figs. 5.28 and 5.29. A comparison between the values of impedance obtained from random excitation and sinusoidal excitation of the servomechanism is shown in Fig. 5.30. Apart from the type of excitation the test conditions were in all other respects identical. It is seen that at low frequency the random excitation of the system gives a lower impedance value than that of sinusoidal excitation, whilst at higher frequencies the situation is reversed. The most likely explanation of this phenomena is that although the signal generator produces a pure white noise signal, due to the sharp attenuation of the vibrator response with increase in frequency, the system under test is not excited by a pure white noise. Thus, at low frequency the servomechanism is excited by a random displacement which has a larger average amplitude in the frequency bandwidth at a low frequency than at high. This is equivalent to sinusoidal excitation with a larger perturbation size at low frequency than at high, resulting in a lower impedance value at low frequency than at high for reasons given in Section 5.10.

5.15 Wide band impedance.

By means of sinusoidal excitation of the servomechanism both stiffness and damping at various frequencies have been determined, as previously shown. The same result could be obtained by exciting the system with a random signal and analysing the force and displacement signals to determine their power spectral densities (PSD) and cross power spectral density (CPSD). If the force and displacement PSD's alone are determined, then information relating to phase is lost from the analysis and thus only the impedance vector value can be determined. In this investigation the CPSD could not be measured due to the inadequacy of the analysis equipment, for this reason the impedance (as opposed to stiffness and damping) was determined for various frequencies, as discussed in the previous section.

If the system was excited by a random signal and the average values of force and displacement measured using detectors having long time constants and wide band frequency responses, then the mean impedance of the system within the bandwidth of the excitation and the detectors can be determined. This has been done in Test Series VII, using an effective frequency bandwidth of 20 - 100 c/s and the results are shown in Fig. 5.31. If the wide band impedance is plotted together with the corresponding impedance determined using sinusoidal excitation at discreet frequencies, Figs. 5.32 and 5.33, it is seen that a good agreement exists between the two methods of excitation and analysis. This is of significance since it suggests that as the impedance varies more with valve opening than with frequency, random excitation provides a rapid method of investigating the impedance characteristics of the servomechanism by the measurement of the wide band impedance for various valve openings.

Excitation of the servomechanism during flight conditions is random in nature. The close comparison between the results obtained by random and sinusoidal excitation suggests that the results obtained from sinusoidal testing in the laboratory are applicable to flight conditions.

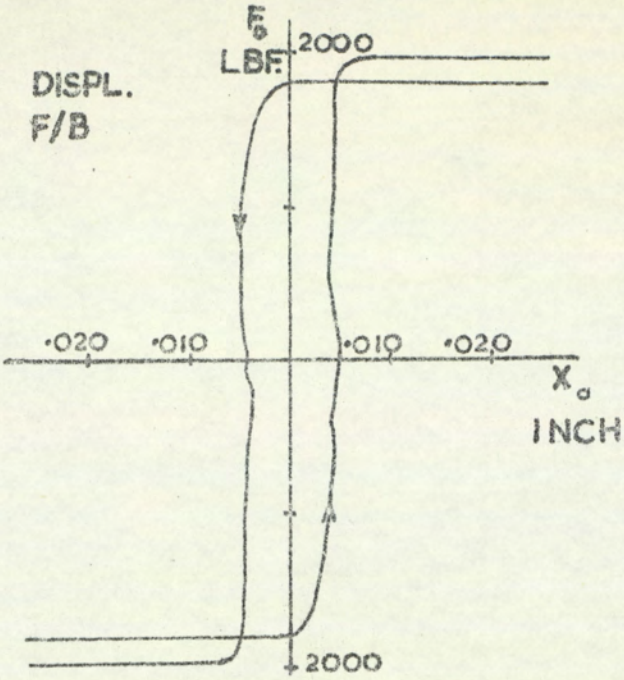

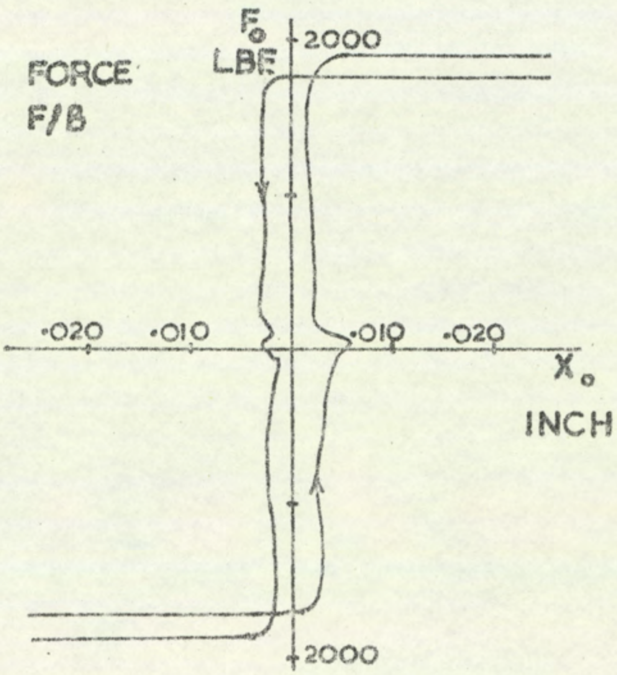

FORCE / DISPLACEMENT

LISSAJOU FIGURES

FREQUENCY 0·01 C/S

FIG 5.1

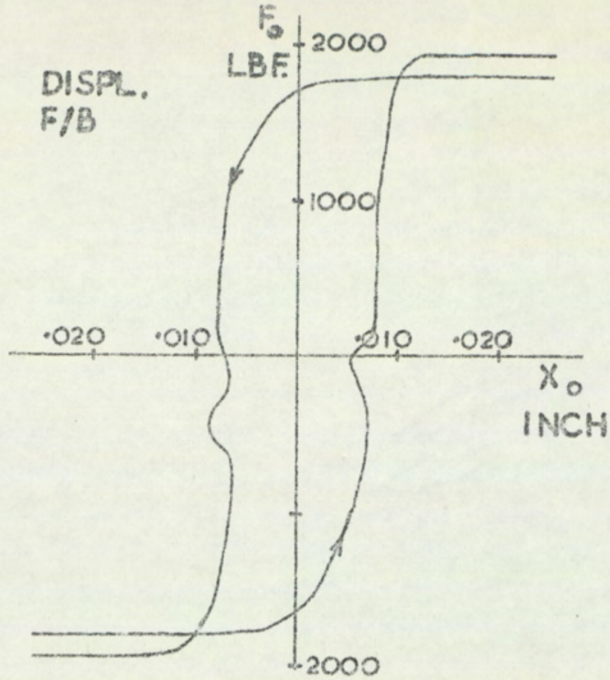

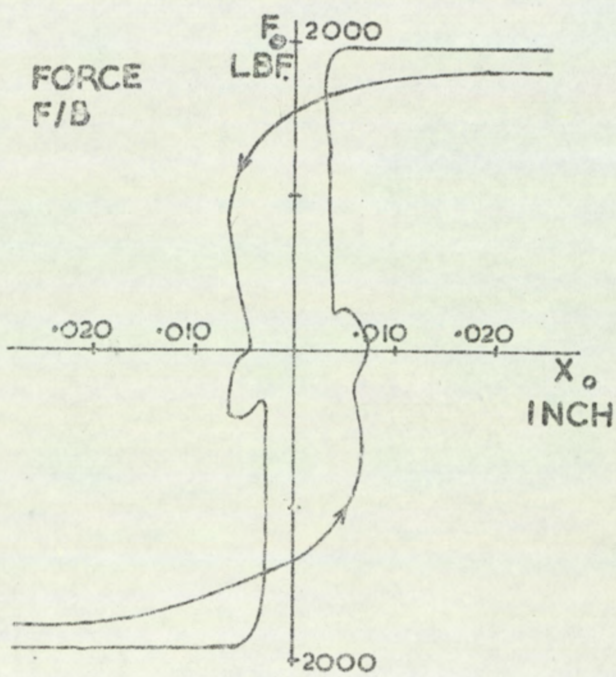

FORCE / DISPLACEMENT

LISSAJOU FIGURES

FREQUENCY 0·5C/S

FIG 5.2

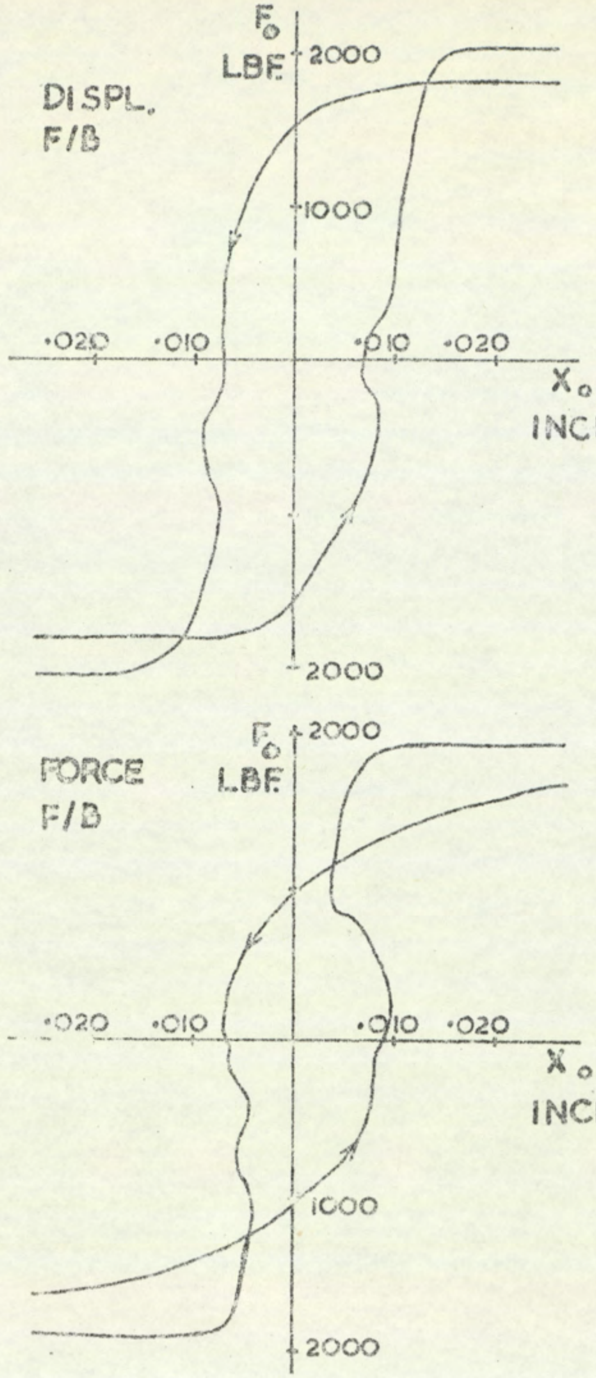

FORCE / DISPLACEMENT
LISSAJOU FIGURES
FREQUENCY 2C/S

FIG 5.3

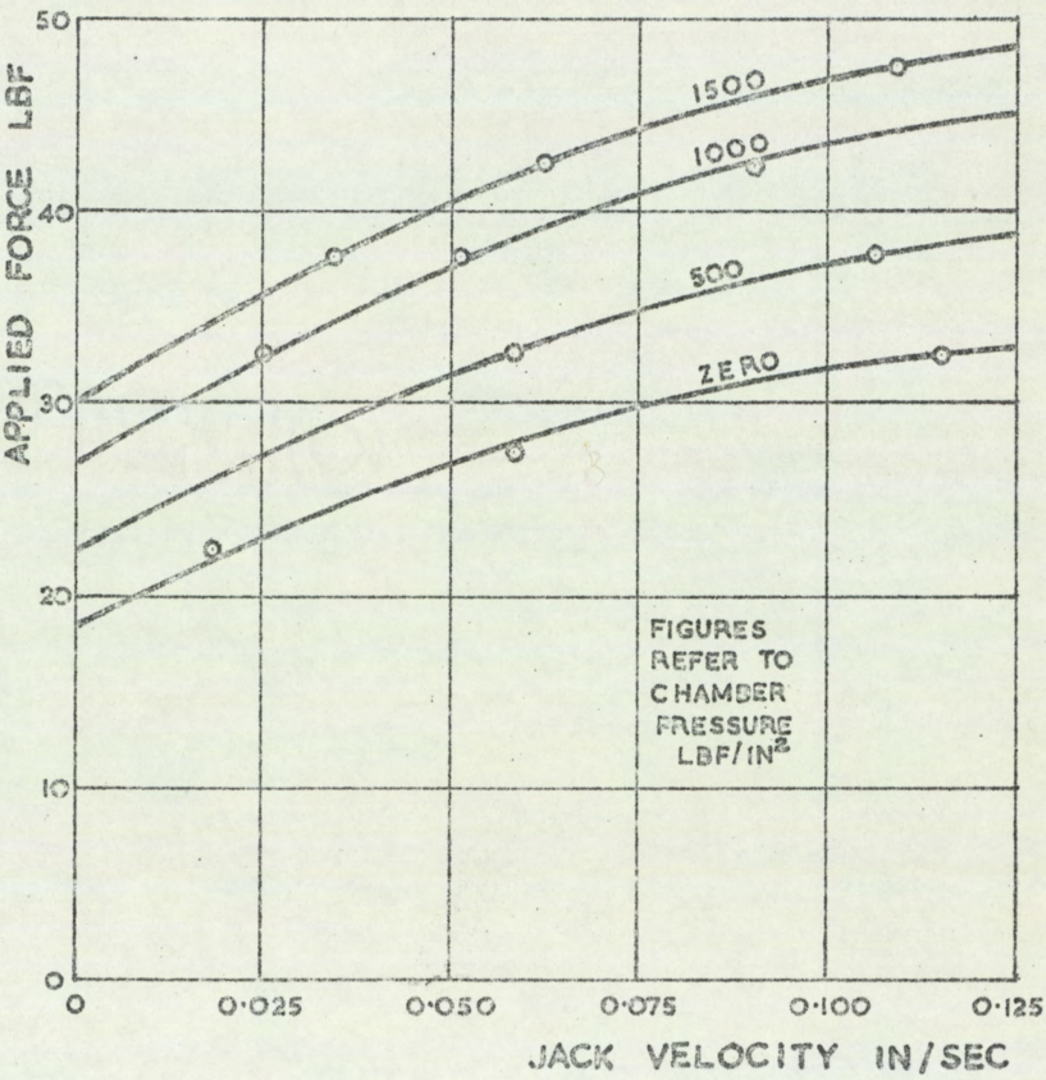

FORCE / VELOCITY CURVES

FOR VARIOUS CHAMBER PRESSURES

FIG 5.4

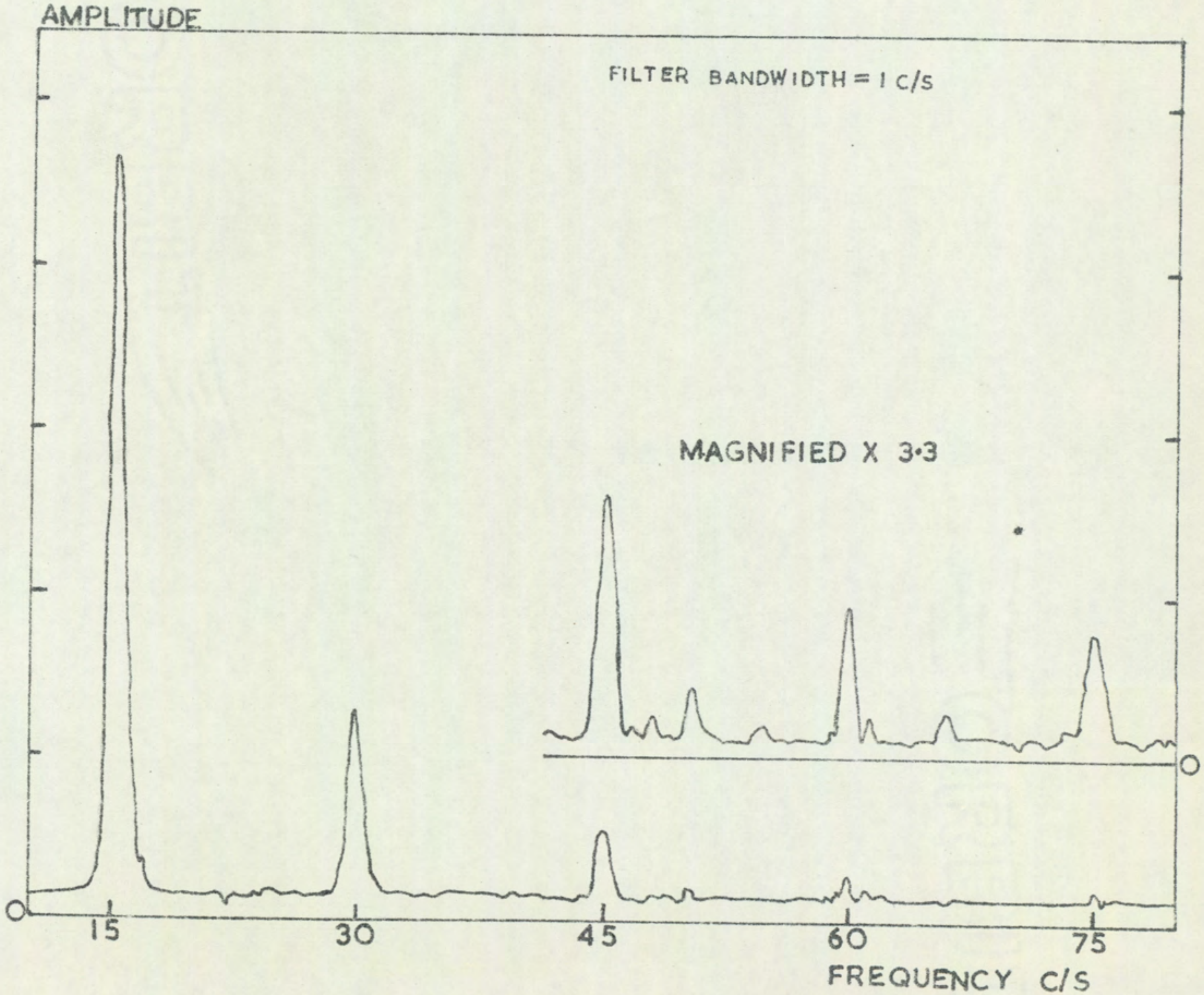

HARMONIC ANALYSIS OF FORCE WAVE FORM
VALVE OPENING = ·010 IN. PERTURBATION AMPLITUDE = ±·005 IN.
EXCITATION FREQUENCY = 15 C/S. DISPL. FEEDBACK CONTROL

FIG 5.5

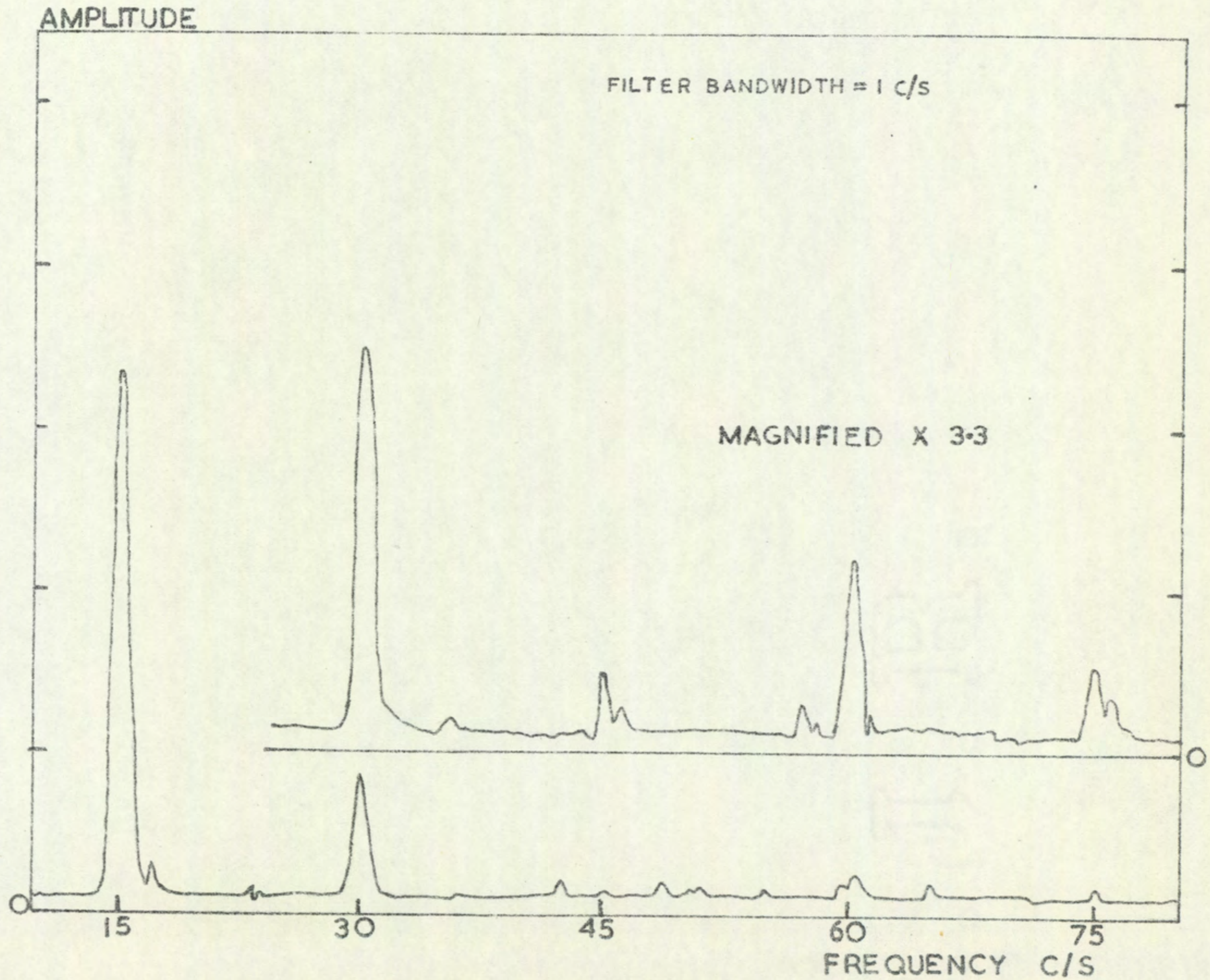

HARMONIC ANALYSIS OF DISPLACEMENT WAVE FORM
VALVE OPENING = ·010 IN. PERTURBATION AMPLITUDE = ± ·005 IN.
EXCITATION FREQUENCY = 15C/S. DISPL. FEEDBACK CONTROL

FIG 5.6

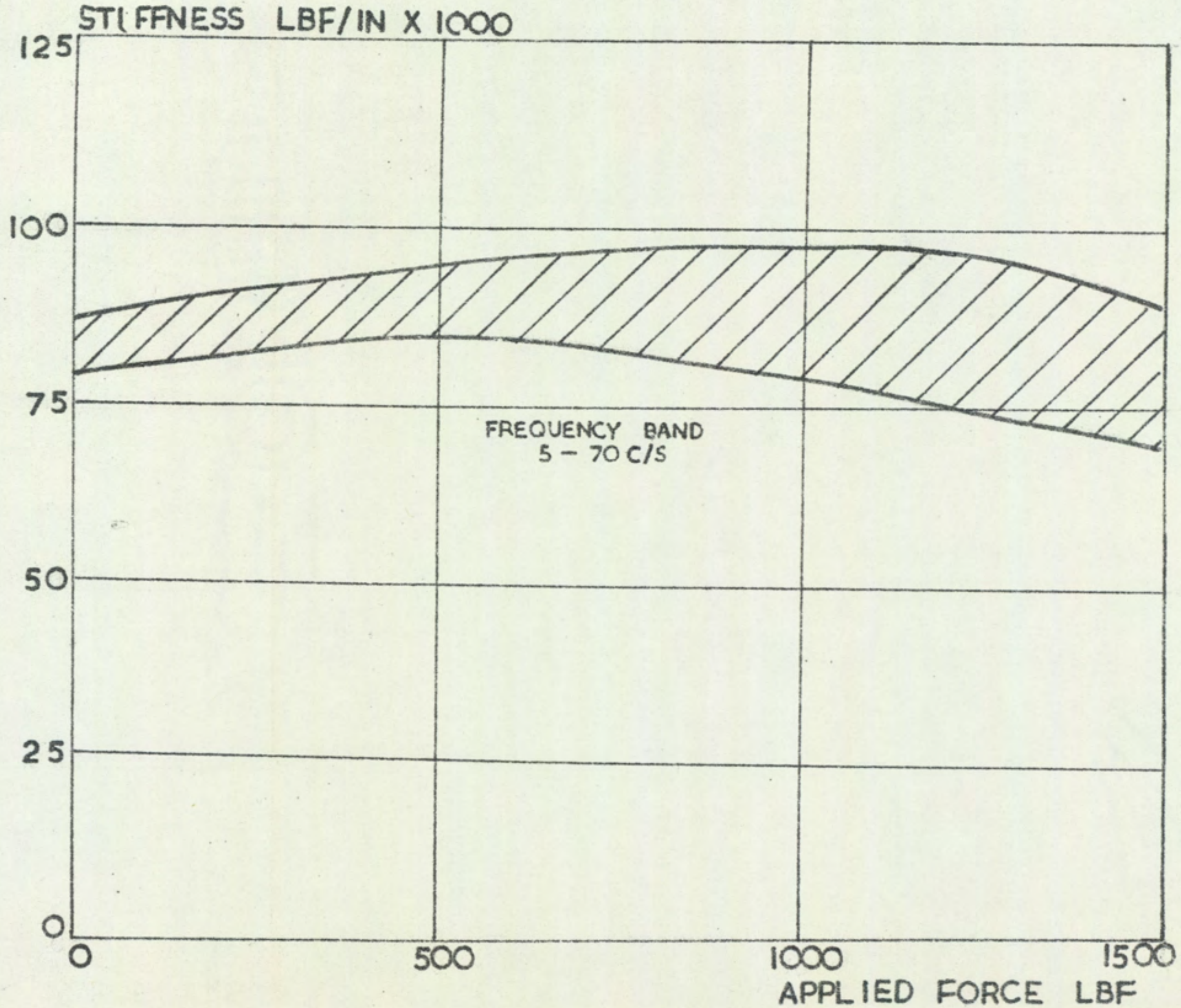

EXPERIMENTAL STIFFNESS CURVES
PERTURBATION AMPLITUDE = ± 200 LBF (± ·002 IN. APPROX.)
FORCE FEEDBACK CONTROL

FIG 5.7

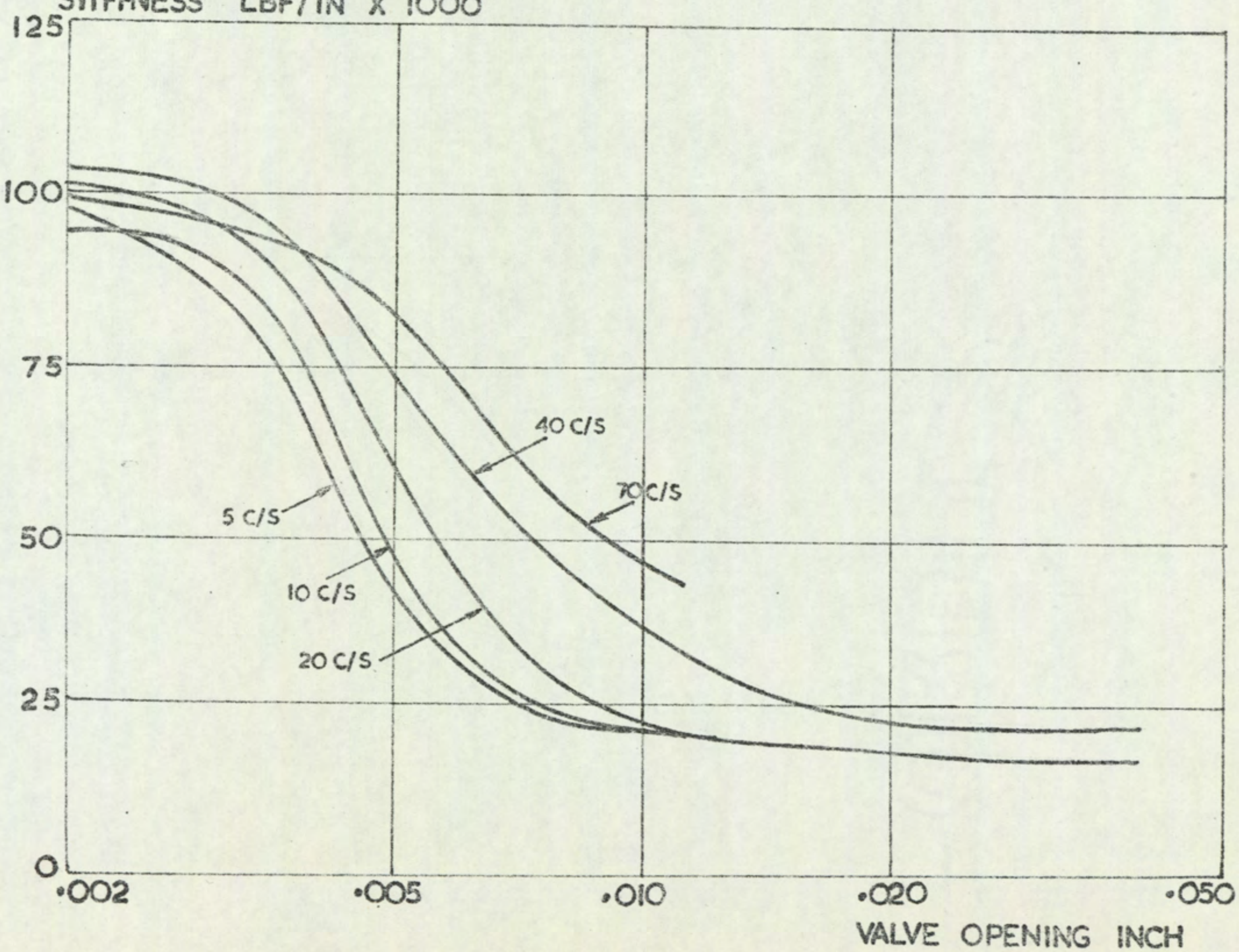

EXPERIMENTAL STIFFNESS CURVES
PERTURBATION AMPLITUDE = ± •002 INCH
DISPLACEMENT FEEDBACK CONTROL

FIG 5.8

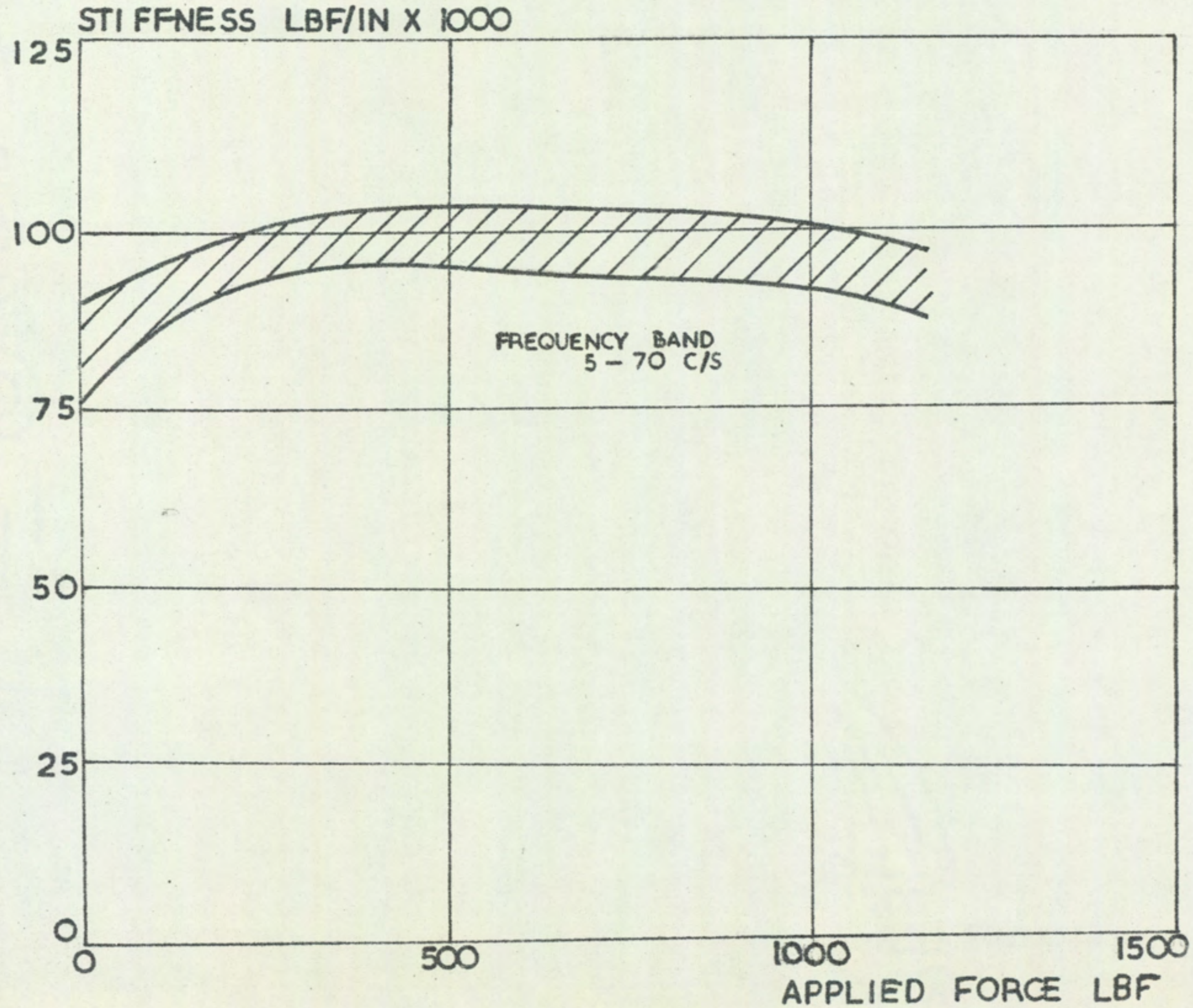

EXPERIMENTAL STIFFNESS CURVES

PERTURBATION AMPLITUDE = ± 500LBF (±.005 IN. APPROX.)

FORCE FEEDBACK CONTROL

FIG 5.9

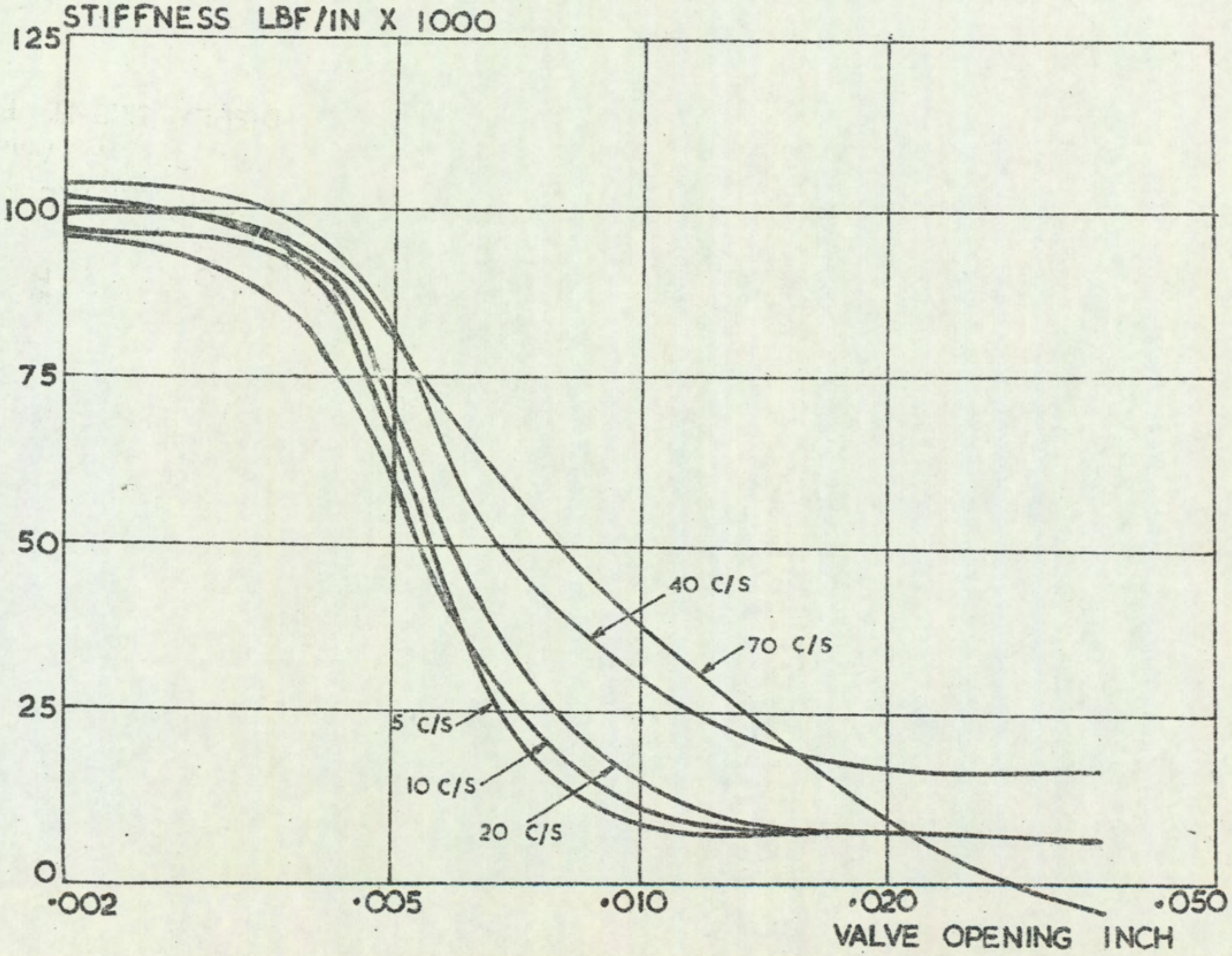

EXPERIMENTAL STIFFNESS CURVES
PERTURBATION AMPLITUDE = ±·005 INCH
DISPLACEMENT FEEDBACK CONTROL

FIG 5.10

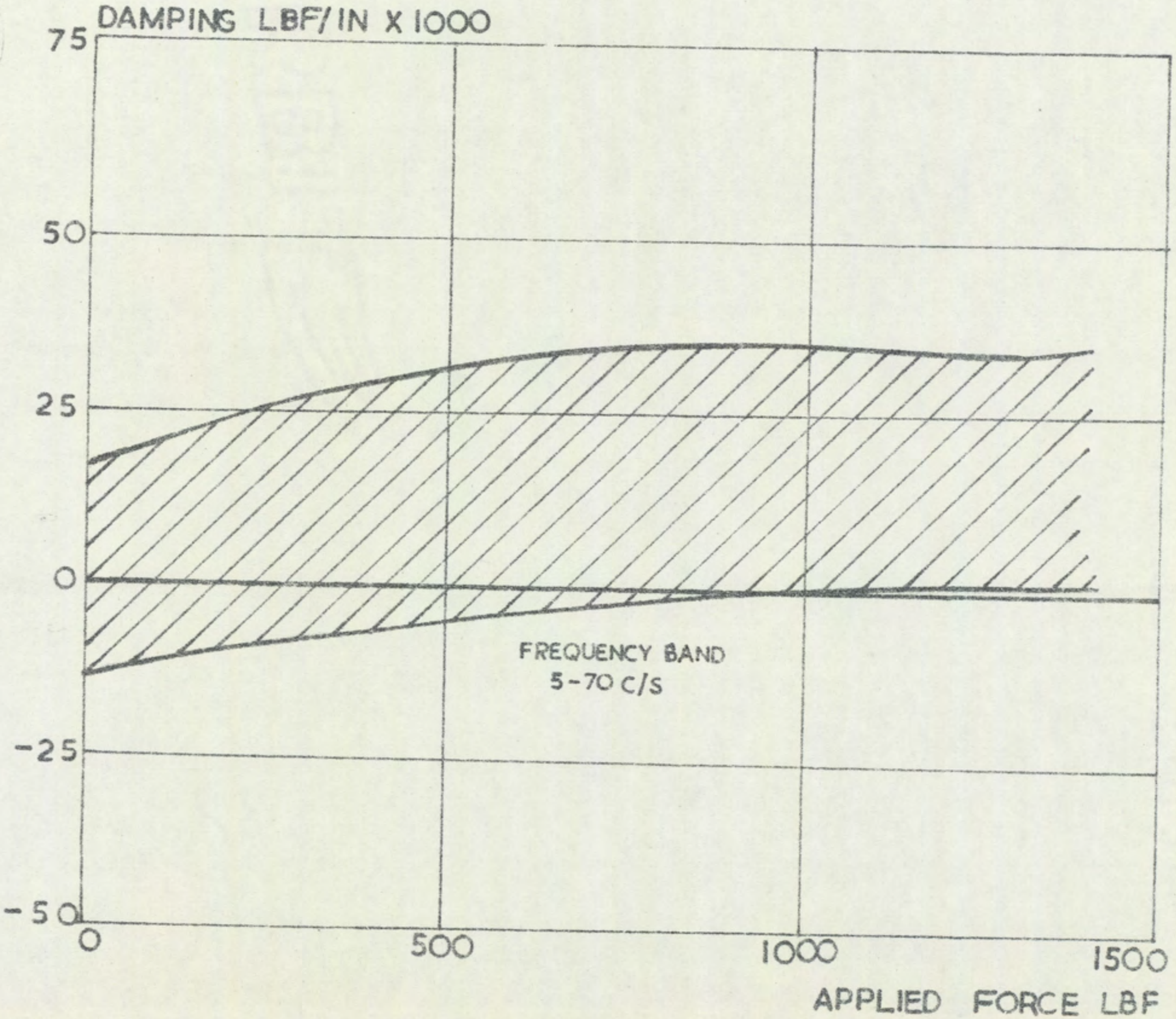

EXPERIMENTAL DAMPING CURVES
PERTURBATION AMPLITUDE = ± 200 LBF (± ·002 IN. APPROX)
FORCE FEEDBACK CONTROL

FIG 5.11

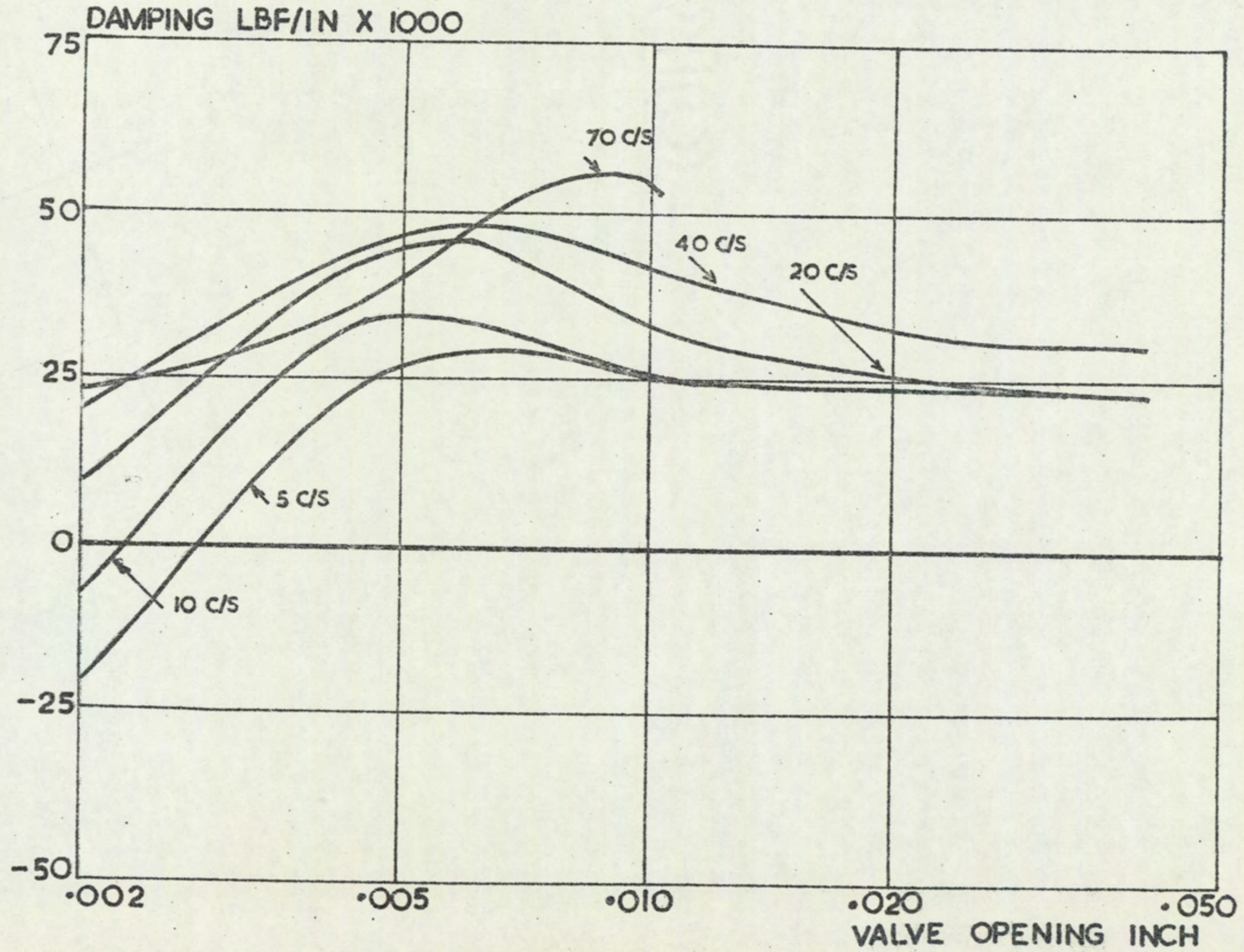

EXPERIMENTAL DAMPING CURVES
PERTURBATION AMPLITUDE = ± •002 INCH
DISPLACEMENT FEEDBACK CONTROL

FIG 5.12

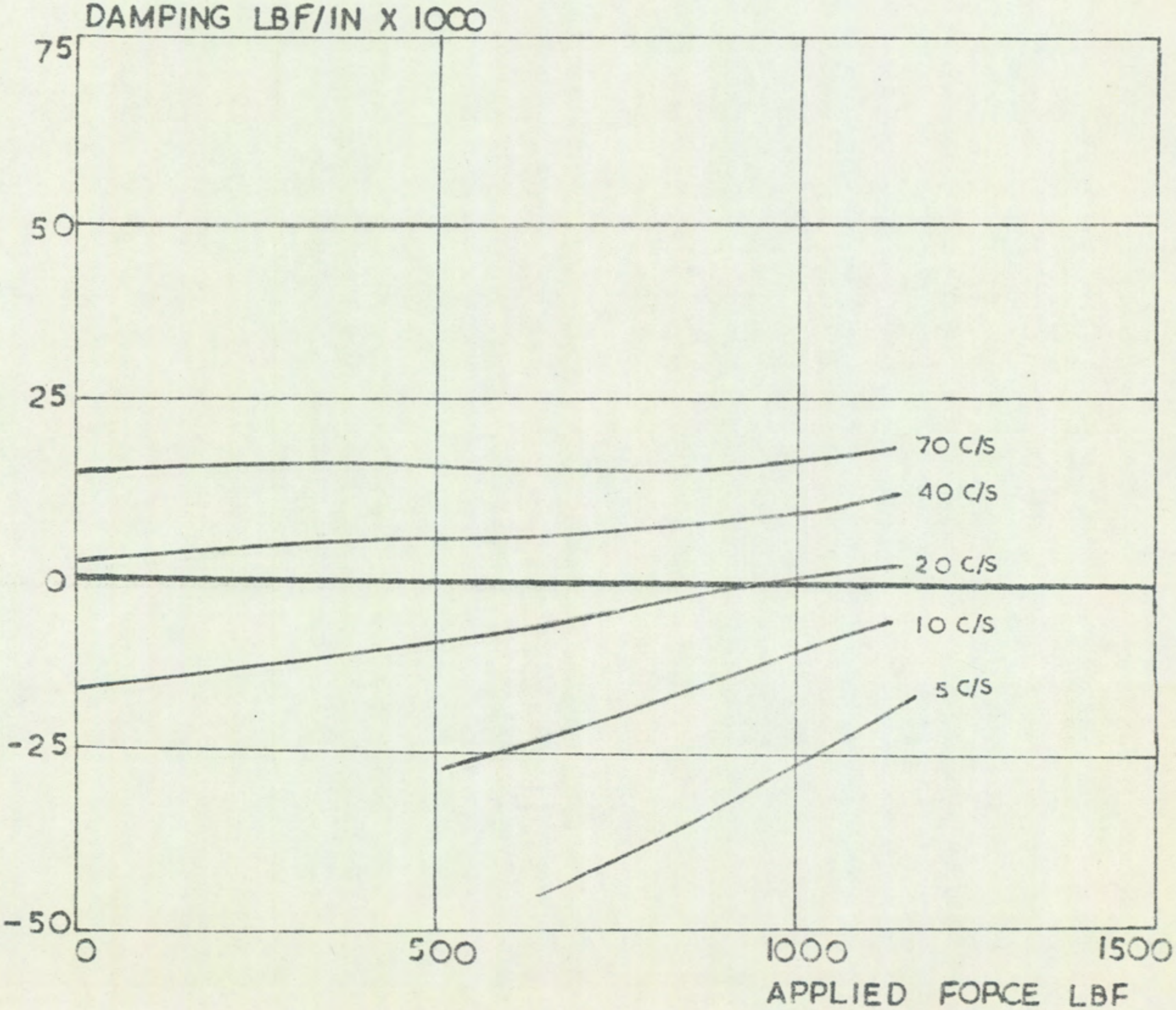

EXPERIMENTAL DAMPING CURVES.
PERTURBATION AMPLITUDE = ±500LBF(±·005 IN. APPROX)
FORCE FEEDBACK CONTROL

FIG 5.13

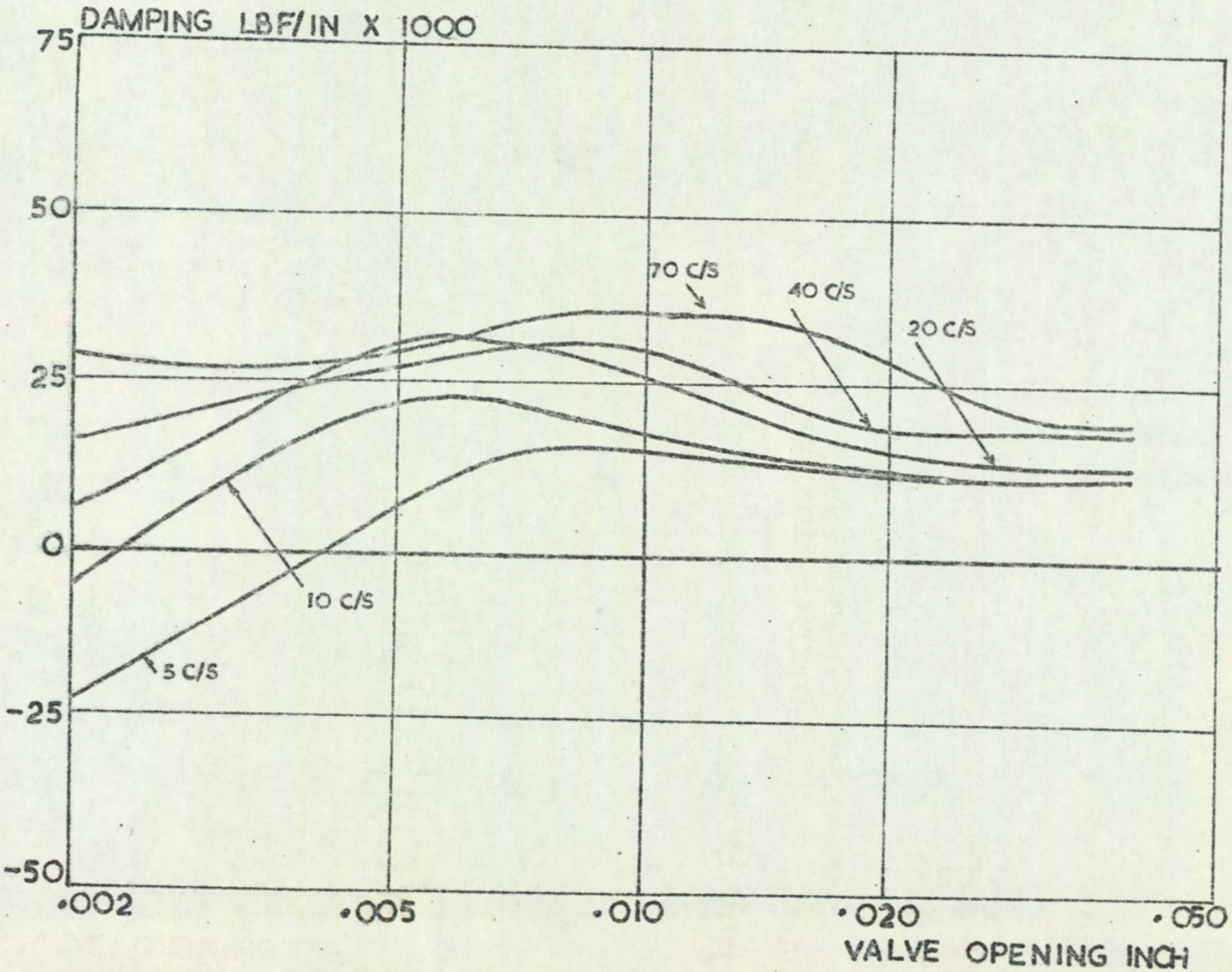

EXPERIMENTAL DAMPING CURVES
PERTURBATION AMPLITUDE = ± ·005 INCH
DISPLACEMENT FEEDBACK CONTROL

FIG 5.14

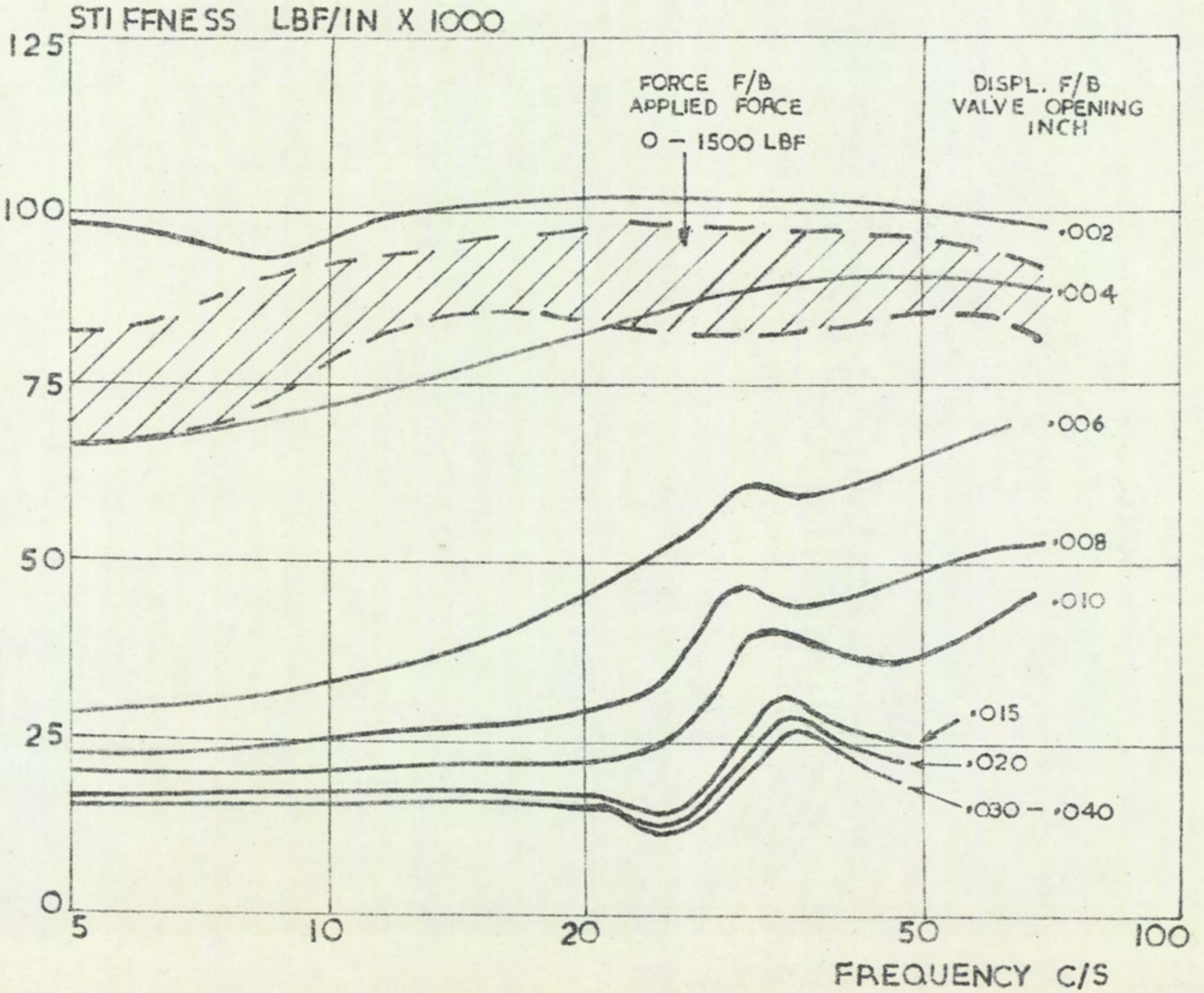

VARIATION OF EXPERIMENTAL STIFFNESS WITH FREQUENCY
DISPL. F/B – PERTURBATION AMPLITUDE = ± ·002 INCH
FORCE F/B – PERTURBATION AMPLITUDE = ± 200 LBF

FIG 5.15

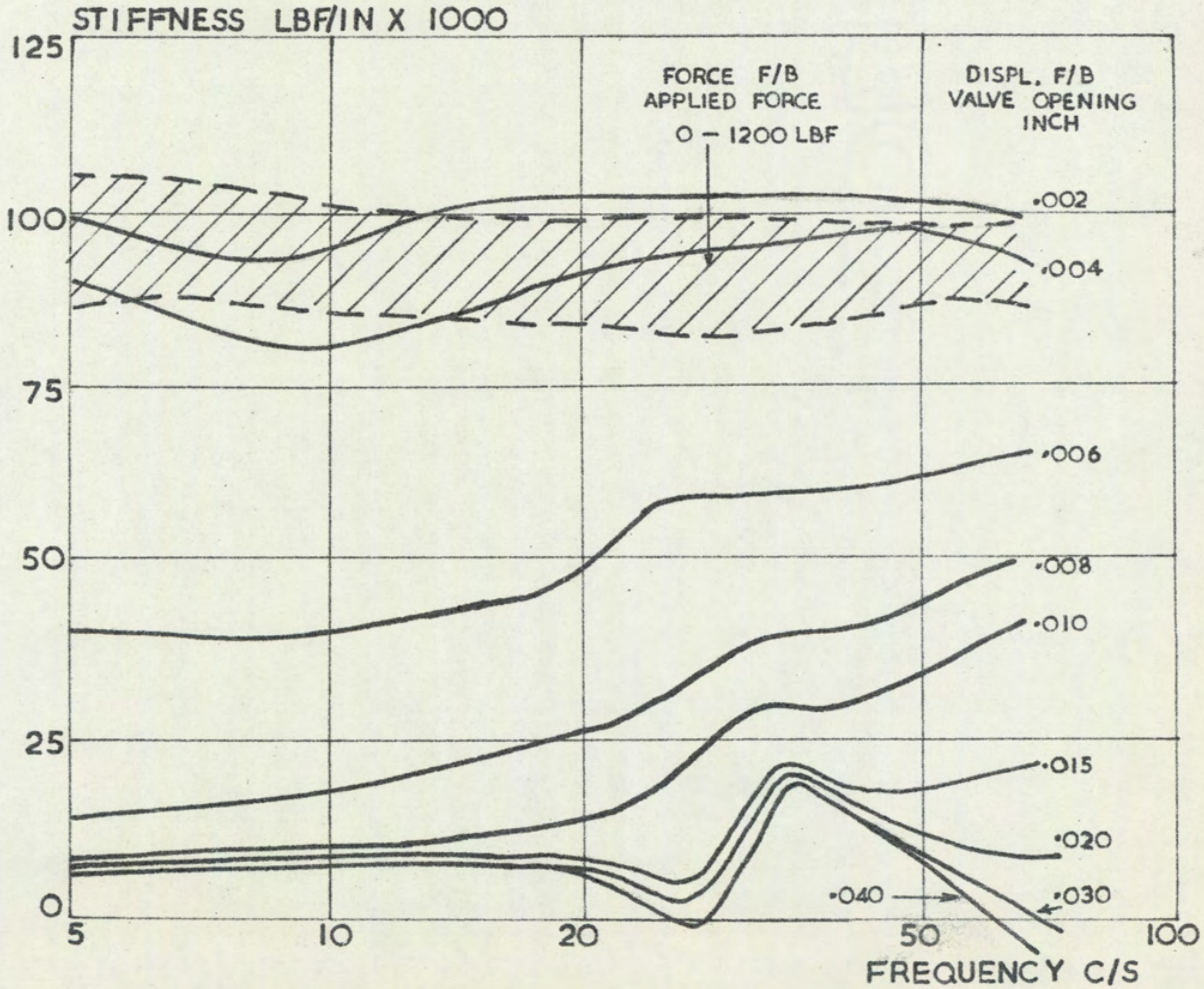

VARIATION OF EXPERIMENTAL STIFFNESS WITH FREQUENCY
DISPL. F/B – PERTURBATION AMPLITUDE = ± •005 INCH
FORCE F/B – PERTURBATION AMPLITUDE = ± 500 LBF

FIG 5.16

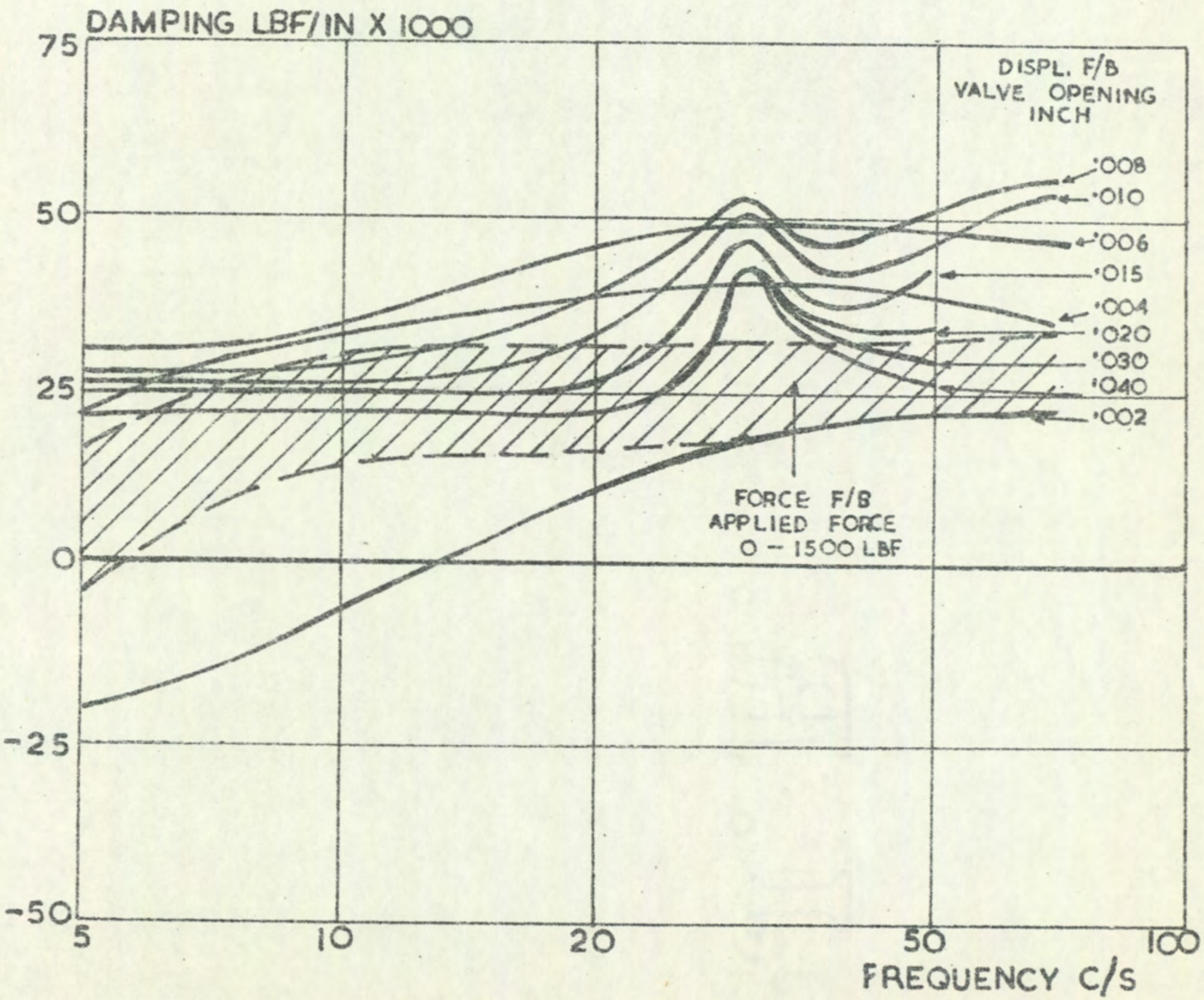

VARIATION OF EXPERIMENTAL DAMPING WITH FREQUENCY
DISPL. F/B – PERTURBATION AMPLITUDE = ± ·002 INCH
FORCE F/B – PERTURBATION AMPLITUDE = ± 200 LBF

FIG 5.17

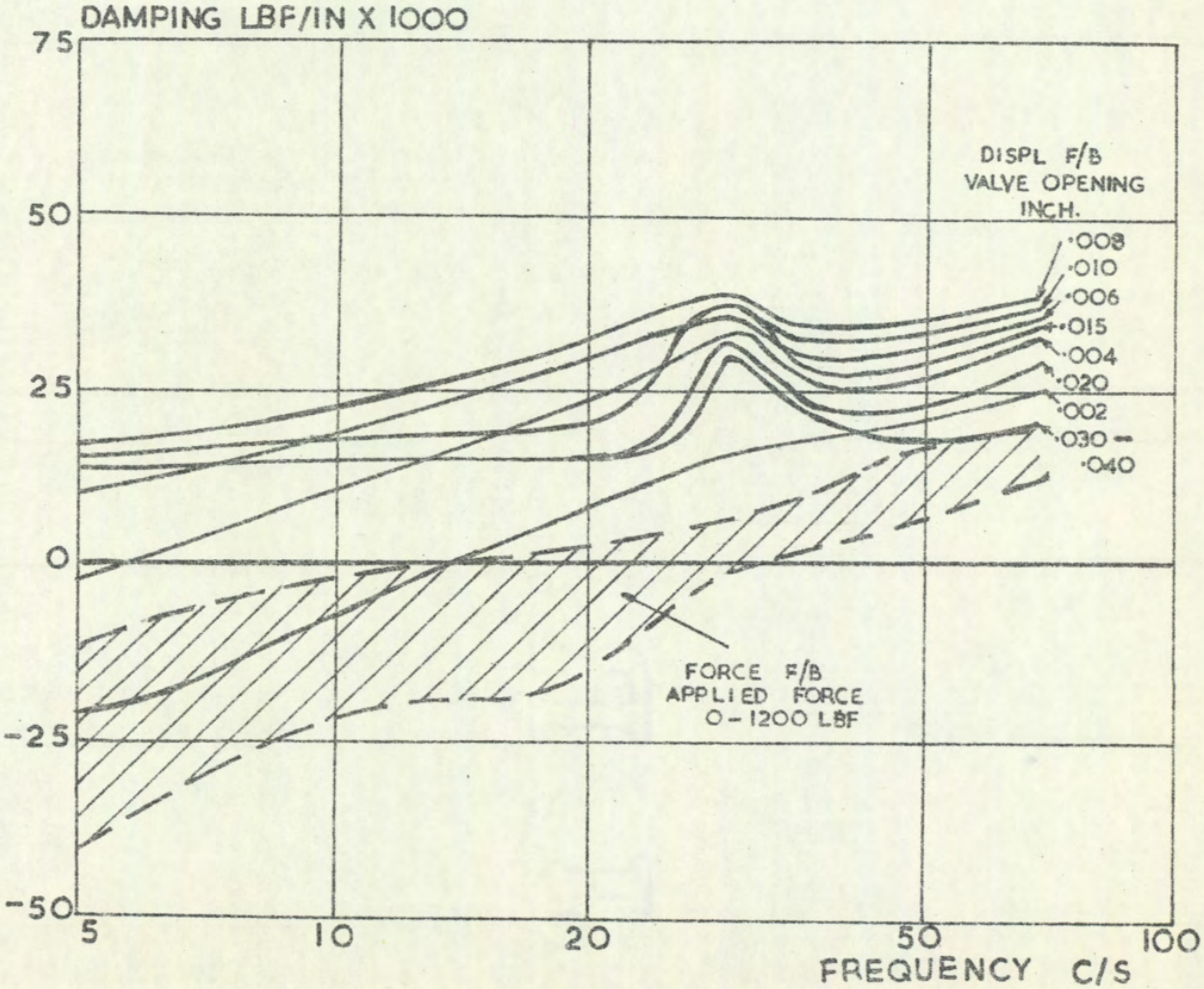

VARIATION OF EXPERIMENTAL DAMPING WITH FREQUENCY
DISPL. F/B - PERTURBATION AMPLITUDE = ± ·005 INCH
FORCE F/B - PERTURBATION AMPLITUDE = ± 500 LBF

FIG 5.18

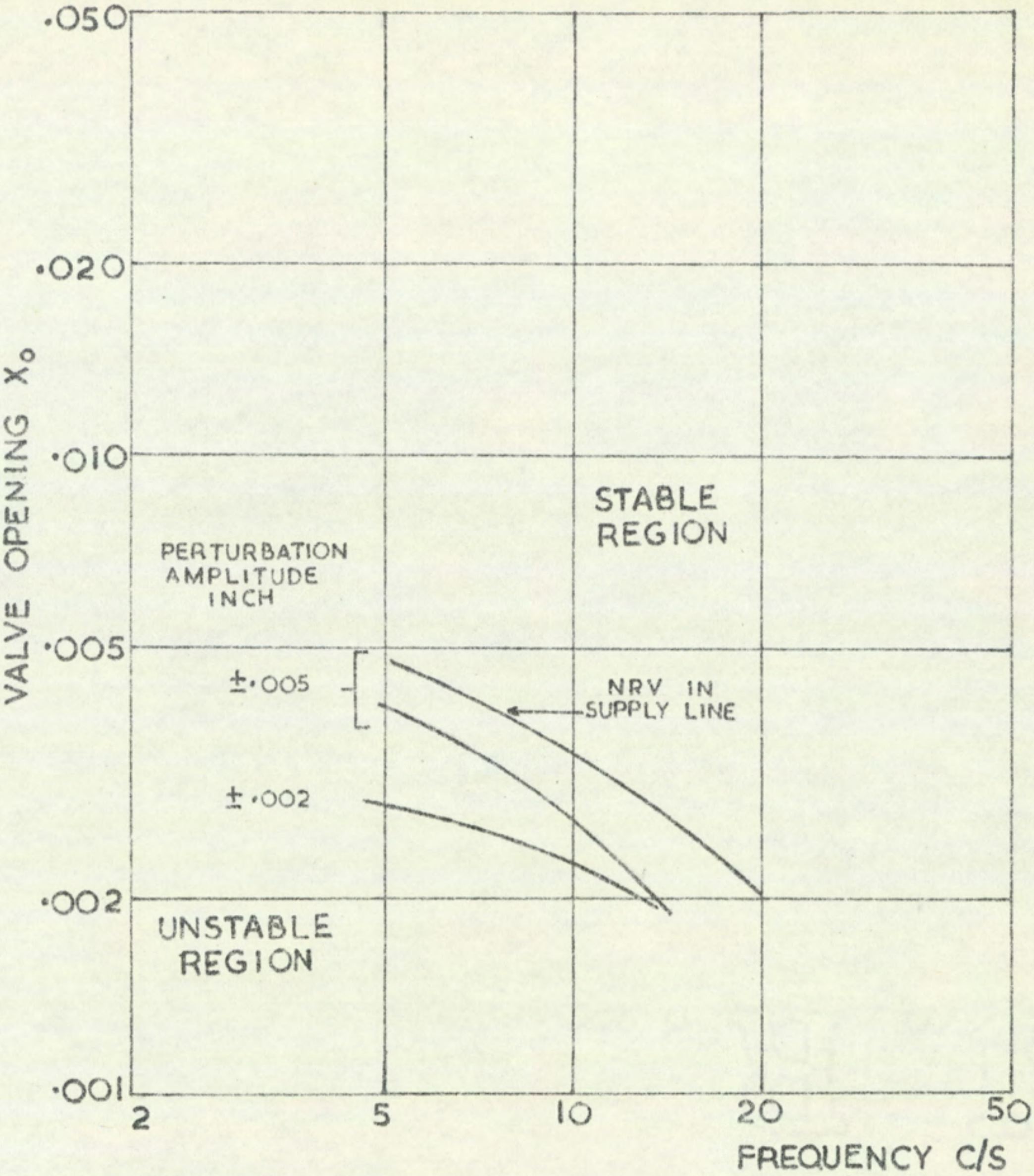

RELATIONSHIP BETWEEN VALVE OPENING AND FREQUENCY FOR ZERO DAMPING

FIG 5.19

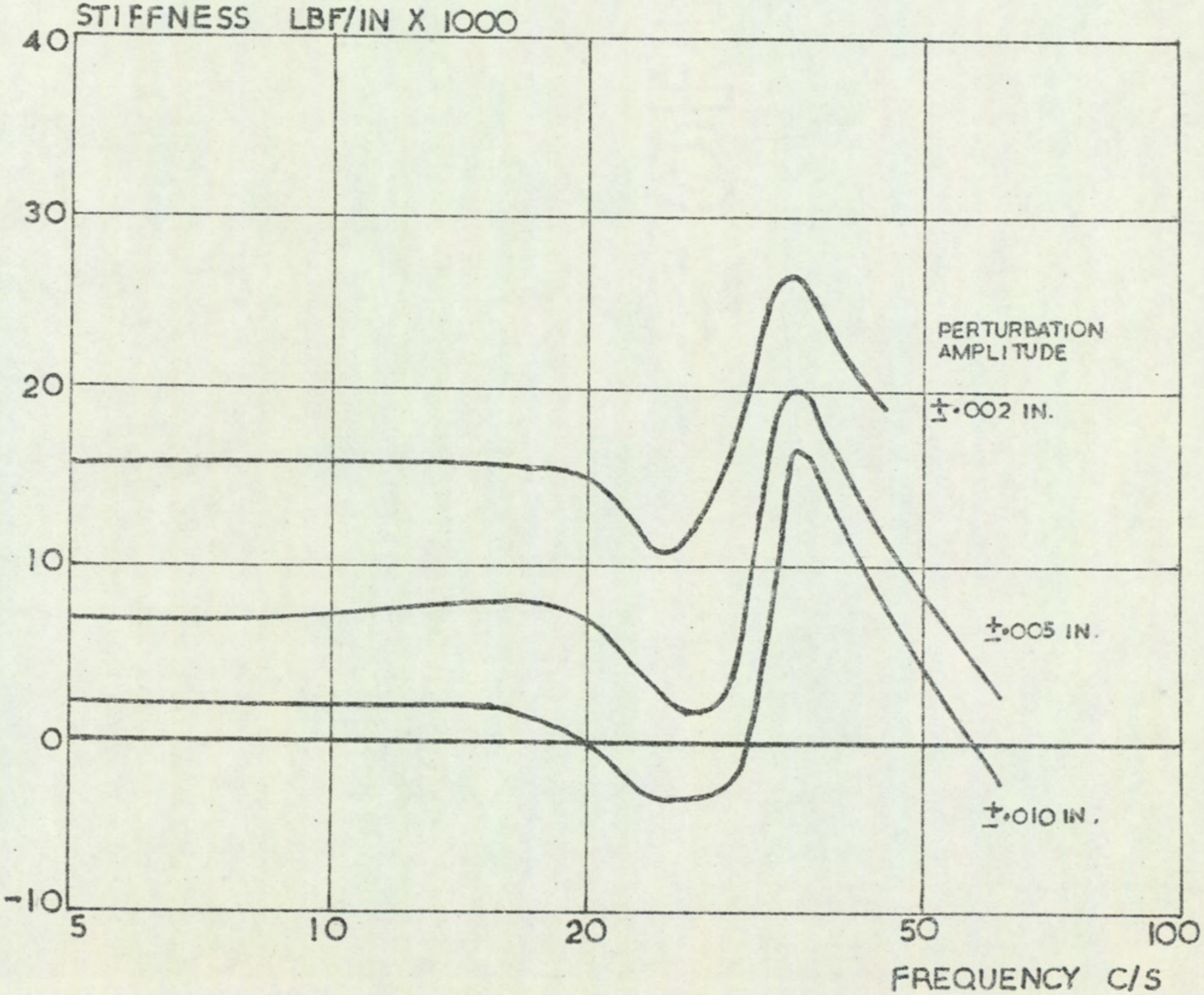

FIG 5.20

EFFECT OF PERTURBATION AMPLITUDE ON EXPERIMENTAL STIFFNESS

VALVE OPENING = ·040 INCH

EFFECT OF PERTURBATION AMPLITUDE
ON EXPERIMENTAL DAMPING
VALVE OPENING = •040 INCH

FIG 5.21

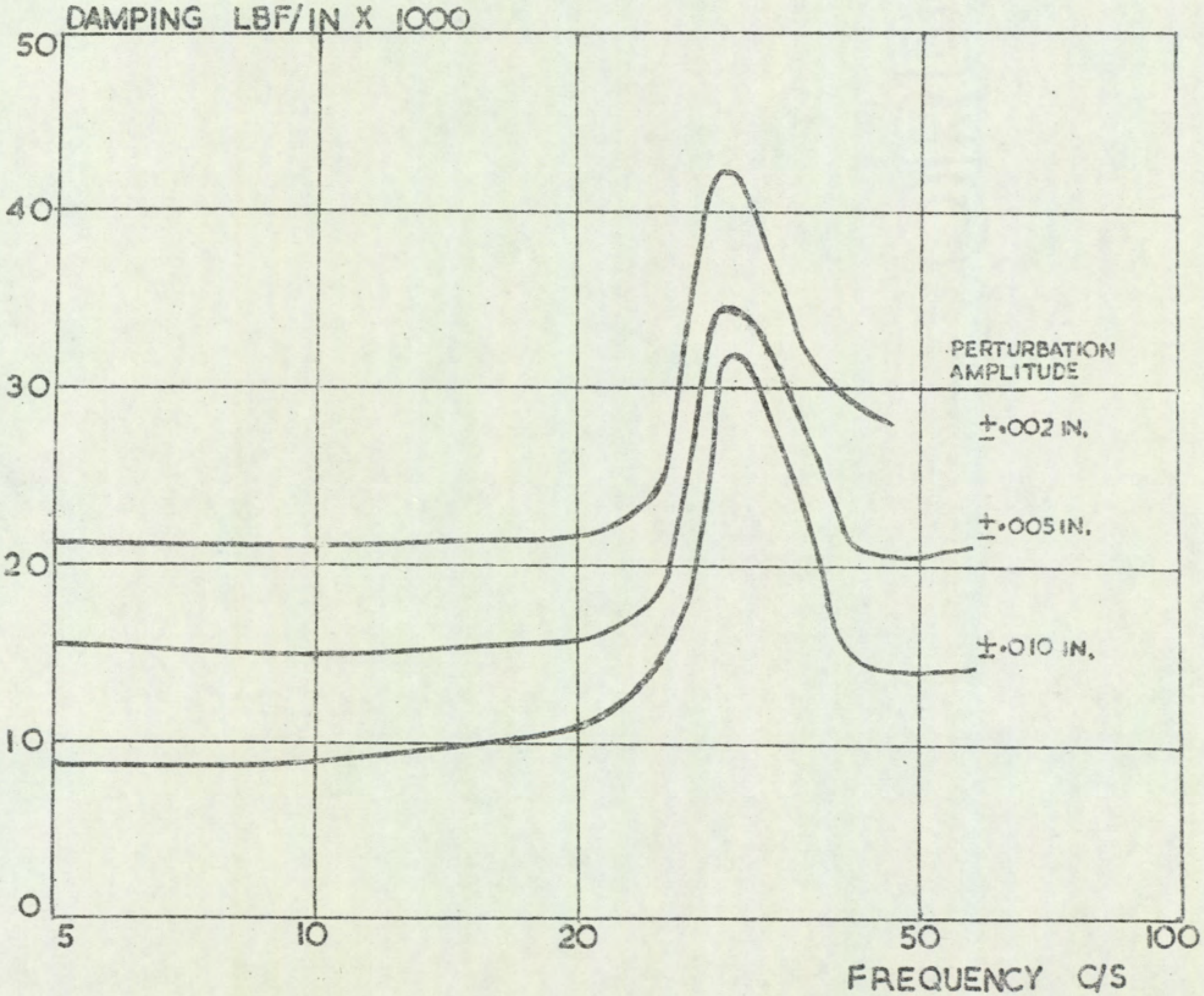

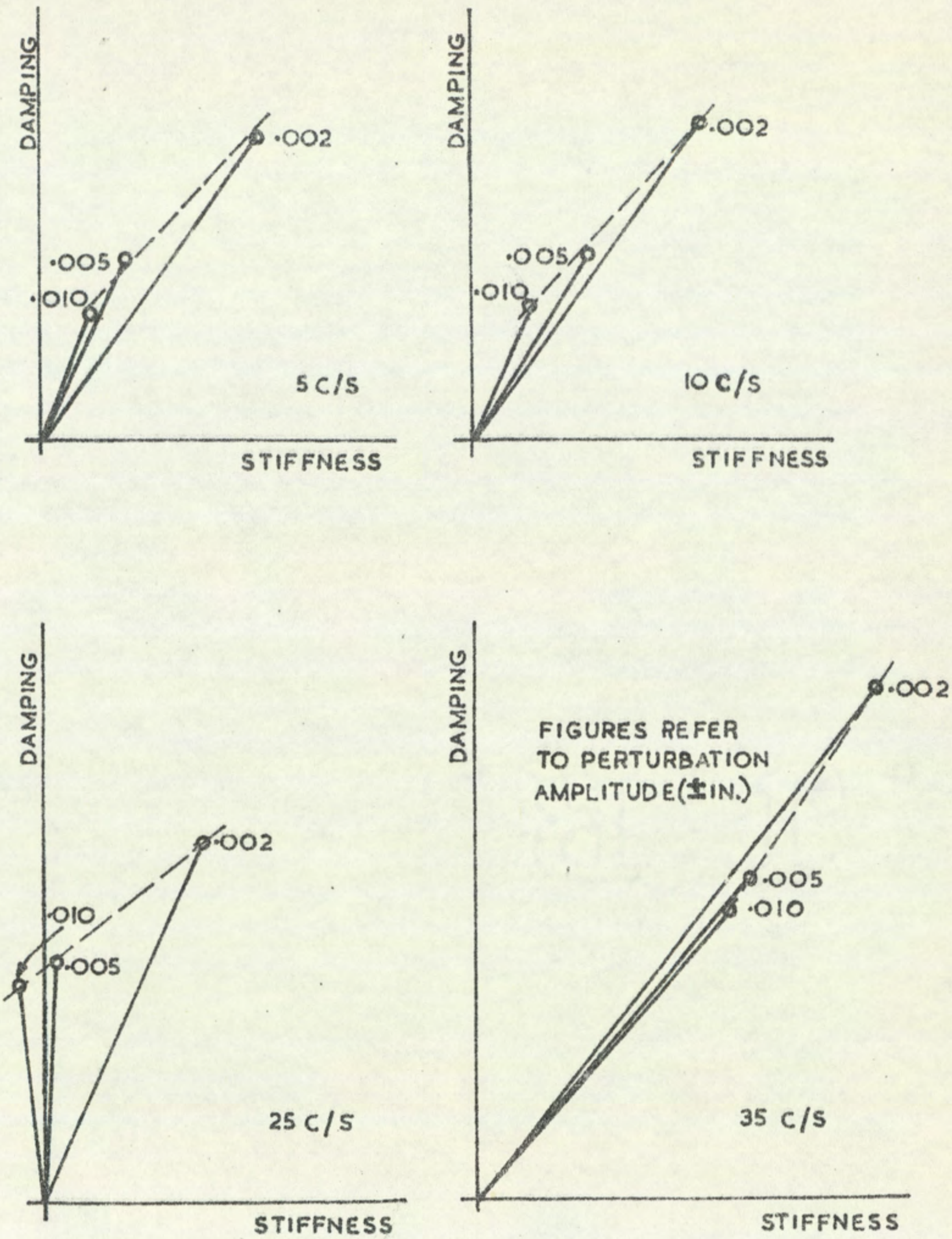

IMPEDANCE VECTOR DIAGRAMS
FOR VARIOUS EXCITATION FREQUENCIES
VALVE OPENING=·030 INCH.

FIG 5.22

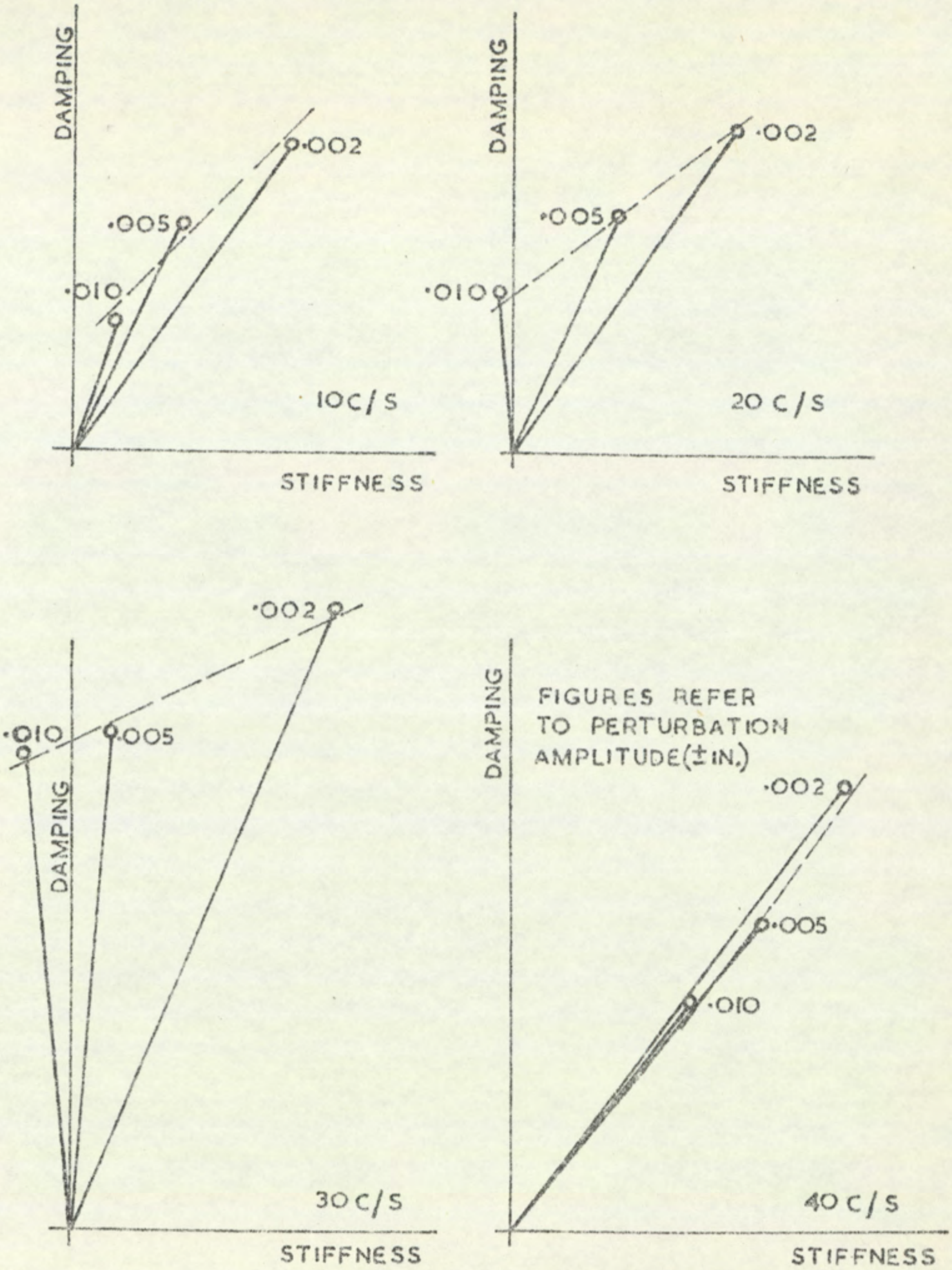

IMPEDANCE VECTOR DIAGRAMS
FOR VARIOUS EXCITATION FREQUENCIES
VALVE OPENING = ·040 INCH.

FIG 5.23.

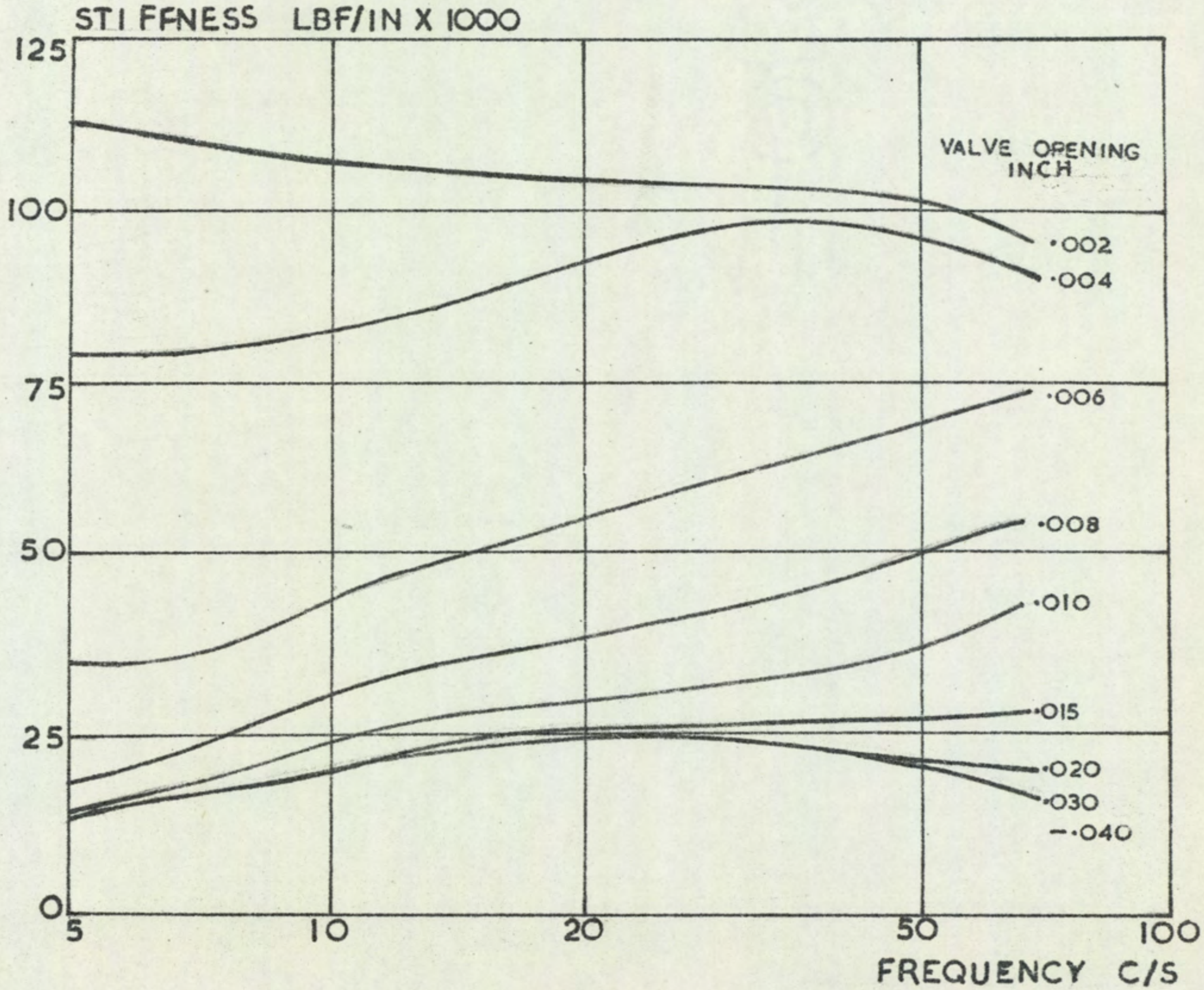

VARIATION OF EXPERIMENTAL STIFFNESS WITH FREQUENCY
PERTURBATION AMPLITUDE = ±·005 INCH
NON RETURN VALVE IN SUPPLY LINE

FIG 5.24

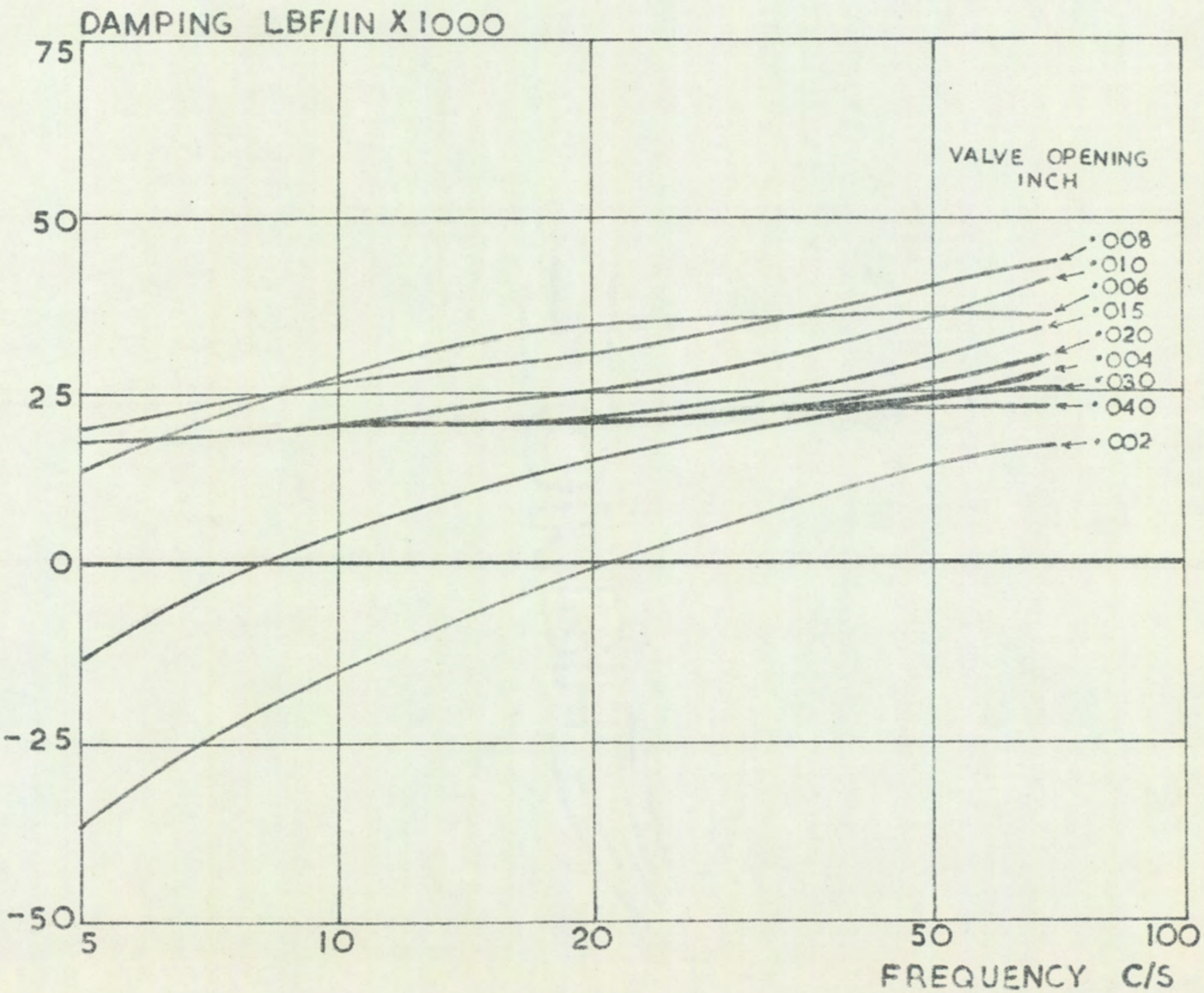

VARIATION OF EXPERIMENTAL DAMPING WITH FREQUENCY
PERTURBATION AMPLITUDE = ±·005 INCH
NON RETURN VALVE IN SUPPLY LINE

FIG 5.25

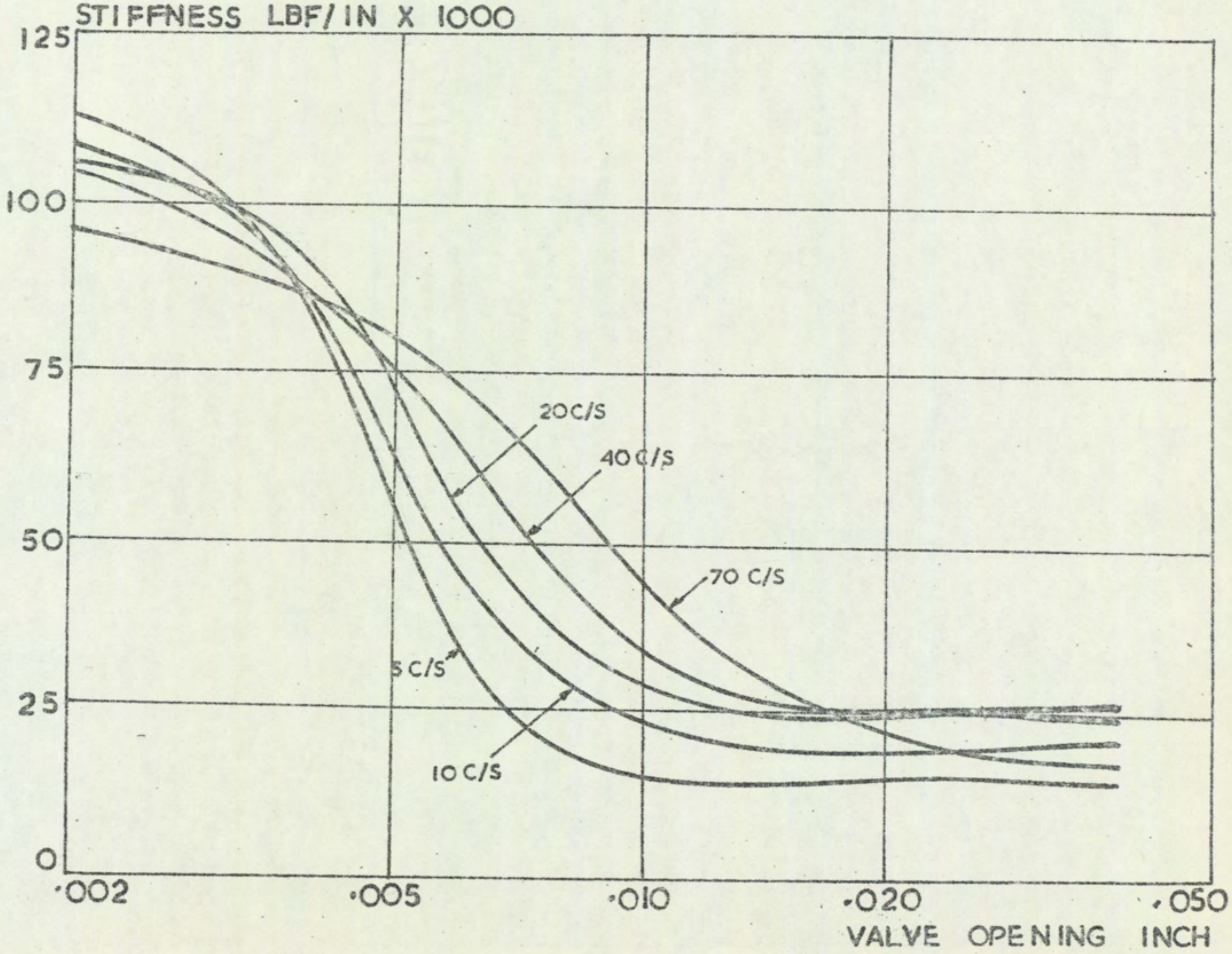

EXPERIMENTAL STIFFNESS CURVES
PERTURBATION AMPLITUDE = ±·005 INCH
NON RETURN VALVE IN SUPPLY LINE

FIG 5.26

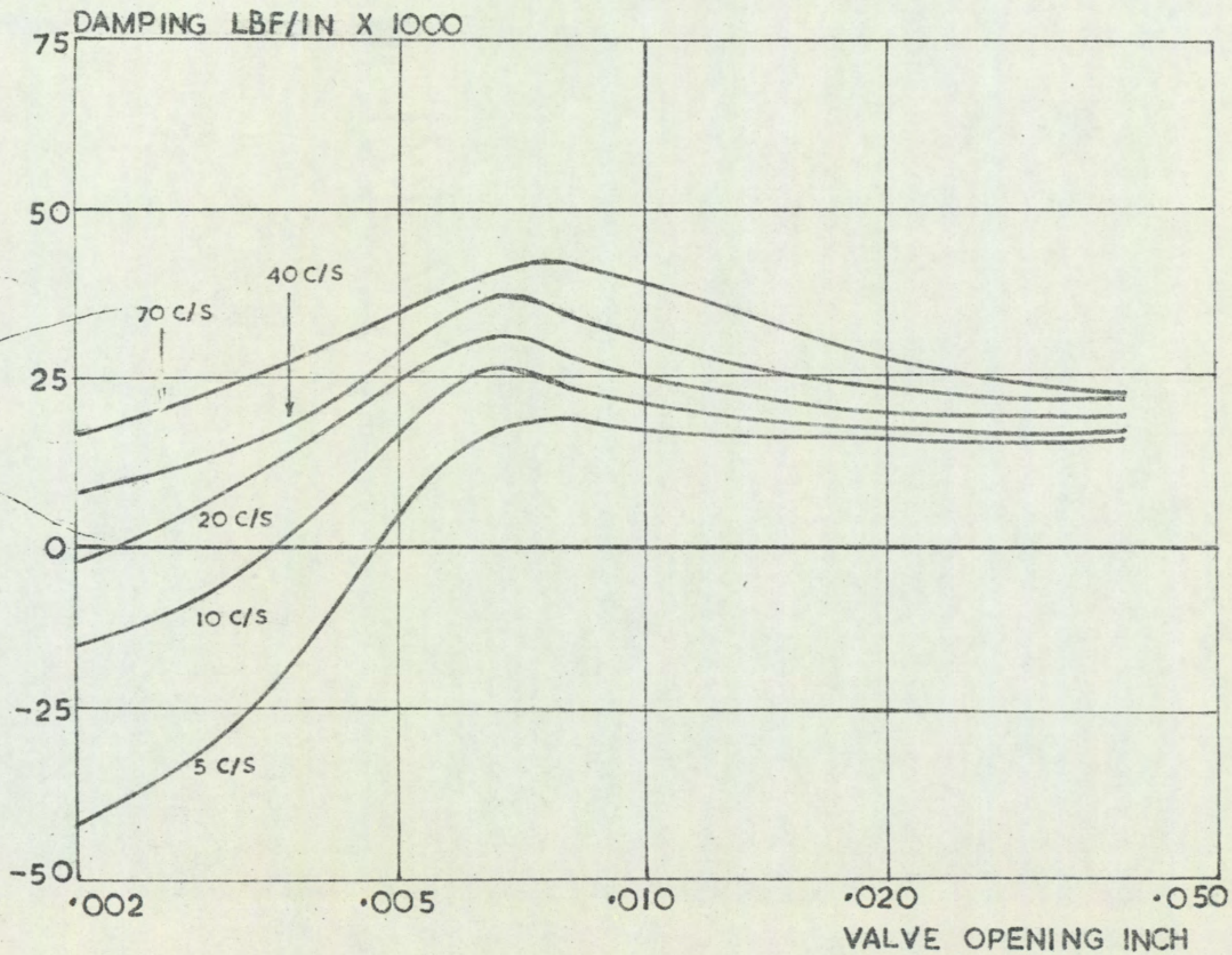

EXPERIMENTAL DAMPING CURVES
PERTURBATION AMPLITUDE = ±.005 INCH
NON RETURN VALVE IN SUPPLY LINE

FIG 5.27

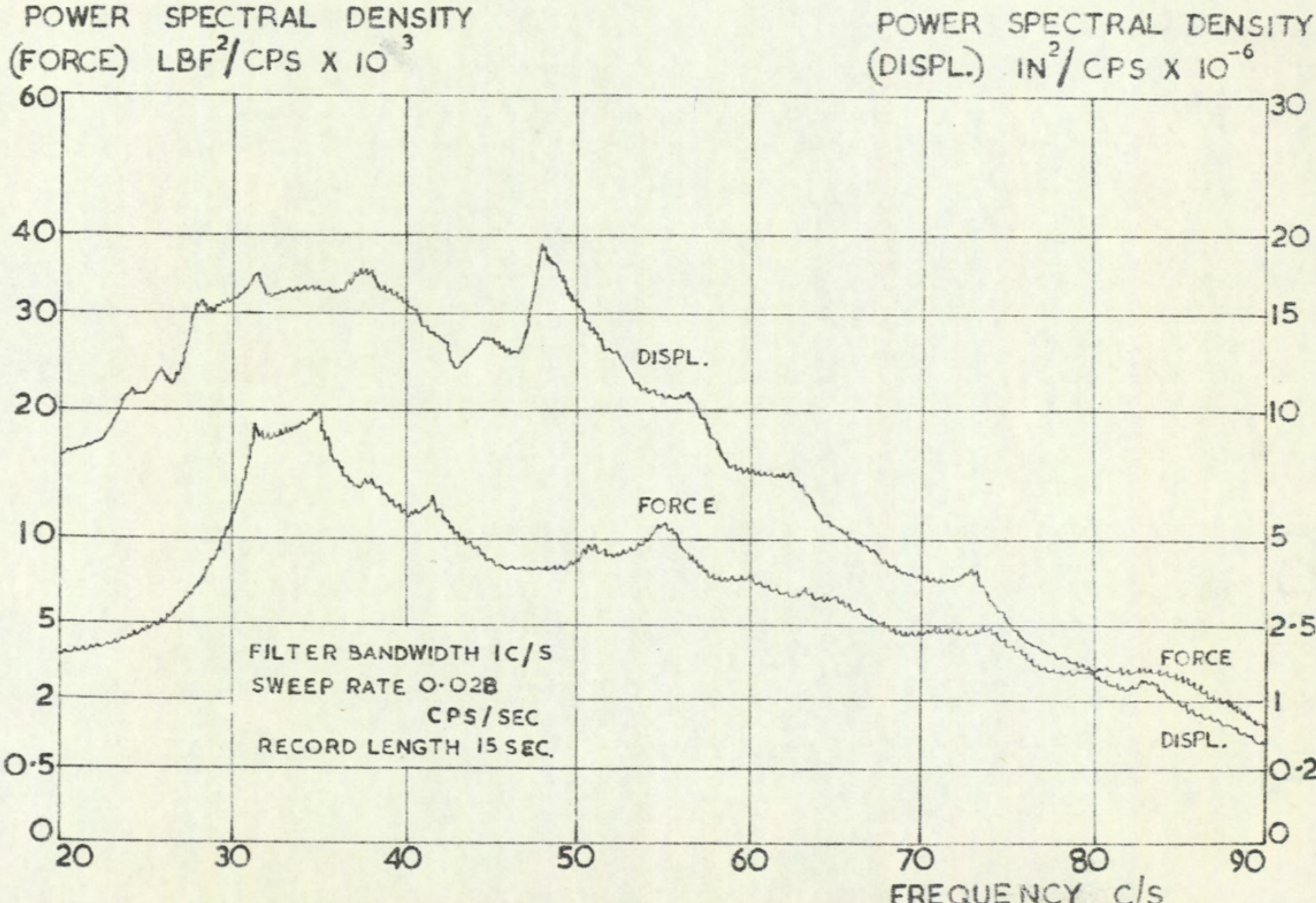

FIG 5.28

FORCE & DISPLACEMENT POWER SPECTRUM

WIDE BAND RANDOM EXCITATION $X_o = 0{\cdot}040$ INCH

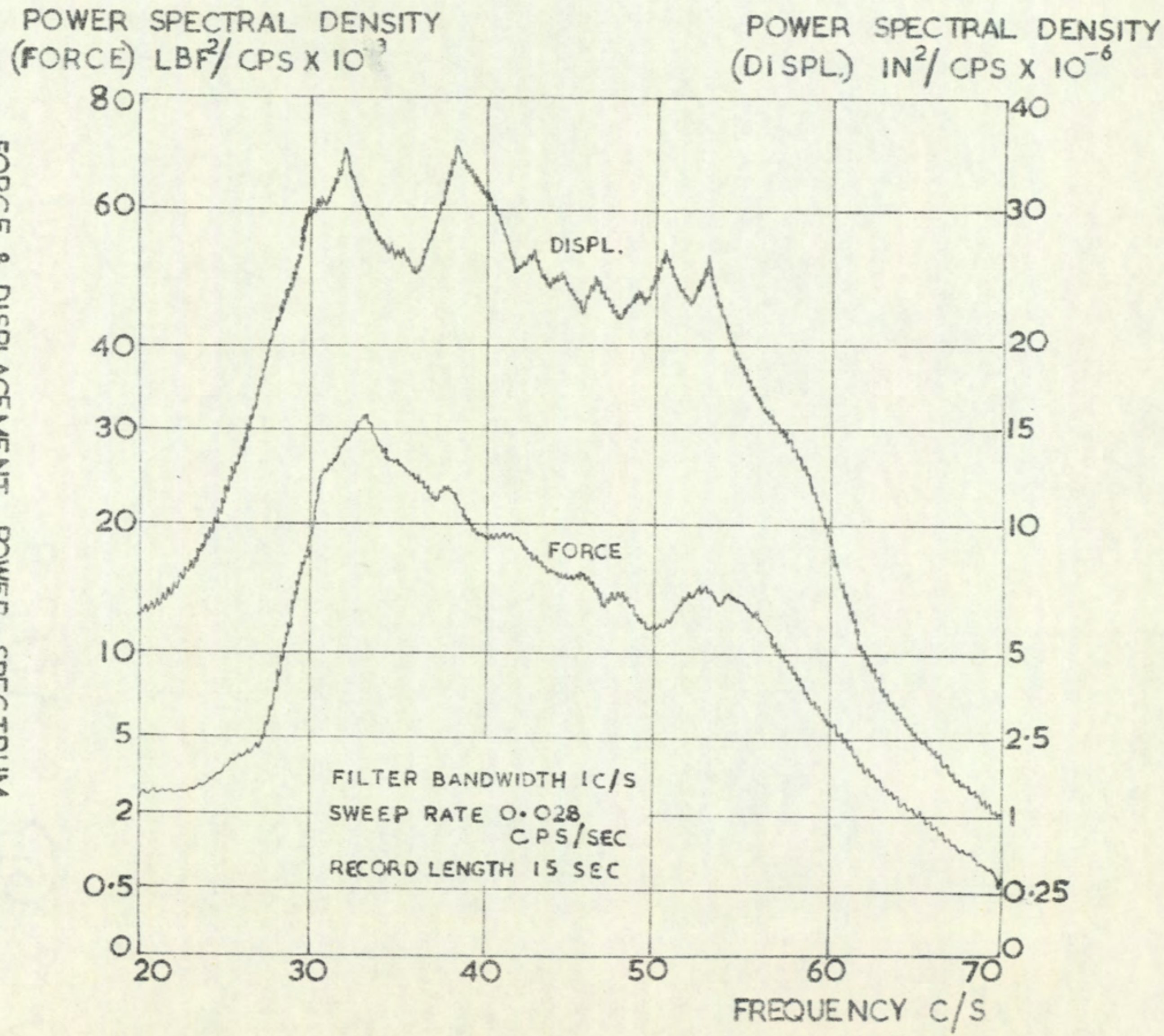

FORCE & DISPLACEMENT POWER SPECTRUM
NARROW BAND (30 C/S) RANDOM EXCITATION CENTRE
FREQUENCY = 45 C/S X_0 = 0·040 INCH

FIG 5.29

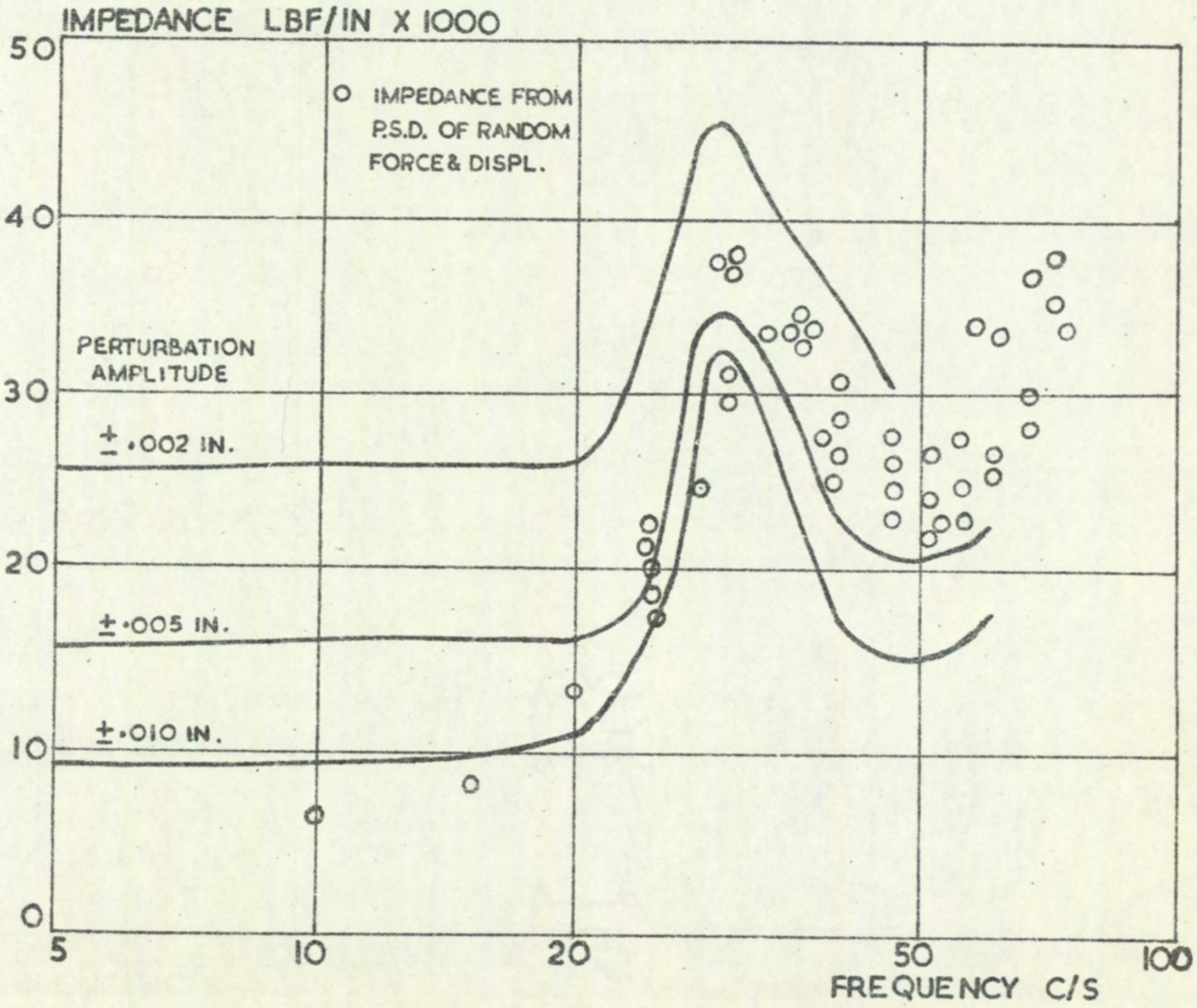

VARIATION OF EXPERIMENTAL IMPEDANCE WITH FREQUENCY
COMPARISON BETWEEN SINUSOIDAL AND RANDOM
EXCITATION OF SERVOMECHANISM
VALVE OPENING = ·040 INCH

FIG 5.30

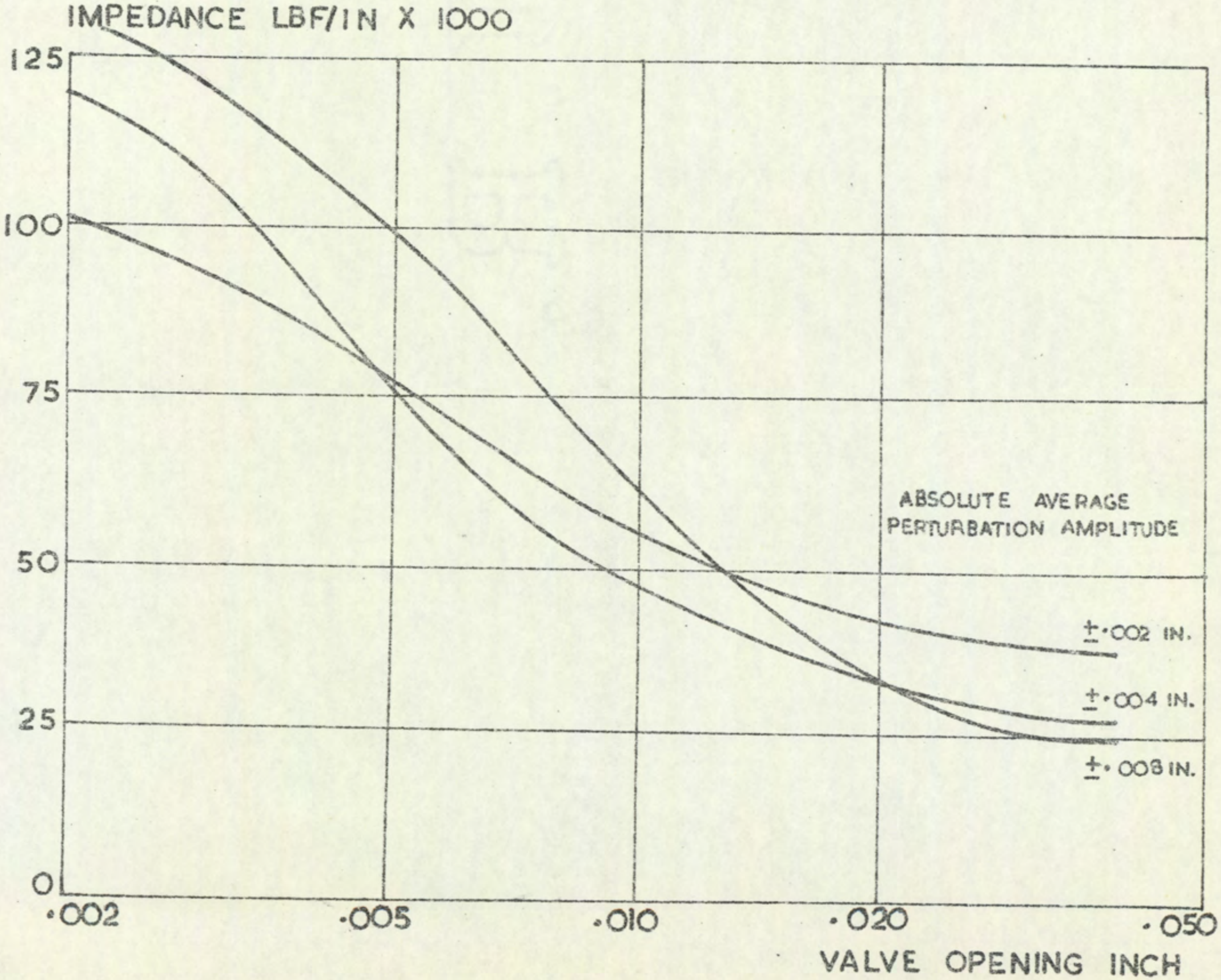

EXPERIMENTAL IMPEDANCE CURVES
WIDE BAND IMPEDANCE DETERMINED FROM RANDOM
EXCITATION OF SERVOMECHANISM
DISPLACEMENT FEEDBACK CONTROL

FIG 5.31

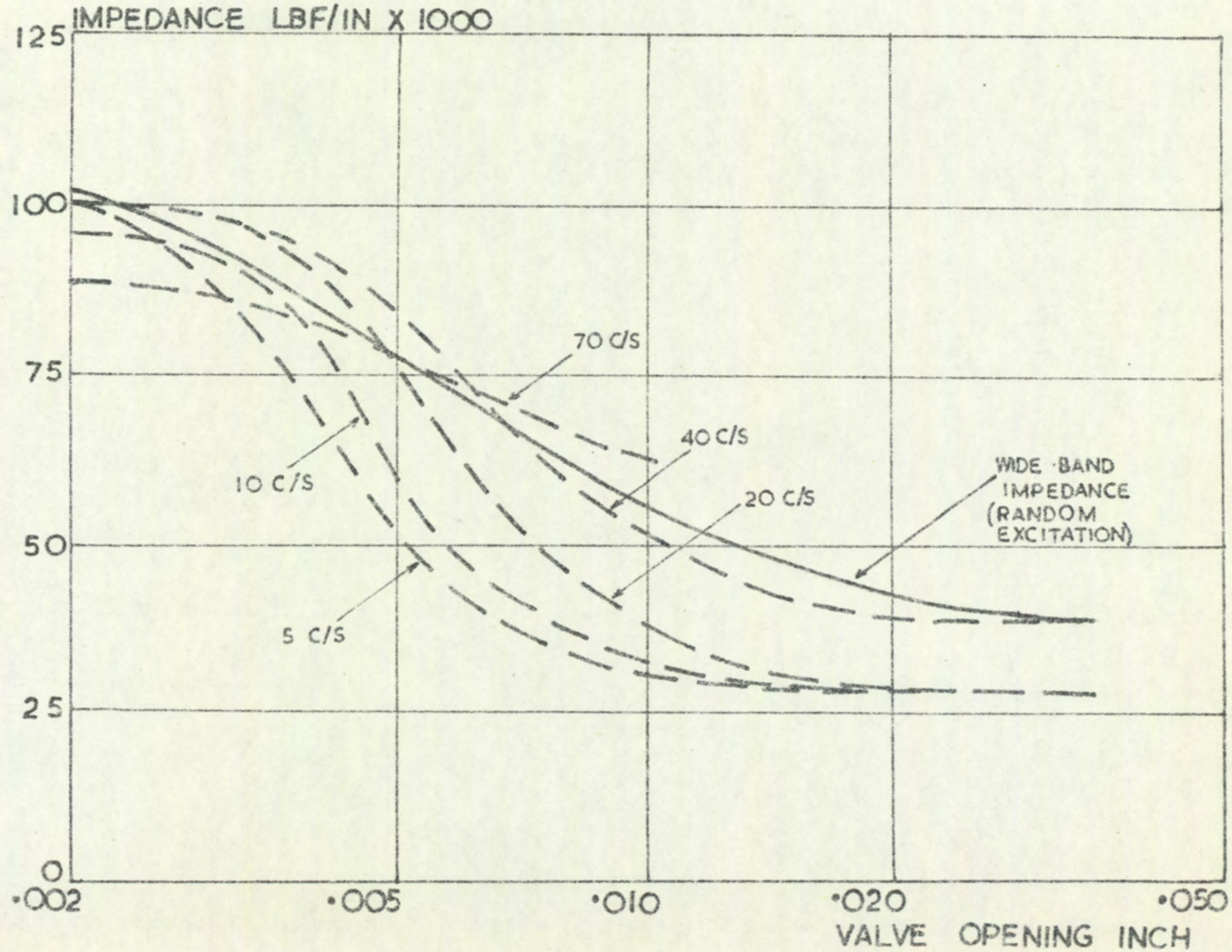

EXPERIMENTAL IMPEDANCE CURVES
COMPARISON BETWEEN WIDE BAND AND DISCREET
FREQUENCY IMPEDANCE
PERTURBATION AMPLITUDE = ±·002 INCH

FIG 5.32

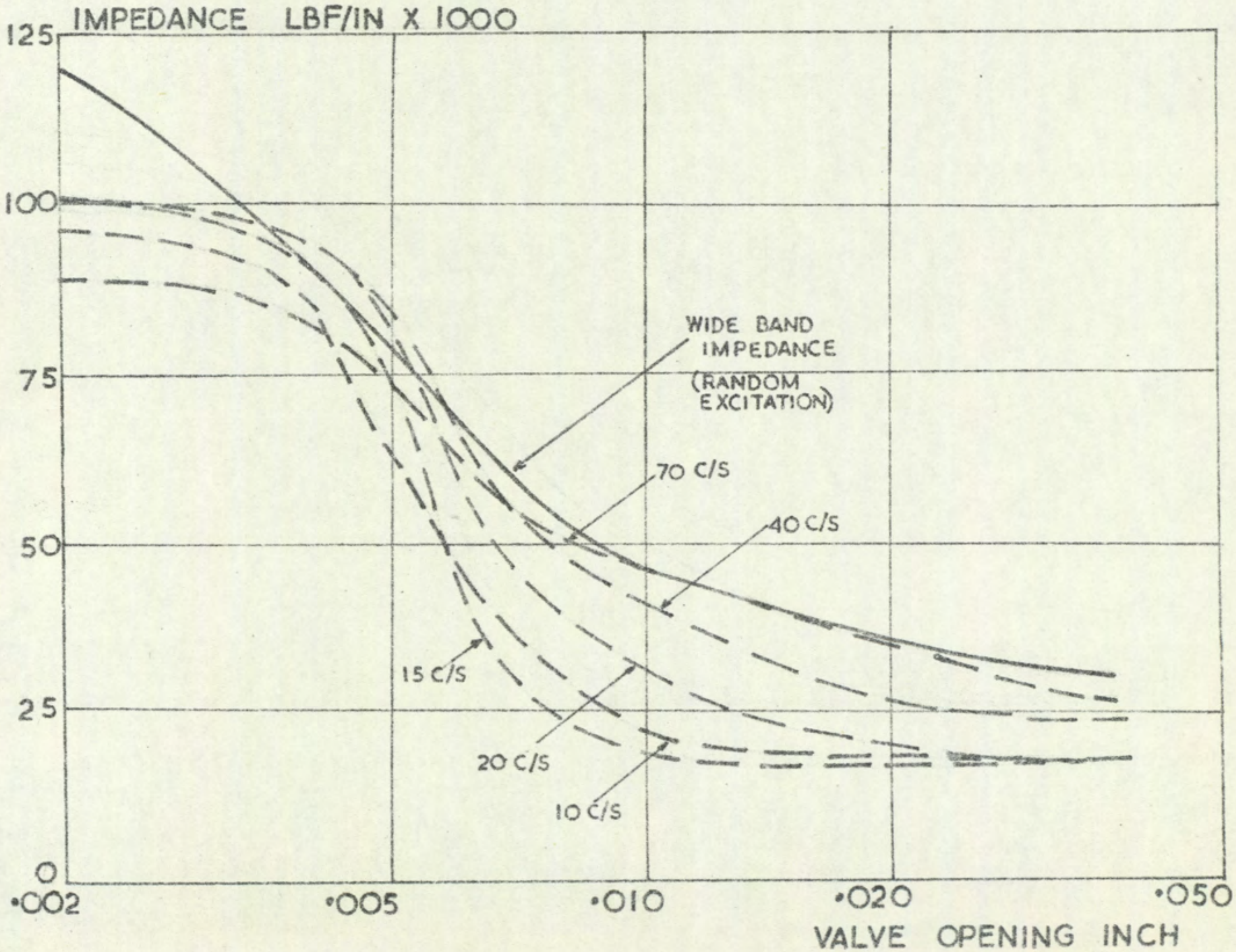

EXPERIMENTAL IMPEDANCE CURVES
COMPARISON BETWEEN WIDE BAND AND DISCREET FREQUENCY IMPEDANCE
PERTURBATION AMPLITUDE = ±•005 INCH

FIG 5.33

CHAPTER VI

Experimental determination of the impedance of a servomechanism in a rigid environment by excitation of its valve input.

The experimental work done to determine the impedance of the servomechanism by exciting its valve input is described and the results discussed. A comparison is made between these results, the experimental results obtained from the output end excitation tests and the results from the theoretical analysis of the servomechanism.

6.1 System under test.

The system under test, a servomechanism excited at the valve input, was described in Section 3.4 and shown in Figs. 3.5 and 3.7.

6.2 Problems involved in the experimental investigation

Whilst f_o^B/x_i can be measured experimentally for various valve openings by offsetting the servo valve, x_o^F/x_i cannot be measured experimentally for various valve openings since when the output is free the servo valve will centre at the neutral position.

If the servomechanism valve was excited with a large amplitude displacement when the output end was free, then X_o^F/X_i would be measured and if this were differentiated dX_o^F/dX_i i.e. x_o^F/x_i would result.

Consequently x_o^F/x_i can be obtained but the effective valve opening or error would not be known. Furthermore, differentiation of X_o^F/X_i would make the measurement of x_o^F/x_i inaccurate. For these reasons it was decided not to attempt to measure the free output response but to use the theoretically predicted values of x_o^F/x_i together with the experimentally obtained values of f_o^B/x_i to obtain the impedance of the servomechanism.

6.3 Calibrations of transducers and instrumentation.

The load cell and displacement transducers were calibrated in the manner described in Section 5.1. The calibration factors were as given in this section. The valve input displacement transducer calibration was set at 50 V/in.

6.4 Excitation of the servomechanism valve input. Output end blocked.

The tests were carried out with the servomechanism piston in the mid stroke position and the servomechanism output end blocked, so that no movement of the output end was possible. Tests were carried out in the frequency range 5 - 70 c/s. The valve input displacement and blocked output force signals were fed into the automatic mechanical impedance analysis system in order to measure the f_o^B/x_i ratio. To tune the analysis system to the frequency of excitation of the valve input (in these tests the oscillator in the analyser was not providing the excitation signal) use was made of the facility for programming the oscillator and in consequence the complete analysis system. The tachogenerator, which was connected to the electric motor driving the valve input eccentric, provided a DC signal proportional to the excitation frequency. This DC signal was attenuated using a potential divider so that when the motor excited the valve input at a particular frequency, the oscillator and the analysis system were tuned to that frequency also. Fine adjustment of the potential divider was made by comparing the valve input displacent and the oscillator output signals on an oscilloscope. In this manner it was possible to tune the analysis system to within 1 c/s of the excitation frequency.

Test Series VIII: The valve input was excited with a perturbation amplitude of $\pm$ 0.005 in. and with valve openings in the range 0.002 in. to 0.040 in. The ratio f_o^B/x_i was measured using the automatic mechanical impedance analysis system as previously described.

6.5 Discussion of results.

The experimental curves for the real and imaginary parts of the f_o^B/x_i ratio are shown in Figs. 6.1 and 6.2. Comparing these with the theoretical predictions for the real and imaginary parts of this function, Figs. 4.24 and 4.25 respectively, it is seen that the experimental curves are of the same shape and size as the theoretical curves. It may be noted that the experimental values of the real part of the function do not increase with increase in valve opening before decreasing as do the theoretical curves. This characteristic has already been observed when comparisons have been made between experimental and theoretical stiffness curves obtained when considering excitation of the servomechanism at its output end. The experimental values of the imaginary parts of the function also show this characteristic. Although the experimental values at the higher frequency increase with increase in valve opening before decreasing, this is not apparently related to the effect under discussion.

The experimental curves for stiffness and damping, which were obtained by the division of the experimental values of f_o^B/x_i by the theoretical values of x_o^F/x_i, are shown in Figs. 6.3 and 6.4. If a comparison is made between these curves and the theoretically predicted curves, Figs. 4.28 and 4.29, it is seen that only a general agreement exists in the form of the curves.

A more significant comparison, however, can be made between the experimental curves for stiffness and damping measured by valve input and servomechanism output end excitation. The reason for this is that it has already been shown in Chapter V that the theoretical analysis does not give a satisfactory prediction for the impedance of the servomechanism even in the more direct case of servomechanism output end excitation.

A comparison between Figs. 6.3 and 5.10 shows that a reasonable agreement exists between the two sets of stiffness curves except that when the valve opening is small the values of stiffness measured for a valve input frequency of 20 c/s and above are too small compared with the values measured using output end excitation. This is probably due to the unexpectedly low values of the imaginary part of the f_o^B/x_i ratio obtained experimentally. At a low frequency, the valve input excitation method gave a value of stiffness which was high compared with the value obtained by using output end excitation of the system. A comparison of the damping curves obtained using the two methods of system excitation, Figs. 5.14 and 6.4, shows that the valve input excitation method apparently measures a considerably greater amount of negative damping in the system than does the method of output end excitation of the servomechanism.

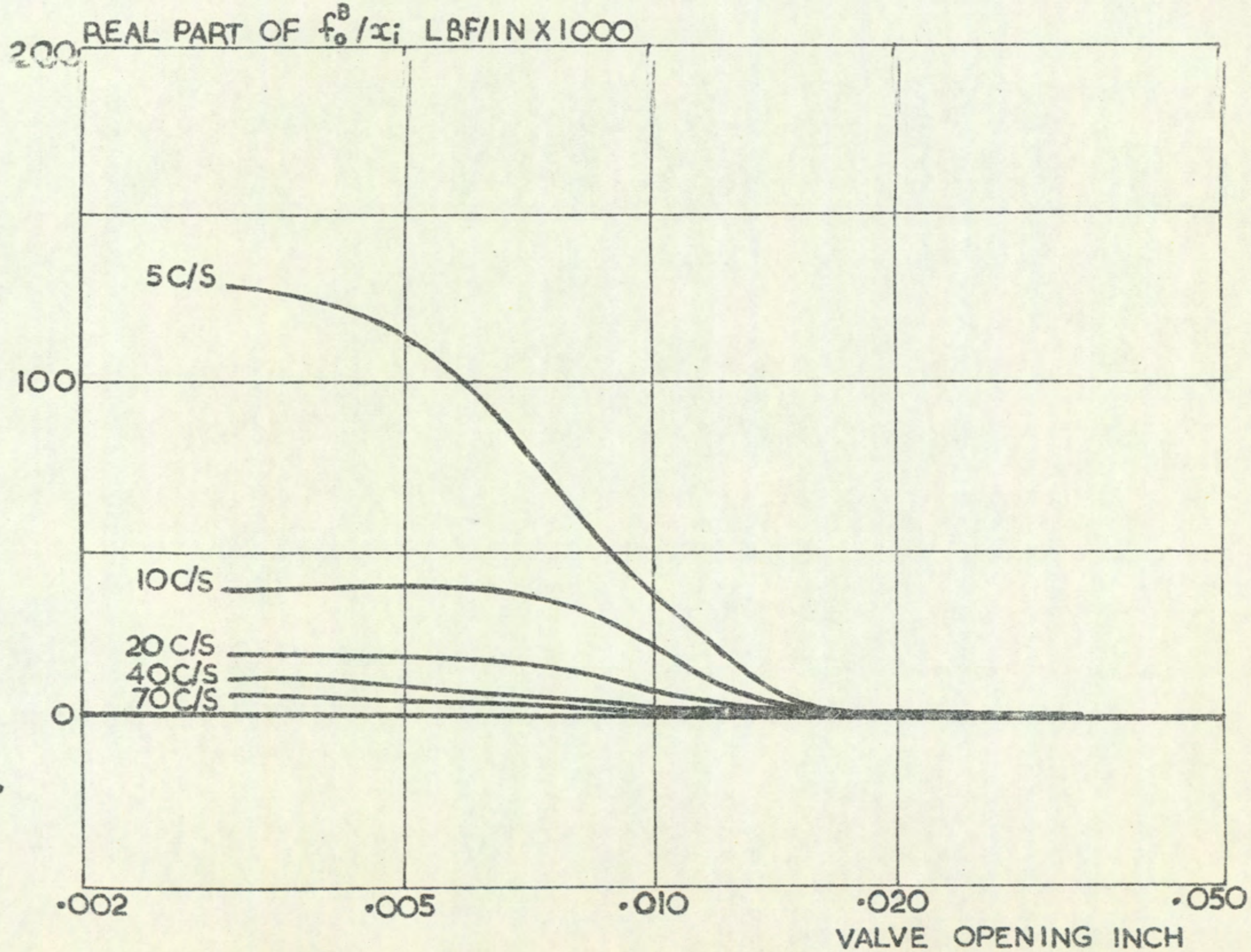

EXPERIMENTAL CURVES FOR REAL PART OF f_o^B/x_i
PERTURBATION AMPLITUDE = ± ·005 INCH

FIG 6.1

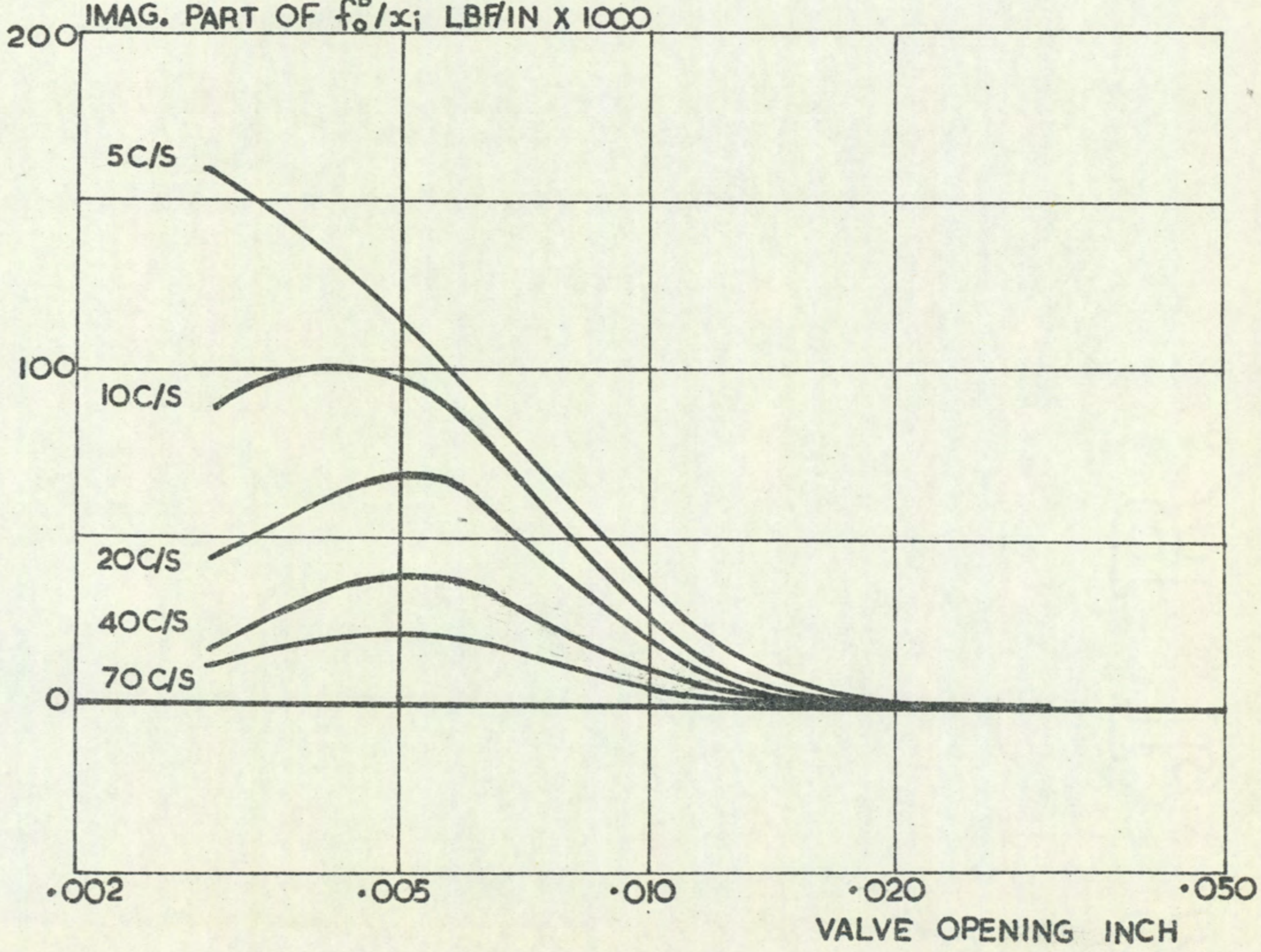

EXPERIMENTAL CURVES FOR IMAG. PART OF f_o^B/x_i

PERTURBATION AMPLITUDE = $\pm$·005 INCH

FIG 6.2

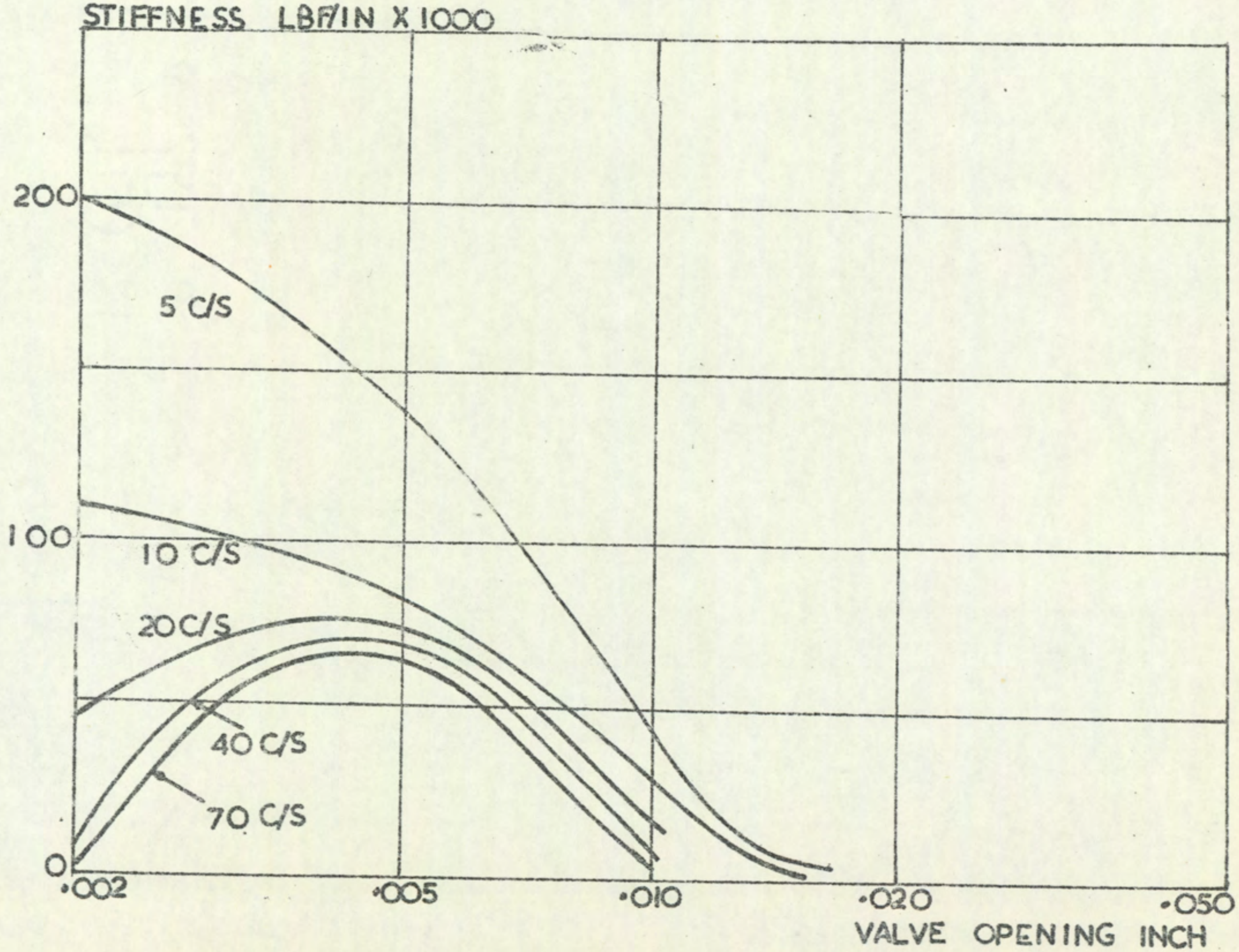

EXPERIMENTAL STIFFNESS CURVES
VALVE INPUT EXCITATION
PERTURBATION AMPLITUDE = ±·005 INCH

FIG 6.3

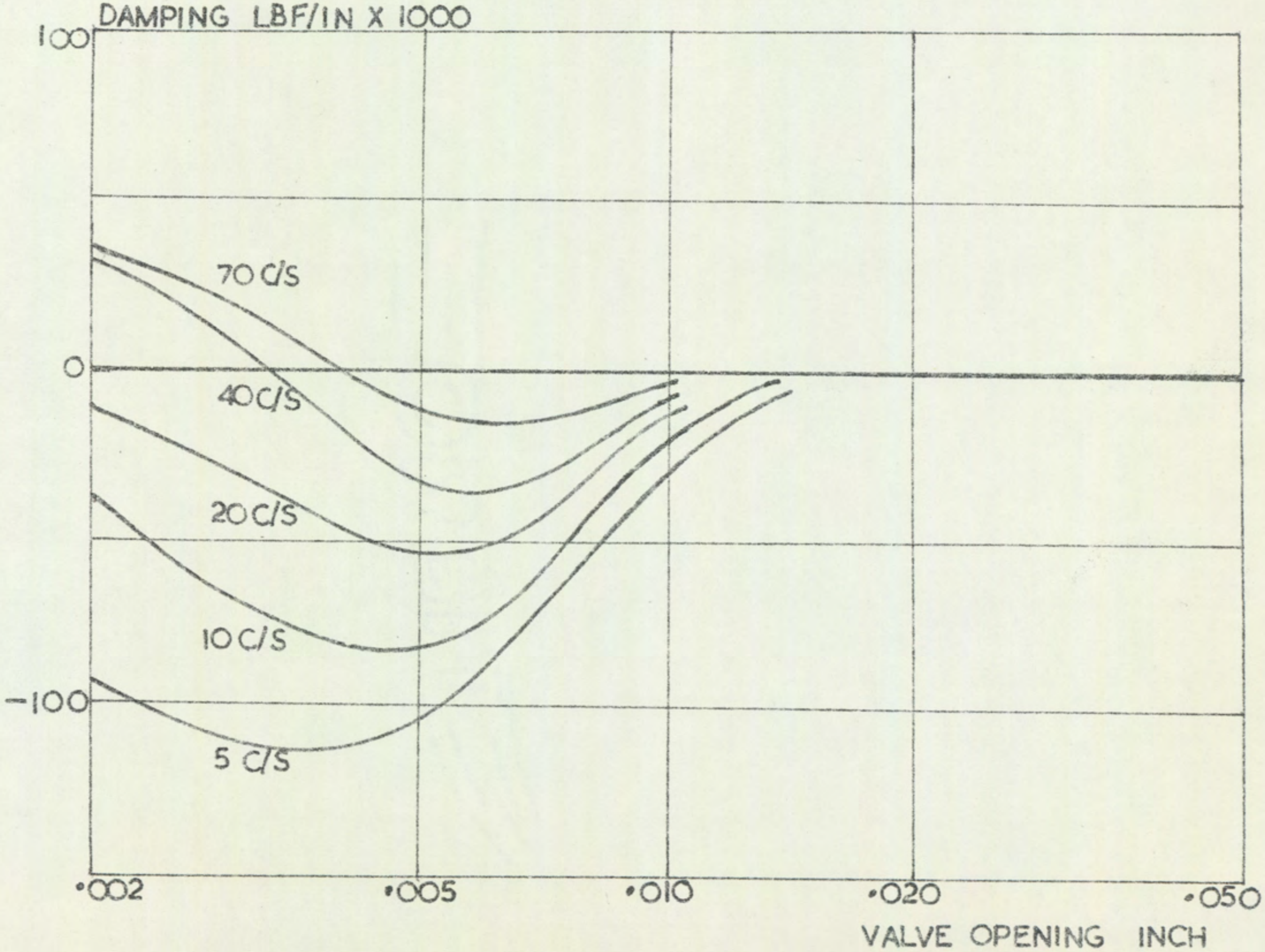

EXPERIMENTAL DAMPING CURVES
VALVE INPUT EXCITATION
PERTURBATION AMPLITUDE = ±·005 INCH

FIG 6.4

PART III

THE IMPEDANCE OF A SYSTEM CONSISTING OF A SERVOMECHANISM CONNECTED TO VARIOUS FLEXIBILITIES.

CHAPTER VII

Theoretical analysis of a system consisting of a hydraulic servomechanism connected to various impedances.

The effect of introducing output end, anchorage and valve input flexibilities on the impedance of the servo system is analysed, the analysis being an extension of that given in Chapter IV.

7.1 Notation.

In addition to the notation defined in Section 4.1 the following notation is used in this chapter.

c	Coefficient of viscous friction in the valve.
G	Oil momentum force factor, $2C_eH_q/(Z_{iR}^2 + Z_{iI}^2)$.
H_p	Oil momentum force coefficient, $\partial F_2/\partial P_2$.
H_q	Oil momentum force coefficient, $\partial F/\partial Q$.
I_p	Modified value of C_p' } To include effect of
J_p	Modified value of K_p } output end impedance.
k_a	Anchorage stiffness.
k_i	Valve input spring stiffness.
k_o	Output end spring stiffness.
L_p	Modified value of C_p' } To include the effect of
M_p	Modified value of K_p } anchorage impedance.

m_a	Mass of moving parts of anchorage.	
m_i	Mass of moving parts of valve spool.	
R_e	Modified value of C_e	To include the effect of valve input impedance. Oil momentum force coupling of valve and spool.
R_p	Modified value of C'_p	
S_e	Modified value of K_e	
S_p	Modified value of K_p	
T_e	Modified value of C_e	To include the effect of valve input impedance. Viscous friction coupling etc.
U_e	Modified value of K_e	
Z_a	Anchorage impedance.	
Z_i	Valve input impedance.	
Z_o	Output end impedance.	
Z_s	Impedance of a particular system.	

In the following notation the upper case letters (left hand column) refer to the steady state condition, and the lower case letters (right hand column) refer to the small perturbation about the steady state condition.

F_1	f_1	Oil momentum forces at each valve port.
F_2	f_2	
F_v	f_v	Viscous friction force onthe valve.
X_a	x_a	Anchorage displacement.
X_s	x_s	Displacement of a particular system.

7.2 Introduction.

In Chapter IV the equations of motion for a hydraulic servomechanism have been formulated and the impedance equation developed. The analysis was then extended to include the effect of an impedance placed in parallel with the servomechanism so that the effect of the mass of moving parts, viscous damping and Coulomb friction could be investigated. In this chapter the analysis is further extended in order that the effect of an impedance placed in series with the servomechanism can be investigated. Two further conditions are analysed, the effect of connecting the servomechanism to a non-rigid anchorage whilst the valve is rigidly connected to earth, and the opposite situation, where the valve is connected non-rigidly to earth whilst the anchorage is rigid.

In the analysis which follows the derivation of equations (4.15), (4.16) & (4.17) is assumed, these equations being restated and renumbered thus,

$$q_1 = -C_p p_1 + C_e e = \frac{V}{2N}\dot{p}_1 + A\dot{x}_o + C_{jp}p_j + C_{op}p_1 \qquad (7.1)$$

$$q_2 = C_p p_2 + C_e e = -\frac{V}{2N}\dot{p}_2 + A\dot{x}_o + C_{jp}p_j - C_{op}p_2 \qquad (7.2)$$

$$2C_e e - p_j C_p' = \frac{V}{2N}\dot{p}_j + 2A\dot{x}_o \qquad (7.3)$$

where $C_p' = C_p + 2C_{jp} + C_{op}$

7.3 Impedance of a system consisting of a servomechanism connected in series to an impedance at its output end.

The system is shown in Fig. 7.1a. The valve is rigidly connected to earth and thus $x_i = 0$ and $e = -x_o$. Considering small force perturbations:

$$f_o = -p_j A = (x_s - x_o)(Z_{oR} + jZ_{oI})$$

and thus

$$x_o = x_s - f_o/(Z_{oR} + jZ_{oI})$$

where Z_{oR} and Z_{oI} are the real and imaginary parts of Z_o respectively.

Substituting for p_j, x_o and e in equation (7.3) and assuming the excitation and response to be sinusoidal

$$(C_p' + j\,\frac{V\omega}{2N})\,\frac{f_o}{A} = 2(C_e + jA\omega)(x_s - \frac{f_o}{Z_{oR} + jZ_{oI}})$$

Writing $V\omega/2N = K_p$ and $A\omega = K_e$

$$[(C_p' + \frac{2AC_e}{Z_{oR} + jZ_{oI}}) + j(K_p + \frac{2AK_e}{Z_{oR} + jZ_{oI}})]\frac{f_o}{A} = 2(C_e + jK_e)x_s$$

$$\left[\left\{C_p' + \frac{2A(C_eZ_{oR} + K_eZ_{oI})}{Z_{oR}^2 + Z_{oI}^2}\right\} + j\left\{K_p + \frac{2A(K_eZ_{oR} - C_eZ_{oI})}{Z_{oR}^2 + Z_{oI}^2}\right\}\right]\frac{f_o}{A}$$

$$= 2(C_e + jK_e)x_s$$

Writing $I_p = C'_p + 2A \dfrac{(C_e Z_{oR} + K_e Z_{oI})}{(Z^2_{oR} + Z^2_{oI})}$

and $$J_p = K_p + 2A \frac{(K_e Z_{oR} - C_e Z_{oI})}{(Z^2_{oR} + Z^2_{oI})}$$

$$Z_s = f_o/x_s$$

$$\therefore Z_s = \frac{2A}{I^2_p + J^2_p} \left[(C_e I_p + K_e J_p) + j(K_e I_p - C_e J_p) \right] \qquad (7.4)$$

It can be shown that the equation can be rearranged into the form

$$1/Z_s = 1/Z_u + 1/Z_o \qquad (7.5)$$

where

$$Z_u = \frac{2A}{C'^2_p + K^2_p} \left[(C_e C'_p + K_e K_p) + j(K_e C'_p - C_e K_p) \right]$$

and $Z_o = Z_{oR} + jZ_{oI}$

This demonstrates that the normal laws of series additions of impedances apply to this system.

7.4 Impedance of a system consisting of a servomechanism connected in series to a flexibility at its output end.

This system, which is shown in Fig. 7.1b is a simplification of the system analysed in the previous section.

In this case $Z_{oR} = k_o$ and $Z_{oI} = 0$

Thus, $I_p = C'_p + 2AC_e/k_o$

and $J_p = K_p + 2AK_e/k_o$

Substituting for I_p and J_p in equation (7.4) gives:

$$Z_s = \frac{2A[\{C_e(C'_p + 2AC_e/k_o) + K_e(K_p + 2AK_e/k_o)\} + j(C'_pK_e - C_eK_p)]}{(C'_p + 2AC_e/k_o)^2 + (K_p + 2AK_e/k_o)^2}$$

or alternatively from equation (7.5)

$$1/Z_s = 1/Z_u + 1/k_o$$

Static stiffness: If $K_e = K_p = 0$ then,

$$Z_s(\text{static}) = 2AC_e/(C'_p + 2AC_e/k_o)$$

Infinite frequency stiffness: As ω tends to infinity, C'_p and C_e become insignificant compared with K_e and K_p

$\therefore$ $Z_s(\text{inf. freq}) = 2AK_e(K_p + 2AK_e/k_o)$

Stability criterion: If the system is to be stable the damping must be positive. Thus,

$$C'_pK_e > C_eK_p \quad \text{or} \quad C'_p/C_e > K_p/K_e$$

The output end flexibility has no effect on the system stability. It can be shown that an alternative form of the criterion is

$$Z_s(\text{inf. freq}) > Z_s(\text{static})$$

7.5 Impedance of a system consisting of a servomechanism connected in series at its output end to a spring/mass combination.

The system is shown in Fig. 7.2. This system was chosen for analysis since it was the practical system used for investigation of output end flexibility, (see Chapter VIII). Although primarily concerned with the investigation of output end flexibility, it was found impossible to design a spring having sufficient strength and stiffness without including a significant mass into the system.

It has been shown in Sections 4.9 and 7.3 that an impedance placed at the servomechanism output end in parallel and in series can be analysed using the normal laws of impedance addition. Thus, it is possible to predict the impedance of this system by combining the theoretical impedance of the servomechanism with the impedance of the springs and masses. In Chapter V, however, it was shown that the theoretical analysis of the servomechanism did not give a value of impedance which compared closely with the measured impedance of the servomechanism. Hence, to determine the impedance of the servomechanism output end flexibility system, it would be more realistic to use the experimentally determined values of stiffness and damping for the servomechanism as a starting point for the impedance calculations. This has been done and the results are discussed in Chapter VIII.

7.6 Impedance of a system consisting of a servomechanism connected to a non-rigid anchorage.

Although primarily concerned with a system containing anchorage flexibility, initially to make the analysis more general, the case will be considered where the anchorage has an impedance $Z_a = Z_{aR} + jZ_{aI}$. The system is shown in Fig. 7.3a. The analysis of the motion of the jack will be unaltered except that equations (7.1) & (7.2) will be modified thus:

$$q_1 = - C_p p_1 + C_e e = \frac{V}{2N} \overset{\circ}{p}_1 + A(\overset{\circ}{x}_o - \overset{\circ}{x}_a) + C_{jp} p_j + C_{op} p_1$$

$$q_2 = C_p p_2 + C_e e = - \frac{V}{2N} \overset{\circ}{p}_2 + A(\overset{\circ}{x}_o - \overset{\circ}{x}_a) + C_{jp} p_j - C_{op} p_2$$

Adding these two equations together gives

$$2C_e e - p_j C'_p = \frac{V}{2N} \overset{\circ}{p}_j + 2A(\overset{\circ}{x}_o - \overset{\circ}{x}_a) \qquad (7.6)$$

The valve is locked so $x_i = 0$ and $e = -x_o$. Considering small force perturbations $Z_a x_a = f_o = -p_j A$

$$\therefore \quad x_a = f_o/Z_a \quad \text{and} \quad p_j = -f_o/A$$

Substituting for p_j, x_a and e in equation (7.6) and assuming the excitation and response to be sinusoidal,

$$(C_p' + j\,\frac{V\omega}{2N})\,\frac{f_o}{A} = 2C_e x_o + j2A\omega(x_o - \frac{f_o}{Z_{aR} + jZ_{oI}})$$

Writing $V\omega/2N = K_p$ and $A\omega = K_e$

$$[C_p' + j(K_p + \frac{2AK_e}{Z_{aR} + jZ_{aI}})]\,\frac{f_o}{A} = 2(C_e + jK_e)x_o$$

$$[(C_p' + \frac{2AK_e Z_{aI}}{Z_{aR}^2 + Z_{aI}^2}) + j(K_p + \frac{2AK_e Z_{aR}}{Z_{aR}^2 + Z_{aI}^2})]\frac{f_o}{A} = 2(C_e + jK_e)x_o$$

If we write $L_p = C_p' + \dfrac{2AK_e Z_{aI}}{Z_{aR}^2 + Z_{aI}^2}$

and $M_p = K_p + \dfrac{2AK_e Z_{aR}}{Z_{aR}^2 + Z_{aI}^2}$

$$\therefore Z_s = \frac{2A}{L_p^2 + M_p^2}[(C_e L_p + K_e M_p) + j(K_e L_p - C_e M_p)] \qquad (7.7)$$

7.7 Impedance of a system consisting of a servomechanism with anchorage flexibility.

This system is shown in Fig. 7.3b, and is a particular case of the system previously analysed. Thus,

$$Z_{oR} = k_a \text{ and } Z_{oI} = 0$$

$$\therefore \quad L_p = C_p' \text{ and } M_p = K_p + 2AK_e/k_a$$

$$\therefore Z_s = \frac{2A[\{C_e C_p' + K_e(K_p + 2AK_e/k_a)\} + j\{C_p'K_e - C_e(K_p + 2AK_e/k_a)\}]}{C_p'^2 + (K_p + 2AK_e/k_a)^2}$$

Static stiffness: If $K_e = K_p = 0$ then

$$Z_s(\text{static}) = 2AC_e/C_p'$$

Comparison between this equation and equation (4.20) shows that the anchorage flexibility has no effect on the static stiffness of the system.

Infinite frequency stiffness: As ω tends to infinity C_p' and C_e become insignificant compared to K_p and K_e

$$\therefore \quad Z_s(\text{inf. freq.}) = 2AK_e/(K_p + 2AK_e/k_a)$$

Rearranging this equation gives

$$\frac{1}{Z_s(\text{inf. freq})} = \frac{K_p}{2AK_e} + \frac{1}{k_a}$$

From equation (4.21) $Z_u(\text{inf. freq.}) = 2AK_e/K_p$

$$\therefore \quad \frac{1}{Z_s(\text{inf. freq.})} = \frac{1}{Z_u(\text{inf. freq.})} + \frac{1}{k_a}$$

Thus, as the frequency of excitation tends to infinity the impedance of the system can be calculated by combining the impedance of the servomechanism in a rigid environment and the impedance of the anchorage flexibility using the normal laws of impedance.

Stability criterion: For the system to be stable the damping must be positive. Hence,

$$C_p'K_e > C_e(K_p + 2AK_e/k_a)$$

The margin of stability is decreased by the anchorage flexibility. It can be shown that an alternative form of the criterion is

$$Z_s(\text{inf. freq.}) > Z_s(\text{static})$$

7.8 Impedance of a system consisting of a servomechanism connected to an anchorage flexibility and mass.

This system, which is shown in Fig. 7.4 was the practical system used for investigation of the effect of anchorage flexibility. As previously mentioned, it was found impossible to design a spring having sufficient stiffness and strength without introducing a significant mass into the system. The effect of this mass is to modify k_a to $(k_a - m_a\omega^2)$ in the impedance equation developed. Using the technique of step by step integration the relationship between valve opening and valve pressure drop could be determined and the impedance equation evaluated in an identical manner to that already described in Chapter IV to investigate the impedance of a servomechanism in a rigid environment. It has been shown in Chapter V that the theoretical analysis of the servomechanism in a rigid environment did not produce a value of impedance which closely compared with the measured value. Hence, it is unlikely that the impedance equation, which includes the effect of anchorage flexibility, will give a closer estimate of the impedance of a system with anchorage flexibility than did the basic equation from which it is developed give an estimate of the impedance of a servomechanism in a rigid environment.

In view of these difficulties it was decided to assume that the low frequency impedance of the system was equal to the low frequency impedance of the servomechanism measured in a rigid environment, and to calculate the high frequency impedance of the system using the high frequency impedance measured in a rigid environment combined with the impedance of the anchorage flexibility using the normal laws of impedance addition. This has been done and the results are discussed in Chapter IX.

7.9 Impedance of a system consisting of a servomechanism with its valve input connected non-rigidly to earth.

Introduction.

Before an anlysis of the system shown in Fig. 7.5a can be undertaken it is necessary to decide what forces are acting on the valve spool in order to excite the subsystem consisting of the spool and impedance Z_i. The forces acting on the valve spool may be classified thus:-

(i) Oil momentum forces.

(ii) Viscous friction forces acting between the valve spool and body.

(iii) Coulomb friction forces acting between the valve spool and body.

In the sections which follow the impedance of the system will be developed for the first and second form of excitation force on the valve. The analysis necessary to develop the impedance equation for a system with Coulomb friction excitation of the valve will not be given since the resulting equations are extremely complicated. Furthermore, since the effect of Coulomb friction must be linearised to be included into the analysis, the resulting equation would be of doubtful value.

7.10 Impedance of a system consisting of a servomechanism with its input connected to earth via an impedance. Oil momentum force excitation of the valve spool.

This analysis is based on (11), in which the effect of oil momentum forces acting on the servo valve are analysed. Equations (7.1) & (7.2) will be unchanged and so equation (7.3) gives

$$2C_e(x_i - x_o) - p_j C'_p = \frac{V}{2N}\mathring{p}_j + 2A\mathring{x}_o = q_1 + q_2$$

Now $\quad F_1 = \phi_1(Q_1 P_1)$

and $\quad F_2 = \phi_2(Q_2 P_2)$

where F_1 and F_2 are the oil momentum forces acting at each valve port.

Taking small perturbations

$$f_1 = \frac{\partial F_1}{\partial Q_1} q_1 + \frac{\partial F_1}{\partial P_1} p_1$$

and
$$f_2 = \frac{\partial F_2}{\partial Q_2} q_2 + \frac{\partial F_2}{\partial P_2} p_2$$

Assuming the valves are symmetrical

$$\frac{\partial F_1}{\partial Q_1} = \frac{\partial F_2}{\partial Q_2} = H_q \quad \text{and} \quad -\frac{\partial F_1}{\partial P_1} = \frac{\partial F_2}{\partial P_2} = H_p$$

$$\therefore \quad f_1 = H_q q_1 - H_p p_1$$

$$f_2 = H_q q_2 + H_p p_2$$

$\therefore f_1 + f_2 = H_q(q_1 + q_2) - H_p(p_1 - p_2)$

Substituting for $(q_1 + q_2)$ from equation (7.3) gives

$$f_1 + f_2 = H_q[\frac{V}{2N}(\dot{p}_1 - \dot{p}_2) + 2A\dot{x}_o] - H_p(p_1 - p_2)$$

Since $f_1 + f_2 = -Z_i x_i$

$$-(Z_{iR} + jZ_{iI})x_i = H_q[(\frac{V}{2N})\dot{p}_j + 2A\dot{x}_o] - H_p p_j$$

Substituting for x_i from above in equation (7.3) and assuming the excitation and response to be sinusoidal

$$(C_p' + j\frac{V\omega}{2N})p_j = 2(C_e + jA\omega)x_o$$

$$+ 2C_e\left[\frac{jH_q[(\frac{V\omega}{2N})p_j + 2A\omega\, x_o] - H_p p_j}{(Z_{iR} + jZ_{iI})} + x_o\right]$$

Substituting for p_j and writing $V\omega/2N = K_p$ and $A\omega = K_e$,

$$\left[C_p' + jK_p + \frac{j2C_eH_qK_p(Z_{iR} - jZ_{iI})}{Z_{iR}^2 + Z_{iI}^2} - \frac{2C_eH_p(Z_{iR} - jZ_{iI})}{Z_{iR}^2 + Z_{iI}^2}\right]\frac{f_o}{A}$$

$$= \left[2x_o \quad C_e + jK_e + j\,\frac{C_e 2K_e H_q(Z_{iR} - jZ_{iI})}{Z_{iR}^2 + Z_{iI}^2}\right]$$

$$\left[\left\{C_p' + \frac{Z_{iI}2C_eH_qK_p - 2C_eH_pZ_{iR}}{Z_{iR}^2 + Z_{iI}^2}\right\} + j\left\{K_p + \frac{2C_eH_qK_pZ_{iR} + 2C_eH_pZ_{iI}}{Z_{iR}^2 + Z_{iI}^2}\right\}\right]\frac{f_o}{A}$$

$$= 2x_o\left[\left\{C_e + \frac{Z_{iI}2K_eC_eH_q}{Z_{iR}^2 + Z_{iI}^2}\right\} + j\left\{K_e + \frac{2C_eK_eZ_{iR}H_q}{Z_{iR}^2 + Z_{iI}^2}\right\}\right]$$

As $H_p = \dfrac{\partial F_2}{\partial P_2}$ then $H_p = \dfrac{\partial F_2}{\partial Q_2} \times \dfrac{\partial Q_2}{\partial P_2} = H_q C_p$

Therefore,

$$\left[\left\{C_p' + 2C_e H_q \frac{(Z_{iI}K_p - Z_{iR}C_p)}{Z_{iR}^2 + Z_{iI}^2}\right\} + j\left\{K_p + 2C_e H_q \frac{(Z_{iR}K_p + C_e Z_{iI})}{Z_{iR}^2 + Z_{iI}^2}\right\}\right]\frac{f_o}{A}$$

$$= 2x_o\left[\left\{C_e + \frac{2K_e C_e H_q Z_{iI}}{Z_{iR}^2 + Z_{iI}^2}\right\} + j\left\{K_e + \frac{2C_e K_e H_q Z_{iR}}{Z_{iR}^2 + Z_{iI}^2}\right\}\right]$$

Writing $2C_e H_q/(Z_{iR}^2 + Z_{iI}^2) = G$, then

$$[\{C_p' - G(Z_{iR}C_p - Z_{iI}K_p)\} + j\{K_p + G(Z_{iR}K_p + Z_{iI}C_e)\}]\,\frac{f_o}{A}$$

$$= 2x_o[(C_e + GK_e Z_{iI}) + j(K_e + GK_e Z_{iR})]$$

If $\quad R_p = C_p' - G(Z_{iR}C_p - Z_{iI}K_p)$

$S_p = K_p + G(Z_{iR}K_p + Z_{iI}C_e)$

$R_e = C_e + GK_e Z_{iI}$

$S_e = K_e + GK_e Z_{iR}$

Then the system impedance is given by

$$Z_s = \frac{2A}{R_p^2 + S_p^2}\,[(R_e R_p + S_e S_p) + j(S_e R_p - R_e S_p)] \tag{7.8}$$

7.11 The impedance of a system consisting of a servomechanism with its input connected to earth via an impedance. Viscous friction force excitation of the valve spool.

Consider a damper (in this sytem, the valve spool - valve body combination) connected in series to an impedance $Z_i = Z_{iR} + jZ_{iI}$

Then $$\frac{1}{Z} = \frac{1}{j\omega c} + \frac{1}{Z_{iR} + jZ_{iI}}$$

$Z = f_v/x_o$ where f_v is the force applied to the valve body and x_o is the displacement of the output end of the servomechanism, i.e. the displacement of the valve body.

$$\therefore \quad f_v = \frac{(-Z_{iI}\omega c + j\omega c Z_{iR})x_o}{Z_{iR} + j(Z_{iI} + \omega c)}$$

As $f_v/(x_o - x_i) = j\omega c$

$$x_o - x_i = \left[\frac{-Z_{iI} + jZ_{iR}}{jZ_{iR} - (Z_{iI} + \omega c)}\right] x_o$$

Therefore,

$$x_o - x_i = \left[\frac{(Z_{iR}^2 + Z_{iI}^2 + Z_{iI}\omega c) - jZ_{iR}\omega c}{Z_{iR}^2 + Z_{iI}^2 + 2Z_{iI}\omega c + (\omega c)^2}\right] x_o$$

As $f_v = j\omega c(x_o - x_i)$

$$f_v = \left[\frac{Z_{iR}(\omega c)^2 + j\omega c[Z_{iR}^2 + Z_{iI}^2 + Z_{iI}\omega c]}{Z_{iR}^2 + Z_{iI}^2 + 2Z_{iI}\,\omega c + (\omega c)^2}\right] x_o$$

$$f_o = -p_j A + f_v$$

Substituting for p_j, f_v and e in equation (7.3) and assuming the excitation and response to be sinusoidal gives

$$\left(C_p' + \frac{jV\omega}{2N}\right)\left[\frac{f_o}{A} - \frac{Z_{iR}(\omega c)^2 + j\omega c[Z_{iR}^2 + Z_{iI}^2 + Z_{iI}\omega c]}{[(Z_{iI} + \omega c)^2 + (Z_{iR}^2)]A}\right] x_o$$

$$= 2Aj\omega x_o + 2C_e\left[\frac{Z_{iR}^2 + Z_{iI}^2 + Z_{iI}\omega c - jZ_{iR}\omega c}{(Z_{iI} + \omega c)^2 + (Z_{iR})^2}\right] x_o$$

Writing $K_p = V\omega/2N$ and $K_e = A\omega$

$$(C_p' + jK_p)\frac{f_o}{A} = 2x_o\left[j\left\{K_e - \frac{Z_{iR}\omega c C_e}{(Z_{iI} + \omega c)^2 + Z_{iR}^2}\right\} + C_e\left\{\frac{Z_{iR}^2 + Z_{iI}^2 + Z_{iI}\omega c}{(Z_{iI} + \omega c)^2 + Z_{iR}^2}\right\}\right]$$

$$+ (C_p' + jK_p)x_o\left[\frac{Z_{iR}(\omega c)^2 + j\omega c(Z_{iR}^2 + Z_{iI}^2 + Z_{iI}\omega c)}{A[(Z_{iI} + \omega c)^2 + Z_{iR}^2]}\right]$$

If we write $T_e = C_e(Z_{iR}^2 + Z_{iI}^2 + Z_{iI}\omega c)/[(Z_{iI} + \omega c)^2 + Z_{iR}^2]$

$$U_e = K_e - (Z_{iR}\omega c C_e)/[(Z_{iI} + \omega c)^2 + Z_{iR}^2]$$

The system impedance is given by

$$Z_s = \frac{2A}{C_p'^2 + K_p^2}[(T_e C_p' + U_e K_p) + j(U_e C_p' - T_e K_p)] + \left[\frac{Z_{iR}(\omega c)^2}{(Z_{iI} + \omega c)^2 + Z_{iR}^2}\right]$$

$$+ j\left[\frac{\omega c(Z_{iR}^2 + Z_{iI}^2 + Z_{iI}\omega c)}{(Z_{iI} + \omega c)^2 + Z_{iR}^2}\right]$$

The effect of the last two terms in this equation is small and thus may be neglected. The resulting impedance equation is given by

$$Z_s = \frac{2A}{C_p'^2 + K_p^2}[(T_eC_p' + U_eK_p) + j(U_eC_p' - T_eK_p)] \qquad (7.9)$$

7.12 <u>The impedance of a servomechanism with its valve connected to earth via a spring.</u>

The system, which is shown in Fig. 7.5b is a particular case of the system which has been previously analysed, and the two hypotheses to account for the valve excitation now simplify as follows:

<u>Oil momentum force excitation of the valve:</u> In this case as $Z_{iR} = k_i$ and $Z_{iI} = 0$, $G = 2C_eH_q/k_i^2$.

$$\therefore \quad R_p = C_p' - \frac{2C_eH_qC_p}{k_i}$$

$$S_p = K_p + \frac{2C_eH_qK_p}{k_i}$$

$$R_e = C_e$$

$$S_e = K_e + \frac{2C_eH_qK_e}{k_i}$$

Z_s may be determined by substituting these values in the following equation, (7.8).

$$Z_s = \frac{2A}{R_p^2 + S_p^2} [(R_e R_p + S_e S_p) + j(S_e R_p - R_e S_p)]$$

Static stiffness (oil momentum force excitation of the valve): From the above equation it can be shown that when $\omega = 0$,

$$Z_s(\text{static}) = 2AC_e/(C_p' - \frac{2C_e C_p H_q}{k_i})$$

Infinite frequency stiffness (oil momentum force excitation of the valve): As ω tends to infinity C_e and C_p' are small compared to K_e and K_p.

$$Z_s(\text{inf. freq.}) = 2AK_e/K_p$$

Stability criterion (oil momentum force excitation of the valve): For the system to be stable the damping must be positive.

$$\therefore \quad K_e(C_p' - \frac{2C_e C_p H_q}{k_i}) > K_p C_e$$

An alternative form of this expression is

$$Z_s(\text{inf. freq.}) > Z_s(\text{static})$$

Viscous friction force excitation of the valve: In this case as $Z_{iR} = k_i$ and $Z_{iI} = 0$,

$$\therefore \quad T_e = C_e k_i^2/(\omega^2 c^2 + k_i^2)$$

and $$U_e = K_e - \frac{k_i \omega c C_e}{\omega^2 c^2 + k_i^2}$$

Z_s may be determined by substituting these values in the following equation, (7.9).

$$Z = \frac{2A}{C_p'^2 + K_p^2}\left[(T_e C_p' + U_e K_p) + j(U_e C_p' - T_e K_p)\right]$$

<u>Static stiffness (viscous friction force excitation of the valve)</u>: From the above equation it can be shown that when $\omega = 0$

$$Z_s(\text{static}) = 2AC_e/C_p'$$

<u>Infinite frequency stiffness (viscous friction force excitation of the valve)</u>: As ω tends to infinity C_e and C_p' are small compared to K_e and K_p

$$Z_s(\text{inf. freq.}) = 2AK_e/K_p$$

<u>Stability criterion (viscous friction force excitation of the valve)</u>: For the system to be stable the damping must be positive. Hence,

$$\left[K_e - \frac{k_i \omega c C_e}{(\omega^2 c^2 + k_i^2)}\right] C_p' > \left[\frac{C_e k_i^2}{(\omega^2 c^2 + k_i^2)}\right] K_p$$

$$\therefore \quad C'_p K_e \left[\frac{\omega c}{k_i}\right]^2 - C_e C'_p \left[\frac{\omega c}{k_i}\right] + K_e C'_p > C_e K_p$$

The effect of the valve input flexibility assuming viscous friction coupling between the valve body and spool, is to increase the stability of the system provided that

$$K_e \left[\frac{\omega c}{k_i}\right] > C_e$$

or $$A\omega^2 c > C_e k_i$$

7.13 The impedance of a servomechanism with its valve input connected to earth via a spring and mass.

The system, which is shown in Fig. 7.6, was the practical system used to carry out the experimental investigation upon the effect of valve input flexibility. The effect of the mass could be included into the analysis by modifying k_i to $(k_i - m_i\omega^2)$. In practice it was found that m_i was sufficiently small to be neglected.

Comparing the two hypotheses used to develop the impedance equation, it can be seen that both of these hypotheses result in an impedance equation of some complexity. Either of the impedance equations could be solved by first obtaining the relationship between valve opening and valve pressure drop by means of a step by step integration process. As previously explained however, in the discussion of the effect of anchorage flexibility, Section 7.8, little purpose would be served by this because the equation developed for a rigid system is not, in itself, an accurate method of predicting impedance.

The analysis of the effect of valve input flexibility shows that depending upon the type of force exciting the valve spool, impedance equations leading to significantly different results are obtained. Hence, prediction of the servomechanism impedance under these conditions cannot be made unless it is known which force, if any, predominates, since the forces which may be acting on the valve spool, e.g. oil momentum, viscous and Coulomb friction, produce effects which might act in conjunction with, or opposition to each other from an impedance consideration.

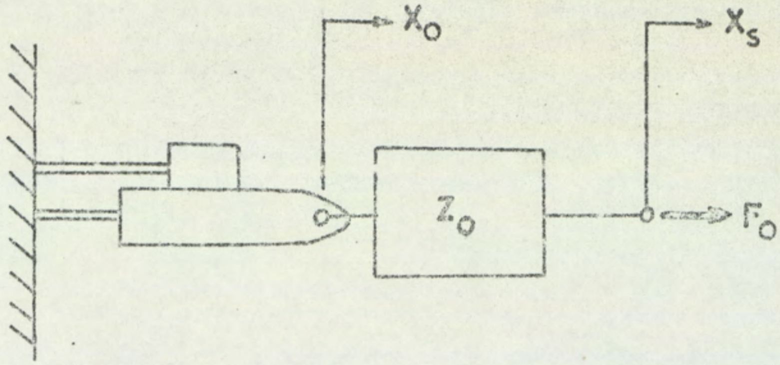

(A) SERVOMECHANISM WITH AN IMPEDANCE CONNECTED IN SERIES AT ITS OUTPUT END

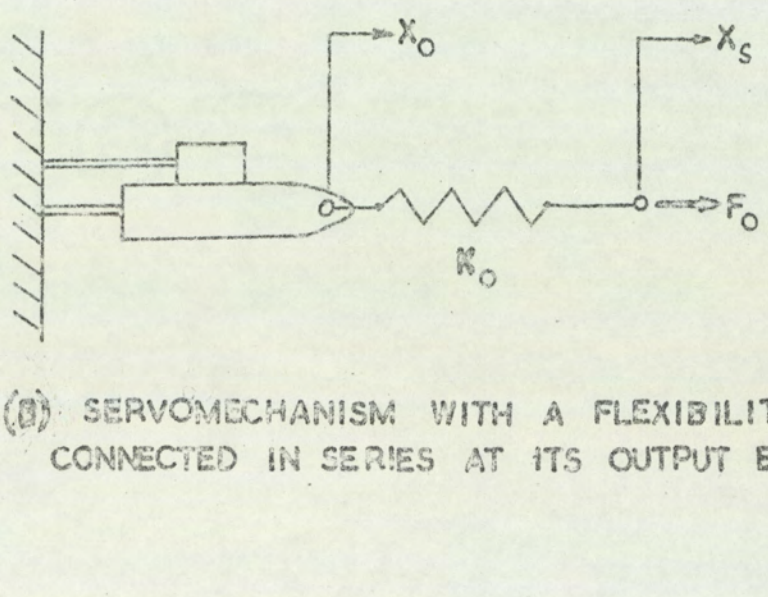

(B) SERVOMECHANISM WITH A FLEXIBILITY CONNECTED IN SERIES AT ITS OUTPUT END

FIG 7.1

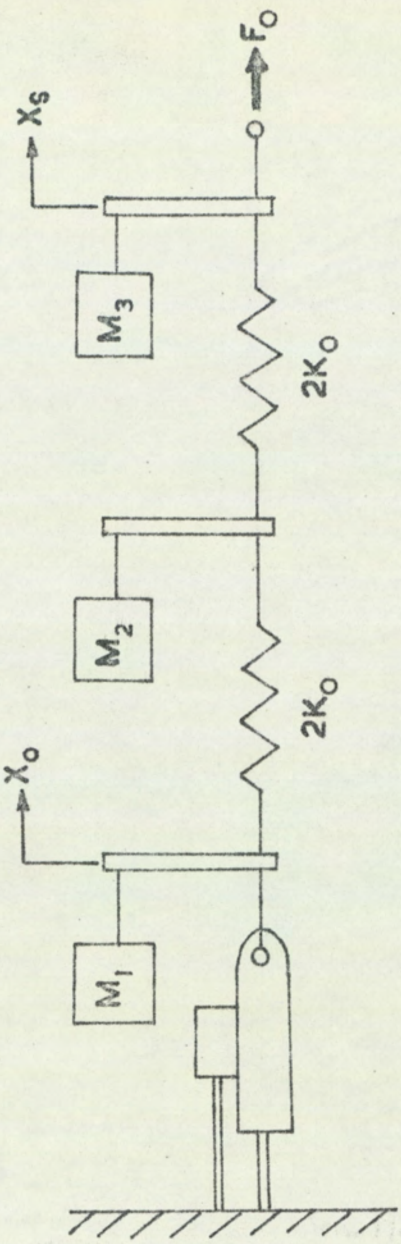

SERVOMECHANISM WITH OUTPUT END FLEXIBILITY
PRACTICAL SYSTEM USED FOR EXPERIMENTAL PROGRAMME

FIG 7.2

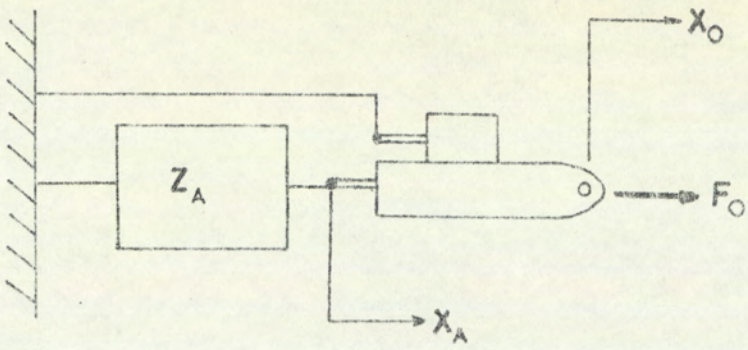

(A) SERVOMECHANISM WITH ITS ANCHORAGE CONNECTED TO AN IMPEDANCE

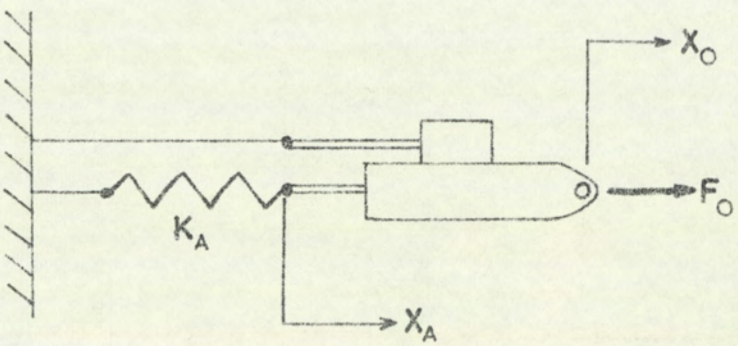

(B) SERVOMECHANISM WITH ITS ANCHORAGE CONNECTED TO A FLEXIBILITY

FIG 7.3

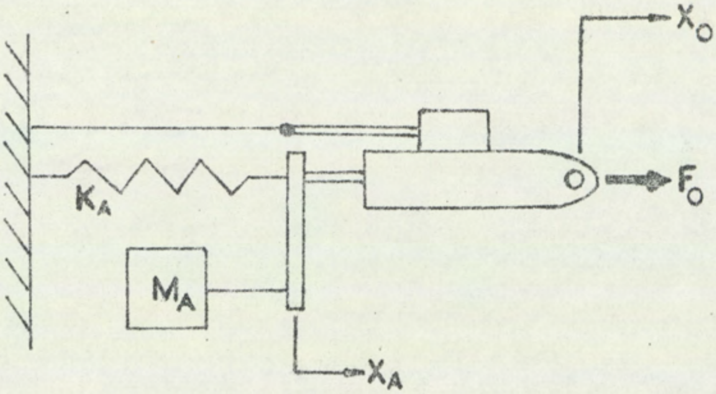

SERVOMECHANISM WITH ANCHORAGE FLEXIBILITY
PRACTICAL SYSTEM USED FOR EXPERIMENTAL
PROGRAMME

FIG 7.4

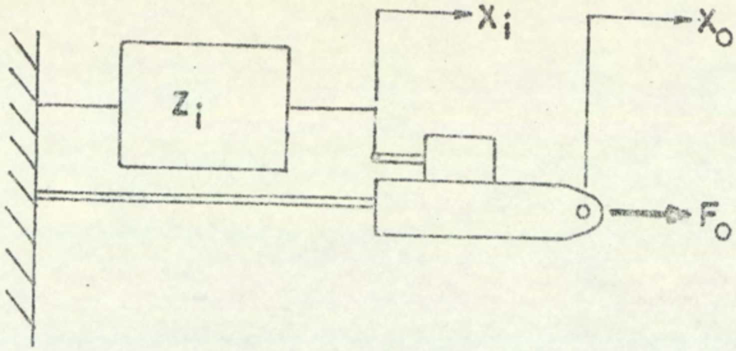

(A) SERVOMECHANISM WITH ITS VALVE INPUT CONNECTED TO AN IMPEDANCE

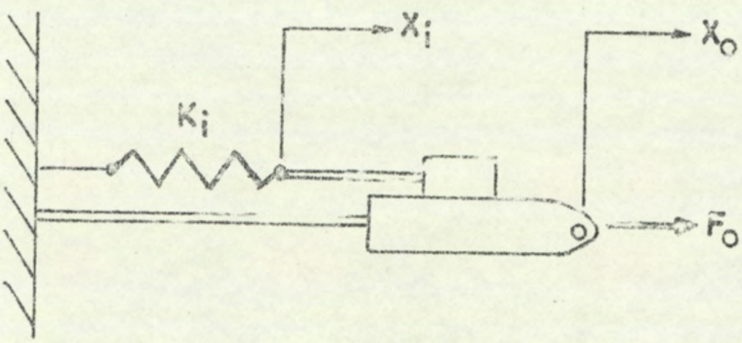

(B) SERVOMECHANISM WITH ITS VALVE INPUT CONNECTED TO A FLEXIBILITY

FIG 7.5

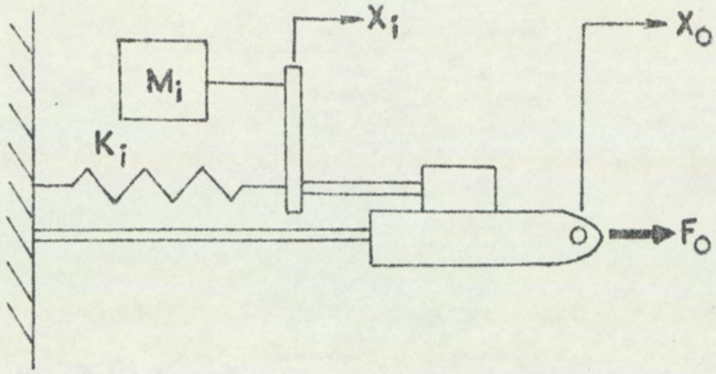

SERVOMECHANISM WITH VALVE INPUT FLEXIBILITY
PRACTICAL SYSTEM USED FOR EXPERIMENTAL
PROGRAMME

FIG 7.6

CHAPTER VIII

Experimental determination of the impedance of a system consisting of a servomechanism connected at its output end to a flexibility.

The experimental work done to determine the impedance of a system consisting of a servomechanism connected to a flexibility at its output end is described. A comparison is made between the measured impedance and the impedance calculated from a knowledge of the impedance of the servomechanism alone, combined with the impedance of the flexibilities using the normal laws of impedance addition.

8.1 System under test.

The system under test, a servomechanism with its output end connected to a flexibility, was described in Section 3.5 and shown in Figs. 3.8 & 3.9. The flexibility, which can be represented by two springs and three masses and the complete servo-spring-mass system under test, are shown diagrammatically in Fig. 7.2.

8.2 Calibration of transducers.

The calibration of the load cell and the displacement transducer measuring the deflexion of the servomechanism was carried out as described in Section 5.1, and the values of the calibration factors were as previously given in this section.

The displacement transducer in the base of the vibrator, which measured the displacement of the vibrator ram, i.e. the displacement of the complete system under test, was calibrated by measuring the output from the transducer when calibrated blocks were inserted between two faces, one of which was fixed to the vibrator ram and the other to the vibrator casing, i.e. earth. In this manner a calibration of the transducer was obtained and was set to 5 V/in.

8.3 Measurement of output end spring stiffness.

The stiffness of the beam spring, which was to be connected to the output end of the servomechanism, was obtained by measuring its deflexion when loaded in both tension and compression in a test machine. The load deflexion relationship for the spring was found to be linear, and the spring stiffness equal to 39,000 lbf/in.

Since the double beam spring was heavy, the effect of the mass of the moving parts of the spring was included into the impedance analysis. To simplify the system it was assumed that the mass of the beams was concentrated at each end and in the middle of the beams. The mass concentrated at the middle of the beams was added to the mass of the connecting links, and the mass concentrated at one end of the beams added to the mass of the shackles joining the beam extremities. In this manner the actual spring system was reduced to the simpler system shown in Fig. 7.2.

8.4 Measurement of system impedance.

Using the technique of small perturbations the impedance of the system under test was determined. Tests were carried out in the frequency range 5 - 70 c/s, the vibrator being controlled by a feedback signal proportional to servomechanism displacement. The servomechanism was operated with its piston in the mid stroke position. The force applied to the system and the displacement across the complete system were measured and fed to the automatic mechanical impedance measuring system to determine the system impedance.

Test Series IX : Using a perturbation amplitude of $\pm$ 0.005 in. tests were carried out with a static valve opening varying from 0.002 in. to 0.030 in. Output end spring stiffness = 39,000 lbf/in.

8.5 Discussion of results.

The variation of stiffness and damping with frequency for the system under test is shown in Figs. 8.1 and 8.2. If a comparison is made between the measured values of stiffness and damping and the theoretically predicted values obtained by combining the impedance of the servomechanism with the impedance of the springs and masses using the normal laws of impedance addition, a reasonably close agreement exists between the two sets of data. This is shown in the tabulation which follows.

Freq. c/s	Valve Opening in.	Stiffness lbf/in		Damping lbf/in	
		Predicted	Actual	Predicted	Actual
5	0.002	27,900	32,000	-1,650	-3,000
	0.020	9,460	7,000	7,950	8,000
70	0.002	2,200	0	3,490	6,000
	0.020	-20,400	-21,000	30,500	40,000

As may be expected, when the stiffness or damping is changing most rapidly with respect to frequency and/or valve opening, the greatest inaccuracy exists between the measured and predicted values of these functions. This is shown in Figs. 8.3 and 8.4, the greatest inaccuracy existing when the valve opening equals 0.020 in. and the frequency of excitation is 70 c/s. When it is considered that the predicted values of the system stiffness and damping are dependent upon experimentally determined values of these functions for the servomechanism alone, the results may be considered to be a satisfactory demonstration of the fact that the normal laws of impedance addition may be applied to a system consisting of a servomechanism with output end flexibility.

This part of the experimental programme had the additional function of allowing experience to be gained in the design, operation and control of a test system which included flexibilities. This experience was of great value when anchorage flexibilities were investigated as described in the chapter which follows.

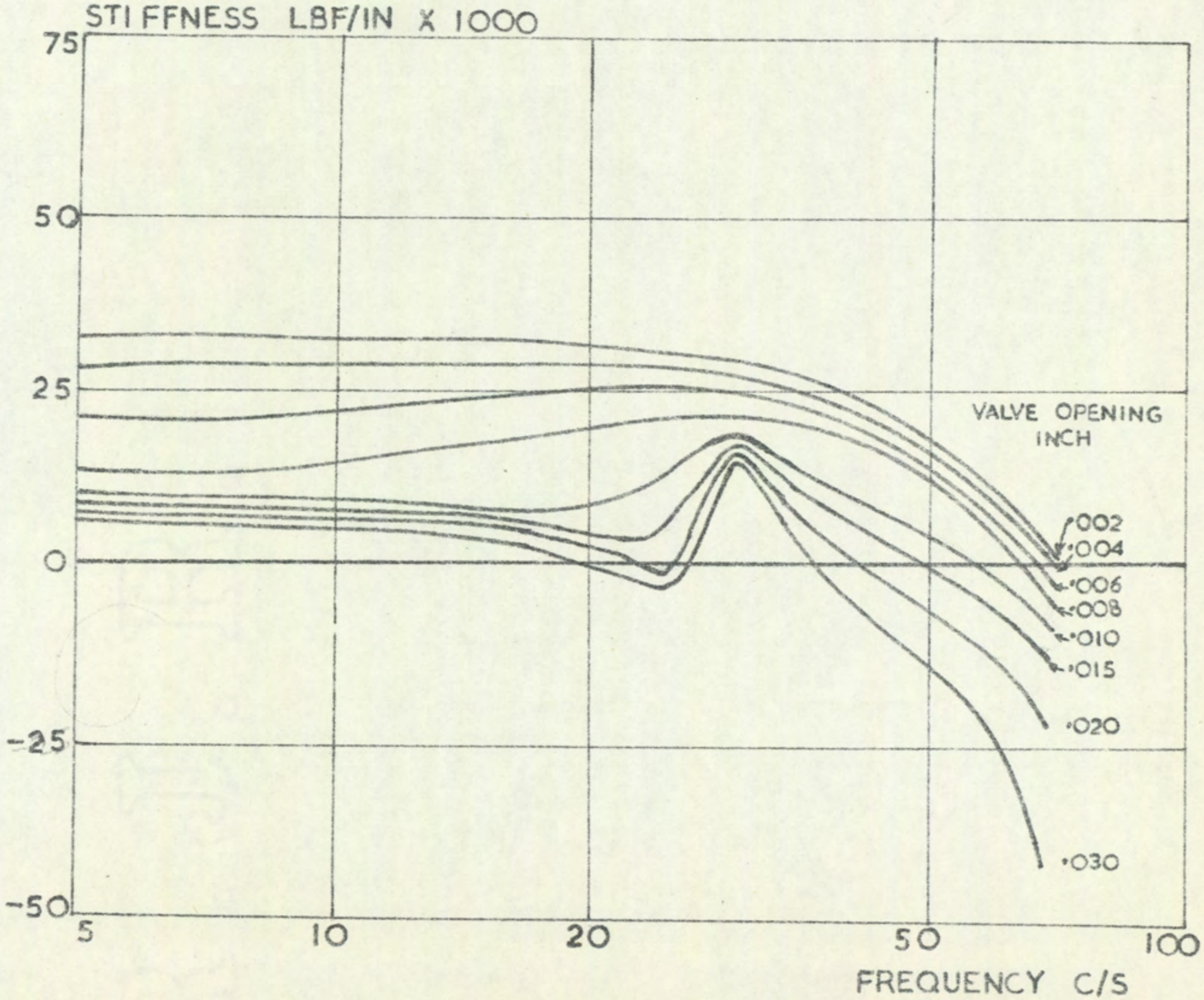

VARIATION OF EXPERIMENTAL STIFFNESS WITH FREQUENCY
OUTPUT END SPRING STIFFNESS = 39,000 LBF/IN
PERTURBATION AMPLITUDE = ±·005 INCH
SERVOMECHANISM DISPL. FEEDBACK CONTROL

FIG 8.1

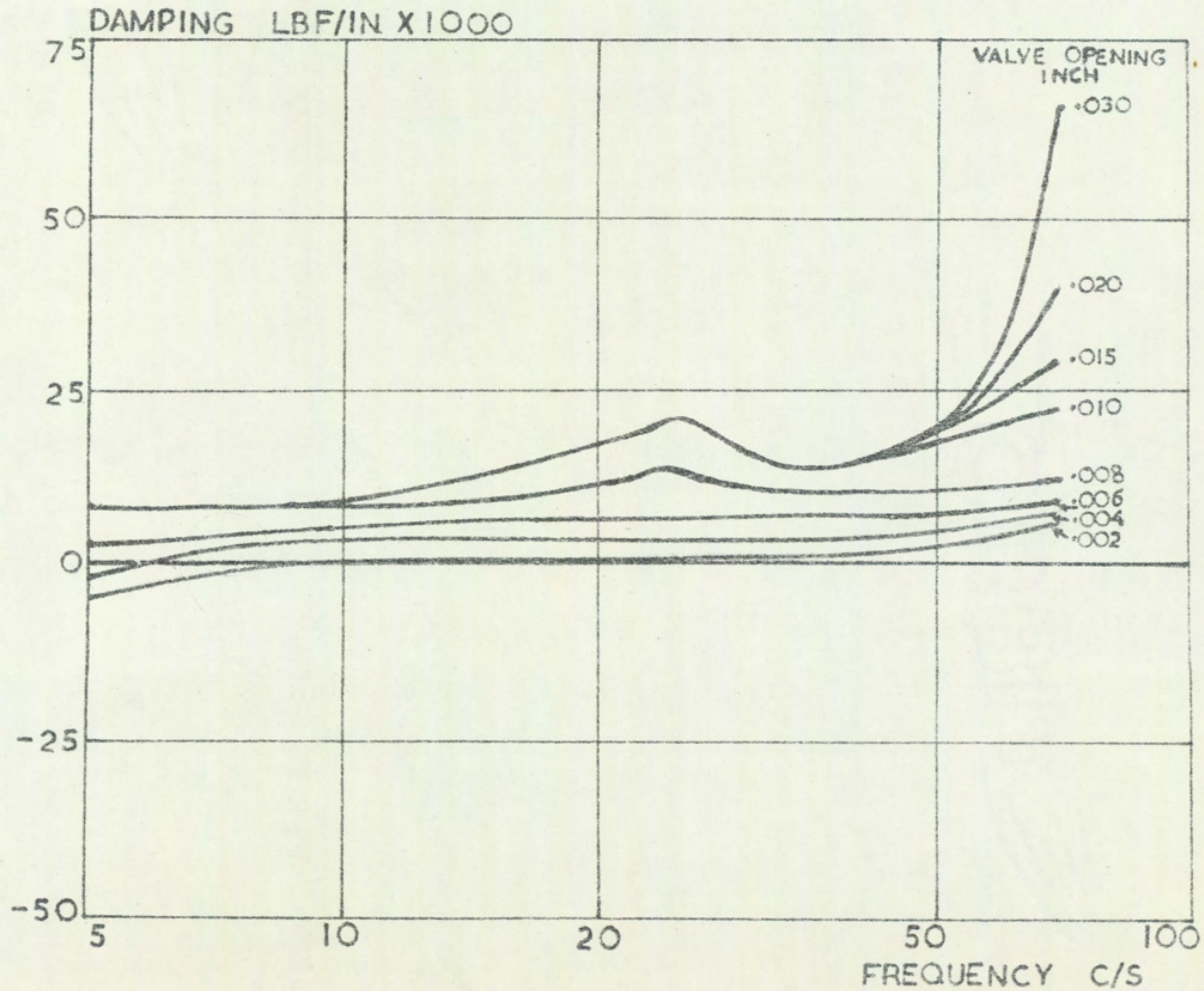

VARIATION OF EXPERIMENTAL DAMPING WITH FREQUENCY
OUTPUT END SPRING STIFFNESS = 39,000 LBF/IN
PERTURBATION AMPLITUDE = ± .005 INCH
SERVOMECHANISM DISPL. FEEDBACK CONTROL

FIG 8.2

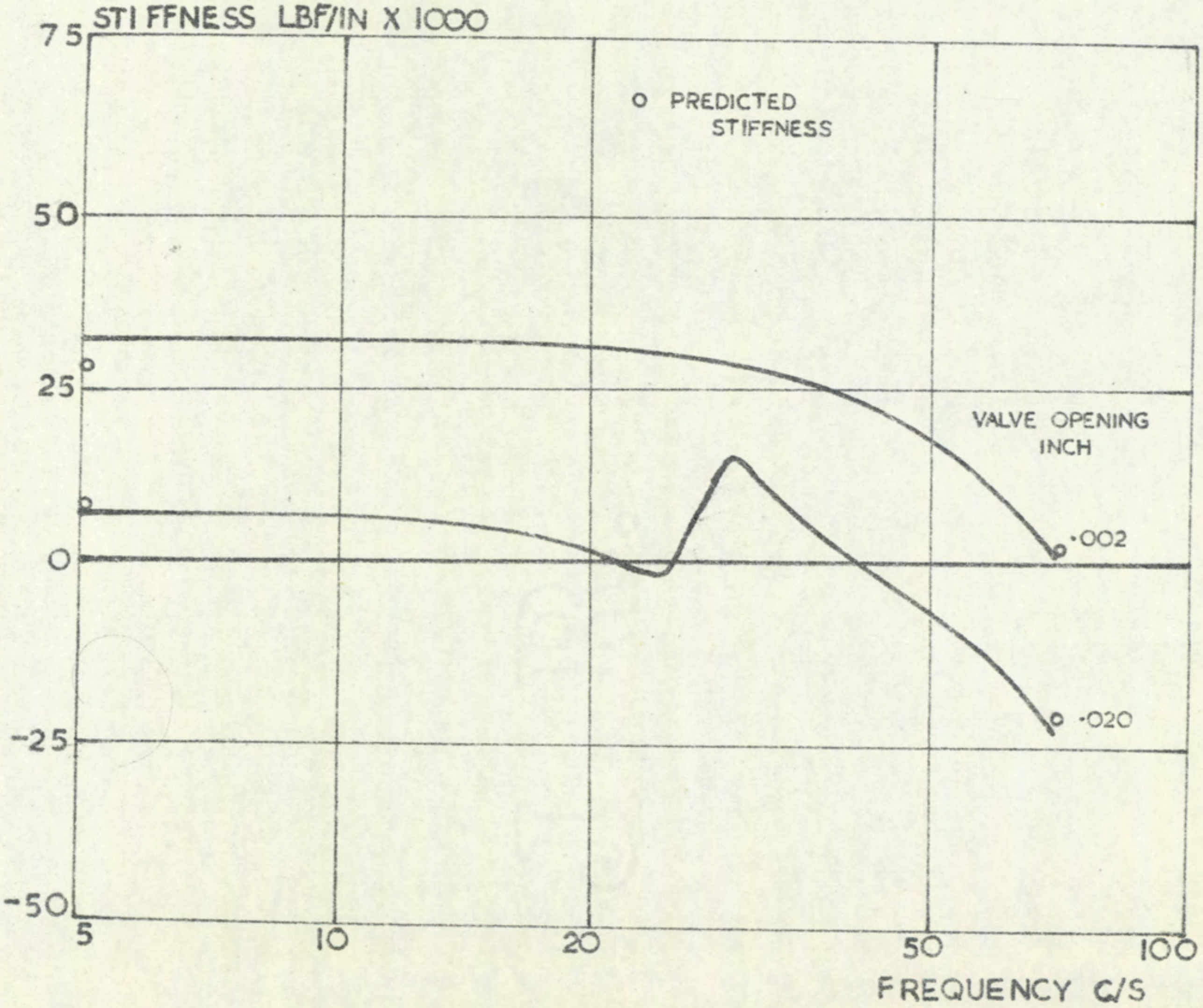

COMPARISON BETWEEN MEASURED & PREDICTED STIFFNESS
OUTPUT END SPRING STIFFNESS = 39,000 LBF/IN
PERTURBATION AMPLITUDE = ±.005 INCH
SERVOMECHANISM DISPL. FEEDBACK CONTROL

FIG 8.3

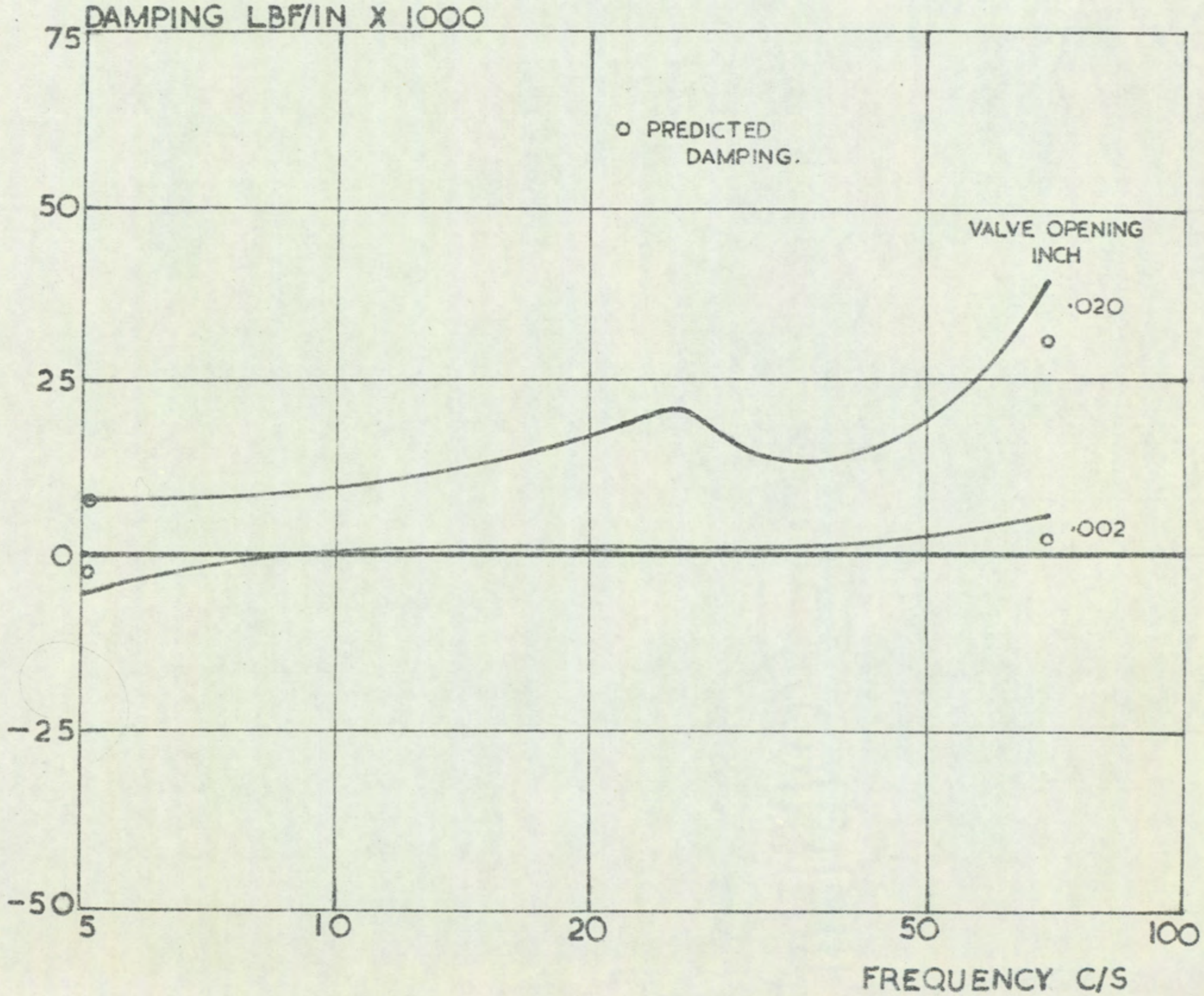

COMPARISON BETWEEN MEASURED & PREDICTED DAMPING
OUTPUT END SPRING STIFFNESS = 39,000 LBF/IN
PERTURBATION AMPLITUDE = ± ·005 INCH
SERVOMECHANISM DISPL. FEEDBACK CONTROL

FIG 8.4

CHAPTER IX

Experimental determination of the impedance of a system consisting of a servomechanism with its anchorage connected to a flexibility.

The experimental work done to determine the impedance of a servomechanism with anchorage flexibility is described and the results discussed. A comparison is drawn between the impedance of this system; the impedance of the system predicted from a knowledge of the impedance of the servomechanism and the impedance of the anchorage flexibility; and the impedance of the servomechanism in a rigid environment.

9.1 System under test.

The system under test, a servomechanism connected to a flexibility, was described in Section 3.5 and shown in Figs. 3.10 and 3.11. The system is shown diagrammatically in Fig. 7.4.

9.2 Calibration of instrumentation and transducers.

The calibration of the load cell and servomechanism displacement transducer was described in Section 5.1 and the calibration of the transducer in the base of the vibrator was carried out as described in Section 8.2. The values of the calibration factors were as previously given in these sections.

9.3 Measurement of the stiffness of the anchorage springs.

The measurement of the stiffness of the anchorage springs was performed in the rig. The servomechanism was replaced by a rigid link and controlling the vibrator by a feedback signal proportional to force, a load was applied to the spring and its deflexion measured by a clock gauge. In this manner the spring stiffnesses were determined and were found to be 60,000 lbf/in. and 20,000 lbf/in. The load deflexion relationship was linear for both springs. The springs and connecting links were weighed and it was assumed that half the mass of the individual springs added to the mass of the moving parts gave their effective mass.

9.4 Measurement of system impedance.

Using the technique of small perturbations, the impedance of the servomechanism-anchorage spring system was measured. With the vibrator controlled by a feedback signal proportional to system displacement and with the servomechanism operating with its piston in the midstroke position, tests were carried out in the frequency range 5 - 70 c/s. The force applied to the system and the displacement across the complete system were measured and fed to the automatic mechanical impedance measuring system to determine the impedance of the system.

Test Series X : With an anchorage stiffness of 60,000 lbf/in. and a perturbation amplitude of $\pm$ 0.005 in., tests were carried out with a static valve opening varying from 0.002 in. to 0.040 in.

Test Series XI : Using an anchorage stiffness of 20,000 lbf/in. Test Series X was repeated.

9.5 Discussion of results.

The families of stiffness curves for a servomechanism rigidly anchored and also anchored by the two differing rate springs, are shown in Figs. 9.1, 9.2 and 9.3. It is seen that the effect of anchorage flexibility is to reduce the stiffness of the system. In Section 7.8 it was shown that as the frequency of the servo-anchorage flexibility system tends to infinity the system stiffness can be predicted by combining the impedance of the servomechanism with the impedance of the anchorage flexibility using the normal laws of impedance addition.

In order to verify this, the stiffness of the system under test was predicted by combining the experimentally determined values of stiffness and damping for the servomechanism alone with the impedance of the anchorage flexibility using the normal laws of impedance addition. The tabulation which follows shows the difference between the value of stiffness predicted in this manner and the measured value of stiffness for the servo-anchorage spring system.

Spring rate	Valve Opening	5 c/s	70 c/s
60,000 lbf/in.	0.002 in.	45,900 (115 x)	5,300 (13.2 x)
	0.020 in.	400 (1)	1,600 (4 x)
20,000 lbf/in.	0.002 in.	23,200 (25.7 x)	900 (1)
	0.020 in.	6,500 (7.2 x)	1,400 (1.5 x)

Note : The figures in brackets refer to the ratio of the error to the smallest error for a particular spring rate.

From this table it is seen that the error between the stiffness predicted by combining the experimentally determined values of stiffness and damping for a servomechanism alone with the impedance of the anchorage flexibility using the normal laws of impedance addition and the measured value of the stiffness for the servo-anchorage spring system is not significant except when the valve opening is small and the excitation frequency is low.

In Chapter VII it was shown that at very low frequencies the stiffness of the servo-anchorage flexibility system tended to that of a rigidly anchored servomechanism. To verify this prediction the difference between the stiffnesses obtained experimentally for the two systems are tabulated below.

Spring rate	Valve Opening	5 c/s	70 c/s
60,000 lbf/in.	0.002 in.	14,500 (14.5 x)	59,000 (59 x)
	0.020 in.	1,000 (1)	10,000 (10 x)
20,000 lbf/in.	0.002 in.	58,000 (29 x)	88,000 (44 x)
	0.020 in.	6,000 (3 x)	2,000 (1)

From this table it is seen that the differences in stiffness between the rigidly anchored servo system and the flexibly anchored system is small at low frequency.

It should be noted that when the anchorage stiffness is as low as 20,000 lbf/in., a frequency of 5 c/s cannot really be considered a low frequency, the tabulated stiffness difference when the valve opening is equal to 0.002 in. is still large. From Fig. 9.4, however, it is seen that at 5 c/s the curves relating to the servomechanism with anchorage flexibility do tend to the curve applicable to the rigidly anchored servomechanism. Also shown in Fig. 9.4 are the high frequency predictions obtained by combining the servomechanism and anchorage impedances using the normal laws of impedance addition.

In Chapter VII no prediction was made with respect to the damping in a servo system with anchorage flexibility, since in all servo systems the damping is zero when the frequency is zero or tends to infinity. The experimental results obtained, Figs. 9.5, 9.6 and 9.7 do show however, that the presence of anchorage flexibility tends to decrease the amount of damping in the servo system and hence to decrease the stability of the system. If the difference between the damping measured in a servo system with anchorage flexibility and the damping predicted by combining the experimentally determined values of stiffness and damping for the servomechanism alone with the impedance of the anchorage flexibility using the normal laws of impedance addition is obtained for various valve opening and frequency conditions, the differences may be tabulated as shown below.

Spring rate	Valve Opening	5 c/s	70 c/s
60,000 lbf/in.	0.002 in.	47,000 (39 x)	2,300 (1.9 x)
	0.020 in.	3,500 (2.9 x)	1,200 (1)
20,000 lbf/in.	0.002 in.	39,600 (14.1 x)	2,800 (1)
	0.020 in.	5,900 (2.1 x)	9,100 (3.2 x)

Inspection of this table shows similar results to those obtained when considering stiffness, i.e. a small difference between the damping in a servomechanism with anchorage flexibility and that using the normal laws of impedance addition except when the frequency of excitation is low and the valve opening is small.

The effect of anchorage flexibility on system stability is shown in Fig. 9.8. As previously stated the presence of anchorage flexibility is to decrease the system stability compared with the rigidly anchored servomechanism thus increasing the region of instability.

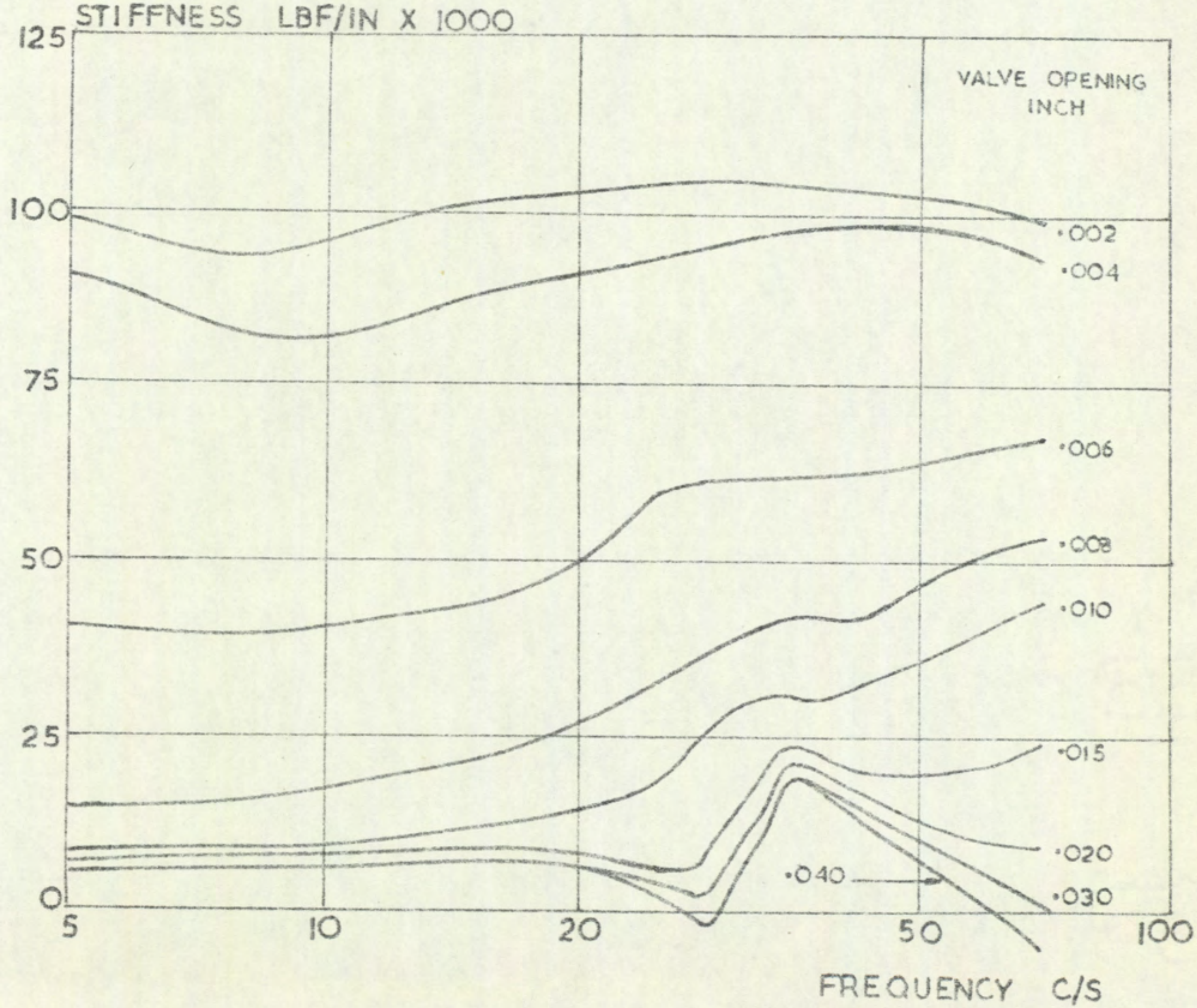

VARIATION OF EXPERIMENTAL STIFFNESS WITH FREQUENCY
ANCHORAGE RIGID
PERTURBATION AMPLITUDE = ± ·005 INCH
SYSTEM DISPL. FEEDBACK CONTROL

FIG 9.1

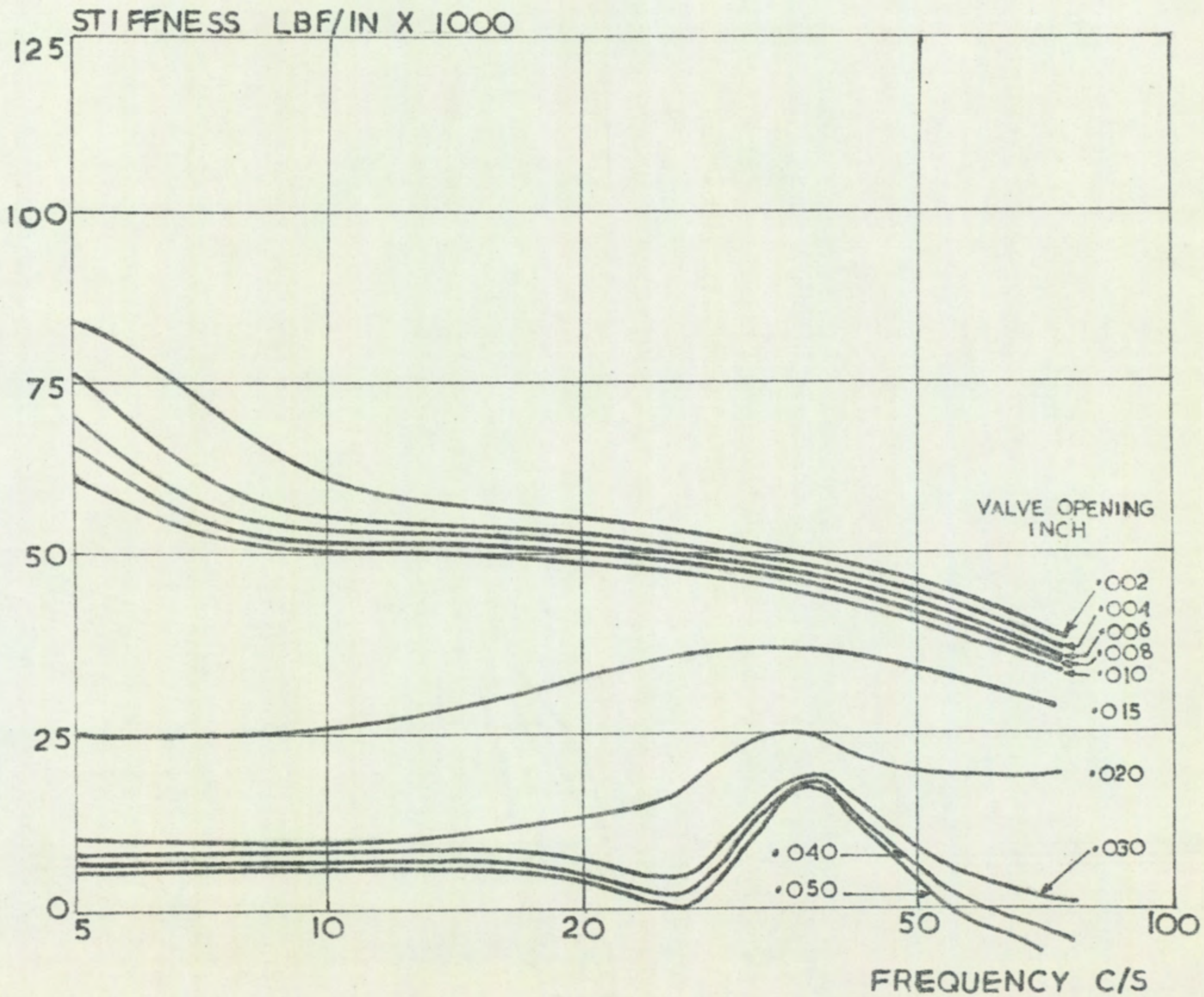

VARIATION OF EXPERIMENTAL STIFFNESS WITH FREQUENCY
ANCHORAGE SPRING STIFFNESS = 60,000 LBF/IN
PERTURBATION AMPLITUDE = ±·005 INCH
SYSTEM DISPL. FEEDBACK CONTROL

FIG 9.2

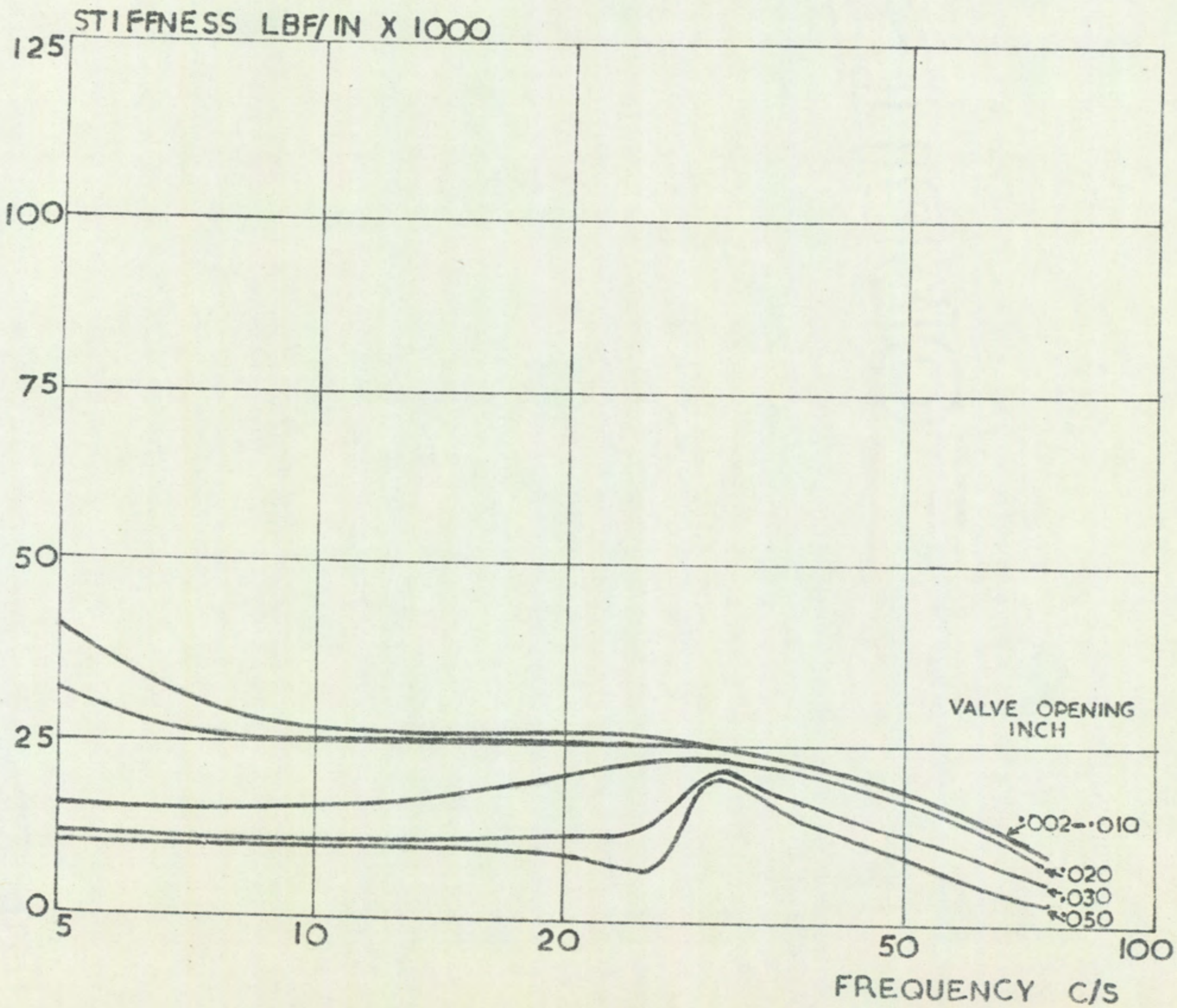

VARIATION OF EXPERIMENTAL STIFFNESS WITH FREQUENCY
ANCHORAGE SPRING STIFFNESS = 20,000 LBF/IN
PERTURBATION AMPLITUDE = ± ·005 INCH
SYSTEM DISPL. FEEDBACK CONTROL

FIG 9.3

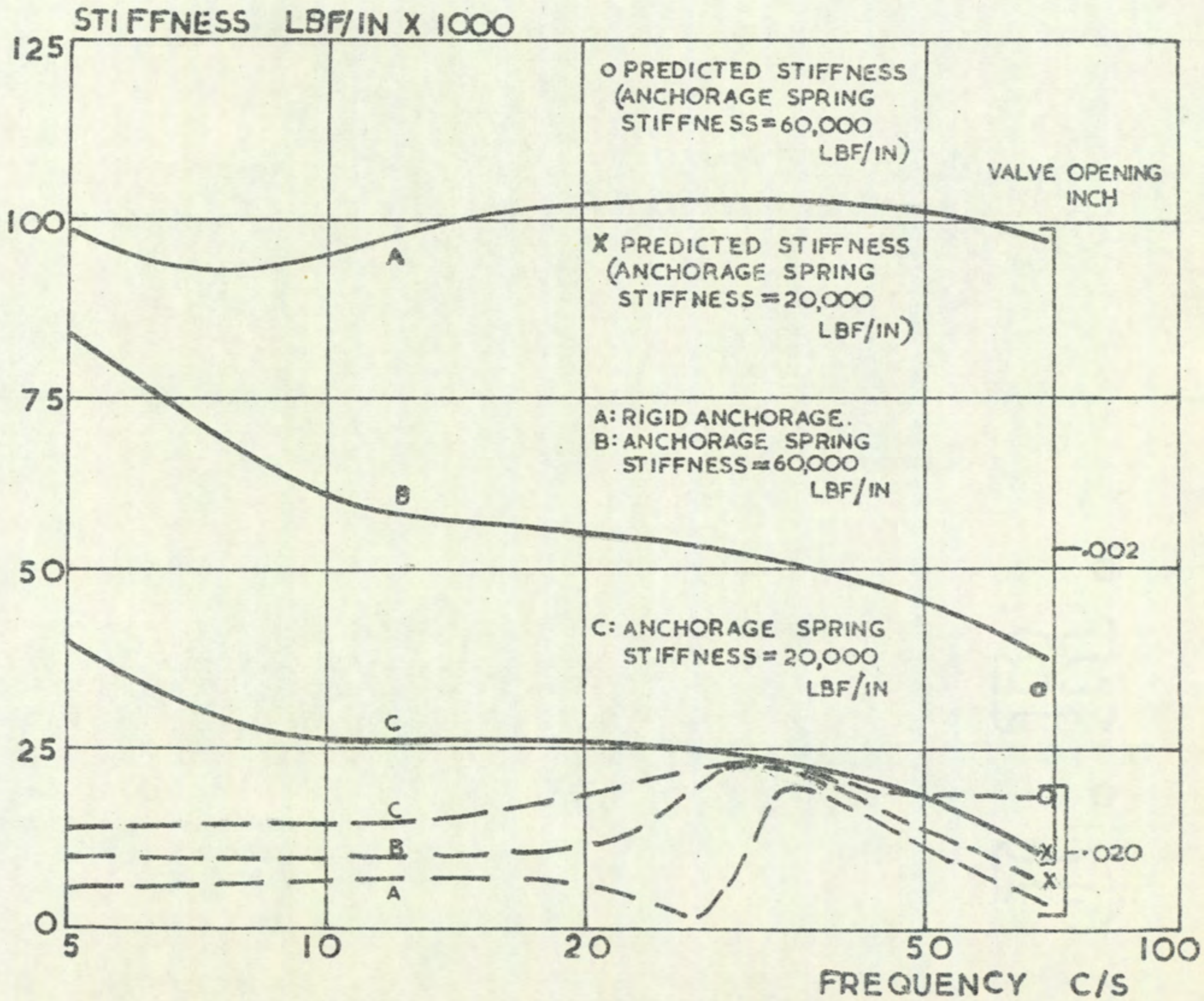

COMPARISON BETWEEN MEASURED & PREDICTED STIFFNESS
FOR VARIOUS ANCHORAGE SPRING STIFFNESSES
PERTURBATION AMPLITUDE = ± ·005 INCH
SYSTEM DISPL. FEEDBACK CONTROL

FIG 9.4

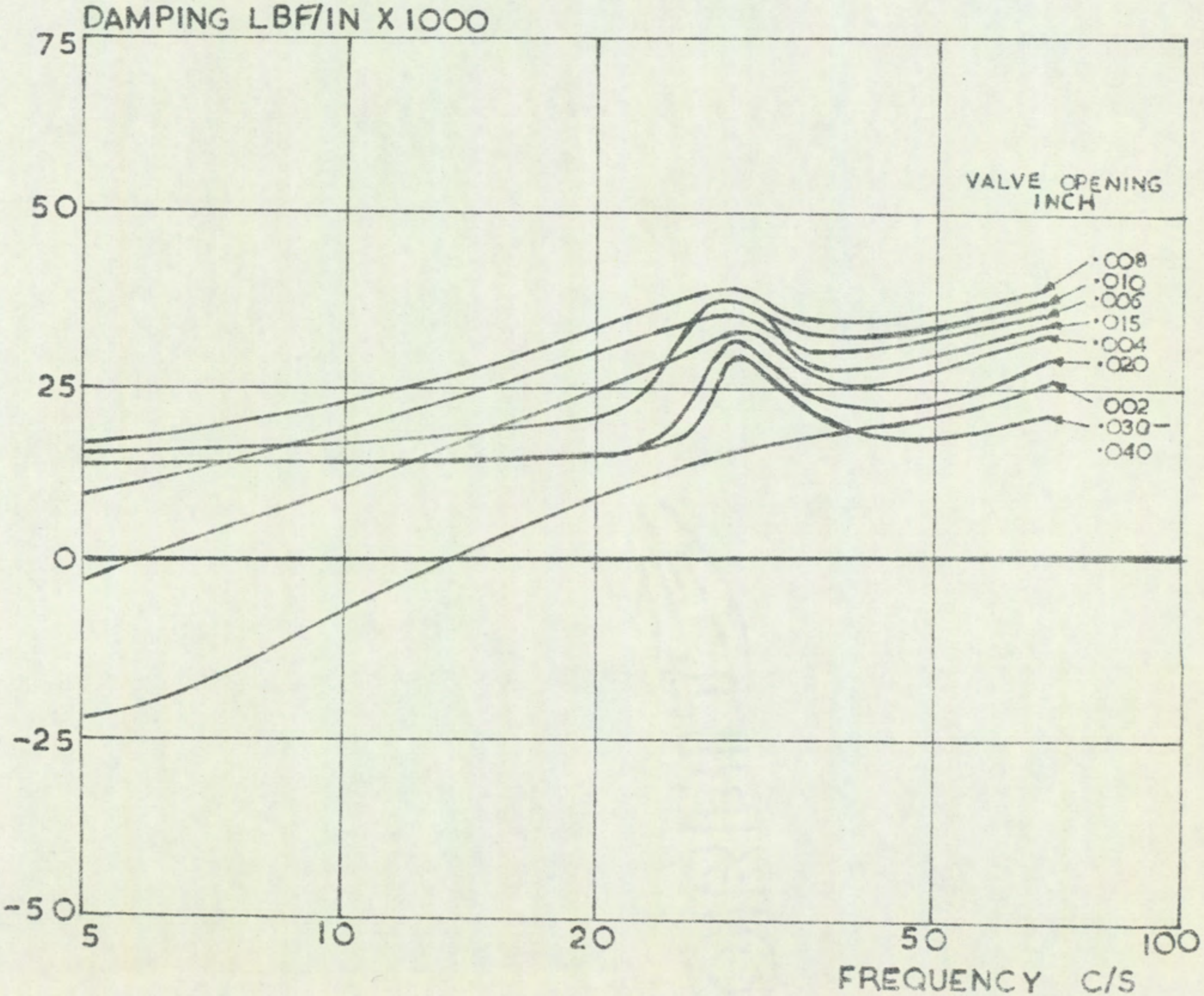

VARIATION OF EXPERIMENTAL DAMPING WITH FREQUENCY
ANCHORAGE RIGID
PERTURBATION AMPLITUDE = ±·005 INCH
SYSTEM DISPL. FEEDBACK CONTROL

FIG 9.5

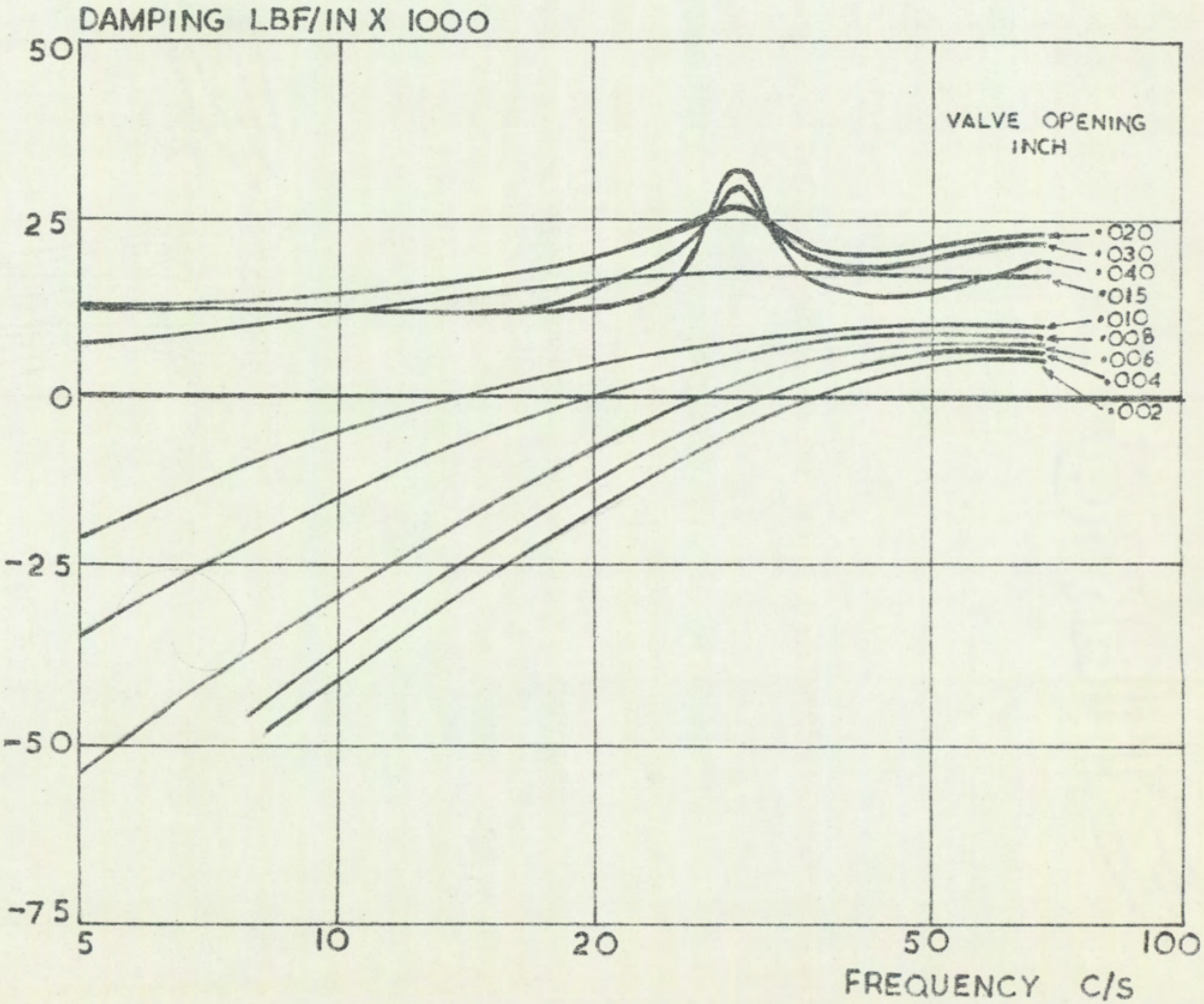

VARIATION OF EXPERIMENTAL DAMPING WITH FREQUENCY
ANCHORAGE SPRING STIFFNESS = 60,000 LBF/IN
PERTURBATION AMPLITUDE = ± ·005 INCH
SYSTEM DISPL. FEEDBACK CONTROL

FIG 9.6

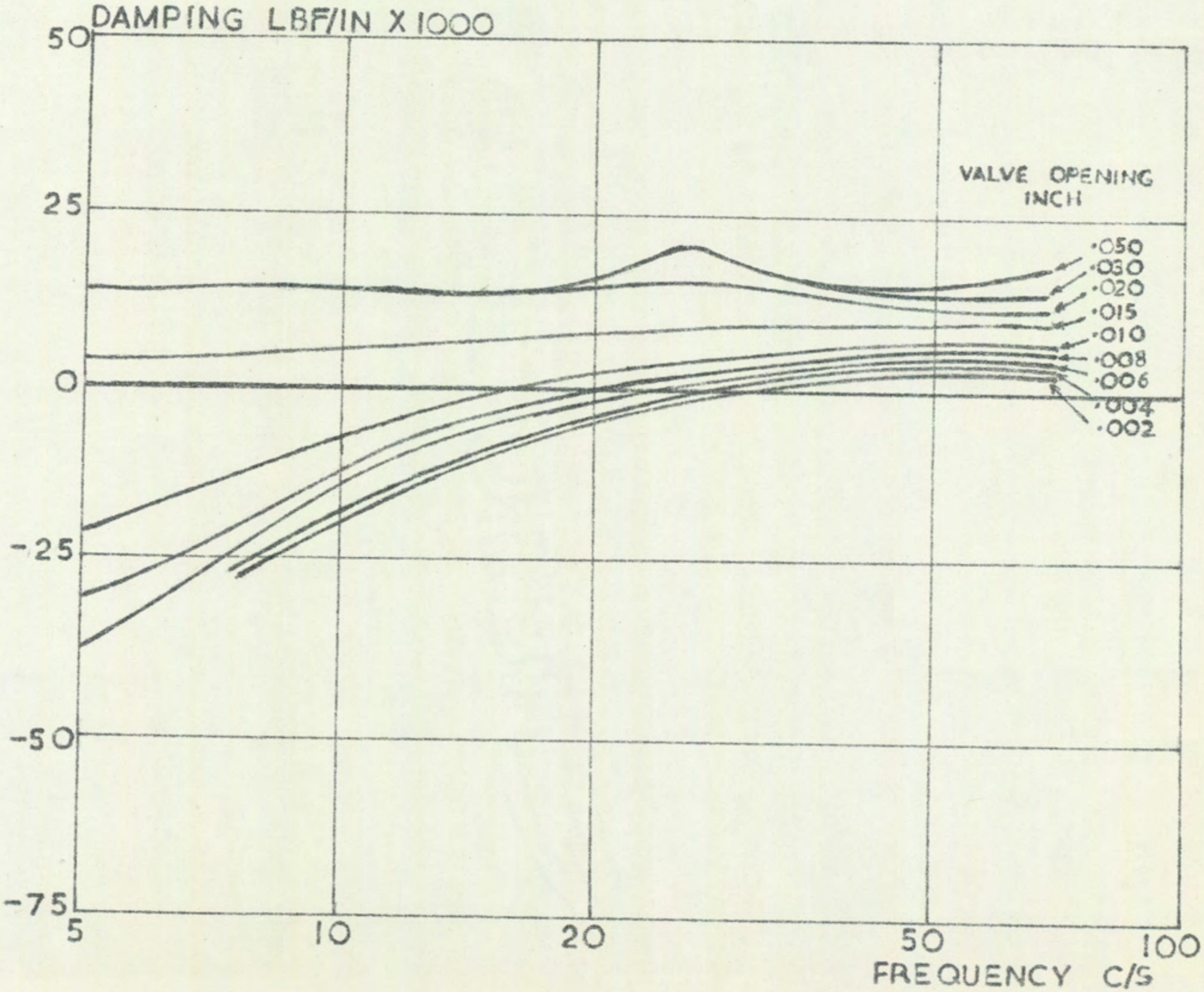

VARIATION OF EXPERIMENTAL DAMPING WITH FREQUENCY
ANCHORAGE SPRING STIFFNESS = 20,000 LBF/IN
PERTURBATION AMPLITUDE = ±·005 INCH
SYSTEM DISPL. FEEDBACK CONTROL

FIG 9.7

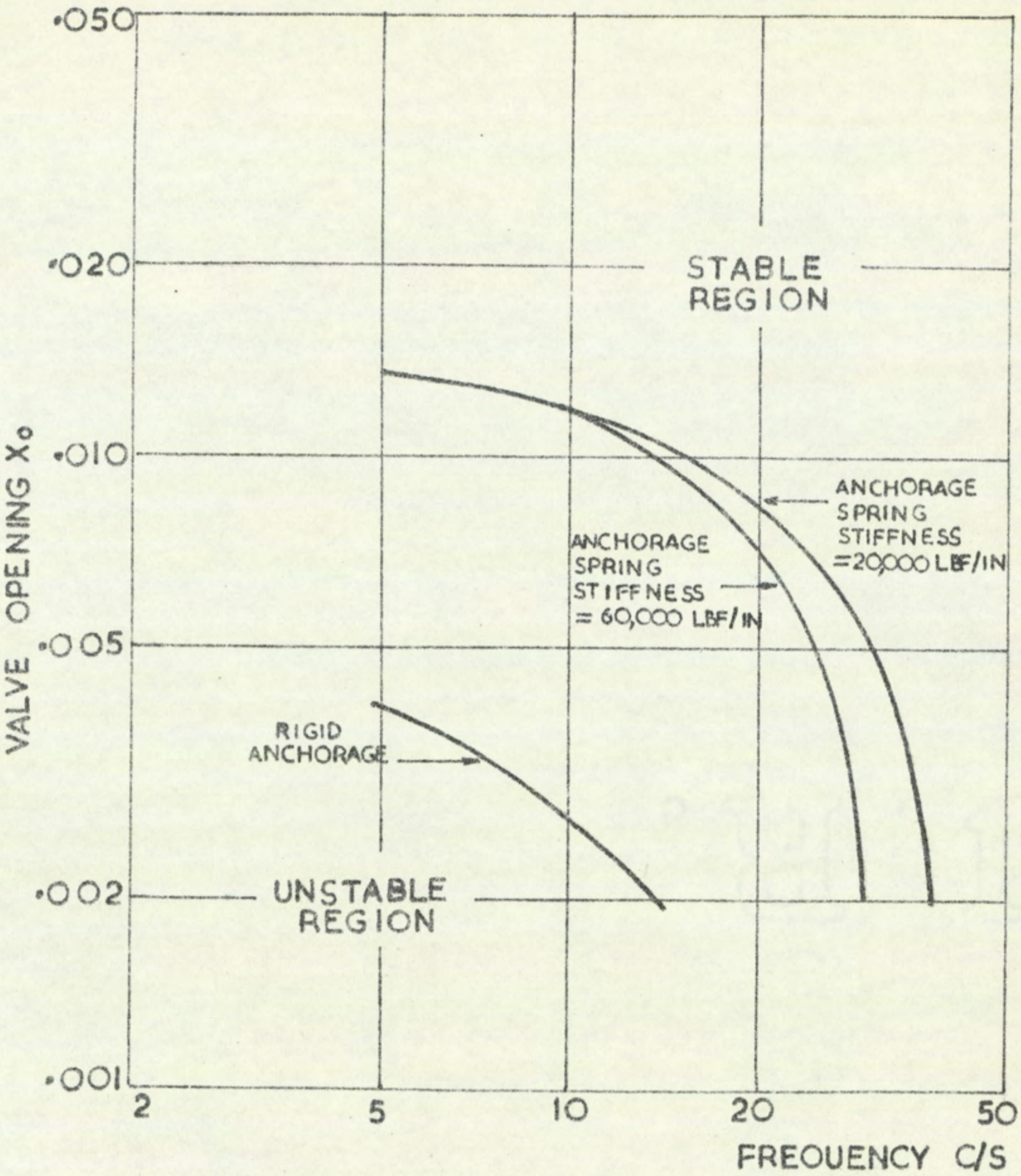

RELATIONSHIP BETWEEN VALVE OPENING AND FREQUENCY FOR ZERO DAMPING

PERTURBATION AMPLITUDE = $\pm$·005 INCH

FIG 9.8

CHAPTER X

Experimental determination of the impedance of a system consisting of a servomechanism with its valve input connected to a flexibility.

The experimental work done to determine the impedance of a servomechanism with its valve connected to a flexibility is described and the results discussed. Reasons are given to show why the results from these tests cannot be applied to the general case of valve input flexibility and are valid only for the particular case examined.

10.1 System under test.

The system under test, a servomechanism with its valve connected to a flexibility, was described in Section 3.5 and shown in Figs. 3.12 and 3.13.

10.2 Calibration of transducers.

The calibration of the load cell and the servomechanism displacement transducer was carried out as described in Section 5.1. The valve spool displacement transducer did not have a micrometer head mounted integral with it and consequently had to be removed from the test rig and mounted into a jig for periodic calibrations. The jig was a device in which the transducer body was rigidly held whilst the core of the transducer was moved under the control of a micrometer, thus enabling a calibration to be made. This calibration was set to 50 V/in.

10.3 Measurement of impedance.

The impedance of the system was measured in the normal manner by means of the small perturbation technique. The tests were carried out in the frequency range 5 - 70 c/s by measuring the force applied to, and the displacement across the servomechanism. The automatic impedance measuring system was used to determine the system impedance and the vibrator was controlled by a signal proportional to the servomechanism displacement. To determine the valve opening it was necessary to subtract the displacement of the valve spool, measured by the valve displacement transducer, from the displacement of the servomechanism body. In practice it was found that as the servomechanism was moved in order to open the valve, friction between the valve and spool caused the spool to move also against the action of the valve input spring. To overcome this 'locking' effect the system was excited for a few seconds at a frequency of 70 c/s in order to free the spool and allow the spring to take up an equilibrium or stable position. It was then possible to measure the valve opening as previously described. Tests were carried out as follows:

Test Series XII: With a valve input spring stiffness of 1,520 lbf/in. and a perturbation amplitude of ± 0.005 in. tests were carried out with a static valve opening varying from 0.002 in. to 0.040 in.

Test Series XIII: Using a valve input spring stiffness of 560 lbf/in. Test Series XII was repeated.

10.4 Discussion of results.

Comparing the families of stiffness curves obtained when the valve was connected to earth rigidly and also by the two springs of differing rates, as shown in Figs. 10.1, 10.2 and 10.3, it is seen that the effect of the flexibility is to decrease the stiffness of the servomechanism. If the stiffness curves obtained from the rigidly and flexibly connected valve tests for a particular valve opening are plotted together, Fig. 10.4, it is seen that the decrease in stiffness is greatest when the valve opening is small and the excitation frequency is low. As the valve opening increases the effect of the flexibility becomes less significant until when the valve is opened by 0.020 in. the flexibility has no apparent effect. At high frequency and small valve opening the flexibility reduces the stiffness but by a smaller amount than at low frequency. Again, as the valve opening is increased the effect of the flexibility tends to become insignificant.

Making a comparison between the families of damping curves as shown in Figs. 10.5, 10.6 and 10.7, it is seen that the damping in the servo system increases when valve flexibility is introduced thus improving the stability of the system.

If a comparison is made between the results obtained experimentally and the theoretical predictions based on the assumption of oil momentum force excitation and also by means of viscous friction force excitation of the valve spool, it is seen that neither assumption appears to be valid. For example, as the excitation frequency tends to zero the oil momentum force excitation hypothesis predicts an increase in the servomechanism stiffness; viscous friction force excitation hypothesis predicts no change; whilst the experimental results give a decrease in the servomechanism stiffness, compared with the stiffness of the servomechanism when the valve input is rigid.

During the experimental programme, however, it was observed that the motion of the servomechanism and the motion of the valve spool remained sensibly in phase for all valve openings tested in the frequency range of interest. This observation suggests that the coupling force causing the excitation of the valve spool was some form of dry friction or stiction force. It seems likely, that due to imperfect alignment of the valve spool and spring, high lateral forces were caused to act on the valve spool and the spool valve and body were thus coupled together. The subject of axial and lateral forces acting on spool valves has been discussed at length by Blackburn (17). If the servomechanism is excited by a perturbation amplitude of $\pm$ 0.005 in., then for the spool valve to have the same displacement it would be necessary for the stiction force to overcome a spring force equal to 2.8 lbf. and 7.6 lbf. in the case of the 560 lbf/in. and the 1520 lbf/in. springs respectively. In view of the possibility of misalignment of the spring valve system and also such factors as wear on the valve and dirt in the hydraulic system, the assumption of a coupling force of up to 8 lbf. does not seem unrealistic. At high frequency this force appeared to break down so that the amplitude of excitation of the spool was attenuated.

Thus we are forced to the conclusion that friction forces are the dominant coupling forces present in this particular servomechanim-valve flexibility system. It should be noted that the results obtained are valid only for the particular servomechanism under test using the particular arrangement of valve flexibility. It would be extremely dangerous to attempt to draw general conclusions for other servomechanisms with valve input flexibility where other forms of coupling, such as oil momentum forces, may be predominant. It would appear that the only reliable method of determining the effect of a particular valve flexibility on a particular servomechanism would be to carry out measurements of impedance on each and every case.

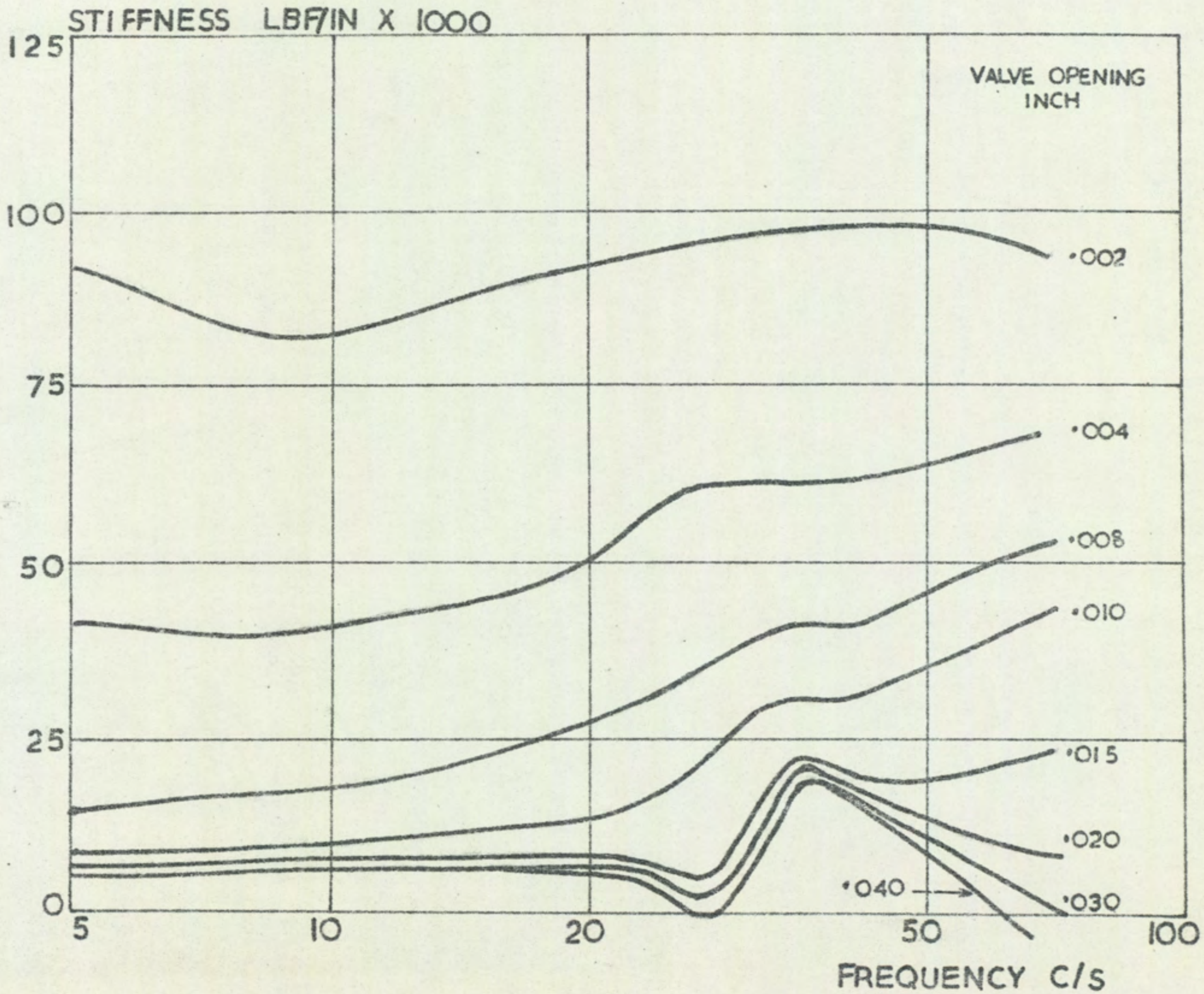

VARIATION OF EXPERIMENTAL STIFFNESS WITH FREQUENCY

VALVE INPUT RIGID

PERTURBATION AMPLITUDE = ± ·005 INCH

SERVOMECHANISM DISPL. FEEDBACK CONTROL

FIG 10.1

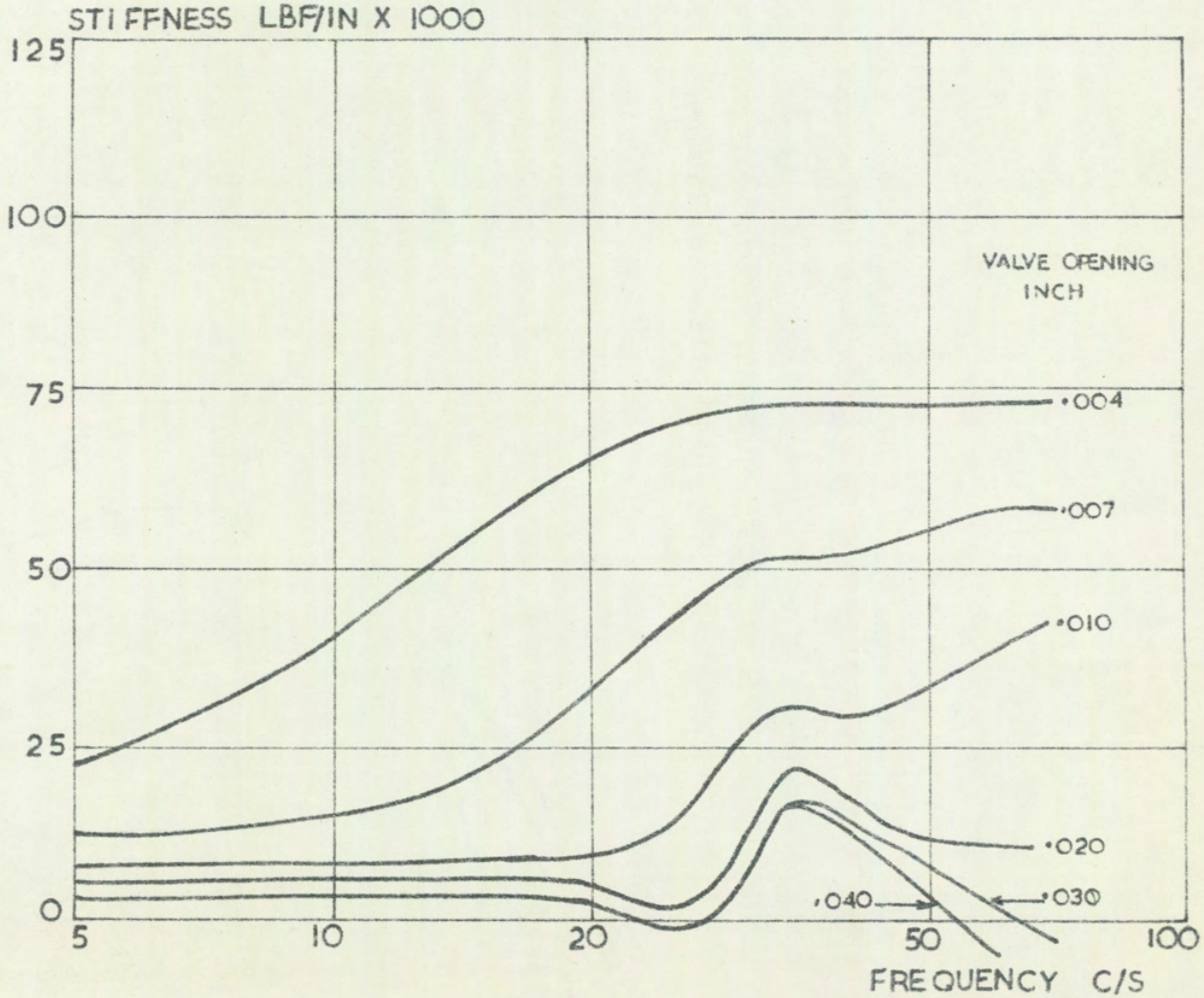

VARIATION OF EXPERIMENTAL STIFFNESS WITH FREQUENCY
VALVE INPUT SPRING STIFFNESS = 1520 LBF/IN
PERTURBATION AMPLITUDE = ±·005 INCH
SERVOMECHANISM DISPL. FEEDBACK CONTROL

FIG 10.2

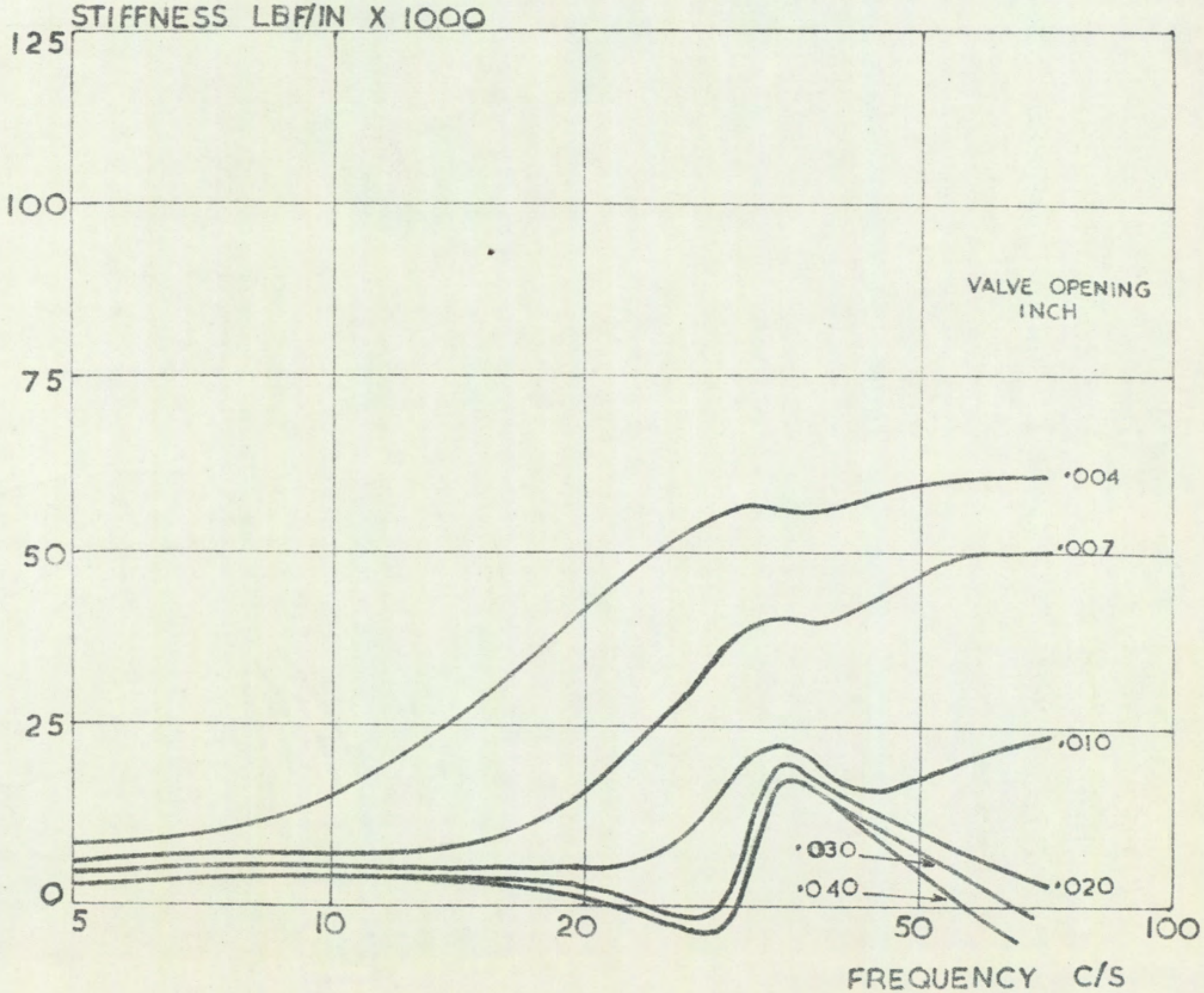

FIG 10.3

VARIATION OF EXPERIMENTAL STIFFNESS WITH FREQUENCY
VALVE INPUT SPRING STIFFNESS = 560 LBF/IN
PERTURBATION AMPLITUDE = ± ·005 INCH
SERVOMECHANISM DISPL. FEEDBACK CONTROL

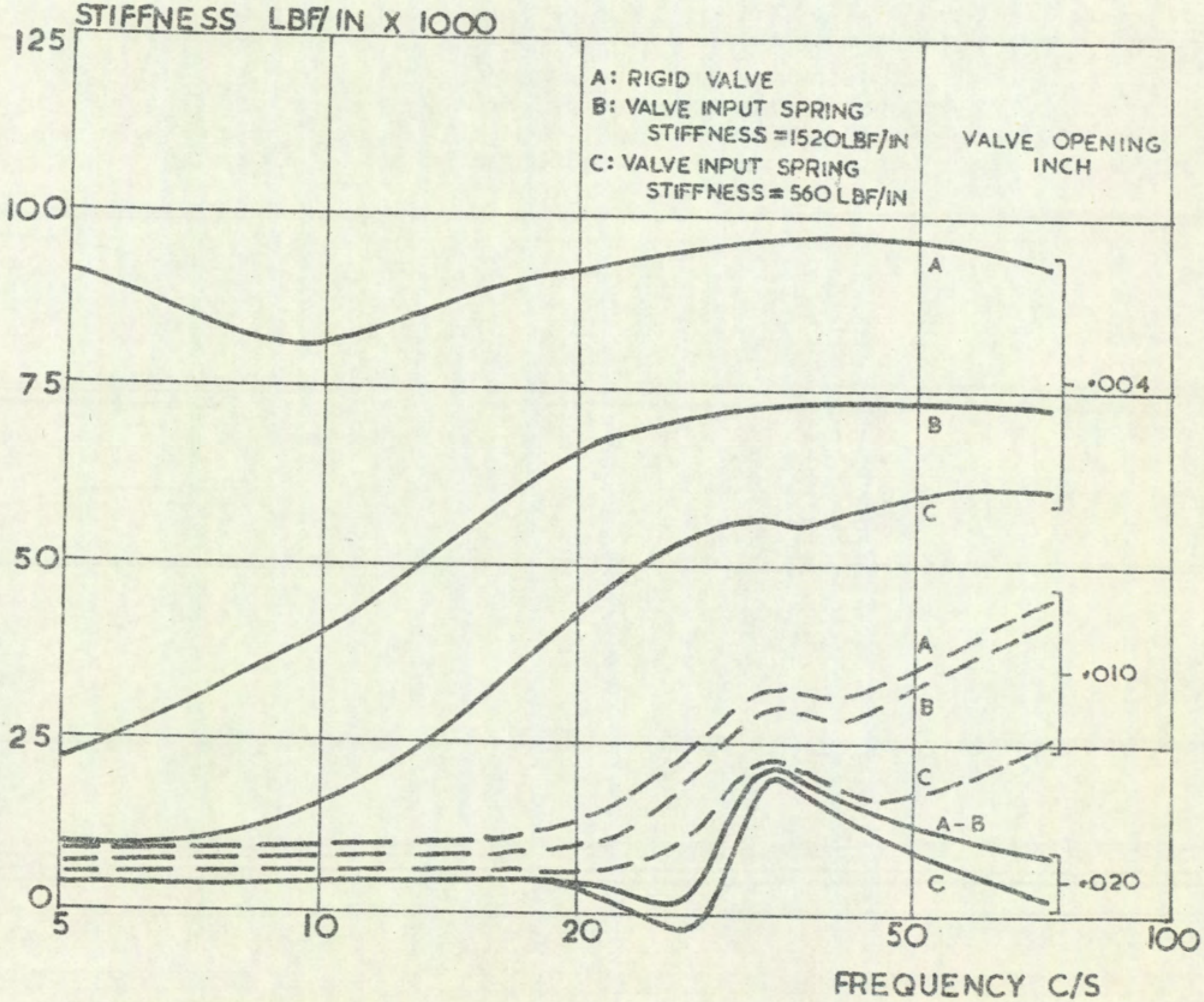

EFFECT OF VALVE INPUT FLEXIBILITY ON STIFFNESS
PERTURBATION AMPLITUDE = ± ·005 INCH
SERVOMECHANISM 'DISPL. FEEDBACK CONTROL

FIG 10.4

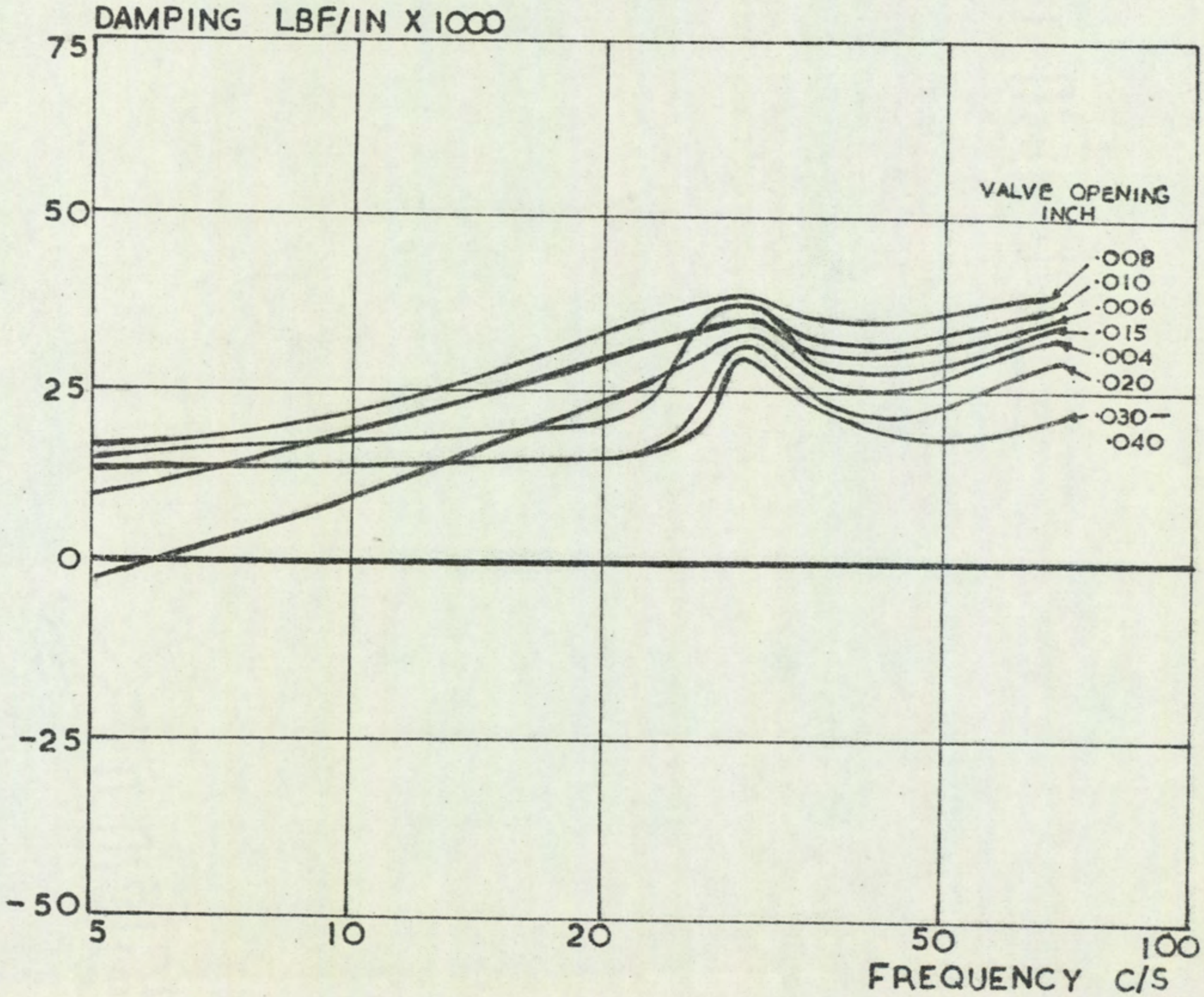

VARIATION OF EXPERIMENTAL DAMPING WITH FREQUENCY
VALVE INPUT RIGID
PERTURBATION AMPLITUDE = ± ·005 INCH
SERVOMECHANISM DISPL. FEEDBACK CONTROL

FIG 10.5

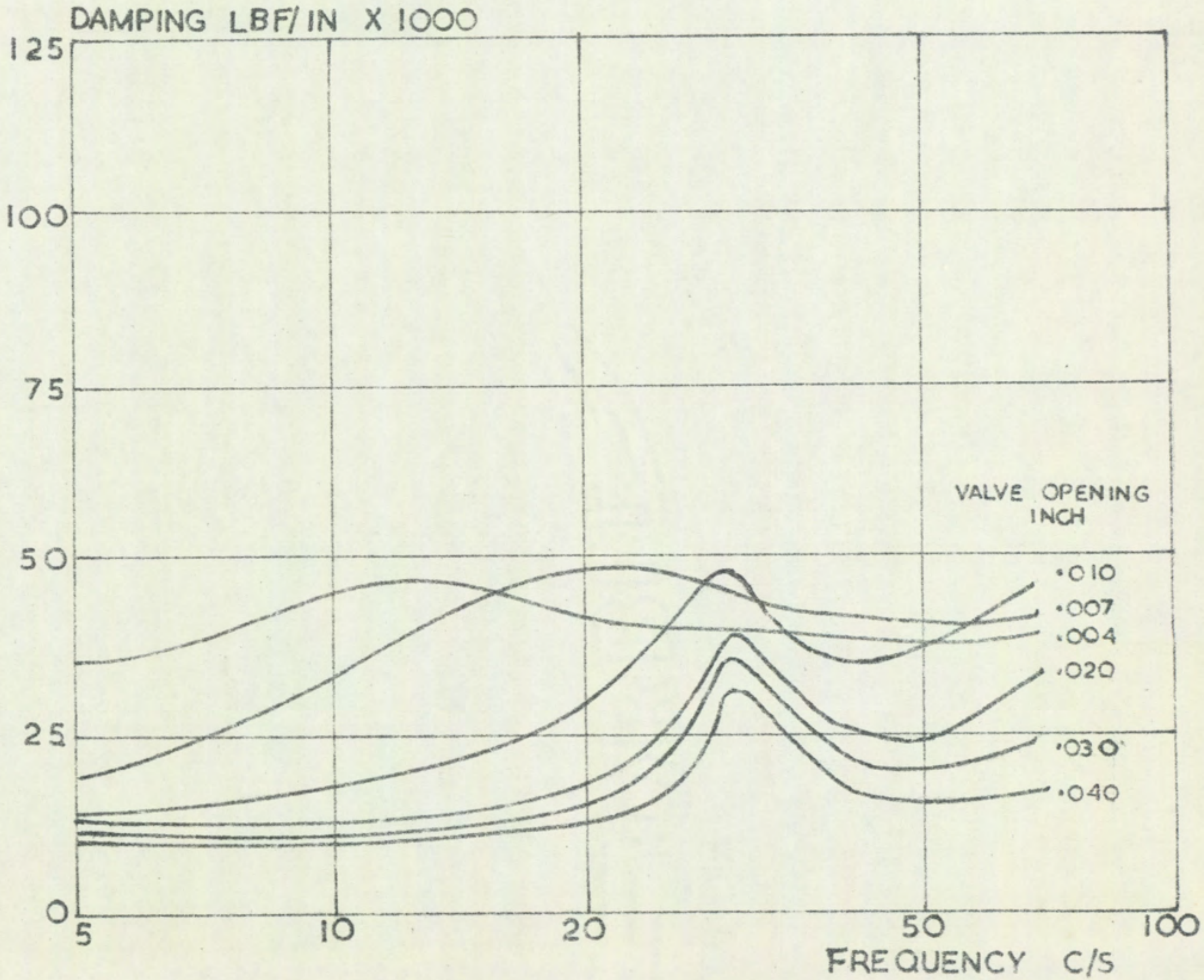

VARIATION OF EXPERIMENTAL DAMPING WITH FREQUENCY
VALVE INPUT SPRING STIFFNESS = 1520 LBF/IN
PERTURBATION AMPLITUDE = ±·005 INCH
SERVOMECHANISM DISPL. FEEDBACK CONTROL

FIG 10.6

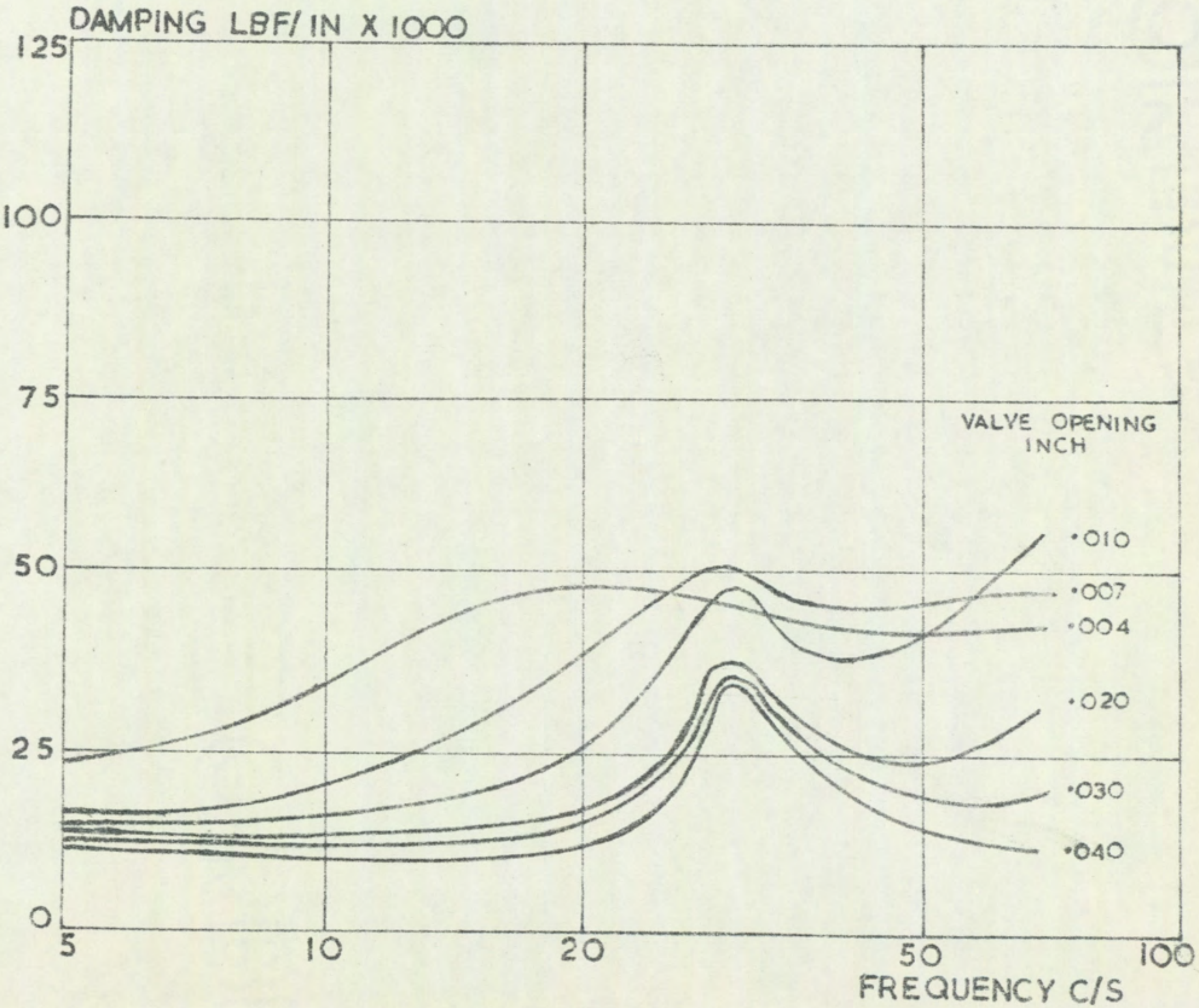

VARIATION OF EXPERIMENTAL DAMPING WITH FREQUENCY
VALVE INPUT SPRING STIFFNESS = 560 LBF/IN
PERTURBATION AMPLITUDE = ±·005 INCH
SERVOMECHANISM DISPL. FEEDBACK CONTROL

FIG 10.7

PART IV

CONCLUSIONS AND PROPOSALS FOR EXTENSION OF THE PROGRAMME.

CHAPTER XI

Conclusions.

These conclusions summarise the more detailed discussions of results which are to be found within the text.

11.1 Impedance of a servomechanism in a rigid environment.

The results obtained from the theoretical analysis of the servomechanism show that when the excitation frequency is low the servo valve characteristics, together with the leakage rate around the jack piston, are the significant parameters of the system in determining the impedance of the servomechanism. The effect of leakage is to decrease the stiffness of the servomechanism when the valve opening is small and to decrease the amount of negative damping predicted in the analysis, thereby improving the stability of the servomechanism.

When the excitation frequency is high (ideally tending to infinity, although in the context of this discussion 40 c/s and above may be considered to be high providing the valve opening is small) the bulk modulus of the working fluid becomes the significant system parameter.

The theoretical analysis shows that the effect of Coulomb and viscous friction in the system is to increase the damping in the servomechanism.

A qualitative agreement has been shown to exist between the theoretical predictions and the experimental results obtained for the servomechanism impedance. The measured stiffness does not, however, reach the large values predicted theoretically at low frequencies and small valve openings. The negative damping, which was predicted theoretically under conditions of small valve opening, occurred in practice but its amplitude was much reduced.

The experimental results showed that the perturbation amplitude of the excitation affected both the measured stiffness and damping of the servomechanism. One possible explanation for this may be due to the effect of Coulomb friction within the servomechanism.

The presence of a non-return valve in the fluid supply line does not have a significant affect upon the servomechanism impedance.

Offsetting the servomechanism piston from the mid stroke position has no affect upon the impedance of the servomechanism.

Since only a qualitative agreement exists between the experimental and theoretical results, it seems that at the present time the only reliable way of determining the impedance of the servomechanism is to measure it in a laboratory test rig. With the experience gained from these tests the measurement of the impedance of any servomechanism could be readily accomplished providing the excitation force required was within the capability of the exciter available.

11.2 Random excitation of the servomechanism.

The impedance of the servomechanism obtained by random excitation of the system followed by analysis of the resulting force and displacement signals to give their power spectral densities and hence the system impedance, shows a good agreement can be achieved with the impedance obtained using sinusoidal excitation of the system. In view of this it would appear that random excitation of the system may well offer a rapid and reliable method of measuring the impedance of the servomechanism. This method has certain attractive advantages since the form of the excitation would often be encountered in flight.

It has also been shown that random excitation of the servomechanism offers an opportunity to measure an average value of its impedance within any bandwidth under consideration. In this manner wide band impedance for a particular valve opening or applied force can be obtained from two simple measurements, providing that phase and frequency information is not required.

11.3 Measurement of servomechanism impedance by excitation of the valve input.

The experimental results obtained in attempting to measure the impedance of the servomechanism by exciting the valve input, gave only a general agreement with the results obtained for the impedance of the servomechanism by direct excitation of its output end.

Although the results obtained up to the present time cannot be considered satisfactory, this method of determining the servomechanism impedance has certain advantages, particularly in that only a low level of force excitation is required and also that the method is closely related to frequency response testing.

11.4 Impedance of a system consisting of a servomechanism connected at its output end to a flexibility.

It has been shown theoretically and demonstrated experimentally that the impedance of a system consisting of a servomechanism with output end flexibility can be calculated by combining the impedance of the servomechanism measured in the laboratory test rig with the impedance of the flexibility using the normal laws of impedance addition.

11.5 Impedance of a system consisting of a servomechanism with its anchorage connected to a flexibility.

The theoretical analysis for a system composed of a servomechanism with anchorage flexibility produces an impedance equation of some complexity. It has, however, been shown theoretically and verified experimentally that as the excitation frequency of the system tends to zero, the stiffness of the system is equal to the stiffness of the servomechanism alone, i.e. the anchorage flexibility has no effect upon the system stiffness. Also, as the excitation frequency of the system becomes high the stiffness of the system may be calculated by combining the impedance of the servomechanism measured in the laboratory test rig with the impedance of the flexibility using the normal laws of impedance addition. The stiffness of the system will vary between these two limits, and thus will always be equal to, or greater than the stiffness predicted using the normal laws of impedance addition.

11.6 Impedance of a system consisting of a servomechanism with its valve input connected to a flexibility.

The theoretical analysis for a system consisting of a servomechanism with valve input flexibility can only be made if the form of the force exciting the valve spool-input flexibility sub system is known. In practice, more than one form of force may cause the excitation and unless one force predominates the analysis cannot be readily made. The experimental results obtained for this system are of limited value since they are valid only for the particular conditions which existed in the test rig.

CHAPTER XII

Proposals for Extension of the Programme.

12.1 Introduction.

In order to complete the investigation proposed in Section 1.4 the following parts of the project remain,

(i) An investigation to determine what mechanical element, if any, may be used to replace the servomechanism in the powered flying control system whilst tests are carried out on the remainder of the system to determine its impedance using a low level of force excitation.

(ii) An investigation to determine the impedance of a powered flying control system in a limited and restricted manner by direct excitation of the control system in the aircraft in order that a comparison can be made between these results and the results obtained by the method proposed in Section 1.4.

In addition to these projects the investigations which follow may be undertaken.

12.2 Measurement of impedance using random excitation of the system.

This would be an extension of the work already carried out (see Chapter V). The investigation would extend the work for more varied conditions of valve opening and perturbation amplitude etc. The analysis of the force and displacement signals could be performed using the automatic mechanical impedance analysis system working in the power spectral density mode. This system would give a better analysis of the signals than would the system previously used and described in Section 3.8. In the event of analysis equipment capable of producing the cross power spectral density of two functions becoming available, the work could be extended to cover this aspect of the analysis.

12.3 The impedance of a servomechanism with valve input flexibility.

In Chapters VII and X the problems involved in predicting and obtaining reliable results for the impedance of a servomechanism with valve input flexibility have been discussed. The results obtained, however, were of restricted value only and the work could be usefully extended to obtain more experimental information for various values of flexibility and designs of valve (see also Section 12.7).

12.4 Measurement of impedance of a servomechanism using valve input excitation.

In Chapter VI the work done in attempts to measure the impedance of the servomechanism using valve input excitation was described. The results obtained from this work did not give a good measurement of impedance compared to those obtained by direct excitation of the servomechanism output end. The method does, however, have certain advantages and it seems desirable that further efforts should be made to overcome the problems, particularly the measurement of x_o^F/x_i, in order to make the method workable. In this manner the measurement of the servomechanism frequency response and impedance can be closely linked.

12.5 Effect of large input forces and displacements on the servomechanism.

Experimental work is required to determine the force displacement relationship for the servomechanism when the input force or displacement is large. Theoretical predictions can be made either by using a digital computer to solve equation (2.61), see section 2.11, or by using an analogue computer to simulate the form of the impedance-valve opening relationship using diode function generators.

12.6 Effect of exciting the servomechanism output end and valve input simultaneously.

This effect has been analysed theoretically in Section 4.23. These predictions can be checked experimentally provided that the necessary excitation and analysis equipment is available. The automatic mechanical impedance analysis system would require slight modifications in order to carry out this work.

12.7 Impedance measurement on various servomechanisms.

By measuring the impedance of several servomechanisms of differing designs the effect of various parameters such as jack piston area, swept volume and valve characteristics could be established. This investigation could be carried out simultaneously with Section 12.3. It would also be of interest to vary leakage rates across the servomechanism ram by artificial means to study the effects experimentally.

12.8 Analogue simulations of the servo system.

One use of an analogue computer already suggested is to simulate the effect of a large force and displacement input to the servomechanism, see Section 12.5. The computer might also be used to simulate the system when attempts are made to combine the impedance of the servomechanism determined in the laboratory test rig with the impedance of the remainder of the control system.

REFERENCES

1. Olson H.F. 'Dynamic Analogies', D. Van Nostrand, New York, 1943.

2. Biot M.A. 'Coupled Oscillations of Aircraft Engine Propeller Systems', J. Aero. Soc., Jan. 1940.

3. Firestone F.A. 'The Mobility and Classical Impedance Analyses', American Institute of Physics Handbook, McGraw-Hill, p.3-140, 1938.

4. Duncan W.J. 'The Admittance Method of Obtaining the Natural Frequencies of Systems', Phil. Magazine Vol. XXXII, Ser. 7, p. 401-409, Nov. 1941.

5. Bendat J.S. 'Principles and Applications of Random Noise Theory', John Wiley & Sons, 1958.

6. Burrow L.R. 'Some Analog Methods for Power Spectral Density Analysis', Instr. Soc. Am., 20th Annual Conf., Los Angeles. Paper No. 1.5-3-65.

7. Van Orstrand C.E. 'Reversion of Power Series', Phil. Magazine, Vol. XIX, March 1910.

8. Conway H.G. & Collinson E.G. 'An Introduction to Hydraulic Servomechanism Theory', Proc. Conf. Hydraulic Servomechanisms 1953, 1 (Instn. Mech. Engrs., London).

9. Harpur N.F. 'Some Design Considerations of Hydraulic Servos of Jack Type', Proc. Conf. Hydraulic Servomechanisms 1953, 41 (Instn. Mech. Engrs., London).

10. Sung C.B. & Watanabe S.F. 'Control of Inertia Loads by Hydraulic Servo-systems through Elastic Structures', Proc. Symp. Recent Mech. Engng. Dev. Automatic Control 1960, 63 (Instn. Mech. Engrs., London).

11. Williams H. 'Effect of Oil Momentum Forces on the Performance of Electro-hydraulic Servomechanisms', Proc. Symp. Recent Mech. Engng. Dev. Automatic Control 1960, 31 (Instn. Mech. Engrs., London).

12. Glaze S.G. 'Analogue Technique and the Non-linear Jack Servomechanism', Proc. Symp. Recent Mech. Engng Dev. Automatic Control 1960, 178 (Instn. Mech. Engrs., London).

13. Lambert T.H. & Davies R.M. 'Investigation of the Response of a Hydraulic Servomechanism with Inertial Load', J. Mech. Engng. Sci. 1963, 5 (No.3), 281.

14. Davies R.M & Lambert T.H. 'Transient Response of an Hydraulic Servomechanism Flexibly Connected to an Inertial Load', J. Mech. Engng. Sci. 1964, 6 (No.1) 32.

15. Watson C.D. 'Variable Hydraulic Pump Servos, and a Method of Impedance Testing', Proc. Conf. Hydraulic Servomechanisms 1953, 12 (Instn. Mech. Engrs., London).

16. Lambert T.H. & Davies R.M. 'Relaxation Oscillation of a Valve Controlled Hydraulic Servomechanism under Steady Load', Proc. Convention Advances Automatic Control 1965, 141 (Instn. Mech. Engrs., London).

17. Blackburn J.F. and others. 'Fluid Power Control', The Technology Press of M.I.T. and John Wiley & Sons, 1960.

ACKNOWLEDGEMENTS

The author wishes to thank and acknowledge:

Professor A.C. Walshaw, for the facilities of the Dept. of Mech. Eng.

Professor E. Downham, under whose supervision the work was carried out, for his help and encouragement at all stages of the project.

The Ministry of Aviation, for providing the necessary financial support for the project.

The numerous members of the academic, technical and workshop staff of the Dept. of Mech. Eng. for the assistance they have so generously given.

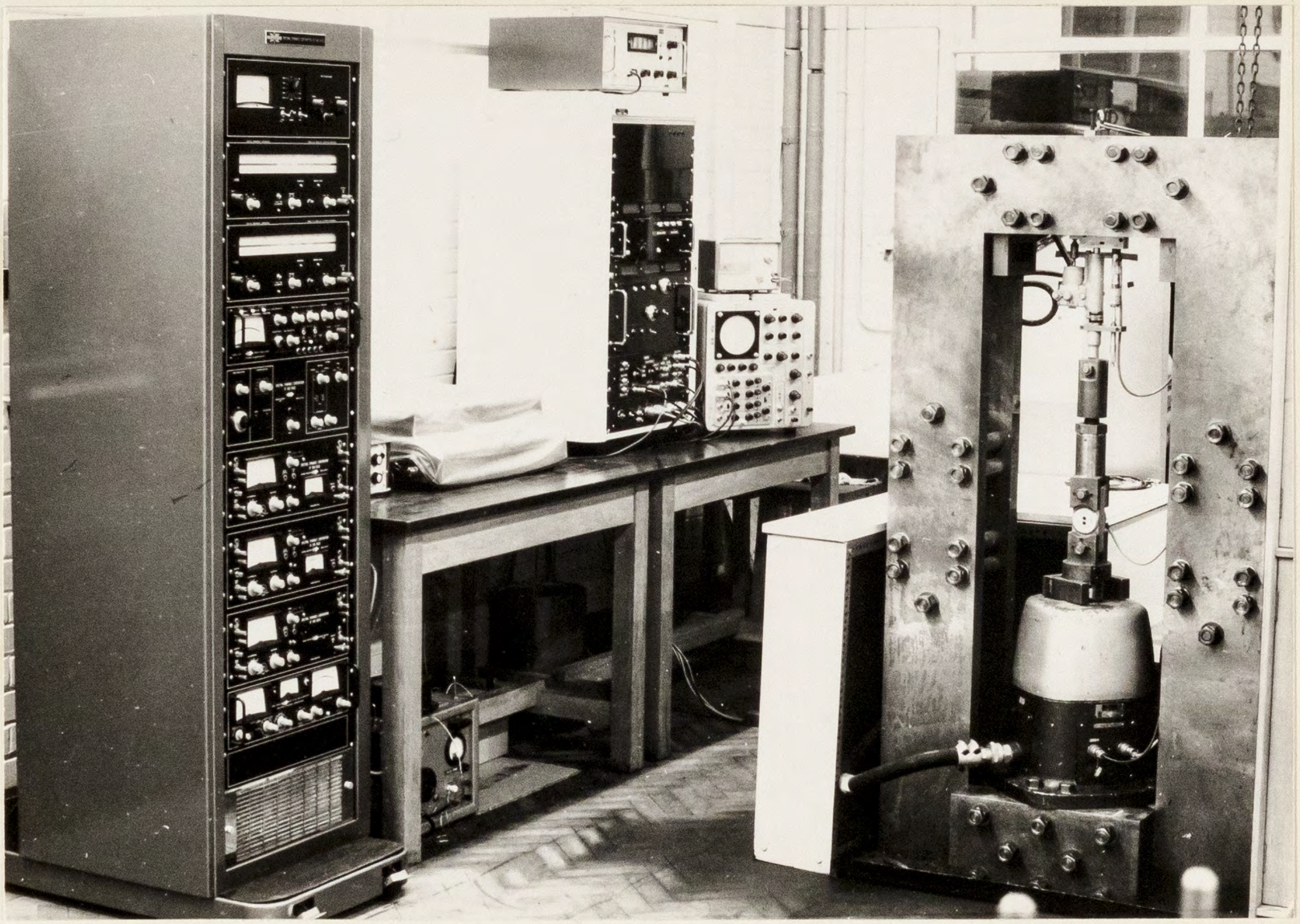

INSTRUMENTATION AND TEST RIG